Role Of The Endothelin B Receptor In Cardiovascular Homeostasis

Dr Alan Bagnall

Thesis presented for the degree of Doctor of Philosophy

University of Edinburgh

February 2004

Declaration

This thesis and the data presented within it are entirely the results of my own efforts, except where stated otherwise. This work contains no material that has been accepted for the award of any other degree or diploma in any university or tertiary institution and, to the best of my knowledge, contains no material previously published or written by another person, except where stated in the text.

28th September 2004

Dr Alan James Bagnall

Table of Contents

DECLARATION ..... **II**

TABLE OF CONTENTS ..... **III**

TABLES AND FIGURES ..... **IX**

LIST OF ABBREVIATIONS ..... **XI**

ACKNOWLEDGEMENTS ..... **XIV**

ABSTRACT ..... **XV**

1 CHAPTER 1 ..... **1**

1.1 INTRODUCTION 1
1.2 ENDOTHELIN GENERATION 3
1.3 ENDOTHELIN CONVERTING ENZYME 5
1.4 SECRETION OF ENDOTHELIN-1 7
1.5 ENDOTHELIN RECEPTORS 7
1.5.1 ENDOTHELIN RECEPTOR GENES 8
1.5.2 DISTRIBUTION OF ENDOTHELIN RECEPTORS 9
1.5.3 STRUCTURE OF ENDOTHELIN RECEPTORS 10
1.5.3.1 *N-terminus* *11*
1.5.3.2 *Transmembrane and extracellular domains* *11*
1.5.3.3 *Cytoplasmic loops* *11*
1.5.3.4 *C-terminus* *12*
1.5.4 POST TRANSLATIONAL MODIFICATION OF ENDOTHELIN RECEPTORS 12
1.5.5 SIGNAL TRANSDUCTION 12
1.5.5.1 *Phospholipase C* *15*
1.5.5.2 *Calcium* *15*
1.5.5.3 *Protein kinase C* *16*
1.5.5.4 *Phospholipase D* *16*
1.5.5.5 *Phospholipase A_2* *17*
1.5.5.6 *Tyrosine kinases* *17*
1.5.5.7 *Nuclear/mitogenic signaling mechanisms* *17*
1.5.5.8 *Nitric oxide and cGMP* *18*
1.5.5.9 *Adenylyl cyclase* *19*
1.5.6 FORMATION, DESENSITISATION AND INTERNALISATION OF RECEPTORS 19
1.5.7 RECEPTOR DOWN REGULATION 21
1.5.8 CLEARANCE OF ENDOTHELINS 21
1.5.9 FURTHER ENDOTHELIN RECEPTOR SUBTYPES 22
1.6 TRANSGENIC AND KNOCKOUT STUDIES OF THE ENDOTHELIN SYSTEM 23
1.6.1 ROLE OF ENDOTHELIN RECEPTORS DURING EMBRYOGENESIS 23
1.6.2 GENETIC KNOCKOUT OF ENDOTHELIN-1 24
1.6.3 TRANSGENIC OVEREXPRESSION OF ENDOTHELINS 25
1.6.4 CURRENT MODELS OF LOSS OF ET_B RECEPTOR FUNCTION 27
1.6.5 HETEROZYGOUS RECEPTOR KNOCKOUTS 30

1.7 CARDIOVASCULAR PHYSIOLOGY OF THE ENDOTHELIN SYSTEM 31
1.7.1 ROLE OF ENDOTHELIN IN THE MAINTENANCE OF VASCULAR TONE 31
1.7.2 THE RENAL ENDOTHELIN SYSTEM AND BLOOD PRESSURE REGULATION 32
1.7.2.1 *Renal tubular effects of ET-1* 33
1.7.2.2 *Renal vascular effects of ET-1* 34
1.7.3 AUTOCRINE AND PARACRINE SIGNALLING IN THE KIDNEY 35
1.7.4 ROLE OF ENDOTHELIN IN THE CENTRAL REGULATION OF BLOOD PRESSURE 36
1.8 ROLE OF ENDOTHELIN IN CARDIOVASCULAR PATHOPHYSIOLOGY 36
1.8.1 WHAT ROLE MAY ENDOTHELIN PLAY IN HYPERTENSION? 37
1.8.1.1 *Experimental models of hypertension involving endothelin* 38
1.8.1.2 *Salt sensitive models of hypertension* 39
1.8.1.3 *Mechanism of increased endothelin expression in hypertension* 40
1.8.1.4 *Vascular remodelling in hypertension* 41
1.8.1.5 *Pathological changes in receptor expression* 42
1.9 GENERAL AIMS 42

2 CHAPTER 2 47

2.1 MATERIALS AND METHODS 47
2.1.1 CONDITIONAL REGULATION OF GENE EXPRESSION 47
2.1.2 THE CRE/LOXP SYSTEM 47
2.1.3 TISSUE SPECIFIC KNOCKOUTS 48
2.1.3.1 *Endothelial cell-specific knockout* 49
2.1.4 CHEMICALS AND SOLUTIONS 49
2.1.5 PRIMERS 50
2.1.6 ENZYMES 54
2.1.7 BACTERIAL STRAINS 55
2.1.8 PROBES, PLASMIDS AND CLONING VECTORS 55
2.1.9 EMBRYONIC STEM CELLS 63
2.1.10 ANIMALS 64
2.1.11 MOLECULAR BIOLOGY METHODS 64
2.1.11.1 *Alkaline lysis miniprep* 64
2.1.11.2 *Large scale plasmid DNA preparation* 65
2.1.11.3 *Quantitation of Nucleic Acids* 66
2.1.11.4 *Sequencing of plasmids* 66
2.1.11.5 *Restriction digestion* 67
2.1.11.6 *Agarose gel electrophoresis* 67
2.1.11.7 *DNA fragment recovery from agarose gels* 68
2.1.11.8 *Ligation* 69
2.1.11.9 *Creating blunt ends for ligation* 69
2.1.11.10 *Dephosphorylation of DNA* 70
2.1.11.11 *Methods for cloning of PCR products* 70
2.1.11.12 *Klenow-Kinase-Ligase* 70
2.1.11.13 *TA Cloning® of PCR products* 71
2.1.11.14 *Preparation of electrocompetent cells* 71
2.1.11.15 *Transformation of E.Coli by electroporation* 72
2.1.11.16 *Colony and Plaque lifts* 73
2.1.11.17 *Preparation of random primed radio-labelled probes* 73
2.1.11.18 *Southern Blot Analysis* 74
2.1.12 SCREENING OF THE BACTERIOPHAGE λ 129/SV MOUSE GENOMIC DNA LIBRARY 75
2.1.12.1 *Preparation of plating bacteria* 75

2.1.12.2 *Plating of bacteriophage λ* ... 75
2.1.12.3 *Picking of bacteriophage λ plaques* ... 76
2.1.12.4 *Screening of bacteriophage λ plaques by in-situ hybridisation* ... 76
2.1.12.5 *Conversion of λ phage P to plasmid pλP* ... 77
2.1.13 TISSUE CULTURE METHODS ... 77
2.1.13.1 *Washing of ES cells* ... 78
2.1.13.2 *Passage of ES cells* ... 78
2.1.13.3 *Thawing of ES cells* ... 78
2.1.13.4 *Freezing of ES cells* ... 79
2.1.13.5 *Freezing of 24 well plates* ... 79
2.1.13.6 *Isolation of ES cell DNA* ... 80
2.1.13.7 *Electroporation of ES cells with pλPW and pλPW(NoDT)* ... 80
2.1.13.8 *Electroporation of targeted ES cells with Cre recombinase-expressing plasmid* ... 81
2.1.13.9 *Production of chimaeric mice* ... 82
2.1.13.10 *Preparation of genomic DNA from tail biopsy* ... 83
2.1.13.11 *Polymerase chain reaction of genomic DNA* ... 84
2.1.14 PHYSIOLOGICAL TECHNIQUES ... 85
2.1.15 WIRE MYOGRAPHY ... 85
2.1.15.1 *Dissection of the mouse aorta and trachea* ... 85
2.1.15.2 *Mounting of aortic and tracheal rings* ... 85
2.1.15.3 *Aortic and Tracheal wake up protocol* ... 87
2.1.15.4 *Preparation of stock solutions* ... 87
2.1.16 BLOOD PRESSURE MEASUREMENT IN CONSCIOUS ANIMALS ... 88
2.1.17 ET-1 BINDING EXPERIMENTS ... 89
2.1.17.1 *Isolation of pulmonary endothelial cell-enriched populations from murine lung tissue* ... 89
2.1.17.2 *Preparation of Biotinylated Griffonia simplicifolia isolectin B4 (GSL I-B4)-coated magnetic beads* ... 89
2.1.18 ANALYSIS OF RESULTS ... 89

3 CHAPTER 3 ... 91

3.1 IDENTIFICATION, CLONING AND PARTIAL SEQUENCING OF PλP ... 91
3.1.1 INTRODUCTION ... 91
3.1.2 METHODS ... 91
3.1.2.1 *PCR amplification of the mouse ET_B receptor gene* ... 91
3.1.2.2 *Cloning of PCR products* ... 92
3.1.2.3 *Construction of a 129/SV mouse genomic DNA library* ... 92
3.1.2.4 *Probes utilised for screening of the λPS 129/SV genomic DNA library* ... 93
3.1.2.5 *Primary and secondary screening of λPS 129/SV genomic DNA library* ... 93
3.1.2.6 *Subcloning of λP into pλP* ... 94
3.1.2.7 *Sequencing and mapping of pλP* ... 94
3.1.3 RESULTS ... 95
3.1.3.1 *PCR amplification of genomic DNA* ... 95
3.1.3.2 *TA cloning® of PCR products* ... 95
3.1.3.3 *Primary and secondary screens of λPS phage library* ... 99
3.1.3.4 *Sequencing of pλP* ... 101
3.1.4 DISCUSSION ... 105

4 CHAPTER 4 ... 106

4.1 DESIGN AND CONSTRUCTION OF THE TARGETING VECTORS PλPW AND PλPW(NODT) ... 106
4.1.1 INTRODUCTION ... 106

4.1.1.1 *Structure of targeting vectors* *106*
4.1.2 METHODS 107
4.1.2.1 *PCR amplification of exons 2 and 3 of the ET_B receptor gene* *107*
4.1.3 PREPARATION OF PλP2-3 108
4.1.3.1 *Preparation of the $LoxP^2ROSA26$ vector* *110*
4.1.3.2 *Cloning of M230F/584R PCR product into $LoxP^2ROSA$ vector* *110*
4.1.4 PREPARATION OF PλP2-3LTNL 110
4.1.4.1 *Isolation of the Xba I fragment of pLTNL* *112*
4.1.4.2 *Preparation of the pλP2-3 vector* *112*
4.1.4.3 *Cloning of Xba I fragment of pLTNL into the pλP2-3 vector* *112*
4.1.4.4 *Destruction of the 5' Xba I site of PλP2-3LTNL* *113*
4.1.5 PREPARATION OF 3' HOMOLOGY ARM 113
4.1.5.1 *Preparation of pλP4-5* *115*
4.1.5.2 *Isolation of the diphtheria toxin gene cassette from pCAGGS-dt* *115*
4.1.5.3 *Preparation of pλP4-dt* *116*
4.1.5.4 *Preparation of pλP2-3LTNL4-dt* *118*
4.1.5.5 *Preparation of pλP2-5LTNL* *118*
4.1.6 PREPARATION OF 5' HOMOLOGY ARM 120
4.1.6.1 *Addition of a Xho Ilinker site to pλP* *120*
4.1.6.2 *Preparation of pλPW and pλPW(NoDT)* *121*
4.1.7 RESULTS 124
4.1.7.1 *Preparation of pλP2-3* *124*
4.1.7.2 *Further analysis of pλP2-3 by restriction digestion mapping* *125*
4.1.7.3 *Direct sequencing of pλP2-3* *126*
4.1.7.4 *Preparation of pλP2-3LTNL* *129*
4.1.7.5 *Destruction of the 5' Xba I site of PλP2-3LTNL* *129*
4.1.7.6 *Preparation of pλP4-5* *130*
4.1.7.7 *Preparation of pCAGGS-dt in pSP72 poly1* *131*
4.1.7.8 *Preparation of pλP4-dt* *132*
4.1.7.9 *Preparation of pλP2-3LTNL4-dt* *133*
4.1.7.10 *Preparation of pλP2-5LTNL* *134*
4.1.7.11 *Addition of Xho I linker site to pλP* *135*
4.1.7.12 *Preparation of pλPW and pλPW(NoDT)* *137*
4.1.8 DISCUSSION 138

5 CHAPTER 5 142

5.1 TARGETING OF THE ET_B RECEPTOR GENE ALLELE AND GERMLINE TRANSMISSION OF THE FLOXED ET_B RECEPTOR ALLELE 142
5.1.1 INTRODUCTION 142
5.1.1.1 *Screening strategies for the detection of homologous recombination events in ES cells* *143*
5.1.1.2 *PCR screening strategy for the detection of recombination events in ES cells* *143*
5.1.1.3 *Southern blot screening strategy for the detection of 3' recombination events* *146*
5.1.1.4 *Screening strategy to identify recombination-mediated removal of the selection cassette from homologously targeted ES cell clones* *147*
5.1.1.5 *Screening strategy for the analysis of 5' recombination events in gancyclovir-resistant clones* *149*
5.1.1.6 *Generation of homozygous 'floxed' ET_B receptor mice* *149*
5.1.2 METHODS 150
5.1.2.1 *Electroporation of ES cells* *150*
5.1.2.2 *Selection of G418-resistant ES cell colonies* *150*
5.1.2.3 *Picking of G418-resistant ES cell colonies* *150*

5.1.2.4 *PCR screening of G418-resistant ES cell colonies following targeting with pλPW or pλPW(NoDT)* 151
5.1.2.5 *3' Southern blot of clones identified by PCR screen* 151
5.1.2.6 *Transient transfection of targeted clones with pMC-Cre* 151
5.1.2.7 *PCR screening of gancyclovir-resistant clones for the presence of the 3' loxP site* 152
5.1.2.8 *PCR screening of gancyclovir-resistant clones for the presence of the 5' loxP site* 152
5.1.2.9 *Generation of chimaeric mice* 153
5.1.3 RESULTS 153
5.1.3.1 *PCR screen of G418-resistant ES cell colonies following targeting with pλPW* 153
5.1.3.2 *PCR screen of G418-resitant ES cell colonies following targeting with either pλPW or pλPW(NoDT)* 154
5.1.3.3 *3' Southern blot of homologously targeted clones identified by PCR screen* 155
5.1.3.4 *Gancyclovir selection of clones following transient transfection with pMC-Cre* 156
5.1.3.5 *PCR screen of gancyclovir-resistant clones for removal of the LTNL selection cassette and presence of the 3' loxP site* 157
5.1.3.6 *PCR screen of gancyclovir-resistant clones for the presence of the 5' loxP site* 158
5.1.3.7 *Sequence of 5' and 3' loxP sites* 159
5.1.3.8 *Generation of chimaeric mice and analysis of progeny* 162
5.1.4 DISCUSSION 163

6 CHAPTER 6 168

6.1 REDUCED ^{125}I ET-1 BINDING TO ENDOTHELIAL CELLS FROM FLOX/FLOX TIE2 MICE 168
6.1.1 INTRODUCTION 168
6.1.1.1 *Endothelial cell specific knockout of the ET_B receptor* 168
6.1.2 METHODS 171
6.1.2.1 *Genotyping of founder and offspring mice* 171
6.1.2.2 *Genotyping for the Tie2Cre transgene* 172
6.1.2.3 *Isolation of pulmonary endothelial cell-enriched populations from murine lung tissue* 173
6.1.2.4 *Pulmonary endothelial cell ^{125}I ET-1 binding* 173
6.1.2.5 *Measurement of plasma ET-1* 173
6.1.3 RESULTS 174
6.1.3.1 *Genotyping of offspring* 174
6.1.3.2 *Genotype and phenotype of piebald mice* 176
6.1.3.3 *Pulmonary EC ^{125}I ET-1 binding* 177
6.1.3.4 *Plasma ET-1 concentration* 178
6.1.4 DISCUSSION 179

7 CHAPTER 7 186

7.1 ENDOTHELIAL CELL SPECIFIC KNOCKOUT OF THE MOUSE ET_B RECEPTOR RESULTS IN SALT-INSENSITIVE HYPERTENSION AND IMPAIRED VASODILATATION TO ET_B RECEPTOR AGONISTS AND ACETYLCHOLINE 186
7.1.1 INTRODUCTION 186
7.1.2 METHODS 188
7.1.2.1 *In vivo measurement of blood pressure* 188
7.1.2.2 *In vitro vascular responses of aortic and tracheal rings* 189
7.1.2.3 *Isolated aortic rings* 189

7.1.2.4 *Tracheal rings* *190*
7.1.2.5 *Analysis of results* *194*
7.1.3 RESULTS 195
7.1.3.1 *In vivo blood pressure* *195*
7.1.3.2 *Aortic vasoconstriction to NE* *196*
7.1.3.3 *Aortic vasodilatation to ACh* *198*
7.1.3.4 *Effect of acute ET_B receptor inhibition upon aortic vasodilatation to ACh* *199*
7.1.3.5 *Aortic vasodilatation to deta/NO* *200*
7.1.3.6 *Aortic vasoconstriction to NE following inhibition of NOS* *201*
7.1.3.7 *Aortic vasodilatation to S6c* *202*
7.1.3.8 *Tracheal constriction to S6c* *204*
7.1.3.9 *Tracheal constriction to carbachol* *204*
7.1.4 DISCUSSION 206

8 CHAPTER 8 214

8.1 CONCLUSIONS 214
8.1.1 GENERATION OF FLOXED ET_B RECEPTOR MICE AND MICE FEATURING ENDOTHELIAL CELL-SPECIFIC ET_B RECEPTOR DOWN-REGULATION 215
8.1.2 RECOMBINATION-MEDIATED REMOVAL OF EXONS 2 AND 3 OF THE ET_B RECEPTOR GENE IS SUFFICIENT TO PREVENT EXPRESSION OF FUNCTIONAL ET_B RECEPTORS 217
8.1.3 ET-1 BINDING BY PULMONARY EC IS SIGNIFICANTLY DECREASED IN FLOX/FLOX TIE2 MICE 218
8.1.4 AORTIC VASODILATATION TO ET_B RECEPTOR AGONISTS IS IMPAIRED IN FLOX/FLOX TIE2 MICE 219
8.1.5 FUNCTIONAL EXPRESSION OF SMOOTH MUSCLE CELL ET_B RECEPTORS IS MAINTAINED IN FLOX/FLOX TIE2 MICE 220
8.1.6 ENDOTHELIAL CELL-SPECIFIC ET_B RECEPTOR KNOCKOUT MICE DEMONSTRATE IMPAIRED ACETYLCHOLINE-INDUCED AORTIC VASODILATATION AND DECREASED BIOAVAILABILITY OF NITRIC OXIDE 221
8.1.7 ENDOTHELIAL CELL-SPECIFIC ET_B RECEPTOR KNOCKOUT MICE EXHIBIT HYPERTENSION THAT IS UNAFFECTED BY INCREASING DIETARY SALT 223
8.1.8 PATHOPHYSIOLOGY OF HYPERTENSION IN ENDOTHELIAL CELL ET_B RECEPTOR-DEFICIENT MICE 224
8.1.9 PLASMA ET-1 CONCENTRATION IS INCREASED FOLLOWING DOWN-REGULATION OF ENDOTHELIAL CELL ET_B RECEPTORS 225
8.2 LIMITATIONS OF THE CURRENT STUDY 226
8.2.1 GENETIC BACKGROUND 226
8.2.2 CRE-LOXP APPROACHES TO CONDITIONAL GENE EXPRESSION 227
8.2.3 INCREASE IN PLASMA ET-1 228
8.2.4 EFFECT OF ENDOTHELIAL CELL-SPECIFIC ET_B RECEPTOR DEFICIENCY UPON GLOMERULAR FILTRATION RATE 229
8.2.5 COMPENSATORY EFFECTS OF OTHER BLOOD PRESSURE REGULATORY PATHWAYS 230
8.3 SUMMARY 230

9 BIBLIOGRAPHY 232

10 APPENDIX 249

10.1 AUTORADIOGRAPHIC STUDIES 249
10.1.1 METHODS 249
10.1.2 RESULTS 249

Tables and figures

FIGURE 1.1 2
FIGURE 1.2 4
FIGURE 1.3 14
FIGURE 2.1 51
FIGURE 2.2 52
FIGURE 2.3 53
FIGURE 2.4 57
FIGURE 2.5 58
FIGURE 2.6 59
FIGURE 2.7 60
FIGURE 2.8 61
FIGURE 2.9 62
FIGURE 2.10 63
FIGURE 2.11 87
FIGURE 3.1 95
FIGURE 3.2 97
FIGURE 3.3 99
FIGURE 3.4 100
FIGURE 3.5 102
FIGURE 3.6 103
FIGURE 3.7 104
FIGURE 4.1 109
FIGURE 4.2 111
FIGURE 4.3 114
FIGURE 4.4 117
FIGURE 4.5 119
FIGURE 4.6 122
FIGURE 4.7 123
FIGURE 4.8 124
FIGURE 4.9 125
FIGURE 4.10 126
FIGURE 4.11 127
FIGURE 4.12 128
FIGURE 4.13 130
FIGURE 4.14 131
FIGURE 4.15 132
FIGURE 4.16 133
FIGURE 4.17 134
FIGURE 4.18 135
FIGURE 4.19 136
FIGURE 4.20 136
FIGURE 4.21 137
FIGURE 4.22 138
FIGURE 5.1 145
FIGURE 5.2 146
FIGURE 5.3 148
FIGURE 5.4 154
FIGURE 5.5 156
FIGURE 5.6 158
FIGURE 5.7 159
FIGURE 5.8 160
FIGURE 5.9 161
FIGURE 5.10 163
FIGURE 6.1 170

FIGURE 6.2 172
FIGURE 6.3 175
FIGURE 6.4 176
FIGURE 6.5 177
FIGURE 6.6 178
FIGURE 6.7 179
FIGURE 7.1 191
FIGURE 7.2 192
FIGURE 7.3 193
FIGURE 7.4 194
FIGURE 7.5 196
FIGURE 7.6 197
FIGURE 7.7 198
FIGURE 7.8 199
FIGURE 7.9 200
FIGURE 7.10 201
FIGURE 7.11 202
FIGURE 7.12 203
FIGURE 7.13 205
FIGURE 7.14 206
FIGURE 10.1 250

TABLE 1.1 8
TABLE 2.1 54
TABLE 5.1 155
TABLE 5.2 157

List of abbreviations

1K/1C	1 Kidney 1 clip
2K/1C	2 kidney 1 clip
A192621	(2R, 3R, 4S)-2-(4-propoxy-phenyl)-4-(1,3-benzodioxol-5-yl)-1-(N-[(2,6-diethylphenyl]ace-tamido)pyrrolidine-3-carboxylate, nitrogen
ACh	Acetylcholine
Ang II	Angiotensin II
ANOVA	Analysis of variance
ANP	Atrial natriuretic peptide
ApoE	Apolipoprotein E
AQ2	Aquaporin 2 promoter
ATP	Adenosine triphosphate
AVP	Arginine vasopressin
bp	Base pairs
BSA	Bovine serum albumin
CAIP	Calf Intestinal Alkaline Phosphatase
cAMP	Cyclic adenosine monophosphate
CCT	Cortical collecting tubule
cDNA	Copy deoxyribonucleic acid
cGMP	Cyclic guanosine monophosphate
CHO	Chinese Hamster Ovary
CMV	Cytomegalovirus
CNS	Central nervous system
Cpm	Counts per minute
Cre	Cre recombinase
DAG	sn1,2-diacylglycerol
dATP	Deoxyadenine triphosphate
DβH	Dopamine ß-hydroxylase promoter
dCTP	Deoxycytosine triphosphate
Deta/NO	2,2'-(hydroxynitrosohydrazono)bis-ethanimine
dGTP	Deoxyguanine triphosphate
DIA/LIF	Differentiation Inhibiting Activity/Leukaemia Inhibitory Factor
DMSO	Dimethyl sulfoxide
DNA	Deoxyribonucleic acid
dNTP	Deoxynucleotide triphosphate
DOCA	Deoxycorticosterone acetate
DT	Diphtheria toxin
dTTP	Deoxythymine triphosphate
EC	Endothelial cell
ECE	Endothelin converting enzyme
EDTA	Ethylene dinitrilo-tetra-acetate
EGF	Epidermal growth factor
ENaC	Epithelial sodium channel
eNOS	Endothelial nitric oxide synthase

ES	Embryonic stem cell
ET	Endothelin
ET_A	Endothelin receptor type A
ET_B	Endothelin receptor type B
ET_C	Endothelin receptor type C
FAK	Focal adhesion kinase
FCS	Foetal calf serum
Flox	Floxed ET_B receptor allele
g	Gravity
G418	Neomycin
GFP	Green fluorescent protein
GFR	Glomerular filtration rate
GPCR	G-protein coupled receptor
GSL I-B4	Griffonia simplicifolia isolectin B4
IL	Interleukin
IMCD	Inner medullary collecting duct
IP_3	Inositol 1,4,5-triphosphate
JAK	Janus kinase
Kb	kilobases
KKL	Klenow-Kinase-Ligase
L-Broth	Luria-Bertani medium
L-NAME	N^G-nitro-L-arginine methyl ester
L-NMMA	L-N^G-monomethyl arginine
LTNL	loxP-thymidine kinase-neomycin-loxP
M	Molar
MAP	Mean arterial pressure
MAPK	Mitogen activated protein kinase
mRNA	Messenger ribonucleic acid
NE	Nor-epinephrine
NeoR	Neomycin resistance
NEP	Neutral endopeptidase
nNOS	Neuronal nitric oxide synthase
NO	Nitric Oxide
NOS	Nitric oxide synthase
OD	Optical density
PA	Phosphatidic acid
PBS	Phosphate buffered saline
pCO_2	Partial pressure of carbon dioxide
PCR	Polymerase chain reaction
PDGF	Platelet derived growth factor
PG	Prostaglandin
PIP_2	Phosphatidylinositol 4,5-bisphosphonate
PKC	Protein kinase C
PLA_2	Phospholipase A_2
PLC	Phospholipase C

PLD	Phospholipase D
PNK	Polyneucleotide kinase
pO_2	Partial pressure of oxygen
PSS	Physiological saline solution
PT	Proximal tubule
RAAS	Renin angiotensin aldosterone system
RBF	Renal blood flow
RIA	Radioimmunoassay
RNA	Ribonucleic acid
RSNA	Renal sympathetic nerve activity
RVR	Renal vascular resistance
s	Piebald allele
S6c	Sarafotoxin 6c
SDS	Sodium dodecyl sulphate
SHR	Spontaneously hypertensive rat
SHR-SP	Spontaneously hypertensive rat-stroke prone
sl	Spotting lethal allele
SMC	Smooth muscle cell
SM-MHC	Smooth muscle myosin heavy chain promoter
STAT	signal transducers and activators of transcription
Tie2	Tie2 promoter/enhancer Cre transgene
TK	Thymidine kinase
TNF	Tumour necrosis factor
TPR	Total peripheral resistance
TVP	Trypsin
UHP	Ultra high purity
UV	Ultra-violet
v/v	Volume per volume
VSMC	Vascular smooth muscle cell
W	Wild type ET_B receptor allele
w/v	Weight per volume

Acknowledgements

I would like to thank my supervisors Professor David Webb and Dr Yuri Kotelevtsev for their untiring help over the duration of this project. Yuri was responsible for the planning, inception and execution of the project and has provided constant support and inspiration. The project could have faltered at many hurdles were it not for his resourcefulness and keen intelligence. I aspire to achieve his level of scientific analysis and rigour. David Webb brought me to Edinburgh for this project and has not faltered in his intellectual and practical support ever since. I hope to repay his faith in me by achieving the same high standards he sets for himself in my future work and career. Fiona Gulliver-Sloan was responsible for training me in the technique of wire myography and completed the *in vitro* sarafotoxin 6c aortic vasodilatation experiments. Dr Nick Kelland was responsible for all *in vivo* surgical procedures and performed all measurements of blood pressure in mice following high salt diet. The completion of this project would not have been possible were it not for the monumental effort of Fiona and Nick and their assistance is greatly appreciated. I am indebted to Nina Kotelevtsev who was responsible for performing the extensive sequencing experiments required for this project. I am also grateful for all the support and advice given over the years by the remaining members of our laboratory, not least Adele Gordon, Mark Miller, Isam Sharif, Gillian Gray and Ian Megson. Finally, I would like to thank Anna Beattie and my parents for their unceasing support and encouragement throughout.

Abstract

INTRODUCTION AND AIMS

Studies in humans and animals have demonstrated the importance of the endothelin (ET) system in the regulation of vascular tone, blood pressure and renal haemodynamics (Gariepy *et al.*, 2000, Haynes and Webb, 1994, King *et al.*, 1989). Two receptors, termed ET_A and ET_B, mediate the cardiovascular and renal effects of the endothelins. The ET_B receptor has multiple roles in different cell types, including vasodilatation (Takayanagi *et al.*, 1991), vasoconstriction (Sumner *et al.*, 1992), inhibition of renal sodium reabsorption (Gariepy *et al.*, 2000) and clearance of ET-1 (Fukuroda *et al.*, 1994). Each of these responses may independently modulate blood pressure and regional blood flow. However, the relative importance of each response to the complex homeostatic mechanisms of blood pressure control, particularly under conditions of high salt intake, has yet to be determined. Currently available selective ET_B receptor antagonists are unable to block ET_B receptors in individual cell types without also causing blockade of ET_B receptors expressed elsewhere. The aim of this project was to precisely determine the role of the EC ET_B receptor in the regulation of vascular tone, blood pressure and clearance of ET-1.

METHODS

To examine the phenotypical effects of loss of EC ET_B receptor signalling without the confounding effects of ET_B receptor blockade, or loss, in other cell types, I utilised Cre-LoxP technology to conditionally regulate ET_B receptor expression. Mice featuring loxP sites flanking exons 2 and 3 of the ET_B receptor gene (floxed ET_B receptor mice) were generated by standard gene targeting techniques in embryonic stem cells. Floxed ET_B mice were crossed with Tie2-Cre transgenic mice to produce mice in which recombination-mediated removal of ET_B receptor coding regions was limited to EC and cells of the haematopoietic lineage (Flox/Flox Tie2). EC ET_B receptor binding of ^{125}I ET-1 and *in vitro* aortic and tracheal ring myography was performed to assess endothelial function and the response to selective ET_B receptor agonists. Blood pressure was measured under conscious, unrestrained

conditions via in-dwelling carotid catheters in male mice aged 8-16 weeks fed for 21 days with either a normal (0.76% NaCl) or high (7.6% NaCl) salt diet. Plasma ET-1 was measured by radioimmunoassay. Wild type (W/W -/-) and single transgenic littermates were used as controls in experiments.

RESULTS

Pulmonary EC ET-1 binding was decreased by ~80% in EC-specific ET_B receptor knockout mice (cpm/50 μg membrane protein ± SEM; Flox/Flox Tie2 581 ± 67; W/W -/- 3175 ± 268; n = 3; $p<0.001$). Cell-specificity of ET_B receptor down-regulation was demonstrated by maintenance of normal ET_B receptor-mediated tracheal constriction. Blood pressure was increased in Flox/Flox Tie2 mice (MAP 137.2 ± 6.4 mmHg (n = 5); W/W -/-, 113.7 ± 4.7 mmHg (n = 6; $p<0.05$) but was not affected by dietary salt. Plasma ET-1 was increased ~4 fold following EC ET_B receptor down-regulation (mean plasma [ET-1] pg/ml ± SEM; Flox/Flox Tie2 12.40 ± 2.95; W/W -/- 2.94 ± 0.83; n = 6; $p<0.001$). Aortic rings from Flox/Flox Tie2 mice demonstrated impaired endothelium dependent vasodilatation to ET_B receptor selective agonists and acetylcholine but normal endothelium-independent vasodilatation.

CONCLUSIONS

Recombination-mediated removal of exons 2 and 3 of the ET_B receptor is sufficient to prevent expression of functional ET_B receptors. The 'floxed' ET_B receptor mouse thereby facilitates the cell type-specific down-regulation of ET_B receptor expression *in vivo*. The EC ET_B receptor plays an important role in the determination of blood pressure under normal physiological conditions. The mechanism underlying this effect may involve loss of EC ET_B receptor-mediated vasodilatation or impaired clearance of ET-1 with a consequent increase in ET_A receptor activity. In contrast to global ET_B receptor deficiency however, maintenance of ET_B receptor signalling in non-EC is sufficient to prevent salt-sensitive hypertension. The EC ET_B receptor may contribute to the clearance of ET-1 from the circulation

1 Chapter 1

1.1 INTRODUCTION

ET-1 is a local hormone and growth factor widely known for its potent vasoconstrictor effects. ET-1 was originally isolated and characterised by Yanagisawa and colleagues (Yanagisawa *et al.*, 1988) from the culture media of aortic EC. Subsequently, two further isoforms, termed ET-2 and ET-3, were identified. The endothelin family share structural homology with the sarafotoxins, 4 potent cardiotoxic peptides isolated from the venom of *Atractaspis engaddensis*. Each of the mature isoforms of endothelin are 21 amino acid peptides with rigid 3-dimensional structures stabilized by two disulphide bonds. A highly conserved C-terminal sequence is mandatory for biological function of the peptide. The structure of these peptides is illustrated in Figure 1.1. ET-1 is the predominant isoform involved in cardiovascular regulation and is the only isoform produced constitutively by EC (Inoue *et al.*, 1989). The rapid development of selective endothelin receptor antagonists has led to an explosion of research into the physiological and pathophysiological roles of the endothelins. This work has demonstrated the potential for pharmacological manipulation of the endothelin system in a range of cardiovascular conditions, including hypertension, congestive cardiac failure, renal failure and pulmonary hypertension.

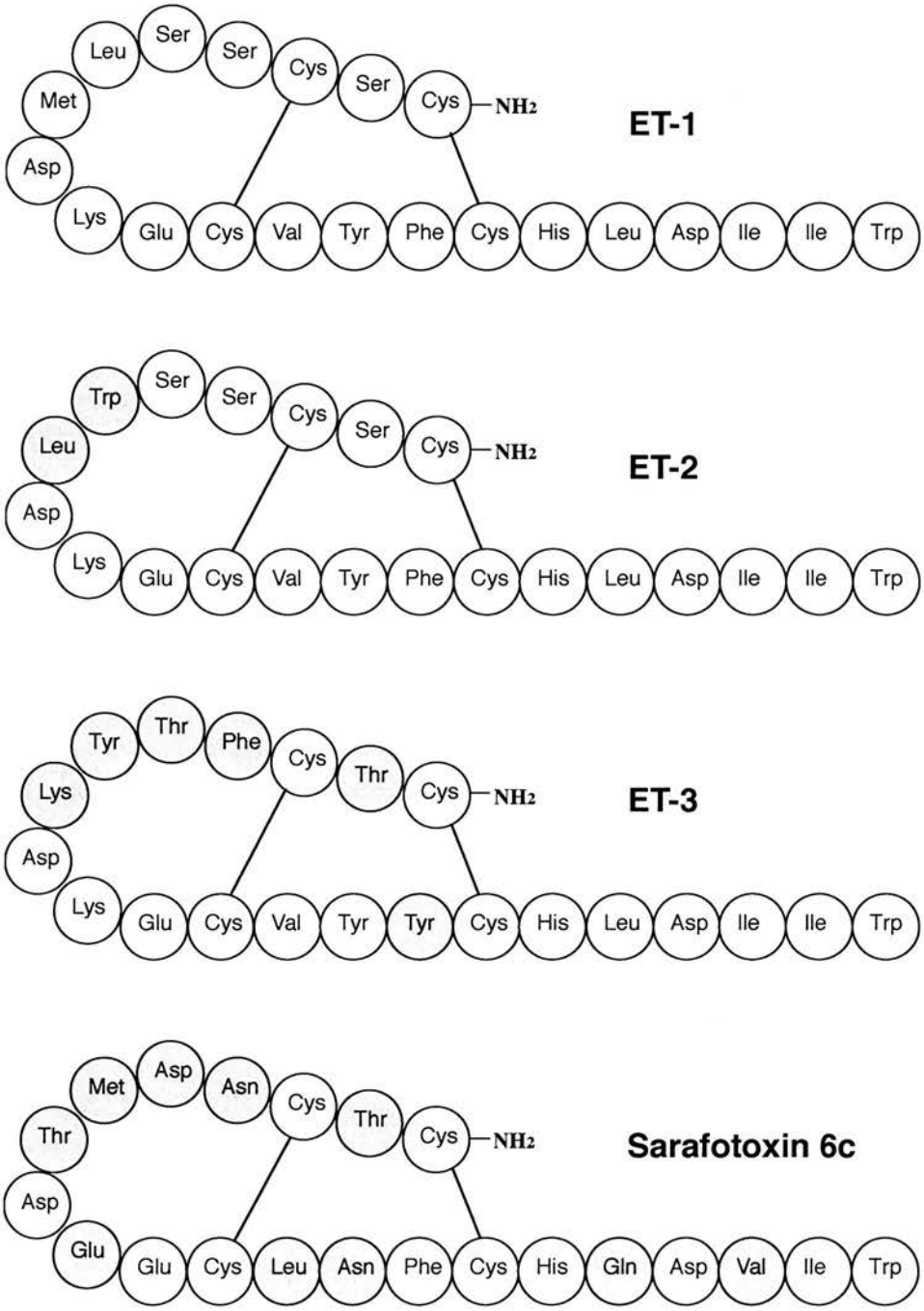

Figure 1.1

Structure of the endothelin family of peptides, and the related snake venom peptide sarafotoxin S6c. Shaded amino acids indicate differences from endothelin-1.

1.2 ENDOTHELIN GENERATION

The human genes for ET-1, ET-2 and ET-3 are located on chromosomes 6, 1 and 20, respectively. Regulation of ET-1 synthesis is determined primarily at the level of transcription of the preproET-1 gene through phorbol-ester-sensitive *c-fos* and *c-jun* complexes (Inoue *et al.*, 1989). Other regulatory sequences located in the upstream (5') promoter region include binding sites for GATA-2 (Dorfman *et al.*, 1992), AP-1 and nuclear factor-1 (Benatti *et al.*, 1994) and a hexanucleotide sequence (Inoue *et al.*, 1989). These sites regulate basal levels of gene transcription and responses to angiotensin II (Ang II), transforming growth factor β and acute phase reactants, respectively (Inoue *et al.*, 1989). Synthesis of ET-1 may also be regulated by post-transcriptional mechanisms. The non-translated 3' region of preproET-1 mRNA contains 'suicide motifs' that may permit its selective destabilisation (Inoue *et al.*, 1989). These motifs determine the short (~15 minute) half-life of preproET-1 mRNA and thereby prevent excessive ET-1 production. Factors known to promote ET-1 production include thrombin, insulin, cyclosporine, epinephrine, Ang II, cortisol, inflammatory mediators, hypoxia and vascular shear stress. ET-1 production is inhibited by NO, NO donor drugs and dilator prostanoids via an increase in cellular cyclic guanosine monophosphate (cGMP), and natriuretic peptides via an increase in cyclic adenosine monophosphate (cAMP) levels (Gray, 1995). The factors affecting ET-1 generation and the synthetic pathways involved are illustrated in Figure 1.2

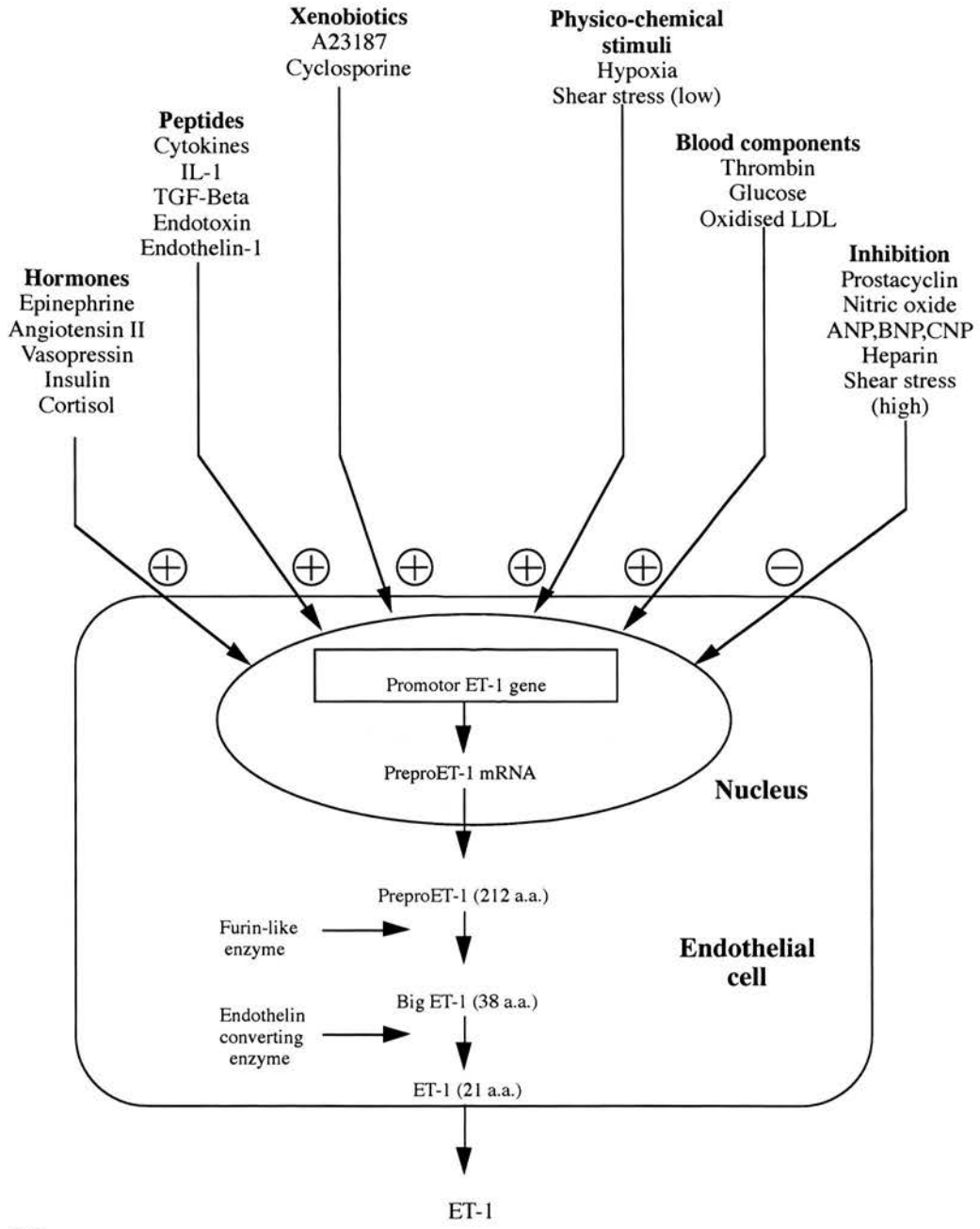

Figure 1.2

Factors that influence ET-1 synthesis and the pathway for ET-1 generation. IL-1 = interleukin-1; TGFβ = transforming growth factor β; LDL = low density lipoprotein; ANP, BNP, CNP = atrial, brain and c-type natriuretic peptides.

The mature ET-1 peptide is generated by sequential enzymatic cleavage of the initial 203 amino acid preproET-1 peptide. A short hydrophobic secretory sequence is first removed to produce proET-1. Cleavage at dibasic amino acid pairs by the endopeptidase furin then generates the 38 amino acid peptide 'big ET-1' (Yanagisawa *et al.*, 1988). Subsequent production of mature ET-1 by a proteolytic cleavage between Trp^{21} and Val^{22} is catalysed by the metalloprotease endothelin-converting enzyme-1 (ECE-1). Recently, a further endothelin peptide has been identified in humans formed by the cleavage of big ET-1 at the Tyr^{31} and Gly^{32} bonds by a human chymase enzyme expressed in mast cells. This product has been termed $ET\text{-}1_{1\text{-}31}$ and has been shown to produce vasoconstriction of airway smooth muscle (Nakano *et al.*, 1997), although its physiological relevance remains unknown.

1.3 ENDOTHELIN CONVERTING ENZYME

ECE-1 was isolated and purified by Ohnaka and colleagues (Ohnaka *et al.*, 1990) from aortic EC. ECE-1 is inhibited by the combined ECE and neutral endopeptidase (NEP) inhibitor phosphoramidon, but not by selective NEP inhibitors such as thiorphan or kelatorphan. The ECE protein is a transmembrane dimer consisting of two 758 amino acid peptide chains linked by a single disulfide bridge. A short (1-56) N-terminal intracellular region is followed by a 21 amino acid transmembrane region. A zinc-binding and catalytic site (595-599) is essential for enzymatic activity. ECE-1 belongs to the Neprilysin family of zinc endopeptidases that also includes NEP and the human Kell blood group protein (Xu *et al.*, 1994). However, ECE is unique in this group in that it recognises a relatively long C-terminal portion of big ET-1 (residues His^{27} to Gly^{34}) in addition to the cleavage site between residues 21 and 22 (Takayanagi *et al.*, 1998). Additional ECE isoforms have been identified in animals (ECE-2 and ECE-3), but only ECE-1 and ECE-2 have been demonstrated in humans (Russell and Davenport, 1999). ECE gene knockout indicates that ECE-1 is the major functional ECE for all three endothelin isoforms, but the presence of mature ET-1 in ECE-1 knockout embryos suggests some degree of redundancy (Yanagisawa *et al.*, 1998). ECE-2 may be

distinguished from ECE-1 by a requirement for a lower pH for optimum activity. It is postulated that ECE-2 is involved in the constitutive pathway of ET-1 release from acidic secretory vesicles and may be particularly important under stress conditions such as ischaemia when the intracellular pH is low (Russell and Davenport, 1999). Combined knockout of both ECE-1 and ECE-2 results in cardiac malformations, indicating a further role for ECE-2 during development (Yanagisawa *et al.*, 2000). ECE-3 has currently only been identified in bovine species where it is selective for the cleavage of bigET-3 (Hasegawa *et al.*, 1999).

The human ECE-1 gene is located on chromosome 1 at the p36 band (Valdenaire *et al.*, 1995). Four splice variants have been identified, termed ECE-1a to ECE-1d. These isoforms differ in structure only at the N-terminus where di-leucine motives may determine the distinct subcellular locations of these isoforms (Valdenaire *et al.*, 1999). In humans, ECE-1c is the predominant isoform, although the relative proportions of each may vary in different tissues. Changes in the isoform expression pattern may further occur in pathophysiological states including atherosclerosis (Davenport and Kuc, 2000). However, controversy still exists concerning the precise sub-cellular locations of each isoform. This has potentially important implications for the design and delivery of pharmacological antagonists of these enzymes. Current opinion suggests that the majority of ECE-1a is found in the plasma membrane, that ECE-1b is exclusively intracellular and ECE-1c is found both in the cytoplasm and at the cell membrane (Valdenaire *et al.*, 2001). However, Barnes and colleagues (Barnes *et al.*, 1998) have demonstrated that in EC, ECE-1 cycles between the Golgi apparatus, cytoplasmic vesicles and the plasma membrane. They propose that ECE-1 is directed into secretory vesicles wherein it generates mature ET-1 from big ET-1 during the passage to the plasma membrane. Following release of ET-1, ECE-1 is re-cycled to the Golgi network via endosomes.

Transfection studies have confirmed that endogenously generated ET-1 secreted abluminaly is the most functionally important source of ET-1. Co-transfection of preproET-1 and ECE-1b genes into cultured cells has shown that ECE-1b expressed at

the cell surface is relatively inefficient at proteolysis of exogenous big ET-1, with only around 10% converted to ET-1. In contrast, between 50-90% of the endothelin peptides secreted by the cells were in the mature ET-1 form (Xu *et al.*, 1994), suggesting significant intracellular ECE-1b activity. This data supports a predominantly autocrine/paracrine mechanism of action for ET-1, a theory given further credence by the low (<5pM) circulating concentration of ET-1 in humans, concentrations probably insufficient to activate endothelin receptors. The concentration of Ang II and atrial natriuretic peptide (ANP) in plasma is normally up to ten times that of circulating ET-1. Also, ET-1 has a half-life of less than five minutes in plasma, with clearance occurring mainly in the lungs and liver (Fukuroda *et al.*, 1994). It is likely that much higher concentrations of ET-1 occur at the junctions between EC and VSMC and that at least some of the plasma ET-1 represents overspill from this site.

1.4 SECRETION OF ENDOTHELIN-1

The secretion of ET-1 may occur by both constitutive and regulated pathways. Russell and colleagues (Russell *et al.*, 1998) have demonstrated the presence of ET-1 immuno-reactivity in both cytoplasmic secretory vesicles and EC-specific storage granules. Whilst constitutive ET-1 secretion is likely to originate from secretory vesicles, storage granules that are sensitive to $[Ca^{2+}]_i$ and mechanical stretch may provide a mechanism of regulated ET-1 release. ECE-1 expression has been co-localised to these granules and the release of mature ET-1 in response to calcium ionophores has been demonstrated *in vitro* (Russell *et al.*, 1998).

1.5 ENDOTHELIN RECEPTORS

Pharmacological analysis of receptor binding suggested the existence of at least two endothelin receptor types in humans, termed ET_A and ET_B. This has been confirmed by molecular characterisation of the receptors (Arai *et al.*, 1990, Sakamoto *et al.*, 1991, Sakurai *et al.*, 1990). The ET_A receptor binds its endogenous ligands with the rank order of affinity ET-1>ET-2>ET-3. The ET_B receptor has equal affinity for each of the

endothelin isoforms. ET_A receptors are located on VSMCs (Arai *et al.*, 1990, Hori *et al.*, 1992) and, when activated, produce a sustained vasoconstriction that is of slow onset. In contrast, ET_B receptors are located on both EC (Takayanagi *et al.*, 1991) and VSMC (Roubert *et al.*, 1991, Sumner *et al.*, 1992). Activation of ET_B receptors on EC causes vasodilatation (Takayanagi *et al.*, 1991) through the release of dilator mediators acting on VSMC, whilst activation of ET_B receptors on VSMC produces vasoconstriction directly (Moreland *et al.*, 1992, Sumner *et al.*, 1992, Williams *et al.*, 1991). The agonist binding characteristics of the endothelin receptors are shown in Table 1.1.

	ET_A	ET_B	
Agonist Potency	ET-1>ET-2>>ET-3	ET-1=ET-2=ET-3	
Tissue	Vascular smooth muscle	Endothelium All vessels	Vascular smooth muscle Resistance and Capacitance vessels
Action	Vasoconstriction	Vasodilatation	Vasoconstriction
Selective Agonists	None	ET-3 (600-fold specific) Sarafotoxin 6c (30000-fold specific)	
Selective Antagonists	A147627, BQ-123	A192621, BQ-788	

Table 1.1

1.5.1 ENDOTHELIN RECEPTOR GENES

The human ET_A gene is located on chromosome 4 and consists of eight exons and seven introns spanning 40 kilobases (kb) (Hosoda *et al.*, 1992). The human ET_B gene on chromosome 13 is somewhat smaller in size, spanning 24 kb and consisting of seven exons and six introns (Arai *et al.*, 1993). In the mouse, the ET_A and ET_B receptor genes are located on chromosomes 8 and 14, respectively (Hosoda *et al.*, 1994, Hosoda *et al.*,

1992). Analysis of cDNA clones predicts an ET_A receptor 427 amino acids in length and an ET_B receptor consisting of 442 amino acids. The sequence homology of these receptor subtypes is ~58%. In a manner analogous to the preproET-1 gene, both the ET_A and ET_B receptor genes have promoter regions which control gene transcription levels in response to factors including nuclear factor-1, nuclear factor kappa-β, RNA polymerase II transcription factor and acute phase response proteins (Arai *et al.*, 1993). The transcription factors AP-1, GATA-2 and CCAAT/enhancer- binding protein (C/EBP) have additionally been shown to regulate ET_B receptor expression in VSMCs (Wagner *et al.*, 2000). Blockade of the interaction between transcription factors and *cis* regulatory promoter regions markedly inhibits gene transcription. Decoy oligonucleotides containing sequences from the ET_A receptor gene promoter region were able to competitively bind a nuclear protein and down-regulate ET_A promoter activity by 75%. Local environmental factors that mediate changes in transcription factor availability may also be able to markedly up or down-regulate receptor expression. Such mechanisms may underlie changes in the number or subtype of receptors expressed by a cell in certain pathological states. For example, Wang and colleagues (Wang *et al.*, 1996) quantitatively and temporally examined mRNA expression following angioplasty of the rat carotid artery. They demonstrated a 30-fold increase in ET_A receptor mRNA 3 days post-angioplasty. ET_B receptor mRNA increased earlier, with a 15-fold induction on day 1. ECE-1 mRNA and preproET-1 mRNA increased 2-fold. This data suggests that the increased expression of ET-1 and of ET_A and ET_B receptors plays an active role in the pathogenesis of angioplasty-induced neointima formation. Furthermore, the local environmental factors that regulate gene expression show quantitative and temporal differences in their influence upon promoter activity of these genes.

1.5.2 DISTRIBUTION OF ENDOTHELIN RECEPTORS

Autoradiography using labelled ET-1 and in situ hybridization has allowed the qualitative and quantitative assessment of both the tissue distribution and the receptor subtype expressed in various tissues and cell lines. Such analysis has demonstrated the

localisation of ET_A receptors predominantly to the VSMCs of large and medium-sized arteries, the highest densities being found in the aorta. In addition, renal arterioles, bronchial SMC and glandular tissues, such as those of the pituitary and adrenal glands, have been shown to preferentially express ET_A receptors (Arai *et al.*, 1990). In contrast, EC are devoid of ET_A receptors (Hosoda *et al.*, 1991). ET_B receptors are found on both VSMC and EC in the vasculature. ET_B receptors are also expressed on glial, striatal, ependymal and choroid plexus cells within the brain and also in the trachea, lung, myocardium, liver, kidney, bowel and adrenal glands. Human kidneys express ET_B receptors as the predominant receptor subtype, with the collecting ducts exhibiting the highest density of ET_B receptors (Hori *et al.*, 1992). A detailed analysis of the distribution of renal ET receptor expression is provided later in section 1.7.3. Human cardiac tissue expresses both ET_A and ET_B receptors throughout the A-V node, His-bundle, myocardium and endocardium (Molenaar *et al.*, 1993).

1.5.3 STRUCTURE OF ENDOTHELIN RECEPTORS

ET_A and ET_B receptors belong to the 7 transmembrane G-protein-coupled receptor superfamily. The consensus ET receptor topology includes three extracellular domains, three intracellular loops and a cytoplasmic COOH-terminal tail, separated by seven hydrophobic helical regions thought to span the lipid bilayer (reviewed by (Rubanyi and Polokoff, 1994). The ET_A and ET_B receptor transmembrane domains and the interconnecting cytoplasmic loops are highly conserved, in contrast to the N-terminal region, which shows only 4% sequence homology between the receptor subtypes (Elshourbagy *et al.*, 1993). Similarly, there is almost no homology between the ET_A and ET_B receptor in the COOH- terminal region (Sakurai *et al.*, 1990, Takagi *et al.*, 1995). Site directed mutagenesis studies and receptor chimeras have each been utilised to determine the structural determinants of receptor function, described below.

1.5.3.1 *N-terminus*

The role of the NH_2-terminal region in ligand binding remains controversial. However, the Asp^{75} and Pro^{93} in this region of the ET_B receptor are thought to be responsible for the high stability of the complex formed between ET-1 and the ET_B receptor, compared to the ET_A receptor (Takasuka *et al.*, 1994). Each ET receptor cDNA contains 2 consensus sequences for N-linked glycosylation of the NH_2-terminal region (Asn-X-Ser), though data on the carbohydrate content of purified receptors is lacking.

1.5.3.2 *Transmembrane and extracellular domains*

Endothelin receptors contain several important ligand interaction subdomains. A 5 amino acid sequence in the second extracellular region of the ET_A receptor is the most important for ligand binding. However, ligand selectivity is determined by the third and fourth extracellular regions and their flanking transmembrane regions (Adachi *et al.*, 1993). Amino acids at the boundary between the first extracellular loop and the second transmembrane domain are essential for binding of the selective ET_A receptor antagonist BQ-123, whist the Lys^{140} in this region is required for the high affinity binding of ET-1 to the ET_A receptor (Adachi *et al.*, 1994). In ET_B receptors, transmembrane domains 4 to 6 and the adjacent loop regions are permissive of the high affinity binding of ET_B receptor agonists (Sakamoto *et al.*, 1993).

1.5.3.3 *Cytoplasmic loops*

The cytoplasmic loops are known to mediate receptor/guanine nucleotide regulatory protein (G-protein) coupling in other rhodopsin-like G protein receptors. Substitution of the C-terminal end of the third cytoplasmic domain with the corresponding section of the β_2-adrenoceptor results in no changes in the affinity of the ET_A receptor for ET-1, but receptor/ligand binding fails to elicit the subsequent rise in intracellular calcium ($[Ca^{2+}]_i$) that normally follows receptor activation (Adachi *et al.*, 1993). The precise structural regions of the receptor that determine G-protein coupling are discussed later in section 1.5.5.

1.5.3.4 *C-terminus*

The COOH-terminal amino acids show marked sequence diversity between ET receptor subtypes. However, a conserved Cys-Leu-Cys-Cys-X-Cys sequence is found close to the end of the seventh transmembrane domain. This region is postulated to mediate correct membrane anchoring via palmitoylation (Roos *et al.*, 1998, Rubanyi and Polokoff, 1994).

1.5.4 POST TRANSLATIONAL MODIFICATION OF ENDOTHELIN RECEPTORS

Both ET_A and ET_B receptors contain regions that may undergo post-translational modification with subsequent alteration of linkage to intracellular effector mechanisms. Most ET_B receptors are phosphorylated at $Ser^{304, 418, 439, 440, 441}$ and palmitoylated at Cys^{402} and Cys^{404}, although non-phosphorylated receptors are also seen (Roos *et al.*, 1998). A $Ser^{304}Asn$ mutation has been identified in patients with Hirschsprung's disease (Auricchio *et al.*, 1996). Loss of phosphorylation at this site may, therefore, critically affect ET_B receptor signal transduction. Differential patterns of post-translational modification may also provide a mechanism for the observation of two distinct ligand affinities of ET_B receptors in the rat brain (Sokolovsky *et al.*, 1992). Palmitoylation of conserved COOH-terminal Cys residues selectively regulates signal transduction by ET_A receptors (Horstmeyer *et al.*, 1996). Replacement of Cys residues with non-palmitoylated serine or alanine residues did not alter ligand binding affinity or stimulation of adenylyl cyclase activity. However, ET-1-induced increases in $[Ca^{2+}]_i$ and phospholipase C activity were abolished by this mutation. The ET_B receptor also contains highly conserved palmitoylated Cys residues in its COOH-terminus suggesting that these may also regulate signal transduction.

1.5.5 SIGNAL TRANSDUCTION

Binding of ET-1 to the ET_A receptor on VSMCs initiates a complex cascade of events resulting in a biphasic rise in $[Ca^{2+}]_i$, and ultimately, cellular contraction. Typically, the

contractions induced by ET-1 develop slowly but are sustained and resistant to agonist removal. These effects are mediated by the interaction of endothelin receptors with specific G-proteins in the cell membrane (Bitar *et al.*, 1992) and subsequent activation of downstream second messengers. G-proteins consist of 3 non-identical subunits and are involved in receptor signal transduction for a wide variety of cellular processes. Evidence from G-protein inhibitors such as *Bordatella pertussis* toxin and subunit-specific antisera suggest that the endothelin receptors can interact with at least 3 different G_{α}-proteins to activate downstream pathways. ET_A and ET_B receptor coupling to phospholipase C (PLC) probably occurs via $G_{\alpha q}$, whilst coupling to adenylate cyclase occurs via $G_{\alpha s}$ in VSMCs (ET_A receptors) and $G_{\alpha i}$ in EC (ET_B receptors) (Rubanyi and Polokoff, 1994). The third and fourth intracellular loops and the COOH-terminal tail of the ET_B receptor contain sequences for the specific binding of the $G\alpha_i$ subtype, whilst the second intracellular loop binds the $G\alpha_s$ subtype (Masaki, 2000). The second messenger systems activated by ET receptor/G-protein signalling are summarised below and illustrated in Figure 1.3. The precise signalling mechanisms utilised by the ET_A and ET_B receptors may exhibit subtle differences, although a consensus opinion in this area is awaited (Douglas and Ohlstein, 1997).

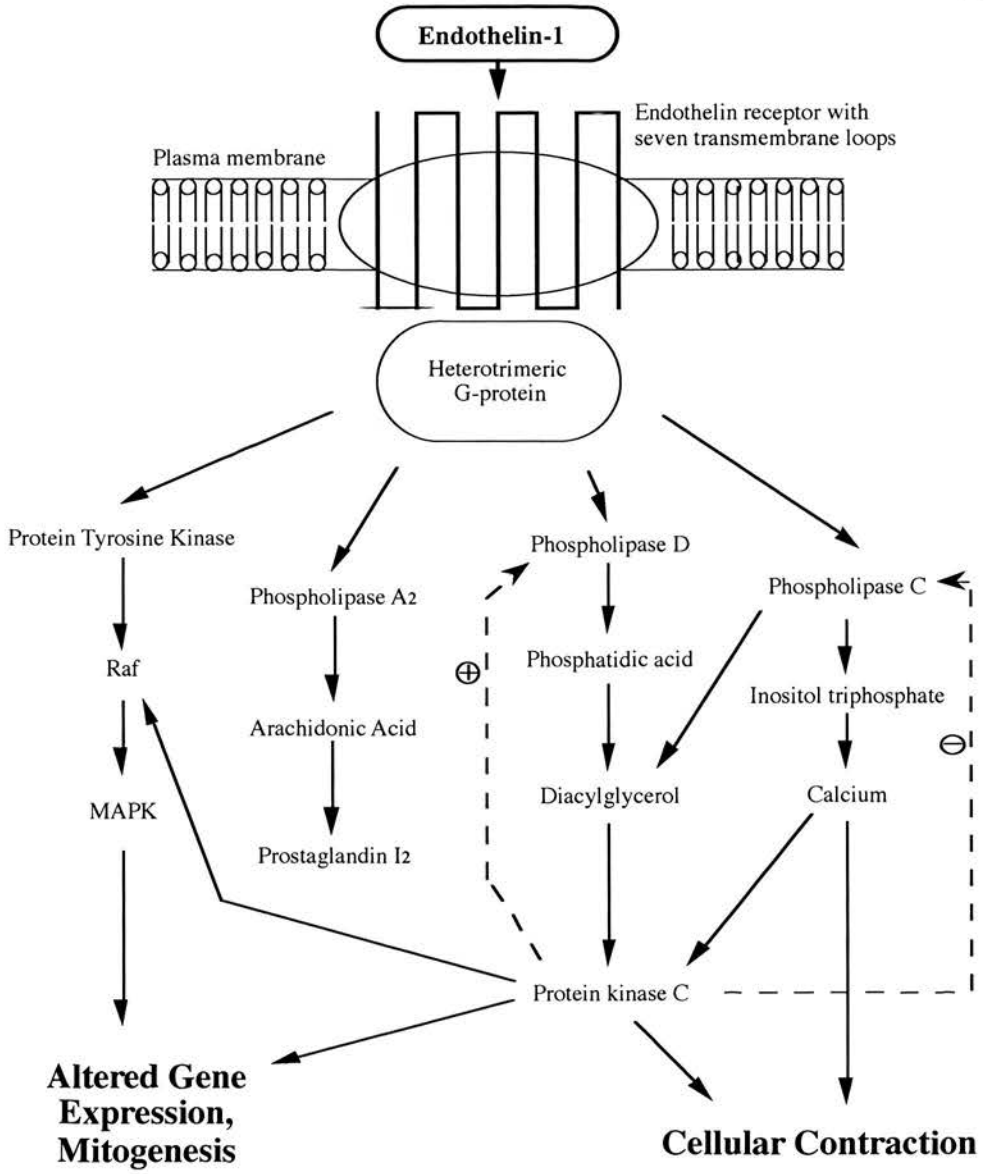

Figure 1.3

Signal transduction pathways of the endothelin receptors. MAPK = mitogen activated protein kinase. Adapted from Decker & Brock, 1998 with kind permission of the authors. See text for details.

1.5.5.1 *Phospholipase C*

$G_{\alpha q}$-protein stimulated activation of PLC (Masaki, 2000) causes hydrolysis of phosphatidylinositol 4,5-bisphosphonate (PIP_2) to produce inositol 1,4,5-triphosphate (IP_3) and *sn*1,2-diacylglycerol (DAG). The rise in IP_3 concentration stimulates release of Ca^{2+} from the sarcoplasmic reticulum via both ryanodine- and IP_3-sensitive Ca^{2+} channels and is responsible for the rapid initial rise in $[Ca^{2+}]_i$ seen following ET-1 (Marsden *et al.*, 1989). DAG activates protein kinase C (PKC) allowing sensitisation of the cellular contractile elements to changes in $[Ca^{2+}]_i$ (see below).

1.5.5.2 *Calcium*

Endothelin receptor activation results in a rapid initial rise in $[Ca^{2+}]_i$ followed by a plateau phase dependent on the presence of extracellular Ca^{2+}. However, although usual, a rise in cellular IP_3 via PLC activation is not mandatory to increase $[Ca^{2+}]_i$. ET-3 and S6c acting on ET_B receptors appear to cause an IP_3-independent rise in $[Ca^{2+}]_i$ in VSMC wherein both the initial and plateau phases of Ca^{2+} mobilisation are dependent on movement of Ca^{2+} into the cell (Little *et al.*, 1992). Entry of extracellular Ca^{2+} appears to be necessary for the sustained increase in $[Ca^{2+}]_i$ that permits prolonged cellular contraction in response to ET-1. Both voltage operated and receptor operated calcium channels are involved in this process. L-type calcium channel blockers (dihydropyridine class) attenuate the sustained rise in $[Ca^{2+}]_i$ by antagonism of voltage operated calcium channels. Prolonged cellular contraction may also be prevented by nickel ions, which selectively block receptor-operated channels. The T-type calcium channel is a putative candidate for the receptor operated channel (Stasch and Kazda, 1989). The opening of voltage dependent L-type calcium channels is dependent upon prolonged membrane depolarisation. The precise mechanism for achieving and maintaining such a period of membrane depolarisation remains controversial but is likely to involve calcium-activated chloride channels with resultant efflux of chloride ions (James *et al.*, 1994), and/or an influx of cations through non-selective cation channels. Other candidates for the mediators of the increased $[Na^+]_i$ that produces membrane depolarisation include ATP-

sensitive K^+ channels, the Na^+/K^+-ATPase, or activation of the Na^+/H^+ antiporter (Danthuluri and Brock, 1990, Meyer-Lehnert *et al.*, 1989, Miyoshi *et al.*, 1992).

1.5.5.3 *Protein kinase C*

PKC exists in multiple isoforms and is one of the key regulatory enzymes involved in the ET-1 signalling process. Activation of endothelin receptors stimulates a rise in DAG levels that, along with phosphatidylserine and Ca^{2+}, results in the activation and translocation of PKC from the cytosol to membranes within VSMC. Activated PKC then catalyses the phosphorylation of heavy and light myosin chains along with caldesmons, thereby increasing the sensitivity of the contractile elements to $[Ca^{2+}]_i$ (Nishimura *et al.*, 1992). Specific PKC inhibitors block the sustained contractile responses to ET-1 and reduce Ca^{2+} sensitivity. PKC also modulates the hydrolysis of PIP_2 following activation of endothelin receptors by exerting an inhibitory effect on PLC and may form part of a negative feedback loop controlling PLD and arachidonic acid metabolism. The mitogenic effects of ET-1 appear to be related to both PKC- and tyrosine kinase-dependent mechanisms.

1.5.5.4 *Phospholipase D*

The rise in intracellular DAG levels in response to ET-1 occurs in a biphasic manner, the initial rise resulting from PIP_2 hydrolysis by PLC. The prolonged secondary rise in DAG levels is thought to originate from phosphatidylcholine hydrolysis mediated by PLD and lasts for up to 20 minutes. Activation of PLD occurs via PKC-dependent and PKC-independent mechanisms (Liu *et al.*, 1992). The phosphatidic acid (PA) produced enhances Ca^{2+} influx and further enhances PLC activity (Shukla and Halenda, 1991). It is proposed that PLD activation may contribute to the mitogenic effects of ET-1 (Boarder, 1994).

1.5.5.5 *Phospholipase A_2*

Phospholipase A_2 (PLA_2) catalyses the generation of arachidonic acid metabolites including the leukotrienes, thromboxane A_2 (TxA_2) and prostacyclin (PGI_2) from membrane lipids. Inhibitors of the arachidonic acid metabolism cascade have been shown to inhibit many of the actions of ET-1, and PGI_2 production by EC can be stimulated by ET-1. Linkage of endothelin-receptors to PLA_2 may be direct via a G-protein, or occur in response to ET-1-activated changes in $[Ca^{2+}]_i$ (Barnett *et al.*, 1994).

1.5.5.6 *Tyrosine kinases*

ET-1-induced tyrosine phosphorylation of cellular proteins modulates activation of PLD and in part regulates its mitogenic effects. Stimulation of ET_A receptors results in phosphorylation of tyrosine residues on cytosolic proteins ranging in size from 45-225 kDa by members of the tyrosine kinase family known as Src, focal adhesion kinase (FAK) and Janus kinase (JAK). Although the precise mechanisms are as yet unknown, it seems likely that activation of transcription factors by these kinases in response to ET-1 stimulation are involved in the mitogenic response.

1.5.5.7 *Nuclear/mitogenic signaling mechanisms*

Alone, ET-1 is a weak mitogen, as measured by thymidine incorporation or expression of the proto-oncogenes c-*jun* and c-*fos*. However, when combined with other growth factors such as platelet derived growth factor (PDGF) and epidermal growth factor (EGF) or co-mitogens such as insulin, it acts synergistically to produce marked mitogenic effects (reviewed by (Rubanyi and Polokoff, 1994). As indicated earlier, a precise mechanistic model is still awaited, but both phorbol ester-sensitive PKCs and tyrosine kinase signal transduction mechanisms are involved. PKCs, activated by the binding of ET-1 to its receptor, initiate the c-Raf-1 cascade leading to activation of mitogen activated protein kinases (MAPKs). MAPKs are known to be critically important in the transduction of mitogenic signals in a number of other growth factor systems. Where the mitogenic response pathways of ET-1 differ from those of other

growth factors, however, is in the proposed coupling of the activated ET_A receptor to the c-Raf-1 cascade via PKC. ET-1 activation of the tyrosine kinases Src, FAK and JAK occurs in a non-PKC dependent manner. Their activation may result in the switching on of transcription factors of the signal transducers and activators of transcription family (STAT) and subsequent translocation of STATs to the nucleus where they interact with promoter regions to initiate gene transcription (Decker and Brock, 1998). The study of the mitogenic responses to ET-1 is currently in its infancy when compared to that of other aspects of endothelin physiology. However, the similarities in the effector mechanisms utilised in response to ET-1 and other growth factors provide interesting parallels. ET_A and ET_B receptor activation is also known to increase the expression of cellular adhesion molecules, induce chemotactic factors such as TNFα, IL-1β, IL-6, and IL-8, and alter matrix synthesis (Douglas and Ohlstein, 1997). Thus, in addition to short-term actions upon cellular contractility, the endothelin isoforms influence cellular growth and differentiation, a process critically linked with the proposed role of ET-1 as a mediator of vascular hypertrophy and cardiac remodelling seen in conditions such as hypertension and chronic cardiac failure.

1.5.5.8 *Nitric oxide and cGMP*

The ET_B receptor present on EC is responsible for vasodilatation in response to activation by ET-1. This effect is produced by ET_B receptor-stimulated release of the vasodilator factors NO (Tsukahara *et al.*, 1994) and PGI_2. Recently, ET_B receptor activation has also been shown to modulate the release of the vasodilator peptide adrenomedullin (Jougasaki *et al.*, 1999). Activation of ET_B receptor-coupled G-proteins leads to an increase in PLC activity with generation of IP_3 and DAG. These release Ca^{2+} from intracellular stores (see above) with a resultant increase in the activity of the constitutive Ca^{2+}/calmodulin-dependent endothelial NO synthase enzyme (eNOS). Liberated NO diffuses to the VSMC layer and initiates production of cGMP by soluble guanylate cyclase. Increasing levels of cGMP activate mechanisms that ultimately decrease $[Ca^{2+}]_i$ leading to cellular relaxation (Lincoln, 1989). Inhibition of eNOS by L-N^G-monomethyl arginine (L-NMMA) has been shown to inhibit the vasodilatation that

follows ET_B receptor stimulation. Further mechanisms of NO production have been proposed. These include a PKC-dependent pathway and direct production of cGMP via activation of a pertussis toxin-insensitive G-protein by ET-1 on the kidney epithelial cell line LLC-PK1 (Ozaki *et al.*, 1994).

1.5.5.9 *Adenylyl cyclase*

ET-1 may directly inhibit the accumulation of cAMP induced by forskolin, cholera toxin and isoproterenol in EC (Ladoux and Frelin, 1991). It is at present unclear whether the effects of ET-1 on cyclic nucleotide levels are mediated directly via adenylyl cyclase or indirectly as a result of PLC activation. However, in LLC-PK1 cells, ET-1-stimulated inhibition of cAMP accumulation was sensitive to *pertussis* toxin, suggesting that this effect is mediated by a *pertussis* toxin-sensitive G-protein (Ozaki *et al.*, 1994). Interestingly, in Chinese Hamster Ovary (CHO) cells expressing ET_A receptors, ET-1 binding was followed by $G\alpha_s$-mediated activation of adenylyl cyclase. In contrast, ET_B receptor activation resulted in $G\alpha_i$-mediated inhibition of this enzyme (Masaki, 2000).

1.5.6 FORMATION, DESENSITISATION AND INTERNALISATION OF RECEPTORS

Bolus injection of ET-1 results in a brief period of vasodilatation mediated by ET_B receptors, followed by a sustained ET_A-mediated vasoconstriction that resists agonist removal by prolonged washout (Spokes *et al.*, 1989). This characteristic pattern of vasodilatation and vasoconstriction to ET-1 is a product of the receptor/ligand binding relationship, the signal transduction mechanisms thereby induced and the subsequent processes of receptor/ligand desensitisation and degradation. Saturation of ET_A receptors occurs within one minute of exposure to ET-1 at 37°C (Marsault *et al.*, 1991). Once bound, the binding of ET-1 to its receptors appears to be a 'pseudo-irreversible' process, with a dissociation half-life in excess of 100 hours (reviewed by (Douglas and Ohlstein, 1997). Prior to this, the rate of dissociation of receptor and ligand are dependent upon the duration of exposure, with studies using radiolabelled ET-1 showing a progressive

decline in the proportion of dissociable ET-1 over 60 minutes (Wilkes and Boarder, 1991). Dissociable ET-1 is thought to represent the presence of surface bound/non-internalised receptor complexes.

The mechanism of inactivation of receptor signalling following agonist binding is controversial but may be receptor subtype-specific. Following agonist binding in CHO cells, phosphorylation and deactivation of ET_B receptor signalling occurs within 5 minutes, as measured by IP_3 generation. In contrast, the ET_A receptor is resistant to ligand-induced phosphorylation and signalling is maintained for over 20 minutes (Cramer *et al.*, 1999). The kinetics of internalisation for each subtype is identical and hence likely to be independent of phosphorylation. Thus, it is proposed that ET_A receptors are slowly inactivated by internalisation, whilst ET_B receptors are rapidly inactivated by ligand-induced phosphorylation (Cramer *et al.*, 1999). This difference in inactivation kinetics may underlie the classical vasodilator/vasoconstrictor response to bolus ET-1. However, both ET_A and ET_B receptor phosphorylation by G-protein coupled receptor kinases has been demonstrated in other cell types and shown to modulate signalling (Freedman *et al.*, 1997). The role of receptor phosphorylation as a mediator of receptor desensitisation, therefore, awaits further clarification.

Agonist binding by ET_B receptors is followed by receptor complex internalisation by a clathrin-mediated endocytic pathway (Oksche *et al.*, 2000). In contrast, ET_A receptors are internalised via caveolae (Chun *et al.*, 1995). This process occurs within 6 minutes for both ET_A and ET_B receptors (Cramer *et al.*, 1999) suggesting that ET_A receptor-mediated signalling may still continue following internalisation. Indeed, studies in CHO cells have demonstrated the presence of internalised but undegraded ET-1/ET_A receptor complexes for up to 2 hours (Chun *et al.*, 1995). Once internalised, separation of the ET-1/endothelin-receptor complex is thought to occur within lysosomes where the local acidic environment favours dissociation. Re-cycling of receptors back to the cell surface then occurs for ET_A (Marsault *et al.*, 1993), but not ET_B receptors (Oksche *et al.*, 2000), perhaps due to a greater resistance of the ET-1/ET_B complex to acid degradation within the lysosome. Reappearance of ET_B receptors at the

cell surface is, therefore, dependent upon *de novo* receptor synthesis. These studies provide a mechanism for the observed tachyphylaxis of ET_B-mediated vasodilatation to repeat bolus ET-1 injection in the face of a relatively preserved ET_A-mediated vasoconstrictor response (Le Monnier de Gouville *et al.*, 1990). Degradation of receptor complexes by neutral endopeptidases located within the plasma membrane may also occur prior to internalisation (Loffler *et al.*, 1991).

1.5.7 RECEPTOR DOWN REGULATION

Repeated exposure of VSMC to ET-1 results in the down-regulation of receptors without a change in their affinity. This is manifest as a progressive decrease in tissue or cellular responsiveness (Hirata *et al.*, 1988). This phenomenon occurs in response to both exogenous and endogenously produced endothelins and receptor downregulation is agonist selective. Pre-treatment of cells with the ET_B receptor-selective agonist S6c results in the loss of further ET_B receptor-agonist-mediated responses, but the response to ET_A receptor agonists is preserved (Henry, 1993). Repeated stimulation with ET-1 may also lead to the heterologous desensitisation of other receptor subtypes including the insulin receptor (Ishibashi *et al.*, 2001) and neurokinin receptor (Cyr *et al.*, 1997) as a result of depletion of common downstream signalling pathways.

1.5.8 CLEARANCE OF ENDOTHELINS

Removal of circulating ET-1 occurs predominantly in the lung and liver, and to a lesser extent, in the kidneys and intestine. This process is mediated by ET_B receptors (Fukuroda *et al.*, 1994). Enzymatic degradation of ET-1 occurs by several different protease pathways, of which neutral endopeptidase is considered to be most important in the kidney (Kohan, 1997). In common with other peptide hormones, clearance is achieved by receptor-mediated endocytosis of bound peptide. This action may be blocked by selective ET_B receptor antagonists (Fukuroda *et al.*, 1994). Following ET_B receptor blockade, circulating concentration of ET-1 increases in proportion to both the dose and the affinity of the antagonist for the ET_B receptor (Willette *et al.*, 1998). This

process is independent of ET_B receptor-mediated NO production. Antagonism of the ET_B receptor may, therefore, produce adverse physiological consequences. In isolated rat coronary arteries ET_B antagonist-mediated increases in ET-1 concentrations were able to stimulate ET_A receptors and provoke coronary vasoconstriction (Brunner and Doherty, 1996).

1.5.9 FURTHER ENDOTHELIN RECEPTOR SUBTYPES

Two further subtypes of endothelin receptor have been isolated in *Xenopus laevis* but not from mammalian species. The first of these receptor subtypes, termed ET_{AX}, displays agonist binding characteristics identical to the ET_A receptor but is insensitive to the selective ET_A receptor antagonist BQ-123 (Kumar *et al.*, 1994). The second, isolated only from *Xenopus laevis* melanocytes, has a greater binding affinity for ET-3 than ET-1 and may represent a third morphological receptor subtype termed ET_C (Karne *et al.*, 1994). The *Xenopus* ET_C receptor cDNA has been isolated and characterised. The predicted amino acid sequence shares 50% homology with the human ET_A and ET_B receptors. Further analysis of human genomic DNA with cDNA probes of low stringency has, as yet, failed to identify any other homologous sequences. Any putative human ET-3-selective ET_C receptor would, therefore, be likely to have a structure that differs widely from the other endothelin receptors (Sakamoto *et al.*, 1991).

Sub-division of the ET_B receptor subtype has also been proposed. This stems from the observation that activation of ET_B receptors may produce either vasodilatation or vasoconstriction. Vasodilatation in response to ET_B receptor stimulation is mediated by ET_B receptors located on vascular EC through the production of NO and dilator prostanoids (Takayanagi *et al.*, 1991). In contrast, vasoconstrictor responses are mediated directly by ET_B receptors located on VSMC (Moreland *et al.*, 1992, Sumner *et al.*, 1992, Williams *et al.*, 1991). However, despite reports that production of two receptor subtypes from a single gene is possible by varying transcription initiation sites or post-translational modification (Shyamala *et al.*, 1993), it is more likely that these differing responses are due to differences in signal transduction pathways within the

effector cell. There is currently no molecular evidence to support subdivision of ET_B receptors. Pharmacological differences in the responses of ET_A receptors in various tissues to antagonists such as BQ-123 have also been demonstrated (Sudjarwo *et al.*, 1994). This has led to suggestions that subtypes of the ET_A receptor may also exist though, again, validation by molecular studies has not been forthcoming.

1.6 TRANSGENIC AND KNOCKOUT STUDIES OF THE ENDOTHELIN SYSTEM

1.6.1 ROLE OF ENDOTHELIN RECEPTORS DURING EMBRYOGENESIS

Targeted gene knockout studies have provided further insight into the multiple physiological roles of the endothelin isoforms. Studies originally conceived to examine the physiological effects of deletion of the genes for ET-1, ECE-1 and the ET_A and ET_B receptors in the adult animal revealed a developmental role for the endothelins. Mouse embryonic stem cells manipulated to carry a non-functional ET-1 allele were utilised to produce ET-1 null mice (ET-1 (-/-)). Homozygous mutation was lethal and characterised by abnormalities of the craniofacial and pharyngeal pouch structures. These structures are derived from neural crest ectomesenchymal cells indicating that ET-1 is crucially involved in the normal ontogeny of the pharyngeal arches (Kurihara *et al.*, 1994). Targeted disruption of the ECE-1 gene produces identical phenotypic abnormalities of the craniofacial structures, as does deletion of the ET_A receptor gene. Deletion of the ET_B receptor or ET-3 gene produces mice characterised by aganglionic megacolon and coat colour spotting (Hosoda *et al.*, 1994). The ET_B receptor/ET-3 interaction, therefore, appears to be critical for the normal migration of epidermal melanocytes and enteric neurons. An elegant series of experiments utilising tetracycline-inducible ET_B receptor transgenes has demonstrated that the critical time period for maintenance of ET_B/ET-3 signalling occurs between embryonic days 10 and 12.5 (Shin *et al.*, 1999). Additionally, ECE-1 knockout mice include the phenotype of ET-3/ET_B knockout mice, suggesting

that ECE-1 is functionally responsible for the conversion of bigET-3 to ET-3 (Baynash *et al.*, 1994).

Mis-sense and nonsense mutations of the human ET_B receptor gene have been documented in the neurocristopathies associated clinically with Hirschsprung's disease (Puffenberger *et al.*, 1994) and the Waardenburg-Shah syndrome (Attie *et al.*, 1995) - both of which are varieties of aganglionic megacolon. The results of endothelin receptor knockout studies have obvious implications for the clinical use of ET_A or ET_B receptor antagonists and ECE-inhibitors, rendering them unsuitable for use during pregnancy or at the time of conception, corresponding abnormalities having been detected in teratogenicity studies with endothelin antagonists in animals.

1.6.2 GENETIC KNOCKOUT OF ENDOTHELIN-1

Mice homozygous for deletion of the ET-1 gene develop a lethal phenotype as described earlier. Interestingly, mice heterozygous (ET-1 (+/-)) for this gene deletion are hypertensive (Kurihara *et al.*, 1994), at odds with the predicted role of ET-1 as a potent pressor agent. ET-1 (+/-) mice produce ~ 60% of the wild type concentrations of ET-1 and are morphologically normal. The expression of ET-2, ET-3 and of endothelin receptors were unaffected by knockout of ET-1 (Maemura *et al.*, 1995). Thus, compensation by redundant expression of the remaining endothelin isoforms and/or receptor upregulation could not explain this phenotype. Similarly, abnormal renal ET-1 signalling was thought unlikely to be responsible since administration of a high salt diet had no increased effect on blood pressure in ET-1 (+/-) mice and changes in urine volume and urinary sodium excretion were not significantly different between wild type and heterozygous mice. However, on the high salt diet renal ET-1 content was suppressed by a further 50% in ET-1 (+/-) mice (Morita *et al.*, 1998).

Interestingly, ET-1 (+/-) mice were found to have a lower arterial pO_2 and a higher arterial pCO_2 than wild type littermates. This was proposed to reflect a disturbance of central cardiorespiratory control, leading ultimately to an increase in mean arterial pressure (MAP) through an increase in sympathetic drive (Kuwaki *et al.*,

1996). Measurement of renal sympathetic nerve activity (RSNA) in anaesthetised heterozygotes confirmed an up-regulation of basal nerve activity and demonstrated an upward resetting of the baroreceptor-mediated relationship between MAP and RSNA (Ling *et al.*, 1998). In addition, heterozygotes had attenuated RSNA responses to hypercapnia but normal responses to hypoxia. The low arterial pO_2, therefore, appears to stimulate an increase in sympathetic activity leading to increased blood pressure. The upward resetting of the MAP-RSNA relationship is permissive of the hypertensive state. The precise mechanism underlying the decrease in arterial pO_2 is unknown but is likely to involve altered ET-1/ET_A signalling in central chemoreceptor areas, since ET_B receptor knockout mice have normal arterial pO_2 and normal ventilatory responses to hypercapnia (Clouthier *et al.*, 1998). The effect on MAP of maintaining normoxia in heterozygous ET-1 knockout mice awaits further investigation.

1.6.3 TRANSGENIC OVEREXPRESSION OF ENDOTHELINS

Transgenic overexpression of a gene of interest can provide a powerful tool for the investigation of the physiological and pathophysiological role of the expressed peptide. This strategy has been employed to investigate the functional role of ET-1 and ET-2 and has provided a number of novel insights. Mice expressing the entire human ET-1 gene under its natural promoter (8 kb of the upstream flanking region) develop age-related glomerulosclerosis, interstitial fibrosis and renal cysts (Hocher *et al.*, 1997). However, despite a marked reduction in glomerular filtration rate (GFR), these mice remained normotensive. Increased expression of human ET-1 was detected in the blood vessels of these mice and lead to an increased media/lumen ratio, consistent with the proposed hypertrophic effect of ET-1. The lack of a significant blood pressure increase in these transgenic mice was unexpected and contrasts with earlier studies in which transient overexpression of a human preproET-1 cDNA transgene under a cytomegalovirus (CMV) promoter was achieved by adenoviral-mediated transfection in the rat (Niranjan *et al.*, 1996). In this model, mean arterial pressure was increased by ~30 mmHg, mediated via an increase in ET_A receptor signalling. This difference in blood pressure response may reflect transgene expression levels. In the mouse model, plasma ET-1

concentration was increased by ~35% but did not differ significantly from controls. A significantly elevated ET-1 was only seen when tissue concentrations were measured in the whole kidney. In contrast, plasma ET-1 in the rat model was 6 times greater than in controls transfected with an adenovirus reporter construct. An alternative hypothesis is that the chronic overexpression of the ET-1 transgene results in the development of counter-regulatory mechanisms that normalise blood pressure, despite an activated endothelin system. Such mechanisms may include up-regulation of the NO system, receptor down-regulation or desensitisation, or changes in post-receptor signalling, though these parameters were not tested in this study. The chronic activation of the renal endothelin system did, however, provide insights into blood-pressure independent mechanisms of progressive renal dysfunction. The mechanism of formation of renal cysts was thought to involve an increase in the rate of apoptotic loss of renal tissue (Hocher *et al.*, 1998), or reflect a disturbance of flow within urinary tubules secondary to interstitial fibrosis (Shindo *et al.*, 2002). However, the pathophysiological mechanisms underlying the observed glomerulosclerosis were less clear. A further strain of ET-1 transgenic mice has been produced in Japan (Shindo *et al.*, 2002). These mice are also normotensive and exhibit age-related pathological changes in the kidney similar to those described by Hocher and colleagues. Detailed electron microscopic examination of glomerular lesions in these animals revealed thickening of the basement membrane and proliferation of the mesangium. This suggests that glomerulosclerosis may have been due to direct ET-1-induced proliferation of epithelial and mesangial cells, respectively. Alternatively, increased ET-1 may have produced glomerular hypertension and subsequent sclerosis due to localised effects upon the afferent and efferent arterioles. Cysts were also found in Bowman's capsule and were similar in appearance to a model of chronic glomerulonephritis, suggesting that ET-1 may have a direct nephritogenic effect (Shindo *et al.*, 2002). The pathophysiological significance of the salt-sensitive hypertension also seen in this model is unresolved, since glomerulosclerosis reduces renal mass and hence the ability of the kidney to excrete a high salt load.

Transgenic rats overexpressing human ET-2 are also normotensive and exhibit progressive renal damage similar, but not identical, to ET-1 transgenic mice (Hocher *et al.*, 1996). In the kidney, transgene expression was limited to the glomerulus and the rats developed age-related glomerulosclerosis and proteinuria but no decrease in GFR. These findings further implicate an activated renal endothelin system as a primary mediator of renal damage. The potential mechanisms underlying the observed normotension despite overexpression of ET-2 have been studied in detail in this model and appear to be related to an increase in the activity of the NO system. Differences were also observed in end-organ structure but no evidence of endothelin receptor down-regulation or desensitisation was found (Liefeldt *et al.*, 1999).

1.6.4 CURRENT MODELS OF LOSS OF ET_B RECEPTOR FUNCTION

A naturally occurring mutation of the ET_B receptor is seen in so-called 'piebald' mice. This mutation consists of a retroposon inserted into intron 1 of the ET_B receptor gene (Ohuchi *et al.*, 1999). Mice homozygous for this mutation (s/s) produce ~1/4 the normal tissue density of ET_B receptors, exhibit reduced coat pigmentation but rarely develop megacolon. These mice have provided a useful tool for the development of alternative strategies to achieve adult ET_B receptor-deficient mice. Ohuchi and colleagues crossed homozygous piebald mice with mice heterozygous (ET_B (+/-)) for targeted disruption of the ET_B gene. ET_B (s/-) mice expressed approximately 1/8th of normal ET_B receptor levels and demonstrated an increase in mean arterial blood pressure of ~20 mmHg compared with wild-type (+/+) or ET_B (s/+) mice on a normal salt diet. The hypertensive phenotype was not ameliorated by treatment with the selective ET_A antagonist BQ-123, and mice demonstrated no abnormalities of cardiorespiratory control. Thus, despite the higher concentrations of circulating ET-1 in ET_B (s/+) and (s/-) mice compared to wild-type controls, an increase in ET_A receptor mediated vasoconstriction did not appear to contribute to the hypertensive state. Treatment of ET_B (s/+) and ET_B (+/+) mice, but not ET_B (s/-) mice, with the ET_B receptor antagonist BQ-788 resulted in an increase in blood pressure. These results suggest that the ET_B receptor is responsible for tonic vasodilatation in the mouse. Further investigation revealed that this hypotensive effect

was mediated predominantly by the release of dilator prostaglandins, rather than NO (Ohuchi *et al.*, 1999). It should be noted, however, that because of the concomitant loss of renal and vascular ET_B receptors in this model, it is not possible to elucidate the site of ET_B receptor-mediated regulation of blood pressure.

A more severe form of ET_B receptor mutation that produces no functional ET_B receptors, termed spotting lethal (sl), has also been utilised in rescue approaches (Gariepy *et al.*, 1998). The sl mutation consists of a 301bp deletion spanning the junction between exon 1 and intron 1. This results in the production of an aberrantly spliced ET_B receptor mRNA that lacks the coding sequence for the first and second putative transmembrane domains of the receptor (Gariepy *et al.*, 1996). Rats homozygous for the spotting lethal mutation (sl/sl) have been rescued from the lethal phenotype by the introduction of transgenes consisting of the wild-type ET_B receptor cDNA under the transcriptional control of the human dopamine ß-hydroxylase promoter (DβH-ET_B;ET_B sl/sl) (Gariepy *et al.*, 1998). This promoter is active in enteric neuronal cell precursors and hence wild-type ET_B receptors are expressed in these cells, allowing normal enteric ganglionic development. All other cells, with the exception of adrenergic tissues and neurons, do not express functional ET_B receptors. On a sodium-deficient diet DβH-ET_B;ET_B sl/sl rats and control DβH-ET_B;ET_B +/+ rats show no significant differences in blood pressure. However, DβH-ET_B;ET_B sl/sl rats develop severe hypertension (~170 mmHg) when fed a high salt (8% NaCl) diet. This salt sensitive hypertension in the setting of functional ET_B receptor deficiency was accompanied by appropriate down-regulation of the renin-angiotensin-aldosterone system. Interestingly, the hypertension could be completely reversed by treatment with doses of amiloride sufficiently low to be selective for epithelial sodium channels (ENaC) in the distal nephron. In contrast, treatment of salt-loaded DβH-ET_B;ET_B +/+ rats with amiloride did not affect blood pressure. Acute administration of the selective ET_A receptor antagonist FR139317 to DβH-ET_B;ET_B sl/sl rats did not completely reverse the hypertension, although an increased acute depressor response was observed compared to ET_B (+/+) rats. Furthermore, no differences in blood pressure responses were observed between

DβH-ET_B;ET_B sl/sl and DβH-ET_B;ET_B +/+ rats treated acutely with either L-NAME or indometacin, each inhibitors of depressor pathways normally associated with ET_B receptor activation. Recent studies in young (21 day old) sl/sl rats have confirmed the finding of a decrease in the fractional excretion of sodium in the setting of ET_B deficiency (Hocher *et al.*, 2001). This effect was similarly reversed following treatment with amiloride. In addition, sl/sl rats were mildly hypertensive (~7 mmHg), although the significance of this finding in the setting of impending intestinal obstruction is debatable.

These findings suggest that ET_B receptor deficiency represents a single locus model of severe salt-sensitivity. The blood pressure response to ENaC-selective doses of amiloride implies that the effects of ET_B receptor deficiency are predominantly mediated through changes in distal tubular sodium transport by ENaC. In the absence of ET_B receptors, ENaC channels exhibit inappropriate sodium reabsorbtion in the face of a high salt load, despite down-regulation of the renin-angiotensin-aldosterone system. In the presence of a mineralocorticoid (DOCA salt), an even greater blood pressure response is seen in ET_B deficient rats (Matsumura *et al.*, 2000). It is likely, therefore, that the normal action of ET_B receptors is one of tonic inhibition of ENaC activity. However, other mechanisms may also contribute to the hypertensive phenotype of these animals. DβH-ET_B;ET_B sl/sl rats have circulating concentrations of ET-1 that are between 5 and 6 times higher than those of DβH-ET_B;ET_B +/+ rats (13.2±2.8 versus 2.1±1.8 pg/ml and 23.9±4.2 versus 4.4±1.4 pg/mL on both normal and high sodium diets respectively). This occurs because ET_B receptors act as clearance receptors for ET-1 (Fukuroda *et al.*, 1994). High plasma concentrations of ET-1 may lead to an enhanced pressor effect mediated through ET_A receptors, as evidenced by the acute depressor response to a selective ET_A antagonist in these rats. Indeed, Matsumura and colleagues recently demonstrated that DOCA salt-induced hypertension in DβH-ET_B;ET_B sl/sl rats could be entirely reversed by chronic administration of the ET_A receptor antagonist ABT-627 (Matsumura *et al.*, 2000). Such an increased ET_A receptor mediated pressor effect could be particularly important in the glomerulus where a subsequent reduction in GFR might affect renal

sodium handling. In addition, the mitogenic effects of high ET-1 concentrations during the development and maturation of the cardiovascular system may alter vascular responses to other pressor agents.

1.6.5 HETEROZYGOUS RECEPTOR KNOCKOUTS

Homozygous ET_A or ET_B receptor knockouts develop lethal phenotypes as described earlier. However, littermates heterozygous for gene deletion at these loci (ET_A (+/-), ET_B (+/-)) survive normally into adulthood and are a useful model for the study of the physiological responses to exogenous and endogenous ET-1. ET_B (+/-) but not ET_A (+/-) mice are hypertensive (MAP ~90 mmHg and ~70 mmHg, respectively) (Berthiaume *et al.*, 2000) by a similar degree to that reported by Ohuchi and colleagues in the ET_B (s/-) model (Ohuchi *et al.*, 1999). In contrast to the results of Ohuchi, however, the hypertension in ET_B (+/-) mice could be reversed with either a mixed or a selective ET_A receptor antagonist, but not with a selective ET_B receptor antagonist. These results might suggest that the hypertension in the ET_B (+/-) mouse is, in fact, mediated by increased binding of ET-1 to ET_A receptors, as a result of an increased plasma ET-1 concentration. This theory is supported by the demonstration that ET_B (+/-) mice have impaired clearance of exogenous ^{125}I-ET-1 and that a similar defect of clearance may be reproduced in wild type mice by the administration of an ET_B receptor antagonist (Berthiaume *et al.*, 2000). Unfortunately, the authors did not report on plasma ET-1 concentrations in ET_B (+/-) or wild type mice and the effects of ET_B receptor down-regulation on renal sodium handling were not investigated.

The pressor response to exogenous ET-1 in ET_A (+/-) and ET_B (+/-) mice is moderated by both selective ET_A and selective ET_B receptor antagonists (Berthiaume *et al.*, 2000). This is in contrast to other animal (Ishikawa *et al.*, 1994) and human studies (Verhaar *et al.*, 1998) where selective ET_B receptor antagonism was shown to potentiate the pressor response to exogenous ET-1, consistent with an endogenous vasodepressor role for the ET_B receptor. The relative contribution of vasoconstrictor VSMC ET_B

receptors and vasodilator endothelial cell ET_B receptors to vascular tone and blood pressure in the mouse remains, therefore, controversial.

1.7 CARDIOVASCULAR PHYSIOLOGY OF THE ENDOTHELIN SYSTEM

The endothelins act in an autocrine and paracrine fashion. Studies involving the administration of the endothelin isoforms, either by bolus or constant infusion are, therefore, unlikely to reproduce the *in vivo* physiological effects of endothelin action. Indeed, such studies may be frankly misleading, despite the presence of increased circulating concentrations of ET-1 having been documented in a number of pathological conditions. Here, studies with antagonists are more informative, since they may reveal more accurately the endogenous activity of an autocrine/paracrine system. These data are reviewed below.

1.7.1 ROLE OF ENDOTHELIN IN THE MAINTENANCE OF VASCULAR TONE

In humans, there is clear evidence that the endothelin system plays an important role in the maintenance of basal vascular tone. Intra-arterial infusion of the selective ET_A receptor antagonist BQ-123 into the forearm results in progressive vasodilatation that persists for up to 1 hour (Haynes and Webb, 1994). These results have since been confirmed by others (Berrazueta *et al.*, 1997, Verhaar *et al.*, 1998) and suggest that endogenous ET-1 increases basal vascular tone mainly via the ET_A receptor. Inhibition of vascular ET_B receptors with the selective ET_B antagonist BQ-788 produces vasoconstriction and, when co-infused with BQ-123, BQ-788 attenuates the vasodilator response (Verhaar *et al.*, 1998). Thus, the summation of effects of endogenous activation of ET_B receptors in the forearm of healthy humans is one of vasodilatation. This effect is largely mediated via the generation of NO. Dilator PGI_2 generation appears to contribute little to this response because pre-treatment with aspirin has no effect. The results of these local studies have since been confirmed in the systemic circulation (Spratt *et al.*, 1999, Strachan *et al.*, 1999).

In the rodent, the evidence for involvement of the ET_B receptor is less clear. Some early studies have shown no effect on vascular tone or blood pressure following endothelin antagonism (reviewed by (Schiffrin, 1999)). However, more recently, investigators have observed significant effects on blood pressure with either genetic or pharmacological perturbation of ET_B receptor function (Gariepy *et al.*, 2000, Giardina *et al.*, 2001, Pollock and Pollock, 2001, Vassileva *et al.*, 2003, Wessale *et al.*, 2002). Taken together, these data suggest that the ET_B receptor mediates an endogenous hypotensive effect in the rodent. This effect appears to become upregulated and assume greater importance during conditions of high salt (Giardina *et al.*, 2001, Pollock and Pollock, 2001). The mechanism of this effect upon blood pressure remains poorly understood and may involve both vascular and renal tubular ET_B receptors and increased ET_A receptor activity.

1.7.2 THE RENAL ENDOTHELIN SYSTEM AND BLOOD PRESSURE REGULATION

The kidney is widely regarded as the most important regulatory organ in the determination of systemic blood pressure. Radio-ligand binding, immunohistochemistry and *in situ* hybridisation techniques have all been used to localise each component of the endothelin system to the renal vasculature and nephrons (reviewed by (Kotelevtsev and Webb, 2001). The greatest tissue concentrations of immunoreactive ET-1 are to be found in the kidney (Kitamura *et al.*, 1993) and urinary ET-1 is almost entirely of renal origin, with little circulating ET-1 cleared into the urine (Abassi *et al.*, 1992). The ET_B receptor is the predominant subtype found in the kidney and is likely, therefore, to contribute importantly to the regulation of blood pressure and fluid balance.

Harris and colleagues (Harris *et al.*, 1991) demonstrated that low doses of exogenous ET-1 produce diuresis and natriuresis in the rat kidney. Higher doses of exogenous ET-1 produce glomerular vasoconstriction, a decrease in sodium delivery to the proximal nephron, and subsequent anti-natriuresis. These results exemplify the difficulties that surround experimental analysis of the effects of ET-1 in the kidney.

Namely, activation of the same receptor within different regions of a single target organ may result in opposing physiological effects. This makes interpretation of antagonist or agonist studies extremely problematic. However, the consensus of opinion now is that intra-renal ET-1 regulates distal tubular sodium transport within the nephron, promoting natriuresis and diuresis. In addition, locally generated ET-1 may also regulate blood flow within the kidney, particularly in the glomeruli and medulla (Gurbanov *et al.*, 1996, Kohan, 1996). In the medulla, ET-1 activates ET_B receptors, increasing medullary blood flow (Gurbanov *et al.*, 1996) and promoting natriuresis. This effect is mediated via the release of NO (Hoffman *et al.*, 2000) and ET_B receptor-dependent medullary vasodilatation appears to be particularly important under high salt conditions (Pollock *et al.*, 2000, Pollock and Pollock, 2001, Vassileva *et al.*, 2003). Specifically, the medullary ET_B receptor appears to regulate the relationship between perfusion pressure and natriuresis during high salt conditions (Vassileva *et al.*, 2003), though the precise cellular location of this effect has not been determined.

1.7.2.1 *Renal tubular effects of ET-1*

In addition to effects in the distal nephron, ET-1 also modulates fluid and electrolyte transport mechanisms within other tubular segments. In the proximal tubule (PT), ET-1 regulates activity of the Na^+/P_i co-transporter, Na^+/H^+ exchanger, Na^+/H^+ antitransporter and the Na^+/HCO_3^- exchange transporter. The effects upon sodium and water transport in the PT are biphasic and dependent on ET-1 concentration, with higher concentrations promoting natriuresis. A biphasic effect is also seen in the distal nephron, although in this region higher concentrations of ET-1 increase sodium reabsorbtion. Analysis of ET-1 concentrations in the PT and CCT suggest that in each of these regions, ET-1 promotes diuresis and natriuresis (Kohan, 1997). The effects of ET-1 are mutually antagonistic with those of arginine vasopressin (AVP) in the CCT and IMCD. Both ET-1 and ET-3 reduce AVP-stimulated increases in osmotic water permeability through inhibition of cAMP accumulation (Kohan and Hughes, 1993). In summary, ET-1 and ET-3 exert a complex array of actions upon renal tubular transport processes throughout the nephron, the net results of which are to promote the excretion of sodium and water.

1.7.2.2 *Renal vascular effects of ET-1*

The renal vasculature is extremely sensitive to the vasoconstrictor action of ET-1, and to a lesser extent, big ET-1. Administration of exogenous ET-1 results in a fall in GFR, an increase in renal vascular resistance and a fall in RBF (reviewed by (Rubanyi and Polokoff, 1994)). Cortical blood vessels appear more sensitive to the vasoconstrictor effects of ET-1 than medullary vessels. Indeed, in Wistar rats, low doses of ET-1 (1 nmol/kg iv.) produce vasoconstriction of cortical vessels but vasodilatation of medullary vessels (Gurbanov *et al.*, 1996). Interestingly, the cortical response appears to be mediated by ET_A receptors, whilst the medullary vasodilator response is ET_B receptor-mediated. Studies in anaesthetised dogs have revealed that the glomerular actions of ET-1 are predominantly mediated by the ET_A receptor, whilst the diuretic and natriuretic effects are mediated by ET_B receptors in the nephron (Clavell *et al.*, 1995). However, inter-species variation in the distribution and function of each receptor subtype is well documented, particularly in relation to the ET_B receptor, which may also mediate glomerular vasoconstriction in some species, including the rat (Matsuura *et al.*, 1996). Although exquisitely sensitive to exogenous ET-1, an endogenous ET_A receptor-mediated vasomotor tone has been more difficult to demonstrate in the kidney. Selective ET_A receptor antagonists do not alter renal vascular resistance in normotensive anaesthetised rats (Matsuura *et al.*, 1997, Qiu *et al.*, 1995). In contrast, a selective ET_B antagonist decreased RBF and increased RVR by ~ 20%, an effect mediated by NO and/or dilator prostaglandins (Matsuura *et al.*, 1997). The recent finding of a markedly decreased GFR in ET_B receptor deficient rats further suggests an overall tonic vasodilator role for glomerular ET_B receptors in healthy rats (Hocher *et al.*, 2001). The balance between vasodilator EC ET_B receptors and vasoconstrictor VSMC ET_B receptors within the glomerulus is, therefore, likely to impact significantly upon glomerular haemodynamics.

1.7.3 AUTOCRINE AND PARACRINE SIGNALLING IN THE KIDNEY

The precise distribution of endothelin receptors within the rodent kidney merits further detailed analysis as it forms the basis of the two current models of renal ET-1 action. Cultured inner medullary collecting duct (IMCD) cells express both ET_A and ET_B receptors and secrete ET-1 (Kohan and Fiedorek, 1991, Kohan *et al.*, 1992). This has prompted an autocrine model of endothelin action in the distal nephron (Kohan and Padilla, 1992). In this model, ET_B receptor activation by IMCD-derived ET-1 directly inhibits sodium transport by the cell. An alternative hypothesis suggests a paracrine signalling mechanism in this region (Kotelevtsev and Webb, 2001). ET-1 secreted from the basolateral side of IMCD cells would activate ET_B receptors located on the adjacent abluminal membrane of EC of the vasa-recta. NO subsequently generated by either the eNOS or nNOS isoforms of NOS found in EC would then diffuse back across to IMCD cells where it would act to inhibit sodium reabsorbtion. A paracrine model would, therefore, require that the ET_B receptor were predominantly expressed upon EC of the vasa-recta. The work of several groups supports this notion. Yukimura and colleagues (Yukimura *et al.*, 1996) used electron microscopic autoradiography with radiolabelled ET-1 and the selective ET_B receptor ligand IRL 1620 to demonstrate the presence of binding sites on the vasa-recta and type 1 interstitial cells of the inner medulla. ET_B receptor binding was also seen on the basolateral membrane of IMCD cells, but to a much lesser extent. This work is supported by *in vitro* and *in vivo* studies with radiolabelled ET-1 and S6c that localised binding to the fenestrated EC of glomerular capillaries and the peritubular capillaries of the rat kidney (Dean *et al.*, 1996). In contrast to these results, other groups have also demonstrated expression of ET_B receptors by cultured IMCD cells (Wong *et al.*, 2000). Insight into whether the renal endothelin system acts by predominantly autocrine or paracrine signalling may be gained by the use of tissue-specific ET_B receptor knockout models, selective for either IMCD cells or EC. Such models will permit study of the effects of selective loss of, for example, IMCD ET_B receptors, without the confounding physiological effect of loss of vasa-recta or glomerular ET_B receptors.

1.7.4 ROLE OF ENDOTHELIN IN THE CENTRAL REGULATION OF BLOOD PRESSURE

Administration of ET-1 directly into the CNS stimulates a dose-dependent increase in blood pressure and sympathetic nerve activity. This effect appears to be mediated by ET_A receptors (Nakamura *et al.*, 1999). However, despite the presence of all the elements of the endothelin system in brain regions responsible for autonomic control, a role for endogenous ET-1 in the central regulation of blood pressure and sympathetic nerve activity in normal rats remains controversial. Central administration of BQ-123 does not affect blood pressure in anaesthetised Wistar-Kyoto or SHR, although an effect was seen in SHR-SP (Nakamura *et al.*, 1999). These findings contrast with the phenotype of ET-1 (+/-) mice in which loss of a single ET-1 gene allele resulted in a marked disturbance of cardiorespiratory control. ET (+/-) mice exhibit increased sympathetic nerve activity, increased blood pressure and show attenuation of hypoxia-induced respiratory reflexes (Kuwaki *et al.*, 1996). Mice deficient in ET-3 demonstrate no similar abnormalities of cardiorespiratory control (Nakamura *et al.*, 2001) despite the demonstration that this peptide is an important neurotransmitter and that there is widespread expression of ET_B receptors within the brain.

1.8 ROLE OF ENDOTHELIN IN CARDIOVASCULAR PATHOPHYSIOLOGY

The normal function of the endothelin system and the balance with other local and hormonal cardiovascular regulatory mechanisms may become disrupted by a number of pathophysiological mechanisms, including increased production, increased sensitivity or decreased clearance of ET-1. Many cardiovascular diseases have been shown to be associated with increased circulating concentrations of plasma ET-1, though whether these represent primary or secondary phenomena is undetermined. Decreases in gene expression for the endothelin precursors, endothelin converting enzymes or endothelin receptors may cause congenital conditions such as Hirschsprung's disease and the Waardenburg-Shah syndromes. More subtle genetic mutations may result in changes in

receptor expression, affinity or selectivity, perhaps contributing to hypertension in some patients. Enhanced receptor number or affinity is thought to mediate the hypertension and renal dysfunction during cyclosporine treatment, and renal dysfunction may reduce peptide clearance, thereby increasing ET-1 concentration. Enhanced production of ET-1, in response to a number of factors including vasoactive hormones and tissue hypoxia, may augment the neurohormonal activation seen in chronic heart failure and enhance the effects of other mediators, such as Ang II. The actions and concentrations of ET-1 would also be potentiated in conditions characterised by dysfunction of the L-arginine/NO system, allowing uncompensated changes in vascular tone and vascular remodelling to occur. This has been suggested as a mechanism for Raynaud's disease and cerebral vasospasm, amongst others. For the purpose of this thesis, the contribution of the endothelin to the pathophysiology of cardiovascular disease will be limited to a discussion of the role of the endothelin system in hypertension.

1.8.1 WHAT ROLE MAY ENDOTHELIN PLAY IN HYPERTENSION?

ET-1 may be involved in the pathogenesis of hypertension through a number of different mechanisms. Firstly, increased expression or decreased clearance of this powerful vasoconstrictor may lead directly to an increase in vascular tone and blood pressure. Alternatively, the balance between the vasoconstrictor and vasodilator responses following ET_B receptor activation may be altered to favour vasoconstriction (Cardillo *et al.*, 1999). Changes in renal endothelin signalling may also result in an increase in blood pressure through increases in sodium reabsorbtion and resultant expansion of circulating volume (Gariepy *et al.*, 2000). Changes in endothelin signalling in the central and peripheral nervous system could lead to alteration of the 'set point' for blood pressure. Finally, the vascular hypertrophic effects of increased ET-1 signalling may lead to an increase in vascular sensitivity to the vasoconstrictor effects of other pressor agents, such as nor-epinephrine (NE) or Ang II. Some of these pathophysiological hypotheses have been tested in experimental animal models of hypertension and in human hypertension and are reviewed below.

1.8.1.1 *Experimental models of hypertension involving endothelin*

Although debate continues concerning the physiological role of the rodent endothelin system in the regulation of normal blood pressure, there is good evidence to support a role for ET-1 in the pathogenesis of hypertension in rats. ET-1 has been particularly implicated in the pathogenesis of salt-sensitive models of hypertension including DOCA-salt hypertension (Lariviere *et al.*, 1993), DOCA-salt treated SHR (Schiffrin *et al.*, 1995), and Dahl salt-sensitive rats (Doucet *et al.*, 1996). In addition, Ang II-infused hypertensive rats (Moreau *et al.*, 1997) and SHR-SP (Sharifi *et al.*, 1998) also exhibit an ET-1-dependent component. Each of these models demonstrates an increase in EC preproET-1 mRNA expression and exhibits a significant hypotensive response to ET antagonists (reviewed by (Schiffrin, 1999)). In contrast, ET receptor antagonists are largely ineffective hypotensive agents in renovascular hypertension. 2 kidney 1 clip (2K/1C) hypertensive (Li *et al.*, 1996), 1 kidney 1 clip (1K/1C) hypertensive (Li *et al.*, 1996) and L-NAME-induced hypertensive rats (Sventek *et al.*, 1997) show no consistent hypotensive response to ET antagonism and feature only modest or no increased expression of preproET-1. The apparent paradox between the involvement of the endothelin system in the hypertension associated with exogenously administered Ang II, but not with endogenously generated Ang II (2K/1C and 1K/1C models) remains unexplained. However, this may relate to a greater permissive effect upon vascular preproET-1 expression of a constant infusion of Ang II compared to the more physiological pulsatile release of Ang II by the kidney. In SHR, the evidence implicating the endothelin system is also contradictory. Some studies have shown no generalised up-regulation of vascular ET-1 (Schiffrin *et al.*, 1995) and no hypotensive effect of ET antagonists (Li and Schiffrin, 1995). Other researchers (Hocher *et al.*, 1995) have demonstrated increased renal ET_A and ET_B receptor expression in SHRs and hypertension that was sensitive to both BQ-123 and bosentan. These apparently conflicting results may reflect SHR strain differences and/or different experimental techniques.

Despite the relatively consistent association between increased vascular expression of ET-1 and sensitivity to endothelin antagonists in rodent models, measurement of plasma and vascular ET-1 content in humans has failed to demonstrate a clear association with hypertension (reviewed by (Schiffrin, 1999)). However, ET-mediated vascular tone is increased in hypertensive patients (Cardillo *et al.*, 1999, Taddei *et al.*, 1999) and ET antagonists lower TPR in normotensive humans (Spratt *et al.*, 1999). Interestingly, following treatment with a selective ET_B receptor antagonist, forearm blood flow is increased in hypertensive patients, but decreased in normotensive controls (Cardillo *et al.*, 1999). This suggests that the balance between vasodilator EC and vasoconstrictor VSMC ET_B receptors may be altered in pathophysiological states, including hypertension. Clinical trial data supports a role for ET-1 in the maintenance of vascular tone, which may be increased in hypertension. Bosentan was found to lower blood pressure by ~6 mmHg in mild to moderate hypertensives (Krum *et al.*, 1998), an effect equivalent to 20 mg of Enalapril.

1.8.1.2 *Salt sensitive models of hypertension*

Defective tubular ET_B receptor signalling may be a causative factor in some forms of salt-sensitive hypertension, as described earlier. In contrast, vascular ET_B receptors may actually play an important protective role in this setting. In DOCA-salt hypertensive rats, ET_A receptor antagonists decrease blood pressure and TPR acutely (Fujita *et al.*, 1996, Yu *et al.*, 1998) and prevent the development of hypertension and cardiac hypertrophy chronically (Matsumura *et al.*, 1995). However, ET_B receptor antagonists significantly worsen the vascular hypertrophy and renal dysfunction in these animals (Matsumura *et al.*, 1999) and promote further increases in blood pressure (Pollock *et al.*, 2000). This may be due to a loss of tonic ET_B-mediated vasodilator responses since selective ET_B antagonists acutely increase systemic blood pressure, decrease renal blood flow and diminish the renal vasodilatation induced by ET_A receptor antagonists in DOCA-salt treated rats (Hashimoto *et al.*, 1998). In addition, chronic ET_B receptor antagonism may further impair renal elimination of the high salt load, thereby increasing circulating volume and blood pressure. DOCA-salt treated rats exhibit increased medullary ET_B

receptor expression (Pollock *et al.*, 2000), perhaps to facilitate the excretion of salt. Indeed, treatment of DOCA-salt rats with ET_B receptor antagonists decreases their ability to excrete salt and water (Pollock *et al.*, 2000). DOCA-salt hypertension appears, therefore, to be characterised by an increase in ET_A receptor-mediated mitogenic and vasoconstrictor effects and by upregulation of protective ET_B receptor-mediated vasodilator and natriuretic responses.

In a genetic model of salt-dependent hypertension, the Dahl salt-sensitive rat, ET_A receptor antagonists prevent the increase in ET-1 expression, vascular hypertrophy and endothelial dysfunction seen during high salt loads (Barton *et al.*, 1998). The activation of the ET-1 system in response to salt may be related to NO release. Dalh-sensitive rats are unable to upregulate renal NOS activity appropriately during salt loading (Barton *et al.*, 2000). In contrast, Dahl-resistant rats increase NOS activity by ~270% in response to salt but do not increase expression of ET-1 or develop hypertension. The failure to upregulate NOS activity may, therefore, permit the increased expression of ET-1 with subsequent renal structural and functional damage mediated through ET_A receptor activation (Barton *et al.*, 2000). These results contrast with the observation that pharmacological inhibition of NOS does not result in upregulation of renal vascular ET-1 expression in Sprague-Dawley rats (Fujita *et al.*, 1995). This suggests that there may be further blood pressure regulatory defects in Dahl salt-sensitive rats or that NOS-inhibitors may prevent ET-1 up-regulation by a mechanism independent of NO.

1.8.1.3 *Mechanism of increased endothelin expression in hypertension*

Increased blood pressure *per se* does not appear sufficient to increase vascular ET-1 expression. Data from Dahl-sensitive rats (Barton and d'Uscio, 2000) and Ang-II infused rats (d'Uscio *et al.*, 1997) suggests that interactions with other vasoactive substances, particularly the local RAAS and NO systems, may also be important. This correlates with *in vitro* studies in which Ang II and NOS inhibition increase the expression of ET-1. In DOCA salt-induced hypertension, AVP may also mediate increased ET-1

expression. Plasma AVP is increased in DOCA salt-treated rats and vasopressin V_1 antagonists prevent the increase in vascular preproET-1 expression, vascular hypertrophy and increased blood pressure seen in this model (Intengan *et al.*, 1998). The observation that vasopressin-deficient rats do not become hypertensive or upregulate preproET-1 expression following DOCA-salt, underlines the important interactions between vasopressin and ET-1 in this pathogenic process (Intengan *et al.*, 1998).

1.8.1.4 *Vascular remodeling in hypertension*

In hypertensive models featuring up-regulation of vascular preproET-1 mRNA, a common pathological feature is vascular hypertrophy of a greater extent than might be expected for the degree of hypertension (Schiffrin *et al.*, 1995). This suggests that an increase in vascular ET-1 expression might be a blood pressure-independent mediator of vascular hypertrophy, as predicted by the *in vitro* mitogenic effect of ET-1 on VSMC (Hirata *et al.*, 1989). Endothelin antagonists reverse the vascular hypertrophy in salt-dependent hypertensive models, particularly in resistance arteries, even if the hypotensive effect is only moderate (Li and Schiffrin, 1995). In contrast, vascular morphology is unchanged by ET antagonists in renovascular hypertension (Li *et al.*, 1996). The presence of vascular hypertrophy in normotensive ET-1 over-expressing transgenic rats (Hocher *et al.*, 1997) further supports a direct vascular hypertrophic role for ET-1. These data suggest that ET antagonists may be particularly useful in human hypertension for the prevention of end-organ damage.

In conclusion, the endothelin system has been strongly implicated in the pathogenesis of experimental and genetic salt-sensitive hypertension, low renin hypertension, exogenous Ang II hypertension and malignant hypertension. A direct vascular hypertrophic effect of ET-1 may further exacerbate end-organ damage in the setting of an increased blood pressure.

1.8.1.5 *Pathological changes in receptor expression*

Genetic models of ET_B receptor down-regulation demonstrate the importance of ET_B receptor signalling in the determination of systemic blood pressure (Gariepy *et al.*, 2000, Ohuchi *et al.*, 1999). However, more subtle changes in the expression of ET_B and ET_A receptors may also influence local blood flow and regulate tissue responses to other vasoconstrictors. Qiu and colleagues recently demonstrated that the mixed endothelin receptor antagonist, tezosentan, lowered RVR and increased RBF in rats with cardiac and renal failure secondary to coronary artery ligation (CAL) (Qiu *et al.*, 2001). This contrasts with previous work in normal rats (Matsuura *et al.*, 1997) demonstrating an endogenous vasodilator role of ET_B receptors in the kidney and suggests that in this pathophysiological state the balance of ET receptor-mediated responses favour vasoconstriction. Increased reactivity to exogenous ET-1 is seen in the coronary arteries of hypertensive rats (Miki *et al.*, 1998) and decreased pulmonary ET_B receptor expression may underlie the increase in circulating ET-1 in congestive heart failure (Kobayshi *et al.*, 1998). An increase in VSMC ET_B receptor and ET-1 expression is also found in atherosclerotic lesions of both humans and ApoE -/- mice (Fan *et al.*, 2000). Changes in the relative balance of vasoconstrictor and vasodilator responses to ET-1 within a particular arterial bed in pathophysiological states including heart failure, hypertension and atherosclerosis may, therefore, have important therapeutic implications. In conditions in which vasodilator ET_B receptor signalling is maintained or increased, selective blockade of ET_A receptors may provide a therapeutic advantage, particularly in view of further potential beneficial effects upon platelet aggregation and vascular growth of ET_B-mediated NO release. In contrast, a non-selective antagonist might be preferable in conditions characterised by increased vasoconstrictor ET_B receptor signalling.

1.9 GENERAL AIMS

The ET_B receptor has multiple roles in different tissues, including vasodilatation (Takayanagi *et al.*, 1991), vasoconstriction (Sumner *et al.*, 1992), inhibition of renal

sodium reabsorbtion (Gariepy *et al.*, 2000) and clearance of ET-1 (Fukuroda *et al.*, 1994). Each of these responses may independently modulate blood pressure and regional blood flow. However, the relative importance of each response to the complex homeostatic mechanisms of blood pressure control, particularly under conditions of high salt intake, has yet to be determined. Currently available pharmacological antagonists are unable to selectively block ET_B receptors in one tissue or cell type without also blocking ET_B receptors remote from the tissue or cell type of interest. Thus, the measured physiological response to the antagonist is a sum of the concurrent effects of receptor blockade upon that physiological variable in several tissues. This has made the interpretation of such data complex. Such complexity might be overcome by utilising drug delivery mechanisms that only release locally active concentrations of antagonists. However, in many tissues the different ET_B expressing effector cells lie in close proximity and it is unlikely that selective targeting of a single cell type would be feasible. Alternatively, the effects of antagonists might be studied *in vitro* and the results extrapolated to an *in vivo* model. This methodology has provided the majority of the data on which understanding of the physiology of the endothelin system is based. Knockout of receptors provides a further mechanism whereby loss of function effects may be studied *in vivo*. However, complete knockouts of ET_B receptor function produce a lethal phenotype that precludes study of *in vivo* adult physiology. Studies on young mice prior to the onset of intestinal obstruction are possible, but the quality of data recorded is likely to be compromised. A great deal of insight has been gained from the study of rescued ET_B receptor-deficient animals. However, the concurrent knockout of ET_B from multiple tissues suffers the same limitations as pharmacological antagonists in terms of data interpretation. The advent of technologies that permit the spatial and temporal regulation of gene expression now provides researchers with a powerful mechanism by which the understanding of the physiological role of the ET_B receptor in an individual cell type may be deepened. Cell-specific regulation of ET_B receptor expression can permit observation of the effects of tissue-specific loss of ET_B receptor function without the confounding effects of receptor down-regulation or blockade at remote sites.

Activation of ET_B receptors on EC results in vasodilatation mediated by the release of NO and/or dilator prostaglandins. In contrast, activation of ET_B receptors on adjacent VSMCs results in vasoconstriction. The relative balance of endothelial and VSMC ET_B receptors is, therefore, likely to influence vascular tone and blood pressure. In humans, the relative balance of endothelial and VSMC ET_B receptor activity appears to favour vasodilatation (Verhaar *et al.*, 1998). However, the contribution of the endogenous endothelin system to the maintenance of normal vascular tone and blood pressure in the mouse remains controversial. ET_B receptor-deficient rats (Gariepy *et al.*, 2000) and mice (Murakoshi *et al.*, 2002) rescued by the expression of a $D\beta H;ET_B$ transgene are hypertensive, an effect that may be secondary to loss of renal ET_B receptor-mediated regulation of ENaC channels. Mice in which expression levels of ET_B receptors are either $1/8^{th}$ of normal (ET_B (s/-)) (Ohuchi *et al.*, 1999) or 1/2 of normal (ET_B (+/-)) (Berthiaume *et al.*, 2000) are also hypertensive. Taken together, these data suggest that the overall effect of ET_B receptor activation is to lower blood pressure. This theory is supported by the observation that acute administration of ET_B receptor antagonists to normal mice produces an increase in blood pressure (Ohuchi *et al.*, 1999). However, other researchers have found that ET_B receptor antagonists have no effect on basal arterial pressure and that ET_B receptors mediate a significant part of the pressor and vasoconstrictive effects of ET-1 (Berthiaume *et al.*, 2000, Giller *et al.*, 1997). The mechanism of the increase in blood pressure in ET_B receptor-deficient mice is controversial. ET_B (+/-) mice show a significant hypotensive response to ET_A receptor antagonists (Berthiaume *et al.*, 2000). In contrast, ET_A receptor antagonists have no effect on blood pressure in ET_B (s/-) mice (Ohuchi *et al.*, 1999). The importance of an increased plasma ET-1 concentration with consequent increase in ET_A receptor binding as a mechanism for the hypertension seen following ET_B receptor blockade or knockout is, therefore, unclear. Debate thus remains over whether or not endogenous ET_B receptor signalling produces a significant hypotensive effect in the mouse, and if so, whether this effect is predominantly mediated by IMCD or vascular EC ET_B receptors, or both. The further role of ET_B receptors in each of these cell types in the regulation of blood

pressure under conditions of high salt also requires further study to clarify the importance of EC ET_B receptors in the regulation of natriuretic pathways.

To more precisely define the role of the ET_B receptor expressed upon different cell types to the regulation of complex homeostatic mechanisms, I have produced a model (the 'floxed' ET_B receptor mouse) that permits the cell-specific down regulation of ET_B receptor expression. The effects of loss of functional ET_B receptors upon the target cell of interest can now be examined in the context of preserved expression of ET_B receptors on all other cells. In order to study the role of the EC ET_B receptor in the regulation of blood pressure and vascular tone, I have produced a model of EC-specific ET_B receptor deficiency with which to test the following hypotheses:

1. The EC ET_B receptor is a critical determinant of resting blood pressure in the mouse.
2. The EC ET_B receptor influences blood pressure through determination of endogenous vascular tone in the mouse.
3. ET_B receptors expressed upon IMCD cells regulate natriuretic pathways under conditions of high salt and determine salt-sensitivity.
4. The EC ET_B receptor is a clearance receptor for ET-1.

EC ET_B receptor deficiency was achieved through intercross of mice featuring loxP sites flanking coding regions of the ET_B receptor gene ('floxed' ET_B receptor mice) with transgenic mice expressing Cre recombinase in an EC-specific pattern (Tie2-Cre mice). Binding of ^{125}I ET-1 was measured in isolated populations of pulmonary EC and functional loss of EC ET_B receptor-mediated vasodilatation was assessed in aortic rings *in vitro*. Maintenance of normal vasoconstrictor ET_B receptor signalling in SMC was examined in the isolated trachea. The effects of loss of EC ET_B receptors upon blood pressure under conditions of normal and high salt diet and upon endothelial function were then investigated. The following chapters describe the generation of the 'floxed' ET_B receptor mouse, its subsequent cross with Tie2-Cre transgenic mice and the

physiological effects of EC-specific down regulation of ET_B receptor expression upon cardiovascular homeostasis.

2 Chapter 2

2.1 MATERIALS AND METHODS

2.1.1 CONDITIONAL REGULATION OF GENE EXPRESSION

Gene targeting provides a mechanism to elucidate definitively the *in vivo* role of a molecule. However, functional analysis of the resultant phenotype may be complex if the molecule subserves different functions in different adult tissues or has a non-redundant role during development. To overcome these difficulties, DNA recombination systems may be used to disrupt gene expression in a pre-determined spatially regulated pattern (Gu *et al.*, 1994).

2.1.2 THE CRE/LOXP SYSTEM

The Cre/loxP system (Orban *et al.*, 1992, Sauer and Henderson, 1989) is the best characterised of the DNA recombination systems and consists of two basic elements. The P1 bacteriophage enzyme Cre recombinase is a 38 kDa protein that catalyses a site-specific recombination reaction between two loxP sites. The 34 bp loxP site consists of two 13 bp inverted repeats separated by an asymmetrical 8 bp core sequence. The core sequence determines the orientation of the loxP site. A recombination reaction is initiated when Cre recombinase binds to the inverted repeat sequence of the loxP site. A synapse is formed consisting of four Cre subunits and two loxP sites orientated in the same direction. Concerted cleavage and rejoining reactions occur between sites in the core sequence region resulting in the excision of a circular molecule containing the loxP flanked sequence of DNA. This system, therefore, enables the deletion of specific regions of genes or chromosomes as determined by the introduction of loxP sites flanking or 'floxing' the region of interest. The use of the Cre/loxP system in mammalian cell systems is facilitated by the lack of requirement for further co-factors or accessory proteins and the presence of basic peptides within Cre that direct it to the mammalian nucleus (Lewandoski, 2001). The efficiency of Cre recombinase to direct

heritable recombination events *in vivo* has been reported as between 87-99% and may be dependent upon factors including the chromosomal location of loxP sites, distance between loxP sites and the expression levels of Cre recombinase within the cell (Orban *et al.*, 1992). Temporal or spatial regulation of Cre-mediated recombination has now become possible through tissue-specific promoters, developmental stage-specific promoters and ligand inducible promoters regulating Cre recombinase expression (Kisanuki *et al.*, 2001).

2.1.3 TISSUE SPECIFIC KNOCKOUTS

In mice genetically targeted to contain a floxed gene, site-specificity of the recombination reaction may be engineered by limiting expression of Cre to the target cell of choice (Gu *et al.*, 1994, Orban *et al.*, 1992). This may be achieved by including tissue-specific promoters within a Cre recombinase transgene. Mice expressing Cre recombinase in a tissue-specific pattern ('effector mice') are usually generated separately and crossed with floxed mice ('target mice') to produce offspring homozygous for the floxed allele, and either homozygous or heterozygous for the Cre recombinase transgene. Although all cells in the offspring contain floxed alleles, expression of Cre recombinase will only occur in cells in which the tissue-specific promoter is active, thereby limiting recombination exclusively to these cells. The success of tissue-specific approaches is critically dependent on the precise restriction of Cre expression to the desired target cell or tissue. 'Leaky' expression of Cre will result in recombination in adjacent cells, whilst 'patchy' expression of Cre in target cells will result in a reduced number of recombination events and a mosaic pattern of gene deletion. Each of these events would serve to complicate the interpretation of any observed phenotype. For many studies, it is also important that the activity of the conditional allele is identical to the wild type allele, in order that normal gene function is maintained in all cells in which Cre is not expressed. To achieve this, loxP sites are generally targeted to intronic regions that are removed by splicing during gene transcription. Antibiotic resistance genes in the targeting construct used for ES cell selection are also usually removed prior to the generation of mice.

2.1.3.1 *Endothelial cell-specific knockout*

Promoter and enhancer elements from the murine Tie2 gene have been used to drive transgene expression in EC and cells of the haematopoietic lineage (Schlaeger *et al.*, 1997). The Tie2 gene encodes the tyrosine kinase angiopoietin receptor and activity of the Tie2 promoter is apparent from the first appearance of EC (late primitive streak stage). The expression pattern of transgenes driven by both promoter and enhancer elements from the Tie2 gene mirror the expression pattern of the Tie2 gene and expression is maintained throughout development into adulthood (Schlaeger *et al.*, 1997). Accurate assessment of the expression pattern of Tie2-Cre transgenic mice is essential for predicting the pattern of recombination events in mice harbouring functional loxP sites. This has been achieved by cross-breeding Tie2-Cre mice with the reporter mouse strains CAG-CAT-Z (Kisanuki *et al.*, 2001), ROSA26R (Kisanuki *et al.*, 2001) and EGFP (Constien *et al.*, 2001), In each of these reporter strains a visible marker (lacZ and GFP, respectively) is expressed only following Cre-mediated recombination. LacZ expression was pan-endothelial in Tie2-Cre;CAG-CAT-Z double transgenic mice and additionally seen in the endocardium and mesenchymal cells of the atrioventricular canal and proximal cardiac outflow tract (Kisanuki *et al.*, 2001). Similarly, recombination rates of up to 90% have been described in haematopoietic cells with no evidence of ectopic expression (Constien *et al.*, 2001). Several groups have now produced Tie2-Cre transgenic mice (Constien *et al.*, 2001, Kisanuki *et al.*, 2001, Theis *et al.*, 2001) using identical promoter and enhancer elements. Small variations in expression patterns are observed between these mice, most likely secondary to differences in transgene insertion sites. For the purposes of this study, we have utilised that of Kisanuki, a kind gift of Professor M. Yanagisawa, University of Texas.

2.1.4 CHEMICALS AND SOLUTIONS

All stock solutions were prepared with autoclaved reverse osmosis water (Elgastat Prima Reverse Osmosis Water Machine; Elga Ltd, High Wicham, UK). All chemicals were supplied by BDH Laboratory Supplies (Merc Ltd, Lutterworth, UK) and were of

analytical grade. Acids, alkalis and organic solvents were supplied by BDH laboratory Supplies with the exception of absolute ethanol and redistilled Tris-buffered phenol (Fischer Scientific, Loughborough, UK). Radionucleotides were supplied by Amersham Pharmacia Biotech UK Ltd. (Little Chalfont, UK) and ICN Pharmaceuticals (Basingstoke, UK). MWG-Biotech AG (Ebersberg, Germany). Hexaneucleotides and dNTPs were supplied by Roche Molecular Biochemicals, Mannheim, Germany. Kodak XOMAT XAR-5 film was used for all autoradiographs and was supplied by IBI Ltd (Cambridge, UK). SeaKem LE agarose (FMC Bioproducts, Rockland, USA) was used for all agarose gel electrophoresis.

2.1.5 PRIMERS

All oligodeoxynucleotide primers for sequencing and PCR reactions were supplied by Sigma Genosys (Pampisford, UK). Primer sequences and the complementary regions of the ET_B receptor gene locus are illustrated in Figure 2.1, Figure 2.2 and Figure 2.3. A list of primer sequences is provided in Table 2.1.

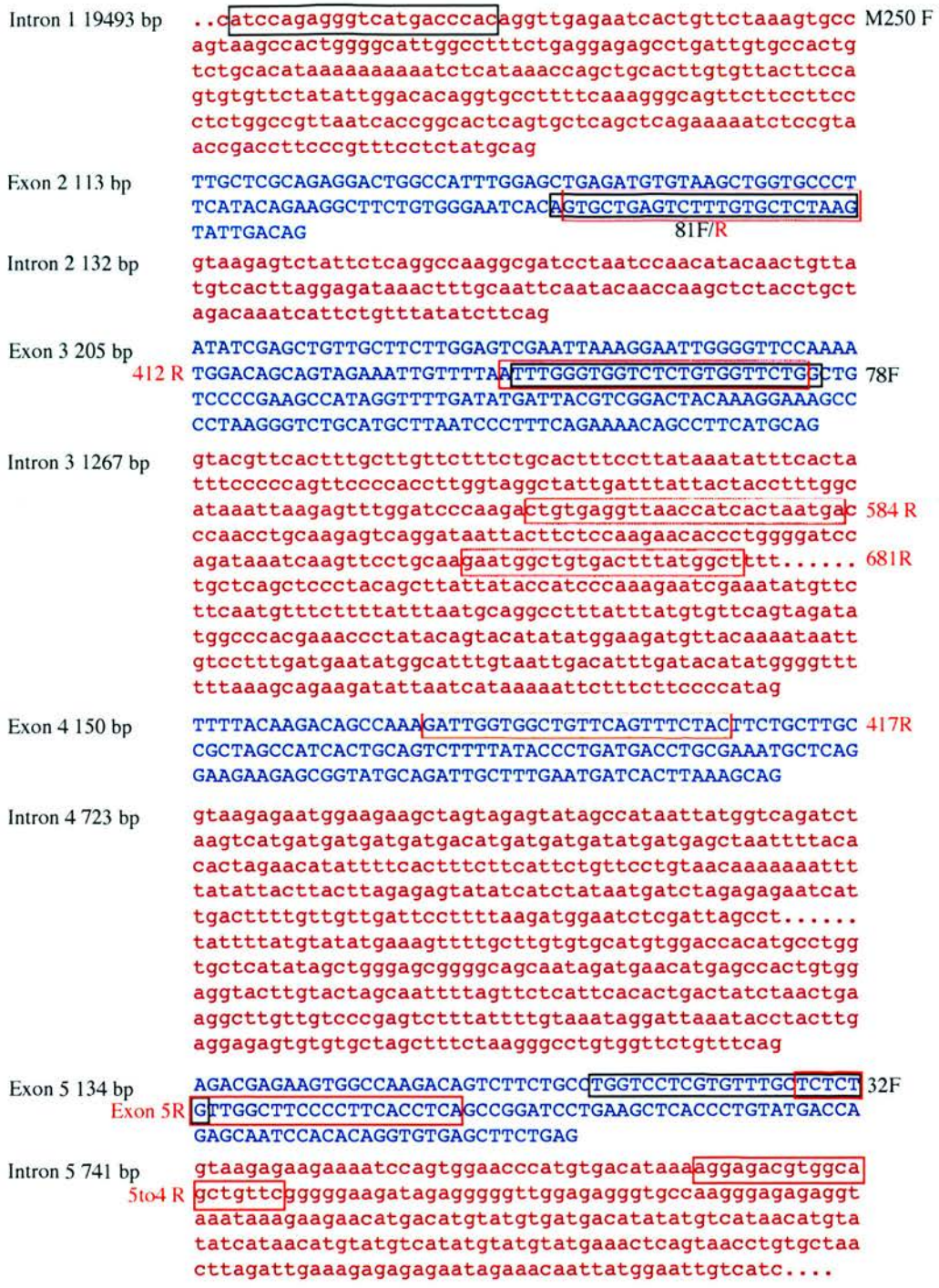

Figure 2.1

Sequence alignment of primers used for PCR and sequencing with complementary regions the ET_B receptor. Black boxes = forward primers; Red boxes = reverse primers.

Figure 2.2

Sequence alignment of primers used for PCR and sequencing with complementary regions the ET_B receptor gene. Black boxes = forward primers; Red boxes = reverse primers.

Figure 2.3

Sequence alignment of primers used for PCR and sequencing with complementary regions the ET_B receptor gene. Black boxes = forward primers; Red boxes = reverse primers.

PRIMER	LOCATION	SEQUENCE
454F	Intron 1	TCAGTTGTAATGAGACACAGAC
M250F	Intron 1	ATCCAGAGGGTCATGACCCAC
671R	Exon 1	GGGTATGTCTATGATGATGTGC
149F	Exon 1	TCCAGACTGAAAACAGCAGAGCGG
81R	Exon 2	CTTAGAGCACAAAGACTCAGCAC
81F	Exon 2	AGTGCTGAGTCTTTGTGCTCTAAG
681R	Intron 3	AGCCATAAAGTCACAGCCATTC
INT 3F	Intron 3	GGATTTGGAATGGCAGCCTG
INT 3R	Intron 3	GTTGTTTAGGACAGTGCT
584R	Intron 3	TCACTAGTGATGGTTAACCTCACAG
412R	Exon 3	CAGAACCACA GAGACCACCCAAAT
78F	Exon 3	TTTGGGTGGTCTCTGTGGTTCTGG
417R	Exon 4	GTAGAAACTGAACAGCCACCAATC
5To4R	Intron 5	GAACAGCTGCCACGTCTC
Exon 5R	Exon 5	TGAGGTGAAGGGGAAGCCAACAGAGA
32F	Exon 5	TGGTCCTCGTGTTTGCTCTCTG
359R	Exon 6	TACAGAGCGATTGGATTGATGC
LTNLF	LTNL cassette	GCCTCTGTTCCACATACACTTCATTC
Tie2 98F	Cre cDNA	CGCATAACCAGTGAAACAGCATTGC

Table 2.1

Sequences of primers used in the generation of EC-specific ET_B receptor knockout mice.

2.1.6 ENZYMES

Genecraft NeoThermMinus (Genecraft, Germany) Taq polymerase or the Expand Long Template PCR system (Roche Molecular Biochemicals, Mannheim, Germany) was utilised for all PCR genotyping reactions. PCR fragments for cloning reactions were prepared using *pfu* DNA polymerase (Promega, Madison,USA) unless otherwise stated. T4 polyneucleotide Kinase (Product number EK0031) and T4 DNA ligase (Product number ELO335) were supplied by MBI Fermentas (St Leon-Rot, Germany). Calf intestinal alkaline phosphatase (CAIP) (Product number 713023) and Klenow enzyme (Product number 1008404) were supplied by Roche Molecular Biochemicals. Roche Molecular Biochemicals supplied all other enzymes used unless otherwise stated.

2.1.7 BACTERIAL STRAINS

All plasmids were maintained in XLI Blue *Escherichia coli* (*E. coli*) of genotype *supE hsdR lac⁻ F' proAB⁺ lacI^q lacZ*ΔM15 (Bullock *et al.*, 1987) unless otherwise stated. λ bacteriophage vectors were propagated in LE392 *E. coli* of genotype *supE supF hsdR* (Borck *et al.*, 1976). λ bacteriophage were converted to plasmids in BNN132 strain *E. coli*, produced by infecting JM107 cells of genotype *endAI, gyr96, thi, hsdR17, supE44, relAI, Δ(lac-proAB), (F', traD36, proAB⁺, lacI^qZΔM15)* with λKC as described by Elledge *et al* (Elledge *et al.*, 1991) .

2.1.8 PROBES, PLASMIDS AND CLONING VECTORS

A probe used for screening of the λPS 129/SV genomic library, consisting of a fragment of the mouse ET_B receptor gene cDNA (Hosoda *et al.*, 1994) spanning from position 563 to 1363, was a kind gift of Dr Paula Smith (University of Edinburgh, Edinburgh, UK). The loxP-thymidine kinase-neomycin-loxP (LTNL) selection cassette (illustrated in Figure 2.4) used in the construction of the pλPW and pλPNoDT targeting vectors was a kind gift of Dr Noboru Komiyama (Centre for Genome Research, University of Edinburgh, Edinburgh, UK) and was cloned into the *Xba* I site of pBluescript® II KS+ (Stratagene, Heidelberg, Germany; illustrated in Figure 2.5). pCAGGS-dt, a plasmid containing a diphtheria toxin gene under the transcriptional regulation of a chicken actin promoter (illustrated in Figure 2.6), the Cre-recombinase expression plasmid pMC-Cre (Araki *et al.*, 1995) and the LoxP²ROSA plasmid (illustrated in Figure 2.7) were kindly donated by Dr A. Smith (Centre for Genome Research, University of Edinburgh, Edinburgh, UK) and were used in the construction of pλPW. The diphtheria toxin gene cassette was subcloned into the plasmid pSP72poly1 (Figure 2.8), a gift of Dr M. Sharp (University of Edinburgh, Edinburgh, UK). This vector was constructed by removal of the polylinker from pSP72 (Promega, Southhampton, UK) and insertion of annealed, complementary oligodeoxynucleotides (S. Morley *et al.*, unpublished data). The plasmid pλP (illustrated in Figure 2.9) was generated by automatic subcloning from a λPS clone

and was subsequently modified through the addition of an *Xho* I site to produce the plasmid pλPXho (Figure 2.10).

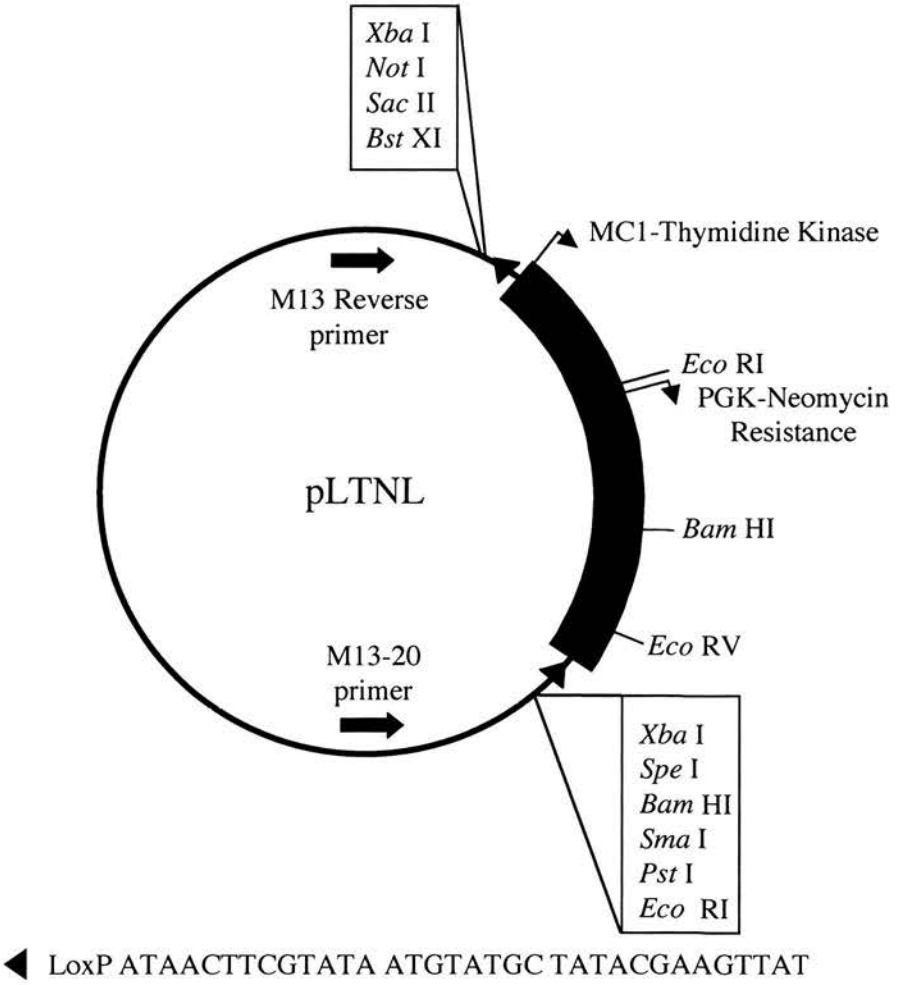

Figure 2.4

LoxP/Thymidine Kinase/Neomycin phosphotransferase/LoxP (LTNL) in pBluescript KS+. MC1; Mario Cappeci-1 promoter. PGK; Phosphoglucokinase promoter. Black triangle; loxP site. Primer sequences are illustrated in Figure 2.5 . The 3.8 kb *Xba* I fragment was sub-cloned into the targeting constructs and permitted the selective propagation of targeted ES cell clones in neomycin-containing culture media.

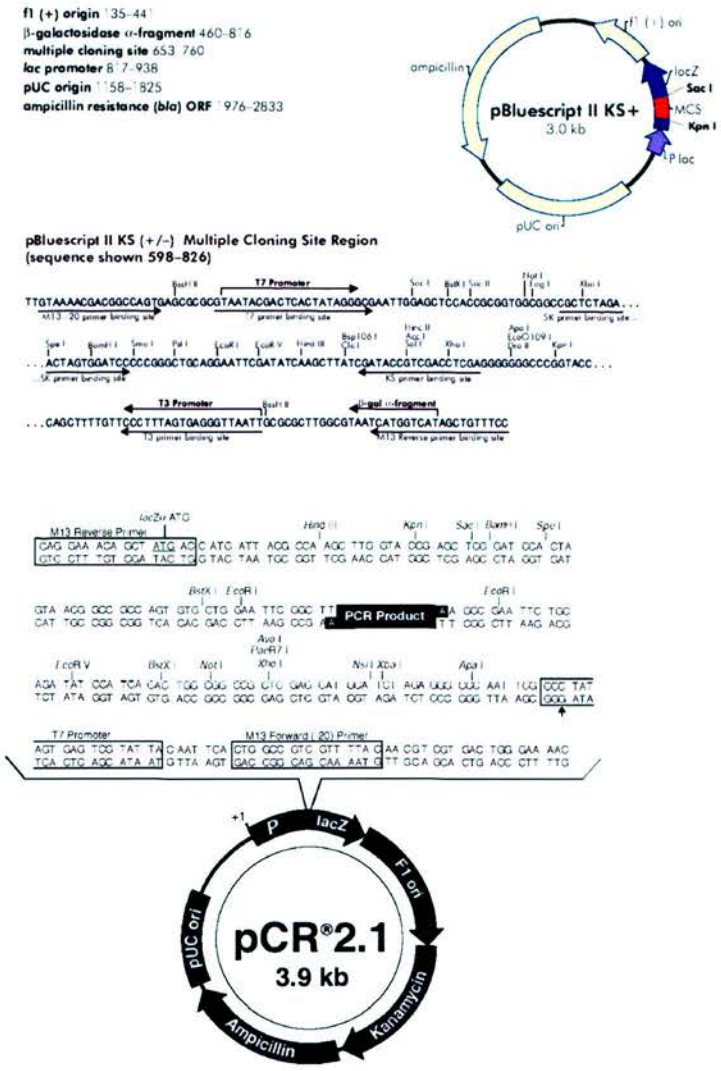

Figure 2.5

The pBluescript KS plasmid (upper panel) was utilised as a vector during preparation of targeting vectors. PCR 2.1 (lower panel) was used for cloning of PCR products. See text for details.

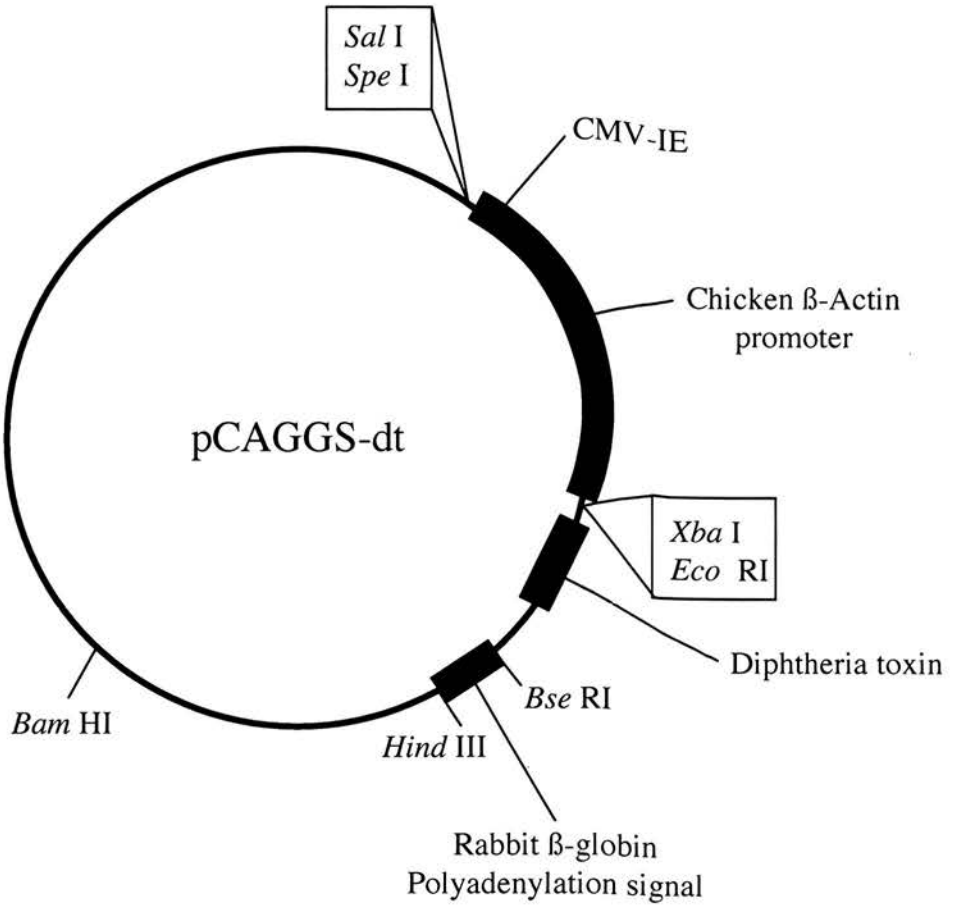

Figure 2.6

pCAGGS-dt; 5372 bp. The Diphtheria toxin (DT) gene and associated human cytomegalovirus immediate early enhancer (CMV-IE), chicken β-actin promoter and rabbit β-globin polyadenylation signal were excised as a 2857 bp *Spe* I – *Hind* III fragment and sub-cloned into a pSP72 poly 1 shuttle vector. The *Xho* I (blunt) – *Not* I fragment was subsequently sub-cloned from the shuttle vector into pλP4-5 to generate pλP4-dt.

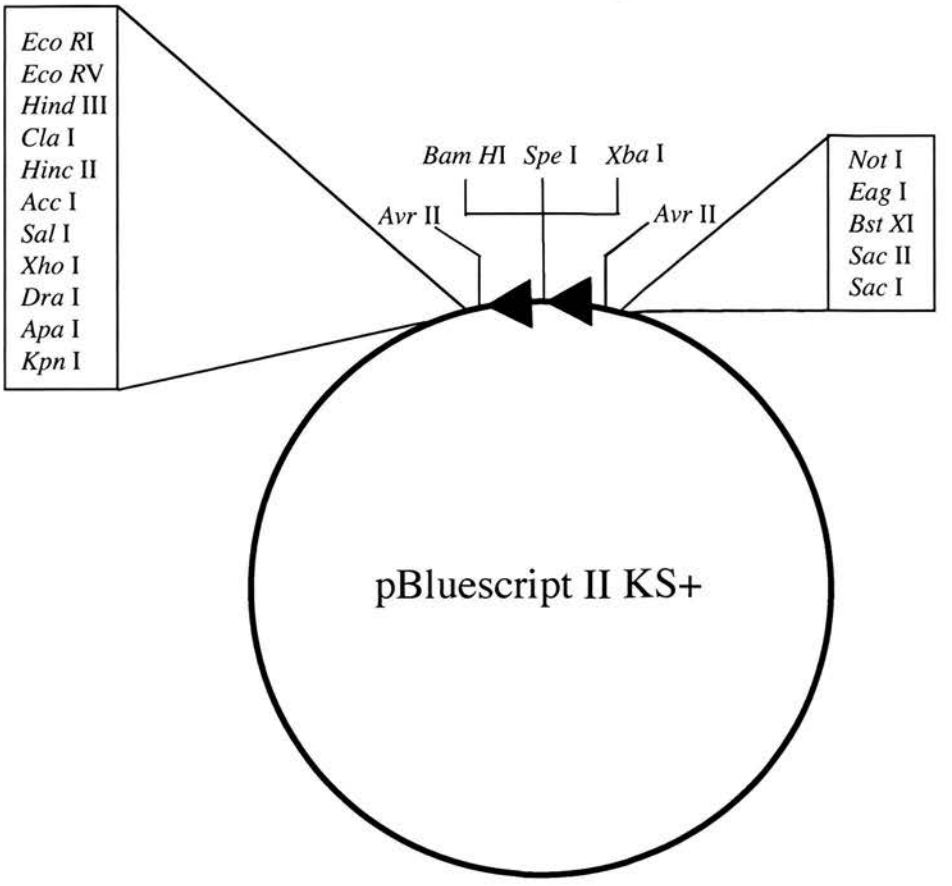

CCT AGG ATA ACT TCG TAT AAT GTA TGC TAT ACG AAG TTA TCC CCT AGG

Avr II — LoxP — *Avr* II

Figure 2.7

LoxP^{2}ROSA construct used during the construction of the targeting vectors pλPW and pλPW(NoDT). LoxP sites (black triangles) are head-to-tail and fragments cloned between loxP sites will be deleted leaving the sequence shown above following Cre recombinase-mediated recombination events.

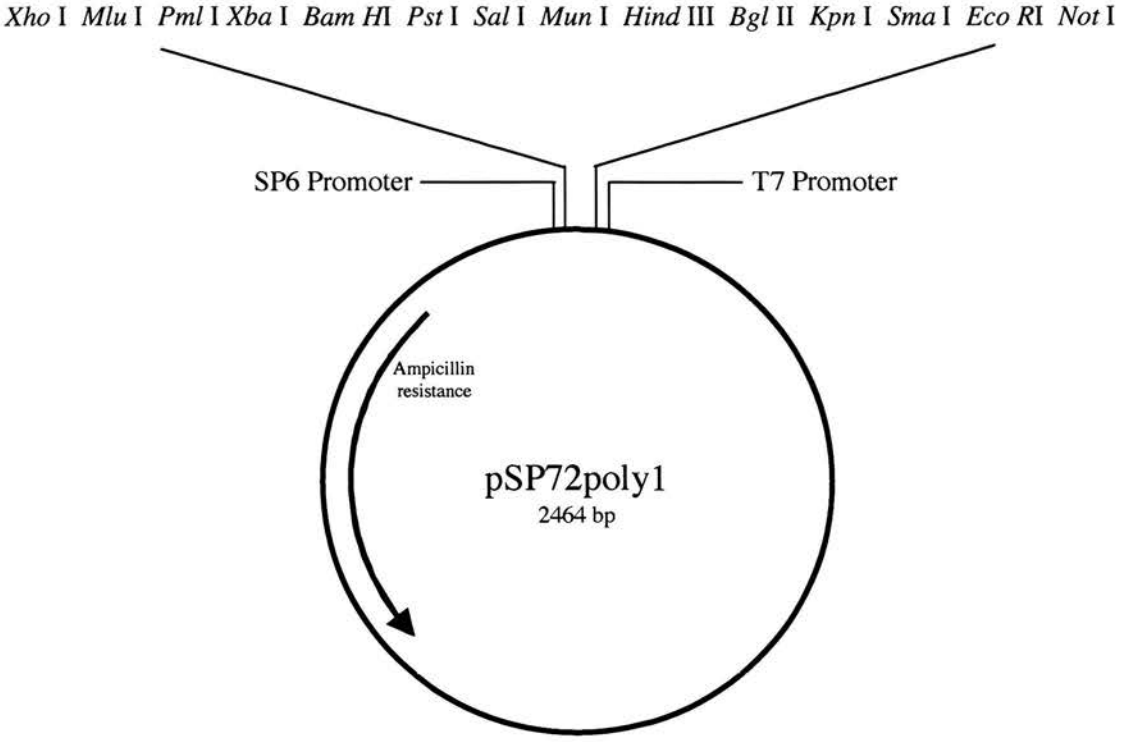

Figure 2.8

pSP72poly1 shuttle vector used in the construction of pλPW. This plasmid was constructed by Dr Steve Morley (University of Edinburgh) through modification of the polylinker region of the pSP72 plasmid (Promega, UK).

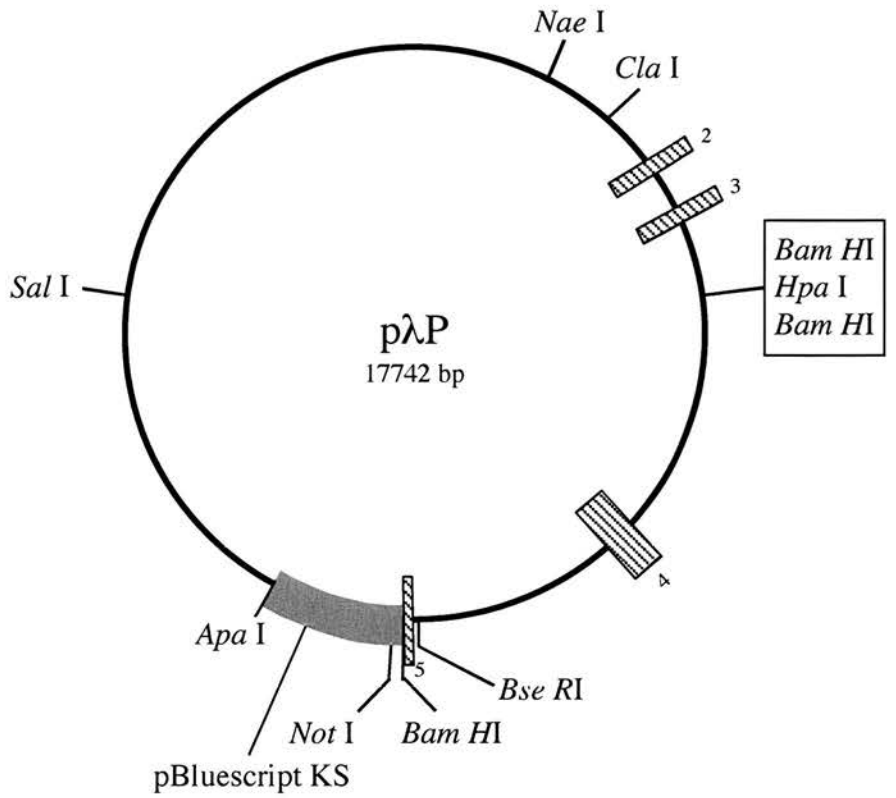

Figure 2.9

The plasmid pλP was produced by automatic subcloning (Nehls *et al.*, 1994) of the bacteriophage λP, identified from a λPS 129/SV mouse genomic DNA library. λP contains a 14748 bp region of the mouse ET_B receptor gene spanning from the final 12104 bp of intron 1 to the *Bam H*I site located 54 bp after the start of exon 5. Shaded rectangles = Exons; single line = introns; solid rectangles = pBluescript KS vector.

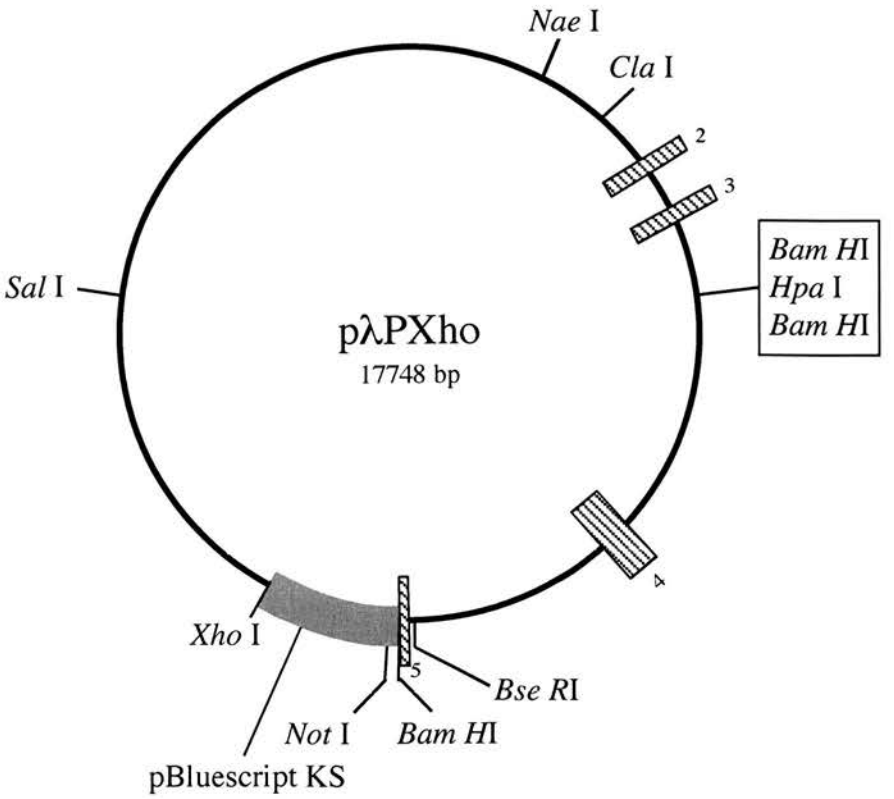

Figure 2.10

pλPXho was produced by the addition of an *Xho* I site adjacent to the *Apa* I site within the pBluescript SK polylinker region of pλP and was used in the construction of targeting vectors. Shaded rectangles = Exons; single line = introns; solid rectangles = pBluescript KS vector.

2.1.9 EMBRYONIC STEM CELLS

E14Tg2a ES cells were a kind gift of Dr J. Ure (Centre for Genome Research, Edinburgh, UK). All culture was performed in media prepared with filter sterilised UHP water (Elgestat Prima Reverse Osmosis Filter and Elgastat UHP water purifier). Media was supplemented with 10% foetal calf serum (FCS) and DIA/LIF (1:1000 dilution of 100 units/ml stock solution, titres prepared by D. Rout, Centre for Genome Research) as previously described (Smith *et al.*, 1988, Williams *et al.*, 1988). Batches of foetal calf

serum were tested prior to use in established ES cell cultures by Mr D. Rout (University of Edinburgh, Edinburgh, UK).

2.1.10 ANIMALS

The inbred mouse line C57BL/6 was used for the derivation of blastocysts for the production of chimaeric mice. Blastocysts were implanted in foster mothers of the outbred MF1 Swiss albino strain. Chimaeric mice were crossbred with BKW mice (B&K Universal Ltd., Hull, UK) to test for germline transmission. Floxed ET_B mice produced in this study were bred at the Centre for Genome Research and the Medical Faculty Animal Area, University of Edinburgh. Tie2-Cre transgenic mice were produced by injection of a Tie2Cre transgene into fertilised C57BL/6 x $SJLF_1$ oocytes (Kisanuki *et al.*, 2001) and were a kind gift of Professor M. Yanagisawa, University of Texas. All mice were ear tagged for identification. Mice were given free access to standard breeding chow (0.8% NaCl) or high salt chow (7.6 % NaCl; Special Diet Services, Witham, UK) and water. Twelve hour diurnal cycles were maintained throughout. Animal house humidity was maintained at 50% ± 10% and the temperature held at 21°C ± 2°C. All breeding, maintenance and experimental protocols were performed in accordance with the Animals (Scientific Procedures) Act (UK) 1986.

2.1.11 MOLECULAR BIOLOGY METHODS

2.1.11.1 *Alkaline lysis miniprep*

Three ml of Luria-Bertani medium (L-Broth; 10g/l bacto-tryptone, 5.0 g/l bacto-yeast extract, 10g/l NaCl, pH 7.2)) containing ampicillin (100 μg/ml) were inoculated with a single bacterial colony and incubated overnight at 37°C with continuous shaking (225-250 rpm). The following day, 1.5 ml of the culture was transferred to an Eppendorf tube and the bacteria pelleted by centrifugation (12,000 x g, 5 minutes). The supernatant was withdrawn and the pellet resuspended by vortexing in 100 μl of lysis buffer (25mM Tris HCl pH 8.0, 10 mM EDTA and 10% (w/v) glucose). Two hundred μl of 0.2M NaOH

and 1% (w/v) SDS were added and the tube inverted gently 5 or 6 times. Tubes were then incubated on ice for 5 minutes before the addition of 150 µl of ice-cold neutralisation buffer (3.0M potassium acetate, 2.0M acetic acid). The contents were mixed by vortexing and incubated on ice for 5 minutes. Tubes were then spun (12,000 x g, 5 minutes) to pellet cell debris and chromosomal DNA. The supernatant containing circular plasmid DNA was removed to a fresh tube and one volume of phenol:chloroform:isoamyl alcohol (25:24:1) added. The aqueous phase was separated by centrifugation (12,000 x g, 5 minutes) and removed to a fresh tube. Two volumes of ice cold 100% ethanol were added and plasmid DNA precipitated by centrifugation at 12,000 x g at 4°C. The pellet was then washed with 70% ethanol and air-dried for 10 minutes. DNA was dissolved in 50 µl of TE, pH 8.0 containing 20 µg/ml DNase-free pancreatic RNase and stored at -20°C until use. This method routinely yielded ~5µg of DNA.

2.1.11.2 *Large scale plasmid DNA preparation*

Up to 200 µg of plasmid were prepared using Qiagen HiSpeed Plasmid Midi kits™ (Qiagen (UK) Ltd, Crawley, UK; Product number 12643). A single colony of bacteria was inoculated into a 3 ml starter culture of L-broth containing 100 µg/ml of ampicillin. The culture was incubated at 37°C with continuous shaking for 8 hours. The starter culture was then diluted in 50 ml of L-broth containing 100µg/ml of ampicillin and incubated overnight at 37°C with continuous shaking. The culture was transferred to a 50 ml Falcon tube and the bacteria harvested by centrifugation (6000 x g, 15 minutes) at 4°C in a Beckmann J6B centrifuge. The supernatant was removed and the bacterial pellet resuspended in 6 ml of ice cold Buffer P1 (50mM Tris Cl pH 8.0, 10mM EDTA and 100 µg/ml of DNase-free RNase). Six ml of Buffer P2 (0.2mM NaOH and 1% (w/v) SDS) were added and the contents mixed by gently inverting the tube 5 times. Samples were incubated at room temperature for 5 minutes before adding 6 ml of ice cold Buffer P3 (3.0M potassium acetate pH 5.5). The contents were mixed by gentle inversion and transferred immediately to a QIAfilter™ cartridge (Qiagen (UK) Ltd, Crawley, UK).

This was left for 10 minutes at room temperature to allow the precipitate of protein, genomic DNA and detergent to float to the surface. The cell lysate was then filtered through the QIAfilter™ cartridge and the cleared lysate collected into a HiSpeed Midi™ column previously equilibrated with 4 ml of Buffer QBT (750mM NaCl, 50mM MOPS pH 7.0, 15% (v/v) isopropanol and 0.15% Triton® X-100 (v/v)). The column selectively binds plasmid DNA and allows degraded RNA, cellular proteins and metabolites to be washed out by the subsequent addition of 20 ml of a medium salt buffer (Buffer QC containing 1.0M NaCl, 50mM MOPS pH 7.0 and 15% isopropanol (v/v)). After washing, plasmid DNA was eluted with 5 ml of a high salt buffer (Buffer QF; 1.25mM NaCl, 50mM Tris Cl pH 8.5 and 15% isopropanol (v/v) and collected into a 15 ml falcon tube. Plasmid DNA was precipitated over 5 minutes with 0.7 volumes of room temperature isopropanol and recovered with a QIAprecipitator Module™ (Qiagen (UK) Ltd, Crawley, UK). This filter traps DNA as a thin layer, allowing removal of isopropanol and air-drying. DNA was eluted into an Eppendorf tube by the addition of 0.5 ml of TE pH 8.0.

2.1.11.3 *Quantitation of Nucleic Acids*

Optical absorbance at 260nm (OD_{260}) of DNA-containing solutions was measured using a Pharmacia Biotech spectrophotometer (model number 80-2092-26). The spectrophotometer was zeroed at 260nm and 280nm with a 200 µl sample of dH_2O prior to sample measurement. DNA samples were diluted 1:100 in dH_2O to a final volume of 200 µl. OD_{260} of samples was multiplied by 50 for double-stranded DNA plasmids and then by 200 to produce a concentration of DNA in µg/ml. For more concentrated solutions, dilutions of the stock plasmid solution were prepared such that spectrophotomeric readings were between 0.1 and 1.

2.1.11.4 *Sequencing of plasmids*

All sequencing reactions were performed by Mrs Nina Kotelevtsev (University of Edinburgh, UK) using an ABI 377 Prism Sequencer (Perkin Elmer Applied Biosystems

Division, Foster City, USA) and the Big Dye Terminator Ready Reaction Kit™ according to the manufacturer's protocol.

2.1.11.5 *Restriction digestion*

All restriction digestion reactions were performed according to the guidelines of Sambrook *et al* (Sambrook *et al.*, 1989) at 37°C unless otherwise stated. DNA was digested at a concentration of 0.1-0.5 μg/μl with less than 10% (v/v) of enzyme (equivalent to less than 5% (v/v) of glycerol). After the appropriate incubation time, reactions were checked for completion by running an aliquot containing 0.1-1.0 μg of DNA on a 0.8% agarose gel. Reactions were terminated by heat inactivation of the enzyme (65°C for 15 minutes) or, for thermostable enzymes, by phenol:chloroform:isoamyl alcohol extraction followed by ethanol precipitation of the digested DNA.

2.1.11.6 *Agarose gel electrophoresis*

DNA molecules were separated according to size using 0.8% agarose gel electrophoresis unless otherwise stated. All gels were prepared with SeaKem LE agarose (FMC Bioproducts, Rockland, USA) using 1 x TAE solution (40mM Tris-acetate, 1mM EDTA) and were stained with 0.5μg/ml of ethidium bromide (Sigma-Aldritch, Steinheim, Germany; Product code E-8752). Samples were mixed with 6 x loading dye solution (0.09% bromophenol blue, 0.015% xylene cyanol FF and 10% glycerol) to a final concentration of 1 x before electrophoresis. All sizes were judged according to standard size markers run concurrently on the same gel. The size markers used were λ DNA digested with *Hind* III (DNA fragment sizes 23130, 9416, 6557, 4361, 2322, 2027, 564 and 125 base pairs), λ DNA digested with *Hind* III and *EcoR* I (DNA sizes 21226,5148, 4973, 4268, 3530, 2027, 1904, 1584, 1375, 947, 831, 564 and 125 base pairs) and the GeneRuler™ 100 bp DNA ladder (DNA fragment sizes 1000, 900, 800, 700, 600, 500, 400, 300, 200, 100 and 80 bp; MBI Fermentas, St Leon-Rot, Germany). DNA was visualised on the gel by UV transillumination and photographed with a

Polaroid MP4 Land Camera (Polaroid (UK) Ltd, St. Albans, UK) with Polaroid 667 (ISO3000/36°) film (Polaroid, UK). Gel images were also digitally photographed using a transilluminator and digital acquisition system (Ultra-Violet Products Ltd., Cambridge, UK.)

2.1.11.7 *DNA fragment recovery from agarose gels*

DNA fragments utilised in ligation reactions were recovered following agarose gel electrophoresis using a QIAEX II™ kit (Qiagen (UK) Ltd, Crawley, UK; Product number 20021) according to the manufacturer's instructions. 3-5 μg of plasmid DNA were digested with the appropriate restriction enzyme(s) at 37°C until completion. Prior to reaction termination, a 2 μl aliquot was run on a 0.8% TAE mini-gel to ensure completion of the restriction digestion. The remaining sample was then loaded into a single slot agarose gel. Following electrophoresis, the desired fragment was cut from the gel with a sterile scalpel and the gel slice dissolved in 3 volumes of solubilisation Buffer QX1 (3.0M NaCl, 4.0M sodium perchlorate, 10mM Tris-HCl pH 7.0, 10mM sodium thiosulphate) for fragments between 100 bp-4 kb, or 3 volumes of Buffer QX1 and 2 volumes of dH_2O for fragments >4 kb. For 2-10 μg of DNA, 30 μl of QIAEX II™ solution containing resuspended silica gel particles was added and the tube incubated at 50°C for 10 minutes with vortexing every 2 minutes. The high salt solution promotes dissociation of DNA binding proteins and the efficient adsorption of DNA to the silica particles. Once completely solubilised, the solution was centrifuged (12,000 x g, 30 seconds) and the supernatant discarded. The pellet was resuspended in a further 500 μl of Buffer QX1 and centrifugation repeated to remove any remaining agarose, proteins, salt or ethidium bromide. The pellet was washed twice with 500 μl of Buffer PE (70% (v/v) ethanol, 100mM NaCl, 10mM Tris-HCl, pH 7.5) and air dried for 20 minutes. The DNA fragment was then eluted from the silica particles by resuspending the pellet in 20 μl of TE buffer, pH 8.0. Following centrifugation, the supernatant containing the DNA fragment was removed and yield checked on a 0.8% agarose gel. The remainder was stored at –20 °C until required.

2.1.11.8 *Ligation*

Ligation of DNA fragments was performed with T4 DNA ligase (MBI Fermentas). Quantification of DNA fragments prior to ligation was achieved by visualisation of an aliquot of each fragment on a 0.8% agarose gel. For cloning small fragments into plasmid vectors, a molar excess of approximately 3:1 (fragment:vector) was used. The DNA fragment and vector cut were mixed with 2 µl of 10 x ligation buffer (400mM Tris HCl, 100mM $MgCl_2$, 100mM DTT and 5mM ATP, pH 7.5), 1 unit of T4 ligase and dH_2O to a final volume of 20 µl. A control reaction containing each of the above ingredients with the exception of the DNA fragment was also set up. Ligations were performed in a MJ Research Peltier Thermal Cycler PT-200, using the following programme: 16°C for 30 seconds, 24°C for 30 seconds, repeated for 60 cycles. The reaction was then held at 16°C until used.

2.1.11.9 *Creating blunt ends for ligation*

The large fragment of DNA polymerase 1 (Klenow fragment) (Roche Diagnostics GmbH, Mannheim, Germany; Product number 1008404) was used to fill the recessed 3' termini created by DNA digestion with restriction enzymes (Klenow and Henningsen, 1970). Reactions were performed in the restriction enzyme buffer used for the preceding digestion reaction following heat inactivation of the enzyme. For heat stable enzymes, the enzyme was removed by phenol:chloroform:isoamyl alcohol extraction, ethanol precipitation of DNA and resuspension in TE buffer. A restriction enzyme buffer required for subsequent digestion reactions or DNA polymerase buffer (50mM Tris-HCl, 15mM $(NH_4)_2SO_4$, 7mM $MgCl_2$, 0.1mM EDTA, 10mM 2-mercaptoethanol, 0.02 mg/ml BSA, pH 8.8) was then added, supplemented with 33 µM dNTPs. Reactions were incubated at 37°C for 30 minutes and terminated by heating the mixture to 65°C for 20 minutes.

2.1.11.10 *Dephosphorylation of DNA*

5' phosphate residues were removed from digested vector DNA with Calf Intestinal Alkaline Phosphatase (CAIP) (Boehringer Mannheim GmbH, Mannheim, Germany; Product number 713023). Restriction enzymes were heat inactivated, 1 unit of CAIP added and the reaction mixture incubated for 30 minutes at 37°C. CAIP was removed prior to subsequent ligation reactions by phenol:chloroform:isoamyl alcohol extraction and the remaining DNA precipitated with ethanol.

2.1.11.11 *Methods for cloning of PCR products*

2.1.11.12 *Klenow-Kinase-Ligase*

PCR products were cloned into plasmid vectors other than PCR2.1 using the Klenow-Kinase-Ligase procedure, as described by Lorens (Lorens, 1991). This method produces cancatemeric DNA molecules that facilitate restriction digestion by the internalisation of enzyme recognition sites. PCR products from 3-5 50μl reactions were pooled and extracted with phenol:chloroform:isoamyl alcohol (25:24:1) followed by precipitation with 2.5 volumes of ice cold 100% ethanol. DNA was pelleted by centrifugation (12,000 x g, 15 minutes) at 4 °C and washed in 70% ethanol. The pellet was then air-dried for 5 minutes and resuspended in 12.6 μl of dH_2O. 2.5 μl of 10 x ligase buffer (400mM Tris-HCl, 100mM $MgCl_2$, 100mM DTT and 5mM ATP, pH 7.8), 0.2mM dNTPs, 5 units of Klenow enzyme, 4 units of T4 polynucleotide kinase and 2 units of T4 DNA ligase were then added such that the final volume of mixture was 25 μl. The mixture was incubated at 25 °C for 60 minutes during which time the PCR products self-ligate to produce multimeric DNA substrates for subsequent cleavage by restriction enzymes. This is achieved by polishing, phosphorylating and ligating PCR termini to produce cancatemeric DNA substrates. Completion of this process was checked on a 0.8% agarose gel to demonstrate the presence of cancatemers of the appropriate molecular weight. The reaction mixture was extracted with phenol:chloroform:isoamyl alcohol (25:24:1) and precipitated with ethanol to remove contaminating enzymes and dNTPs.

The pellet was then washed with 70% ethanol, air-dried and resuspended in 10 µl of TE, pH 8.0. 2 µl of 10 x restriction enzyme buffer, 1µl of restriction enzyme and 7 µl of dH_2O were added. Enzymatic cleavage of cancatemeric DNA at 37°C for 4 hours was followed by a further phenol:chloroform:isoamyl alcohol (25:24:1) extraction and ethanol precipitation. The washed and dried pellet was resuspended in 20 µl of TE pH 8.0.

2.1.11.13 *TA Cloning® of PCR products*

PCR products were cloned into the vector PCR®2.1 using the TA Cloning® kit (Invitrogen BV, The Netherlands). Genomic DNA was amplified with *Taq* polymerase to produce PCR products with a single deoxyadenosine at the 3' terminus. One µl of the PCR reaction mixture was mixed with 1 µl of 10x ligation buffer (60mM Tris-HCl pH 7.5, 60mM $MgCl_2$, 50mM NaCl, 1mg/ml bovine serum albumin (BSA), 70mM β-mercaptoethanol, 1mM ATP, 20mM dithiothreitol and 10mM spermidine), 50 ng of PCR2.1 vector, 1 µl of T4 DNA Ligase (4.0 Weiss units) and dH_2O to a final volume of 10 µl. The linear PCR2.1® vector (illustrated in figure Figure 2.5) contains a single 3' deoxythymidine residue in the cloning site that facilitates the ligation of PCR products with 3' deoxyadenosine overhangs. Reactions were incubated for 16 hours at 14 °C before being centrifugation briefly and placed on ice. Two µl of the ligation mixture were then used for electroporation of XLI *E. coli*. Colonies were plated on LB agar plates containing ampicillin (100 µg/ml) and grown overnight at 37°C. Individual colonies were selected at random and plasmid DNA isolated by alkaline lysis miniprep. Restriction enzyme digestion and DNA sequencing were used to confirm the presence and orientation of the ligated PCR product.

2.1.11.14 *Preparation of electrocompetent cells*

Electroporation was performed with the XLI Blue strain of *E. coli* prepared using a method adapted from Chung (Chung *et al.*, 1989). This method typically produces 1-10 x 10^8 transformants/µg of DNA. A scraping of a frozen aliquot of *E. Coli* was streaked

on an LB plate and incubated overnight at 37°C. Fifty ml of LB media were inoculated with a single bacterial colony and incubated for 12-16 hours at 37°C with continuous shaking at 200-225 rpm in a 250 ml flask. This starter culture was diluted into 1 L of LB medium and grown at 37°C with continuous shaking until the optical density at 550 nm (OD_{550}) was between 0.5 and 0.6. The culture was transferred to 4 x 250 ml pre-chilled centrifuge bottles. All subsequent manipulations were performed at 4°C to achieve maximum electrocompetence of the bacteria. Cultures were spun at 2000 x g for 15 minutes and the supernatant decanted. The cell pellet was resuspended in 250 ml of ice-cold sterile dH_2O and the cells centrifuged at 2000 x g for a further 15 minutes. The supernatant was decanted and the cells resuspended in 125 ml of ice-cold dH_2O. Following a further 15 minute centrifugation step, the supernatant was decanted and the cells resuspended in 10 ml of sterile 10% glycerol using a pre-chilled pipette. The solution was transferred to a sterile 50 ml centrifuge tube, spun (4000 x g, 15 minutes) and the glycerol decanted. Cells were resuspended in 1 ml of ice-cold sterile 10% glycerol. The cell suspension was snap frozen in 100 µl aliquots using an ethanol/dry ice bath and stored at -80°C.

2.1.11.15 *Transformation of E.Coli by electroporation*

Electroporation of competent XLI Blue *E. Coli* was performed using a Bio-Rad Gene Pulser II (Bio-Rad Inc., Hemel Hempstead, UK; Product number 165 2112) with the capacitor set to 25 µF, 2.5 KV and pulse controller at 200 Ω. Forty µl of competent cells were defrosted on ice and immediately mixed with 3-4 µl of ligation mix (~0.5-2 µg of DNA). The mixture was transferred to an ice cold sterile electroporation cuvette and the pulse applied, typically producing a pulse of 12.5 KV/cm with a time constant of 4.6-4.8 msec. Cells were immediately resuspended in 300 µl of room temperature SOB medium (5mM $MgSO_4$, 5mM $MgCl_2$, 20mM glucose) and incubated at 37°C for 40 minutes to permit the expression of plasmid antibiotic resistance genes. Aliquots of 5, 50 and 200 µl were plated out on L-agar plates containing ampicillin (100 µg/ml) and grown overnight at 37°C.

2.1.11.16 *Colony and Plaque lifts*

Bacterial cells or bacteriophage plaques were plated at suitable density onto the appropriate selection media and incubated overnight at 37°C. Petri dishes were then pre-cooled for 30 minutes at 4°C to prevent smearing of colonies before lifts were taken. Using blunt ended clean forceps, 8cm diameter Hybond N™ (Amersham Pharmacia Biotech) positively charged nylon membranes were gently lowered onto the surface of the agar and marked asymmetrically with 5 pinholes to facilitate orientation of the final autoradiograph. For bacterial colonies, the membrane was transferred colony-side up onto a fresh agar plate and both plates were incubated for 2 hours at 37 °C to allow further growth of the transferred and residual colonies. DNA was recovered from colonies or bacteriophage particles by denaturing membranes for 3 minutes on 3MM paper soaked with a solution of 0.5M NaOH and 1.5M NaCl. Membranes were neutralised for 3 minutes with 1.5M NaCl, 0.5M Trizma base solution (pH 7.4) before being washed vigorously in 2 x SSC to remove cellular debris. Discs were then air-dried and DNA fixed to the membrane by oven baking for 2 hours at 80°C or by UV crosslinking at a constant energy of 1200J (UVP CL-1000 UV crosslinker, UVP Inc, Upland, USA; Product number 95-0174-02).

2.1.11.17 *Preparation of random primed radio-labeled probes*

Probes were synthesised using a protocol modified from Feinberg (Feinberg and Vogelstein, 1983). Approximately 50 ng of gel purified template DNA, 2.5 µl of 1x hexanucleotide solution (55 O.D. units/ml) and dH_2O were mixed to a final volume of 14 µl and boiled for 5 minutes. The solution was cooled immediately to -20°C and centrifuged briefly before the addition of 5 µl of 5x oligodeoxynucleotide labelling buffer (250mM Tris-HCl pH 8.0, 25mM $MgCl_2$, 5mM β-mercaptoethanol, 2.0mM DTT, 2.0mM dATP, 2.0mM dGTP, 2.0mM dTTP, 1M HEPES pH 6.6 and 1mg/ml oligonucleotides), 5 µl α^{32}P-dCTP (3000 Ci/mmol; 10µCi/µl) and 1 µl of Klenow enzyme (2.0 units/µl). The probe was labelled for 2 hours at 37°C before removal of unincorporated nucleotides using a NAP-5 column (Pharmacia Biotech). The reaction

mixture was diluted to a final volume of 400 µl with TE (pH 8.0) and loaded onto an equilibrated column. The sample was eluted in 600µl of TE and denatured by boiling for 5 minutes. The probe was immediately cooled on ice before addition to the hybridisation solution. Radioactivity of a 2 µl aliquot of the probe diluted into 2.5 ml of Ultragold solution was measured using a Packard 1600CA Series scintillation counter (Packard, Pangborne, UK). Only probes with activity of 2.5-5.0x10^7 counts/minute (cpm) were used for hybridisation experiments.

2.1.11.18 *Southern Blot Analysis*

Approximately 5 µg of genomic DNA were digested overnight with 10 units of restriction enzyme. Reactions were terminated by heat-inactivation of the enzyme at 65°C for 15 minutes. The entire sample was loaded on a 0.8% agarose gel and DNA fragments separated by electrophoresis. A photograph of the gel was taken alongside a transparent ruler. The DNA fragments were transferred by capillary action onto a positively charged nylon membrane (Boehringer Maanheim, Germany; Product number 1209272) as described by Southern *et al* (Southern, 1975). Capillary transfer was performed by a modified rapid alkaline (0.4M NaOH, 1M NaCl) transfer procedure as described previously (Chomczynski and Qasba, 1984, Reed and Mann, 1985). Nylon membranes were then neutralised with 2 x SSC for 15 minutes and DNA fixed to the membrane by UV crosslinking at 254nm followed by baking at 80°C for 2 hours. Membranes were washed in 25ml of pre-hybridisation solution (0.25M Na_2HPO_4 (pH 7.2), 7% (w/v) SDS, 1.0mM EDTA and 50-200 µg/ml of sheared and denatured salmon sperm DNA) in a pre-warmed Techne hybridisation bottle (Techne (Cambridge) Ltd, Cambridge, UK) at 68°C for 1 hour. The bottles were continuously rotated using a Techne hybridisation oven (Techne (Cambridge) Ltd, Cambridge, UK. Product number HB-1D). The pre-hybridisation solution was then discarded and replaced with a further 25 ml pre-warmed to 68°C and containing the heat denatured radio-labelled probe at 10^6-2.5 x 10^6 cpm)/ml. Membranes were washed for 16 hours by continuous rotation at 68 °C before the hybridisation solution was discarded. Membranes were then washed

twice for 10 minutes in 25 ml of 20mM Na_2HPO_4 (pH 7.2), 1.0mM EDTA (pH 8.0) and 5% (w/v) SDS, followed by 2 further 10 minute washes in 20mM Na_2HPO_4 (pH 7.2), 1.0mM EDTA (pH 8.0) and 1% (w/v) SDS. Once dried, membranes were covered with Saran Wrap and placed in an autoradiography cassette with two enhancement screens and Kodak X-Omat film. Autoradiographs were exposed for a minimum of 16 hours at -70°C prior to development.

2.1.12 SCREENING OF THE BACTERIOPHAGE λ 129/SV MOUSE GENOMIC DNA LIBRARY

The λ 129/SV library (Nehls *et al.*, 1994) was a kind gift of Dr Andrew Smith (University of Edinburgh, Edinburgh, UK).

2.1.12.1 *Preparation of plating bacteria*

A single colony of LE392 *E. coli* was inoculated into 50 ml of LB media supplemented with 0.2% maltose and grown overnight at 37°C with continuous shaking. Bacteria were collected by centrifugation at 4000 x g for 10 minutes and the supernatant discarded. The pellet was resuspended in sterile 0.01M $MgSO_4$ to an $OD_{600} = 2$ (~1.6×10^9 cells/ml) before storage at 4°C.

2.1.12.2 *Plating of bacteriophage λ*

Tenfold serial dilutions of bacteriophage plaques were prepared in SM media (50mM Tris Cl (pH 7.5), 10mM $MgSO_4$, 0.1M NaCl, 0.01% geletin). One hundred µl of each bacteriophage dilution were then mixed with 100 µl of plating bacteria and incubated at 37°C for 20 minutes. The bacteriophage/bacteria mixture was mixed with 3 ml of molten (45°C) top agar (L broth supplemented with 1% agar and 10mM $MgSO_4$), vortexed briefly and poured onto pre-dried LB agar plates. Plates were gently rotated to ensure an even distribution of bacteria before overnight incubation at 37°C.

2.1.12.3 *Picking of bacteriophage λ plaques*

A plug of plaque and underlying agar was picked using a Pasteur pipette. Plugs were inoculated into 1 ml of SM containing a single drop of chloroform and left at room temperature for 2 hours before storage at 4°C. For long term storage, DMSO (7% v/v) was added and the solutions stored at -70°C.

2.1.12.4 *Screening of bacteriophage λ plaques by in-situ hybridization*

Bacteriophage λPS was grown at an appropriate density on agar plates as described in section 2.1.12.2. Bacteriophage particles and DNA were then transferred to nitrocellulose membranes using a protocol modified from the method of Benton and Davies (Benton and Davis, 1977). Once baked, membranes were wetted with 2 x SSC and transferred to a glass crystallising dish containing 60 ml of pre-hybridisation solution (50% formamide, 5 x SSPPE and 0.5% SDS) and 0.5 ml of salmon sperm DNA (a kind gift of Nina Kotelevtsev, University of Edinburgh) denatured by boiling for 5 minutes. The dish was gently rotated for 60 minutes at 42°C before the pre-hybridisation solution was replaced with a further 60 ml containing 0.5 ml of denatured salmon sperm DNA and denatured ^{32}P-labelled probe at a concentration of 2 x 10^5 - 1 x 10^6 cpm/ml. Probes were prepared according to the method described in 2.1.11.17. Membranes were incubated overnight at 42°C with continuous rotation then washed twice for 15 minutes at 42°C in 500 ml of 2 x SSC and 0.1% SDS, followed by a further wash at 68°C for 15 minutes in 500 ml of 1 x SSC and 0.1% SDS. Membranes were then dried and covered with Saran Wrap. In a dark room, the membranes were attached to Kodak X-Omat film and 'pre-flashed' with UV light to facilitate later orientation of the filters. The film and filters were placed in an autoradiography cassette with two enhancement screens and exposed for a minimum of 16 hours at -70°C prior to development. Positive plaques were identified by alignment of the pinholes in the filters with the corresponding image on the autoradiograph and then identifying positive hybridisation signals.

2.1.12.5 *Conversion of λ phage P to plasmid pλP*

10^8 phage were incubated with 1 ml of a fresh overnight culture of Cre recombinase-expressing BNN132 cells in 10mM $MgCl_2$ for 30 minutes. Two ml of LB were added and the mixture incubated for 1 hour at 30°C with continuous shaking. Cultures were plated on 150 mm LB + ampicillin plates (100 μg/ml) supplemented with 0.1% glucose and incubated overnight at 37°C. Scrapings of cells were cultured in 50 ml aliquots of Terrific Broth containing ampicillin (100 μg/ml) until the stationary phase. Plasmid DNA was isolated from cultures using a Qiagen HiSpeed Midi-prep kit as described in section 2.1.11.2. Isolated plasmid DNA was used to transform *XL* I *E. coli* as described in section 2.1.11.15.

2.1.13 TISSUE CULTURE METHODS

E14 TG2a IV ES cells were grown at 37°C in a humidified incubator (Heraeus; model B5060 EC/CO_2) with CO_2 maintained between 6.0 and 7.5% as previously described (Smith *et al.*, 1988). All manipulations were performed inside a laminar flow hood (Gelair ICN Flow Hood (Class 3), ICN Pharmaceuticals Ltd, Thame, UK). Sterilisation of the hood interior and of hands and forearms was performed on each occasion with 70% industrial methylated spirits (BDH). ES cells were grown on Corning culture grade plasticware (Bibby Sterilin, Stone, UK) coated with 0.1% geletin (Sigma-Aldritch, Steinheim, Germany; Product number G-2500). Standard ES cell culture media consisted of 1 x GMEM (Gibco-BRL; Product number 12541-025) supplemented with 10% (v/v) foetal calf serum (Globepharm, Surrey, UK), 0.23% (w/v) sodium bicarbonate (Gibco-BRL; Product number 11140-035), 1.0 x MEM non-essential amino acids (Gibco-BRL; Product number 118110-017), 2.0mM L-glutamine (Gibco-BRL; Product number 25030-024), 1.0mM sodium pyruvate (Gibco-BRL; Product number 11360-039) and 0.1μM β-mercaptoethanol (Sigma-Aldritch, Steinheim, Germany). Media was prepared in a laminar flow hood in 500ml aliquots and stored at 4°C. Newly prepared media was tested for bacterial contamination by incubating a 5ml aliquot with 5ml of Tryptose Phosphate broth at 37°C for at least 2 days prior to use. Immediately before use

the media was supplemented with DIA/LIF (1:1000 dilution). The term 'ES cell media' will be used throughout to refer to DIA/LIF-supplemented media. Cells were routinely frozen in ES cell media containing 10% (v/v) DMSO as described later.

2.1.13.1 *Washing of ES cells*

ES cells were washed between manipulations with filter sterilised phosphate buffered saline (PBS; 137mM NaCl, 4.3mM Na_2HPO_4, 2.7mM KCl and 1.4mM KH_2PO_4, pH 7.3) prepared by dissolving 1 PBS tablet (Unipath, Basingstoke, UK; Product number BR14A) in 100 ml of UHP filter sterilised H_2O. PBS was added to flasks by gently running the solution down the flask wall opposite the cell layer.

2.1.13.2 *Passage of ES cells*

Media was aspirated and cells washed twice with 5 ml of PBS. Sufficient TVP (0.025% trypsin (Gibco-BRL; Product number 25090-010), 1.0% chicken serum (Gibco-BRL; product code 16110-033) and 0.5mM EDTA dissolved in PBS) was added to just cover the cells. Flasks were then incubated at 37°C for 1-2 minutes and tapped to dissociate cells. The trypsin was neutralised by the addition of 4 ml ES cell culture medium/ml of TVP added. Dissociated cells were pelletted by centrifugation (1,200 rpm; 5 minutes (200 x g in a Denley BS400 bench top centrifuge; Supplied by Life Sciences International (UK) Ltd, Basingstoke, UK)) then resuspended in 5 ml of media. Cells were counted in a haemocytometer and 1 x 10^6 cells seeded into a 25 cm^2 flask coated with 0.1% geletin and containing 10 ml of warmed ES cell media. Proportionately larger volumes of media were used for larger flasks. Flasks were gassed with 5% CO_2, 95% air for 10 seconds prior to incubation.

2.1.13.3 *Thawing of ES cells*

Vials of ES cells were retrieved from liquid nitrogen storage (Minnesota Valley Engineering Cryogenics; Product number XLC110) and immediately defrosted by floatation in a 37°C water bath. Once thawed, the vial was dried, sprayed with 70% IMS

and transferred to the laminar flow hood. Cells were diluted into 9.5 ml of pre-warmed ES cell media and pelleted by centrifugation (1,200 rpm; 3 minutes). The cell pellet was gently resuspended in 10 ml of pre-warmed media and transferred to a 25 cm^2 coated-coated flask, gassed with 5% CO_2/95% air and incubated at 37°C. ES cell media was replaced after 8 hours to remove dead cells and to further dilute remaining DMSO. For cells frozen in 24 well plates, the entire plate was thawed by floatation in a water bath for 1 minute. Freezing media was aspirated and 2 ml of ES cell media added to the appropriate wells. The cell suspension was then transferred to a 1% coated-coated 12 well plate and incubated overnight at 37°C. Cells were then washed twice with PBS to remove dead cells and the ES cell media refreshed.

2.1.13.4 *Freezing of ES cells*

Cells were washed twice with PBS and dissociated with TVP as previously described. Cells were resuspended in 9 ml of ES cell media and 10% (v/v) DMSO added. Cells were then collected by centrifugation (1,200 rpm; 3 minutes), resuspended in 1 ml of ES cell media containing 10% (v/v) DMSO and divided equally between 2 labelled freezing vials. Vials were immediately frozen at -80°C and transferred the following day to a liquid nitrogen cell bank for long-term storage.

2.1.13.5 *Freezing of 24 well plates*

Prior to freezing, confluent wells were washed twice with 1 ml of PBS and dissociated by adding 100 µl of TVP and incubating at 37°C for 2 minutes. Once completely dissociated, typsinisation was terminated by the addition of 200 µl of 'Quenching' media (1:1 (v/v) 100% FCS: ES cell media containing G418 (200 µg/ml)). Three hundred µl of ES cell media supplemented with G418 (200 µg/ml) and 20% (v/v) DMSO was added to each well, resulting in a final DMSO concentration of 10% (v/v). The media and cells were mixed by gentle rotation, the plate sealed with adhesive tape, labelled and immediately stored at -80°C. Wherever possible, whole plates were brought to confluence simultaneously in order that they could be frozen *in situ*. Where this was

not possible, the preceding method was used but the final cell suspension in 10% (v/v) DMSO was transferred to a fresh plate and the lid labelled with the clone identity.

2.1.13.6 *Isolation of ES cell DNA*

In contrast to 'freezing' plates, 'DNA' plates were allowed to grow beyond confluence in order that all cells could be lysed simultaneously. The following protocol was modified from Laird *et al* (Laird *et al.*, 1991). Cells were washed twice with 1 ml of PBS before the addition of 500 µl of 'lysis buffer' (100mM Tris-HCl pH 8.5, 5mM EDTA, 0.2% (w/v) SDS, 200mM NaCl and 100 µg/ml Proteinase K (Boehringer Maanheim, Germany; Product number 745723)). Plates were incubated overnight at 37°C and the lysate transferred to appropriately labelled Eppendorf tubes. One volume of phenol:chloroform:isoamyl alcohol (25:24:1) was added to each and the phases separated by centrifugation at 12,000 x g for 5 minutes. The aqueous phase was reserved and transferred to a fresh tube. DNA was then precipitated by the addition of 2 volumes of ice cold ethanol and gentle inversion of the tube for 5 minutes. DNA was pelleted by spinning at 12,000 x g for 10 minutes. The pellet was washed with 70% ethanol, air dried for 10 minutes and then dissolved in 100 µl of TE (pH 8.0) containing 50 µg/ml DNase-free RNase (Sigma-Aldritch, Steinheim, Germany). To completely dissolve the DNA, many samples required incubation at 37°C for 1-2 hours followed by gentle pipetting up and down using a 'cut-off' blue tip.

2.1.13.7 *Electroporation of ES cells with pλPW and pλPW(NoDT)*

Seventy five µg of targeting vector were digested overnight with 10 units of the appropriate restriction enzyme. Aliquots of each were checked for complete digestion by electrophoresis on a 0.8% agarose gel. Reaction mixtures were extracted with phenol:chloroform:isoamyl alcohol and DNA precipitated by the addition of 2.5 volumes of ice cold ethanol. DNA was pelleted by centrifugation at 4°C (12,000 x g; 15 minutes) and the pellet dissolved in 150 µl of TE (pH 8.0). The sample was transferred to the laminar flow hood and the DNA re-precipitated with 2.5 volumes of ethanol. The

pellet was recovered by centrifugation (12,000 x g; 5 minutes), washed with 70% ethanol, air-dried, then dissolved in 150 µl of TE (pH 8.0). To prepare ES cells for electroporation, 2 confluent 175cm^2 flasks were washed 3 times each with 20 ml of PBS. Cells were dissociated with 5 ml of TVP as previously described, resuspended in 10ml of pre-warmed ES cell media and transferred to two 50 ml universal tubes. Cells were pelletted by centrifugation (1,200g; 3 minutes), resuspended in 5ml of ES cell media and pooled. A 50 µl aliquot diluted x 10 with media was used for counting cells. 5 x 10^7 - 1 x 10^8 cells were taken, pelletted by centrifugation (1,200 rpm; 3 minutes) and resuspended in PBS to a final volume of 600 µl. 75 µg of targeting vector was added and the mixture incubated at 37°C for 10 minutes. Electroporation was performed in a 40 mm cuvette using a Biorad Gene Pulser (Biorad Laboratories Ltd; Model number 1652087) and Capacitance Expander (Biorad Laboratories Ltd; Model number 1652078) with to the following settings: 0.8 kV, 3.0 µF, capacitance expander 960 µF. This typically produced a time constant of 0.1 seconds. Mixtures were transferred to a universal and left for 10 minutes at 37°C before the cells were resuspended in 10 ml of ES cell media. 5 ml of the suspension was divided equally between five 90 mm 0.1% geletin-coated petri dishes. A further 10 ml of ES cell media was added to each dish and the dish rotated gently to spread the cells before incubation at 37°C. The remaining cells were diluted x 2 with ES cell media and a further 5 ml plated out as described. This process was repeated until 5 plates each of 1:1, 1:2, 1:4 and 1:8 dilutions were established. Duplicate plates of cells electroporated with no plasmid DNA were also established as controls for the later selection of G418-resistant colonies.

2.1.13.8 *Electroporation of targeted ES cells with Cre recombinase-expressing plasmid*

ES cell clones identified as having undergone a homologous recombination event following targeting with either pλPW or pλPW(NoDT) were grown to confluence in 25 cm^2 flasks. G418 selection was removed 48 hours prior to electroporation. Cells were washed, dissociated and resuspended for counting as described in section 2.1.13.1. A

total of 5 x 10^6 cells were mixed with 50 μg of pMC-Cre (Araki *et al.*, 1995) in a final volume of 600 μl using a plasmid preparation and electroporation protocol identical to that described in section 2.1.13.8. A further 5 x 10^6 cells of the same clone underwent electroporation without the addition of pMC-Cre. Following electroporation, cells were seeded into 75 cm^2 flasks pre-coated with 1% geletin and grown without G418 selection for 4 days until confluent. Cells were again washed, dissociated and counted and the following cell numbers seeded onto individual 1% coated-coated petri-dishes: 1 x 10^2, 5 x 10^2, 1 x 10^3, 5 x 10^3 and 1 x 10^4. Duplicate dilution series were cultured either with or without 2.5 μM Gancyclovir (Sigma-Aldritch, Steinheim, Germany).

2.1.13.9 *Production of chimaeric mice*

Chimaeric mice were generated by a modification of the method described by Bradley (Bradley, 1987). With the exception of the expansion of targeted ES cells, Dr J. Ure, (Centre for Genome Research, University of Edinburgh) performed all procedures. A total of 40 blastocysts were harvested from the fallopian tubes of C57BL/6J female mice on day 4 of pregnancy by flushing with Buffer PB1 (prepared by dissolving 822 mg NaCl, 300 mg Na_2HPO_4, 104 mg glucose, 21 mg KCl, 20 mg KH_2PO_4, 6.2 mg penicillin, 4.5 mg sodium pyruvate and 1.0 mg $MgCl_2$ in 100 ml of dH_2O and adding 0.01% (v/v) phenol red, pH 7.0-7.2)). The buffer was supplemented with 10% (v/v) FCS prior to use. Harvested blastocysts were transferred to pre-warmed ES cell media and incubated at 37°C to promote development of the blastocoel cavity. Blastocysts and trypsinised ES cells were then transferred to hanging drops of PB1 buffer supplemented with 10% FCS suspended on a siliconised (Repelcote™; BDH; Product number 63216 4J) coverslip. The coverslip was placed over a custom-made manipulation chamber (G. Robertson, Centre for Genome Research, University of Edinburgh) containing liquid paraffin and the chamber chilled at 4°C for 10 minutes. Injection of blastocysts was performed using vacuum pressure to immobilise the blastocyst on a rounded holding pipette (20 μm internal diameter). ES cells were then individually collected by vacuum pressure onto a heat-polished, flat-ended injection pipette (15 μm internal diameter). Between 15 and 20

ES cells were injected into each blastocyst. The procedure was visualised with an IMT2 image-corrected microscope (Olympus Optical Company (UK) Ltd, London, UK). Injection and holding pipettes were manufactured in-house by stretching 100μm internal diameter glass capillary tubes with an electrode puller (Camden Instruments, Loughborough, UK) followed by heat polishing with a microforge (DeFonbrune; Supplied by Micro Instruments Ltd., Witney, UK). The pipettes were attached to instrument holders and manoeuvred with precision manipulators (both produced by Ernst Leitz, Wetzlar, Germany). Vacuum pressure was adjusted by means of injectors (Narashige International Ltd., London, UK for the holding pipette; DeFonbrune for the injection pipette) connected via paraffin-filled plastic tubes to the pipettes.

Following injection, blastocysts were transferred to pre-warmed ES cell media and incubated at 37°C for 2-3 hours prior to implantation in pseudo-pregnant MF1 mice. The recipient females were mated with vasectomised MF1 males 2.5 days prior to implantation and successful coitus was confirmed by the presence of 'plugging'. Five to ten blastocysts were typically implanted in the uterine horn of each recipient mouse. Chimaeric pups derived from this procedure were identified by the presence of sandy-coloured patches amidst the normally black fur. Germline transmission of targeted ES cell DNA was assessed by the coat colour of pups produced by the cross of chimaeric mice with BKW mice. Black pups will have inherited a full complement of C57Bl/6 chromosomes derived from the parent blastocyst and, hence, will not carry the targeted mutation. In contrast, sandy coloured pups will have inherited a complement of chromosomes derived from 129/SV ES cells and have, therefore, a 1 in 2 chance of carrying the targeted mutation. PCR screening and sequencing of tail tip DNA was used to confirm germline transmission. Heterozygous mice were then inter-crossed to produce offspring homozygous for the targeted mutation.

2.1.13.10 *Preparation of genomic DNA from tail biopsy*

Tail tip biopsy was performed under either general (Halothane-Vet, Merial Animal Health Ltd., Harlow, UK; Product number H3006/2) or local (ethyl chloride B.P. spray,

Roche, Welwyn Garden City, UK) anaesthesia in weaned pups up to 28 days old. A 1 cm length of tail was cut and stored at -20°C until DNA extraction. Mice were ear-tagged as appropriate. Tail biopsies were minced with scissors in 600 µl of tail buffer (200 mM Tris HCl pH 8.0, 400 mM EDTA, 4.0M NaCl and 10% (v/v) SDS) and 35 µl of 10 mg/ml Proteinase K. Tails were then rotated continuously overnight at 55°C in a Techne Hybridiser HB-1D oven (Techne (Cambridge) Ltd, Cambridge, UK). The following day, 20 µl of 20 µg/ml DNase-free RNase (Sigma-Aldritch, Steinheim, Germany) was added and tails incubated for 60 minutes at 37°C. Six hundred µl of Tris-saturated phenol and 37.5 µl of 2 M mercaptoethanol were added to each tube. Tubes were rotated on a vertical rotor (horizontal axis of rotation) for 15 minutes, followed by centrifugation at 12,000 x g for 5 minutes. The aqueous phase and interphase were transferred to a fresh Eppendorf tube and extracted with 1 volume of phenol:chloroform:isoamyl alcohol (25:24:1), followed by 1 volume of chloroform:isoamyl alcohol (24:1). DNA was precipitated from the aqueous phase with 600 µl of room temperature isopropanol by gentle rotation for 5 minutes. The stringy genomic DNA precipitate was pelleted by centrifugation (12,000 x g, 2 minutes) and washed in 200 µl of 70% ethanol. DNA was air dried for 10 minutes then dissolved in 200 µl of TE, pH 8.0. Samples were then left to dissolve completely for 30 minutes at 37°C before being mixed gently and stored at –20°C until required.

2.1.13.11 *Polymerase chain reaction of genomic DNA*

Approximately 1 µg of genomic tail tip DNA was used for PCR screening of floxed ET_B receptor mice. Reactions were performed in a total volume of 25 µl containing 500µM of each deoxyribonucleotide, 300nM of each primer, 1 µg of genomic DNA, 2.5 µl of 10 x Expand™ Buffer number 3 (22.5mM $MgCl_2$, detergents, pH 9.2, Roche Pharmaceuticals) and 1.875 units of Genecraft Biotherm™ Taq polymerase. Samples were amplified using a MJ Research Peltier Thermal Cycler PT-200 with a heated lid with the following protocol: initial denaturation at 92°C for 5 minutes followed by 30 cycles of 92°C for 30 seconds, 60°C for 30 seconds and 68°C for 2 minutes. A final

extension period of 10 minutes at 68°C completed the reaction. Reaction mixtures were mixed with 2 μl of 6 x loading dye and 18 μl of this mixture was then run on a 2% agarose gel stained with ethidium bromide.

2.1.14 PHYSIOLOGICAL TECHNIQUES

2.1.15 WIRE MYOGRAPHY

The isometric tension developed in mouse aortic rings in response to agonists was measured using the technique of wire myography as originally described by Mulvany (Mulvany and Halpern, 1976) and according to their later modifications of this technique (Mulvany *et al.*, 1978).

2.1.15.1 *Dissection of the mouse aorta and trachea*

Mice were culled by inhalation of increasing concentrations of CO_2 and immediately transported to the laboratory for dissection of the aorta and trachea. The trachea was exposed and cut at the level of the larynx and 8-9 tracheal rings removed. The excised trachea was covered with ice-cold physiological saline solution (PSS; 119mM NaCl, 4.7mM KCl, 2.5mM $CaCl_2$, 1.17mM $MgSO_4$, 25mM $NaHCO_3$, 1.18mM KH_2PO_4, 0.027 EDTA and 5.5mM Glucose) and dissected free of connective tissue. The trachea was bisected and the two segments mounted individually onto the wire myograph as described in section 2.1.15.2. The thoracic aorta was carefully dissected off the posterior thoracic wall and removed along with the heart and lungs. The heart was removed and weighed. The aorta was then cleaned of connective tissue and divided at the junction of the thoracic aorta and the aortic arch. Proximal and distal aortic rings (~2 mm each) were mounted on the wire myograph as described in section 2.1.15.2.

2.1.15.2 *Mounting of aortic and tracheal rings*

The mounting procedure is illustrated in Figure 2.11. Briefly, vessel rings were suspended between two intra-luminal mounting wires (40 μm diameter, ~2.2 cm in

length) in a 10 ml myograph organ bath (Multi-myograph model 610M; JP Trading, Aarhus, Denmark). One wire was attached to the stationary support driven by a micrometer whilst the second wire was attached to an isometric force transducer. Care was taken not to damage the endothelium during the mounting procedure. Vessels were bathed in PSS at 37°C and, following a 10 minute equilibration period, vessel dimensions were normalised as previously described (Mulvany *et al.*, 1978). Previous studies in our laboratory had determined that a tension of 1.5 g (7.36 mN) was required for aortic rings and 0.5 g (2.45 mN) for tracheal rings. Periodic adjustments were made to maintain this tension over the subsequent 60 minute equilibration period. This tension was defined as zero for all following measurements. 95%/5% O_2/CO_2 was bubbled through the solution of PSS at all times during the experiment. Signals from the myograph were processed by a MacLab/4e analogue-digital converter and displayed through Chart™ software (ADInstruments; Chalgrove, Oxfordshire, UK).

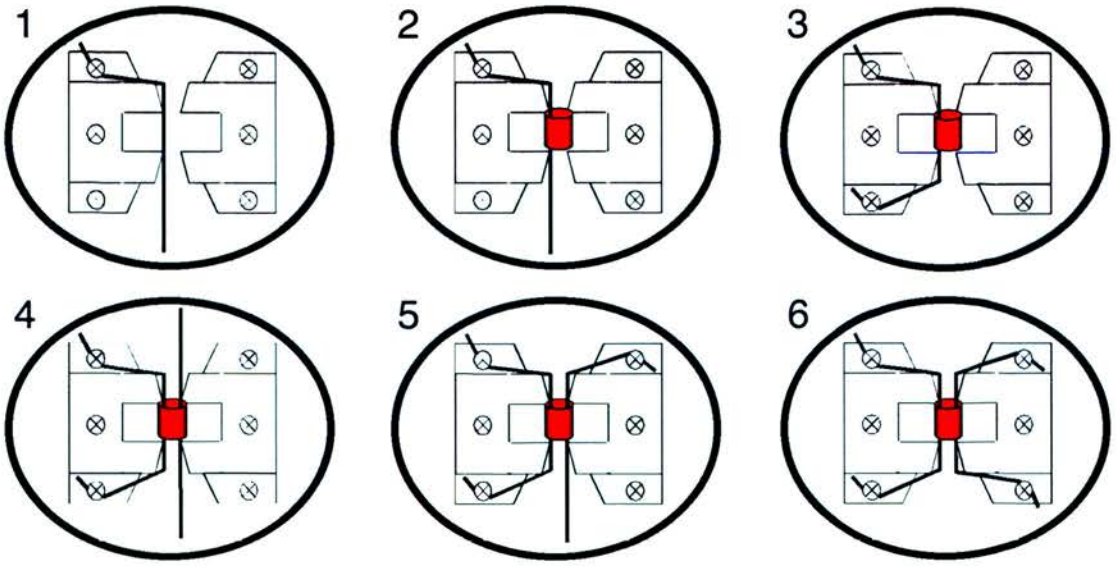

Figure 2.11

Mounting of vascular and tracheal rings upon the wire myograph.

2.1.15.3 *Aortic and Tracheal wake up protocol*

Following equilibration, aortic and tracheal rings were contracted three times to obtain the maximum contraction to KPSS solution (123.7mmol KCl, 2.5mmol $CaCl_2.2H_2O$, 1.17mmol $MgSO_4.7H_2O$, 25mmol $NaHCO_3$, 1.18mmol KH_2PO_4, 0.027mmol EDTA, 5.5mmol Glucose). A 10 minute wash with PSS was performed prior to each treatment with KPSS. Rings were then given a final wash with PSS solution and allowed return to baseline over a 10 minute period prior to further experiments. The complete experimental protocols are illustrated in Figure 7.1, Figure 7.2, Figure 7.3 and Figure 7.4.

2.1.15.4 *Preparation of stock solutions*

Stock solutions of 10^{-2}M carbachol (Sigma-Aldritch, Steinheim, Germany; product number C-4382), ACh (10^{-2}M; Sigma-Aldritch, Steinheim, Germany; product number A7000) and 2,2'-(hydroxynitrosohydrazono)bis-ethanimine (a diazeniumdiolate, henceforth referred to as deta/NO); 10^{-2}M; Sigma-Aldritch, Steinheim, Germany;

product number D-185) were each prepared in dH_2O. Stock solutions of 10^{-4}M S6c (Calbiochem, La Jolla, USA; product number 05-23-3813) were prepared in 5% acetic acid and diluted with PSS containing 10mg/ml of BSA. A192621 (2R, 3R, 4S)-2-(4-propoxy-phenyl)-4-(1,3-benzodioxol-5-yl)-1-(N-[(2,6-diethylphenyl]ace-tamido)pyrrolidine-3-carboxylate, nitrogen; 10^{-4}M; Abbott Pharmaceuticals) and L-NAME (N_W-nitro-L-arginine methyl ester hydrochloride; 10^{-4}M; Sigma-Aldritch, Steinheim, Germany; product number N5751) were dissolved in DMSO. NE (10^{-2}M; Sigma-Aldritch, Steinheim, Germany; product number A-0937) was dissolved in 0.1M ascorbic acid.

2.1.16 BLOOD PRESSURE MEASUREMENT IN CONSCIOUS ANIMALS

Mean blood pressure was measured by direct cannulation of the right common carotid artery in adult mice (8-12 weeks old) as previously described (Davisson *et al.*, 1998). Cannulae were produced by flaming and stretching the tip of a section of Micro Renathane tubing (internal diameter = 12 μm; Braintree Laboratories Inc., Braintree, Massachusetts, USA; Product number MRE025). Animals were anaesthetised by continuous inhalation of isoflurane and body temperature maintained throughout with a heating pad. The common carotid was exposed via a mid-line incision and ligated distally. With the proximal end held under tension, the cannula was inserted and secured in place with a further silk suture. The cannula was then tunnelled beneath the skin to emerge in the intra-scapular region where it was secured with Germolene Newskin™ tissue adhesive. After flushing with heparinised saline (100 IU/ml), the cannula was plugged with a blunted 26G needle filled with paraffin wax. Carotid cannulation and measurement of blood pressure following high salt diet was performed by Dr Nick Kelland (University of Edinburgh, Edinburgh, UK).

2.1.17 ET-1 BINDING EXPERIMENTS

2.1.17.1 *Isolation of pulmonary endothelial cell-enriched populations from murine lung tissue*

Pulmonary endothelial cell-enriched populations were isolated using the general approach described by Dong (Dong *et al.*, 1997). Briefly, 150 mg of pulmonary tissue were removed from freshly culled 8-10 week old mice and minced into ~1mm particles. The tissue was then digested for 60 minutes in 1ml of HEPES-Ringer buffer (118mM NaCl, 17mM Hepes, 16mM Na Hepes, 14mM Glucose, 3.2mM KCl, 2.5mM $CaCl_2$, 1.8mM $MgSO_4$, 1.8mM KH_2PO_4; pH 7.4; 285 mosm) containing 1mg/ml of Collagenase A (Boehringer Mannheim, Germany). Digested tissue was then and forced through a 100 μm Falcon Strainer filter using a 'cut off' blue pipette tip and the resultant suspension was washed twice with PBS and re-suspended in 1 ml of PBS.

2.1.17.2 *Preparation of Biotinylated Griffonia simplicifolia isolectin B4 (GSL I-B4)-coated magnetic beads*

GSL I-B4 (Vector Laboratories, Peterborough, UK; product number B-1205) was bound to streptavidin-coated Dynabeads (CELLection™ Biotin Binder Kit, Dynal Ltd., Bromborough, UK; product number 115.21) according to the manufacturer's instructions. Briefly, 100 μl of Dynabeads (~4 x 10^7 beads) were washed with 1 ml of PBS with 0.1% tween and resuspended in 100 μl of this buffer. Eight μg of GSL I-B4 were added and the mixture incubated at room temperature for 30 minutes. The beads were recovered with a magnetic particle concentrator, washed 3 times with 1 ml of PBS and 0.1 % tween and resuspended in a final volume of 100 μl.

2.1.18 ANALYSIS OF RESULTS

Blood pressure on standard and higher salt chow was compared by 2 factor ANOVA with Bonferroni post-test analysis. Pulmonary EC ^{125}I ET-1 binding was analysed using an unpaired student's t test. Concentration response curves were analysed by 2 factor

ANOVA. EC_{50} and E_{Max} values, S6c-induced vasodilatation and plasma ET-1 concentration were each compared by repeated measures ANOVA with Dunnett's multiple comparison post-test analysis. *P*-values quoted in the text were accepted as statistically significant when $p<0.05$.

3 Chapter 3

3.1 IDENTIFICATION, CLONING AND PARTIAL SEQUENCING OF PλP

3.1.1 INTRODUCTION

Manipulation of the mammalian genome has been achieved through the technique of gene targeting. This process involves the homologous recombination of exogenous DNA sequences with chromosomal DNA. In order to maximise the efficiency of homologous recombination, the homology arms of the replacement-type targeting construct are designed to be isogenic to the locus of interest. Homology arms may be produced by PCR or by the cloning of fragments of isogenic genomic DNA from phage display libraries. This chapter describes the identification of a bacteriophage clone, λP, from a 129/SV mouse genomic DNA library constructed using the λPS vector (Nehls *et al.*, 1994). λP contains a 14748 bp region of the mouse ET_B receptor gene spanning from the last 12104 bp of intron one to 54 bp after the start of exon 5. λP was converted by automatic subcloning to the plasmid pλP from which the 5' and 3' homology arms of the targeting vectors pλPW and pλPW(NoDT) were constructed. In addition, the amplification by PCR of regions of the mouse ET_B receptor gene using a genomic DNA template is described. These PCR products were used to sequence intronic regions of the ET_B receptor gene for the first time. Although not available at the start of the cloning experiments, the complete sequence of the mouse ET_B receptor gene (27.02 kb) has now been published as part of the mouse genome sequencing project (Ensembl gene reference number: ENSMUSG00000022122).

3.1.2 METHODS

3.1.2.1 *PCR amplification of the mouse ET_B receptor gene*

129/SV genomic tail tip DNA was provided by Dr Matthew Sharp (University of Edinburgh, Edinburgh, UK) and used as a template for the amplification of short regions

of the ET_B receptor locus by PCR. Primers were designed complementary to sequences of the mouse ET_B receptor cDNA (PubMed accession number NM 007904 (Hosoda *et al.*, 1994) using Gene Con Kit™ software. Regions of the ET_B receptor locus complementary to the primers used are illustrated in Figure 2.1, Figure 2.2 and Figure 2.3. PCR was performed using the Expand™ Long Template PCR system (500μM of each deoxyribonucleotide, 300nM of each primer, 1 μg of genomic DNA, 2.5 μl of 10 x Expand™ Buffer number 3 (22.5mM $MgCl_2$, detergents, pH 9.2) and 1.875 units of Genecraft Biotherm™ Taq polymerase) in a final volume of 25 μl. Amplification was achieved using the following cycling parameters: 92°C for 2 minutes, 35 cycles of 92°C for 30 seconds, 50°C for 30 seconds and 68°C for 3 minutes, followed by a final extension period of 15 minutes at 68°C.

3.1.2.2 *Cloning of PCR products*

The Expand™ PCR system generates PCR fragments with mainly 3' single A overhangs. Cloning of PCR products into a pCR2.1® vector (Figure 2.5) was achieved using the TA cloning® kit as described in section 2.1.11.13. Successful cloning results in PCR products flanked by *EcoR* I sites. Plasmid DNA isolated from overnight cultures of XLI Blue *E. coli* was screened for the fragment of interest by restriction digestion with *EcoR* I.

3.1.2.3 *Construction of a 129/SV mouse genomic DNA library*

The 129/SV mouse genomic DNA library was a kind gift of Dr Andrew Smith (University of Edinburgh, Edinburgh, UK). The library was constructed by partial *Sau*3AI digestion of high molecular weight genomic DNA isolated from 129/SV-derived ES cells. Fragments between 18-22 kb in length were selected by sucrose gradient centrifugation and then cloned into a λPS vector as described by Nehls and colleagues (Nehls *et al.*, 1994). The λPS vector features an automatic subcloning facility based upon Cre-recombinase-loxP-mediated recombination. The plasmid portion of λPS is flanked by direct repeats of loxP sites. In the presence of Cre recombinase, a site-

specific recombination reaction is catalysed, resulting in the conversion of the phage form of the vector to a plasmid. Recombination reactions may be initiated by transforming Cre recombinase expressing BNN132 cells with λPS vectors (Elledge *et al.*, 1991).

3.1.2.4 *Probes utilized for screening of the λPS 129/SV genomic DNA library*

In-situ hybridisation using ^{32}P-labelled DNA probes was utilised to identify λPS clones containing regions of the ET_B receptor gene as described in section 2.1.12.4. Two probes were used for this purpose. The first probe was complementary to exon 1 of the ET_B receptor gene and was produced by PCR amplification of 129/SV mouse genomic DNA using the primers Exon 1 149F (TCCAGACTGAAAACAGCAGAGCGG) and Exon 1 671R (GGGTATGTCTATGATGATGTGC; illustrated in Figure 2.2). PCR was performed using the Expand™ PCR system and the following parameters: 92°C for 2 minutes, 30 cycles of 92°C for 30 seconds, 62°C for 30 seconds and 68°C for 2 minutes, followed by a final extension period of 10 minutes at 68°C. A Mg^{2+} concentration of 1.7 mM was found to be optimal. Contaminating dNTPs and primers were separated from the 522 bp PCR product as described in section 2.1.11.7. The second probe, a fragment of the mouse ET_B receptor gene cDNA (Hosoda *et al.*, 1994) spanning from position 563 to 1363, was a kind gift of Dr Paula Smith (University of Edinburgh, Edinburgh, UK). Probes were labelled with ^{32}dCTP as described in section 2.1.11.17 and the library screened as described in section 2.1.12.

3.1.2.5 *Primary and secondary screening of λPS 129/SV genomic DNA library*

The primary library screen was performed by simultaneous hybridisation with both radiolabelled probes. Multiple agar plugs from the regions corresponding to strong hybridisation signals were picked as described in section 2.1.12.3 for each of the clones identified. Serial dilutions of each clone were prepared and plated out as previously described. Bacteriophage particles from each plate were then transferred in duplicate to nitrocellulose membranes and a secondary screen performed. For the secondary screen,

duplicate membranes were individually incubated with either the radiolabelled Exon 1 probe or the ET_B cDNA probe to identify the particular regions of the ET_B receptor gene contained within the λPS vector. This process was repeated until all colonies derived from a single agar plug produced positive hybridisation signals with the appropriate probe, thus indicating that a pure clonal population had been isolated

3.1.2.6 *Subcloning of λP into pλP*

The phage vector λP was converted to the plasmid pλP by the automatic subcloning technique described by Nehls (Nehls *et al.*, 1994) and outlined in section 2.1.12.5. Plasmids isolated using this technique were subsequently electroporated into the *XL* I Blue strain of *E. coli* that lacks Cre-recombinase expression.

3.1.2.7 *Sequencing and mapping of pλP*

The plasmid pλP (illustrated in Figure 2.9) was mapped by direct sequencing and restriction digestion. All sequencing reactions were performed as described in section 2.1.11.4. The primers M13-20 (GTAAAACGACGGCCAGT) and M13R (AACAGCTATGACCATG), complementary to regions of the pBluescript™ vector flanking the polylinker site (illustrated in Figure 2.5), were used to sequence the 3' and 5' regions of pλP, respectively, and to determine insert orientation. Intronic regions were sequenced with the primers 81R (CTTAGAGCACAAAGACTCAGCAC), 78F (TTTGGGTGGTCTCTGTGGTTCTGG), and 417R (GTAGAAACTGAACAGCCACCAATC). The regions complementary to all sequencing primers are illustrated in Figure 2.1, Figure 2.2 and Figure 2.3. Sequence data were compared to the available published ET_B receptor gene sequences using Genejockey II for the MacIntosh.

3.1.3 RESULTS

3.1.3.1 *PCR amplification of genomic DNA*

Exons and intronic regions of the ET_B receptor locus were amplified by PCR from a 129/SV mouse genomic template. The results are illustrated in Figure 3.1. The entire genomic region from exon 2 to exon 6 was amplified using the primers 81F and 359R.

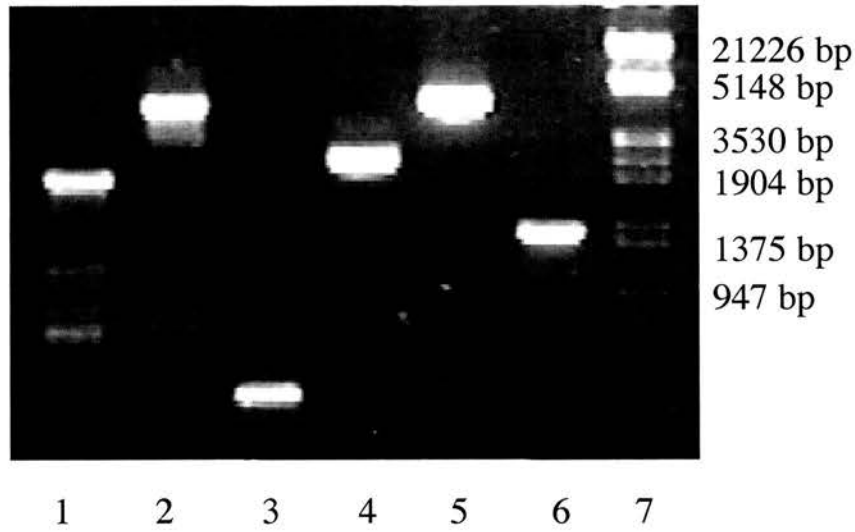

Figure 3.1

PCR amplification of regions within the ET_B receptor locus from a genomic DNA template. Lane 1, 78F/417R (exon 3 – exon 4); Lane 2, 78F/359R (exon 3 – exon 6); Lane 3, 81F/412R (exon 2 – exon 3); Lane 4, 81F/417R (exon 2 – exon 4); Lane 5, 81F/359R (exon 2 – exon 6); Lane 6, 32F/359R (exon 5 – exon 6); Lane 7, λ/*Eco RI*/*Hind* III. PCR products were later subcloned into the pCR2.1 plasmid vector.

3.1.3.2 *TA cloning® of PCR products*

The results of *EcoR* I restriction digestion of plasmid DNA following TA cloning® of PCR products amplified from genomic DNA are illustrated in Figure 3.2. Successful

cloning of cells electroporated with the 81F/359R PCR product (upper panel) resulted in 2 additional bands (lane 2). The sum of the sizes of the 2 addition bands was similar to the size of the original PCR product, suggesting that this region contains an internal *EcoR* I site. Cells electroporated with the 32F/359R PCR product (lower panel) produced a single additional band (lane 2) of ~1.2 kb, consistent with successful cloning of this gene fragment. No plasmids containing the 78F/417R PCR product were identified following attempts to clone this fragment.

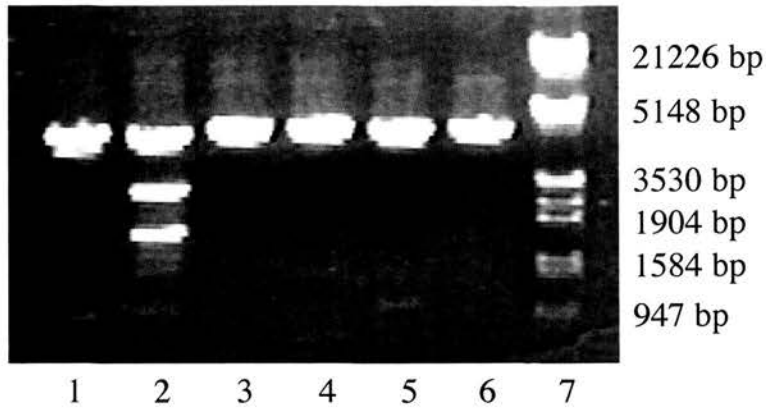

Figure 3.2

Restriction digestion of pCR2.1 plasmid DNA with *Eco R*I following TA cloning of PCR products amplified using the primers 81F/359R (above) and 32F/359 (below). Along with the 3.9 kb vector, lane 2 in each case demonstrates additional bands of the predicted size consistent with successful cloning. Lane 7 λ/*Eco R*I/*Hind* III DNA.

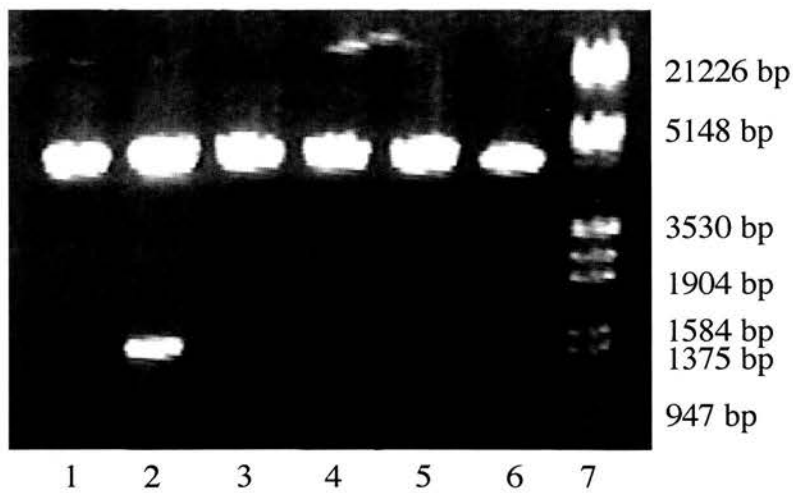

Plasmids featuring the 81F/359 PCR product insert were termed pCR2-6 and insert orientation was determined by restriction digestion with *Bam HI*, illustrated in Figure 3.3. Plasmids pCR2-6.2 and pCR2-6.20 (lanes 3 and 5 respectively) demonstrate an insert orientation opposite to that of pCR2-6.18 (lane 4). Insert orientation was confirmed by direct sequencing of pCR2-6.2 and pCR2-6.18 with the primers M13-20 and M13R, complementary to regions of the pCR2.1 vector polylinker. In the plasmid pCR2-6.18, exon 2 of the ET_B receptor gene lay immediately 3' of the *Bam*H I site of the plasmid polylinker. Detailed sequencing of pCR2-6.18 was performed with the primers 78F, 412R (CAGAACCACAGAGACCACCCAAAT) and 417R. pCR5-6 (lane 2) was sequenced using the primers M13-20, M13R, 32F and 359R. Alignment of these sequencing data permitted the formation of a contiguous sequence of the mouse ET_B receptor gene spanning from exon 2 to exon 6. Sequence data obtained by this method were compared with the available published ET_B receptor gene sequences and found to be homologous (data not shown).

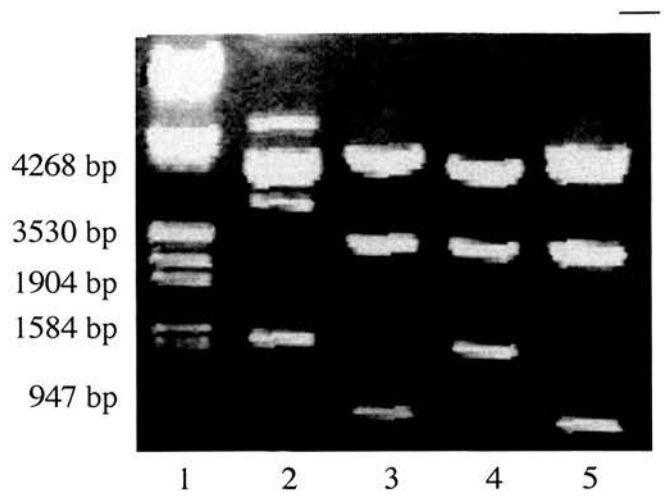

Figure 3.3

The insert orientation of ligated 81F/359R PCR products within the PCR2.1 plasmid was determined by *Bam HI* digestion. PCR2-6.18 (lane 4) demonstrates an insert orientation opposite to that of pCR2-6.2 and pCR2-6.20 (lanes 3 and 5, respectively). Lane 2 demonstrates a band of ~1200 bp following *Eco RI* digestion, consistent with successful cloning of the 32F/359R PCR product into the PCR2.1 plasmid. Lane 1 λ/*Eco RI*/*Hind* III DNA.

3.1.3.3 *Primary and secondary screens of λPS phage library*

An initial screen of the library identified 3 clones, λP, λH and λI, each of which produced a positive hybridisation signal when simultaneously incubated with the Exon 1 and ET_B cDNA probes. In the secondary screen, λP produced positive hybridisation signals only with the ET_B cDNA probe, suggesting that this phage did not contain any sequences originating in exon 1. In contrast, λH and λI produced positive hybridisation signals only with the Exon 1 probe and were unlikely, therefore, to contain any further exons of the ET_B receptor gene. Representative autoradiographs of the library screening process are illustrated in Figure 3.4.

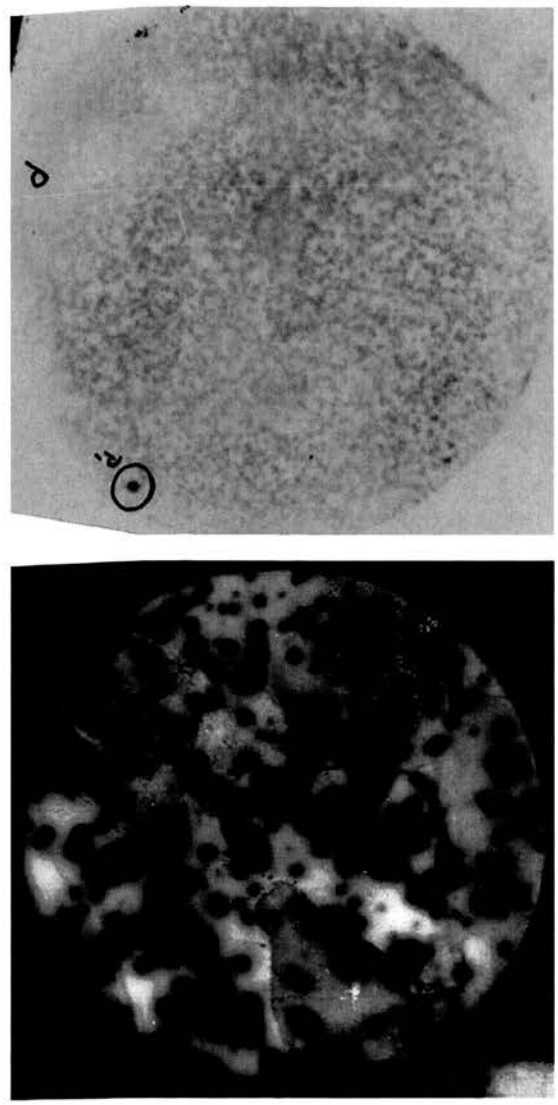

Figure 3.4

Upper panel: Autoradiograph of primary screen of λPS phage library by hybridisation with probes complementary to exon 1 of the ET_B receptor gene and to a fragment of the ET_B receptor cDNA. The circled colony P was selected and serially diluted until a pure clonal population was achieved. Hybridisation of the ET_B receptor cDNA probe to all colonies is illustrated in the lower panel.

3.1.3.4 *Sequencing of pλP*

Sequenced regions of pλP were isogenic with available publishes sequences. The 3' region of pλP terminated at a *BamH* I site 54 bp downstream of the start of exon 5, consistent with the method used to construct the λPS library. In addition, the presence of intronic restriction sites predicted from pCR.2-6.18 sequencing data and available published data were confirmed by analytical restriction digestion of pλP (data not shown). pλP plasmid DNA was used as a template for PCR amplification using the primer pairs and reaction conditions utilised for genomic templates. With the exception of primer pairs complementary to sequences within exon 1, all primer pairs successfully directed amplification of the appropriate regions, producing PCR products of identical size to those seen with a genomic DNA template. Examples of sequence alignment between published sequences and pλP are illustrated in Figure 3.6 , Figure 3.7 and Figure 3.7.

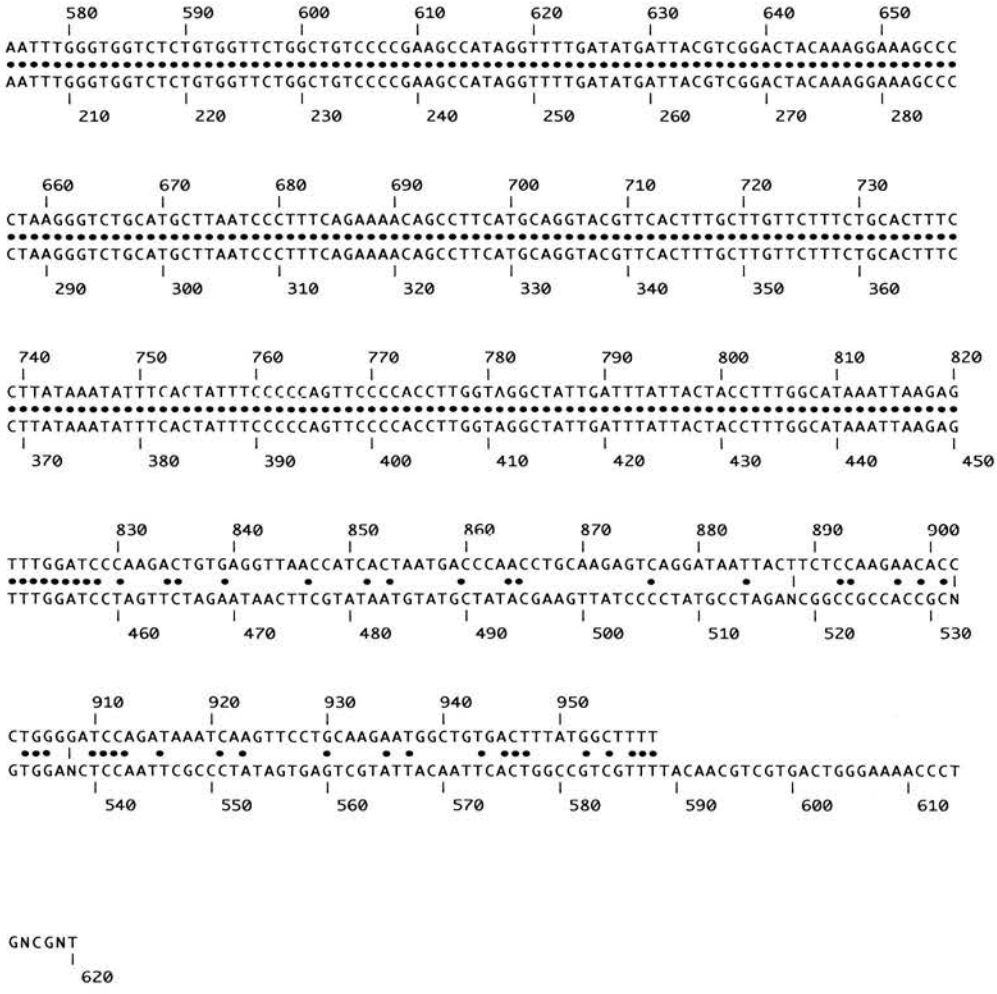

Figure 3.5

Sequence alignment of pλP sequenced with the 81F primer (top) with the published ET_B receptor sequence from exon 2 to the first 254 bp of intron 3 (bottom).

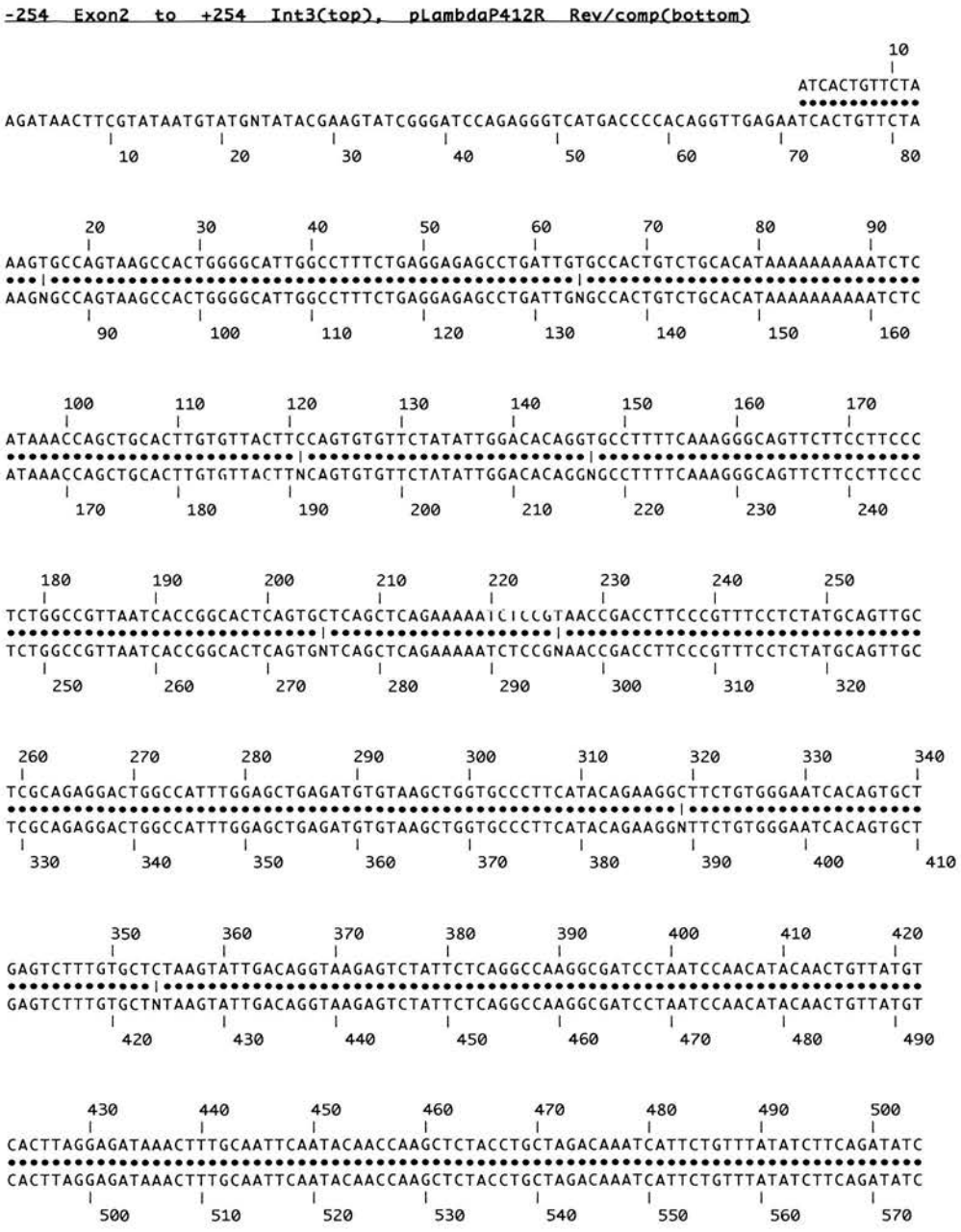

Figure 3.6

Sequence alignment of pλP sequenced with the 412R primer (bottom) with published ET_B receptor sequences spanning from the final 254 bp of intron 1 to intron 3 (top).

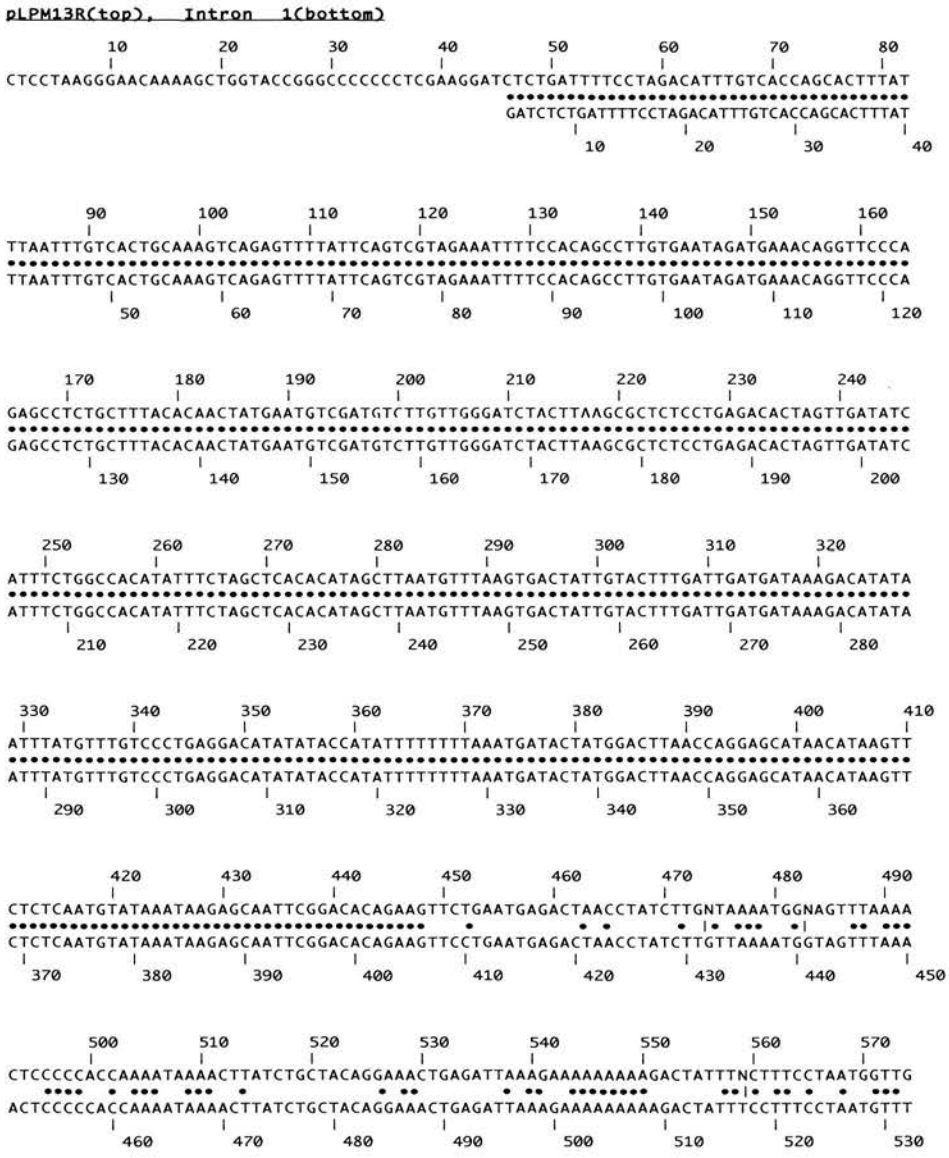

Figure 3.7

Sequence alignment of the 5' end of pλP sequenced with the M13R primer (bottom) with the published sequence of the ET_B receptor gene from position 7388 of intron 1 (top).

3.1.4 DISCUSSION

The successful PCR amplification of the ET_B receptor gene region spanning from exon 2 to exon 6 from genomic DNA permitted detailed sequencing of intronic regions of the mouse ET_B receptor gene for the first time. Interrogation of this sequence data were utilised to predict the presence of restriction sites within this region and to formulate a cloning strategy for the production of targeting vectors as described in chapter 4. However, it was not possible to amplify intron 1 in its entirety (19493 bp), despite the use of the Expand™ Long Template PCR system. This system has previously been shown to amplify fragments of up to 22 kb from human genomic DNA (Cheng *et al.*, 1994) with a low error frequency. Failure to amplify this region and the potential for the introduction of significant mutations during PCR amplification, prompted the adoption of a cloning strategy based upon the use of fragments of the ET_B receptor gene isolated from a λPS phage genomic DNA library.

The λPS phage library was constructed from 129/SV genomic DNA isogenic to the ES cells utilised for subsequent targeting experiments. This has been shown to increase the efficiency of targeting events (te Riele *et al.*, 1992). Traditionally, the characterisation of DNA clones isolated from such phage display libraries involved the subcloning of insert fragments into plasmid vectors. This process is often time consuming and of limited efficiency. The use of phage vectors featuring automatic plasmid excision greatly simplifies the mapping of genomic DNA inserts and the subsequent construction of targeting vectors. λPS libraries prepared by cloning size-selected partially *Sau*3AI-digested genomic DNA typically feature inserts of between 15 kb and 19 kb (Nehls *et al.*, 1994). It was predicted, therefore, that inserts would encompass a significant portion of the ET_B receptor gene locus. In addition, the relatively large insert size permitted the design of constructs with large regions of isogenic DNA flanking the genetic marker. Thus, it was possible to generate a targeting construct fulfilling the optimal design requirements for efficient replacement of the endogenous locus.

4 Chapter 4

4.1 DESIGN AND CONSTRUCTION OF THE TARGETING VECTORS PλPW AND PλPW(NODT)

4.1.1 INTRODUCTION

The advent of techniques to introduce site-specific modifications into the genome by homologous recombination (gene targeting) has revolutionised the field of mouse genetics and the study of *in vivo* gene function. This chapter will describe the design and construction of two gene targeting vectors, pλPW and pλPW(NoDT). These 'tri-lox' replacement targeting vectors were designed to introduce loxP sites into the intronic regions flanking exons 2 and 3 of the ET_B receptor gene locus. A removable selection marker was included in each vector to permit selective propagation of targeted ES cell clones. Following clone selection, this marker was removed from the targeted locus to prevent possible interference with gene expression (reviewed by (Muller, 1999). To maximise the efficiency of homologous recombination events, vectors were designed with long regions of homology flanking the targeted locus and, with the exception of a short PCR-generated fragment spanning exons 2 and 3, all genomic regions of the vectors were constructed from isogenic fragments of the ET_B receptor gene subcloned from the plasmid pλP. The addition of a diphtheria toxin gene to the extreme 3' end of pλPW was further intended to reduce the number of clones featuring random integration of the targeting vector (Yagi *et al.*, 1990). Such events would result in the stable integration and transcription of the diphtheria toxin gene and consequent cell death. In contrast, during homologous recombination the non-homologous diphtheria toxin gene would be excised, thereby permitting cell survival.

4.1.1.1 *Structure of targeting vectors*

The targeting vectors each consisted of a 5' homology arm comprising ~11.9 kb of the 3' region of intron 1, loxP sites flanking exons 2 and 3, and a neomycin

resistance/thymidine kinase selection cassette flanked by a third loxP site. The 3' homology arm consisted of intron 3, exon 4, intron 4 and either the first 54 bp of exon 5 (for pλPW(NoDT) or a diphtheria toxin gene cassette (for pλPW). Briefly, the targeting vectors were constructed by the following steps (illustrated in Figures 4.1-4.7): Firstly, PCR directed amplification of a 956 bp region of the ET_B receptor gene spanning from intron 1 to intron 3 was performed. A *Bam*H I site was incorporated into the 5' end of the PCR product to facilitate cloning into the $LoxP^2$ROSA targeting vector. The LTNL selection cassette was then sub-cloned downstream of the PCR product. The 3' homology arm of pλPW(NoDT) consisted of the *Hpa* I-*Not* I fragment of pλP, spanning from intron 3 to first 54 bp of exon 5. In pλPW, the *Hpa* I-*Not* I fragment was cut with *Bse*RI to remove part of intron 4 and exon 5. This region was replaced with a Diphtheria toxin gene cassette. The 3' homology arm of each construct was then sub-cloned downstream of the LTNL selection cassette. The 5' homology arm was prepared by the addition of a *Xho* I site to the 5' end of pλP and subsequent subcloning of the ~11.9 kb *Xho* I-*Nae* I fragment of pλP into the 5' $LoxP^2$ ROSA polylinker region.

4.1.2 METHODS

4.1.2.1 *PCR amplification of exons 2 and 3 of the ET_B receptor gene*

The region comprising the final 288 bp of intron 1 to the first 155 bp of intron 3 was amplified by PCR using the primers M230F (TCCGGATCCAGAGGGTCATGACCCAC) and 584R (TCACTAGTGATGGTTAACCTCACAG; illustrated in Figure 2.1). This region encompasses exons 2 and 3 of the ET_B receptor gene, essential for the production of functional ET_B receptors during embryonic development and adult life. PCR was, therefore, performed using high fidelity proof-reading *Pfu* DNA polymerase enzyme to minimise the potential for the introduction of mutations. Twenty pg of pλP template DNA were amplified using 1.25 units of *Pfu* DNA polymerase, 0.5 μM of each primer, 200 μM dNTPs and 1 x *Pfu* DNA polymerase buffer (20mM Tris-HCl (pH 8.8), 10mM

KCl, 10mM $(NH_4)_2SO_4$, 2.0mM $MgSO_4$, 0.1 mg/ml nuclease-free BSA and 0.1% Triton® X-100) in a final volume of 50 µl. Reactions were performed with the following cycling parameters: denaturation at 94°C for 5 minutes followed by 30 cycles of 94°C for 45 seconds, 60°C for 45 seconds and 72°C for 2 minutes. A final extension was performed at 72°C for 10 minutes before cooling to 4°C. A 5 µl aliquot of the reaction mixture was run on a gel to confirm successful amplification of the desired region. The remaining mixture was extracted with phenol:chloroform:isoamyl alcohol, ethanol precipitated, re-dissolved in dH_2O and cancatermerised by the Klenow-Kinase-Ligase technique, as described in section 2.1.11.12. Following this procedure, PCR products were cut with 40 units of *Bam*H I for 2 hours at 37°C before further phenol:chloroform:isoamyl alcohol extraction, ethanol precipitation and resuspension in TE buffer. All PCR products were sequenced extensively prior to further use.

4.1.3 PREPARATION OF PλP2-3

This process is illustrated in Figure 4.1 and described below.

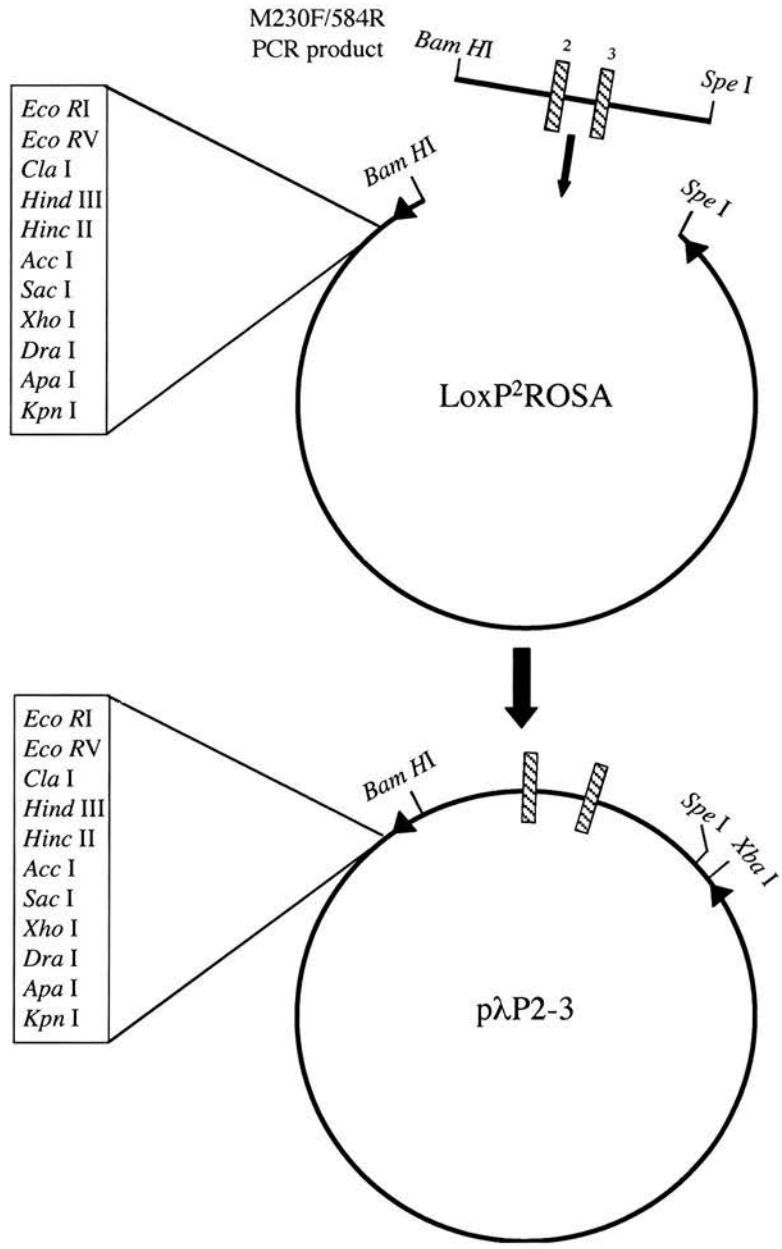

Figure 4.1

The loxP²ROSA vector was linearised by restriction digestion with *Bam HI* and *Spe* I. The M250F/512R PCR product was then ligated into this vector to create the plasmid pλP2-3. Filled triangles (◂), LoxP sites; Shaded rectangles, exons.

4.1.3.1 *Preparation of the LoxP²ROSA26 vector*

Ten μg of the vector LoxP²ROSA were linearized by overnight digestion with *Bam*H I. Following heat inactivation of *Bam*H I, cut ends of the vector were dephosphorylated with 1 unit of CIAP to minimise self re-ligation. The mixture was extracted with phenol:chloroform:isoamylalcohol to inactivate CAIP, ethanol precipitated and resuspended in 20 μl of TE. A 5 μl aliquot of the reaction mixture was run on a gel to check for complete linearization of the vector.

4.1.3.2 *Cloning of M230F/584R PCR product into LoxP²ROSA vector*

Prepared vector and insert were mixed in an approximate 1:3 molar ratio and mixed with 1x ligation buffer, 1 unit of T4 DNA ligase and dH_2O to a final volume of 20 μl. A control reaction was set up containing each of the above reagents with the exception of the PCR fragment insert. Ligation was performed as described in section 2.1.11.8. Following ligation, 3 μl of the reaction mixture were used to transform 40 μl of electrocompetent XLI Blue *E. Coli* by electroporation as described in section 2.1.11.15. Plasmid DNA was isolated by alkaline lysis of overnight cultures and analysed by restriction digestion with *Xho* I, *Cla* I, *Xba* I and *Bam*H I. Plasmids featuring successful cloning events were termed pλP2-3 and underwent extensive sequencing prior to further use. Large-scale preparation of pλP2-3 was performed using a Qiagen Midi prep kit as described in section 2.1.11.2.

4.1.4 PREPARATION OF PλP2-3LTNL

This process is illustrated in Figure 4.2 and described below.

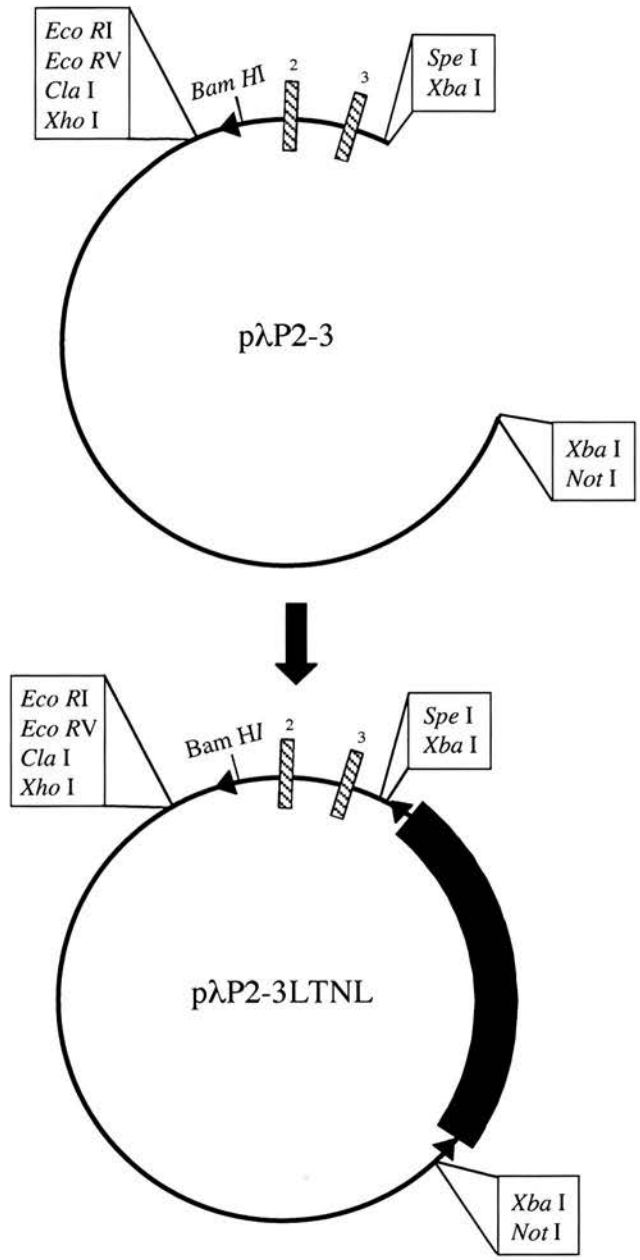

Figure 4.2

The 3.8 kb *Xba* I fragment of pLTNL was ligated into the *Xba* I site of pλP2-3 to create the plasmid pλP2-3LTNL. Black triangle, loxP site; black rectangle, LTNL selection cassette.

4.1.4.1 *Isolation of the Xba I fragment of pLTNL*

The plasmid pLTNL is illustrated in Figure 2.4 and consists of the Thymidine Kinase gene under the transcriptional regulation of the MC1 promoter and a PGK-driven neomycin phosphotransferase gene. LoxP sites flank the 3.8 kb selection cassette. This entire region was isolated by overnight digestion of 20μg of pLTNL with 40 units of *Xba* I. The reaction mixture was loaded into a single well agarose gel and, following electrophoresis, the 3.8 kb fragment was isolated using a QIAEX II kit as described in section 2.1.11.7.

4.1.4.2 *Preparation of the pλP2-3 vector*

Ten μg of pλP2-3 were digested with 10 units of *Xba* I for 4 hours. *Xba* I was heat inactivated and 1 unit of CAIP added to dephosphorylate the cut ends to minimise vector self-ligation. Following incubation for 30 minutes at 37°C, CAIP was inactivated by phenol:chloroform:isoamyl alcohol extraction. The linearised vector was then precipitated with ethanol and resuspended in TE buffer. An aliquot of the vector and LTNL insert were then run on a gel to visually assess the yield of each.

4.1.4.3 *Cloning of Xba I fragment of pLTNL into the pλP2-3 vector*

The insert and vector were mixed in an approximate 3:1 ratio and ligation performed as described in section 2.1.11.8. A negative control ligation reaction containing no insert was also performed. Five μl of the ligation mix were used to transform 40 μl of electrocompetent XLI Blue *E. Coli* as previously described. Colonies were screened by plasmid miniprep and *Xba* I digestion. Plasmids featuring successful cloning events were termed pλP2-3LTNL and prepared on a large scale using a Qiagen Midi-prep kit as described in section 2.1.11.2.

4.1.4.4 *Destruction of the 5' Xba I site of PλP2-3LTNL*

The plasmid pλP2-3LTNL contained 2 *Xba* I sites flanking the LTNL insert as illustrated in Figure 4.2. The cloning strategy for the insertion of the 3' homology arm necessitated the destruction of the 5' *Xba* I site. This was achieved by partial digestion of pλP2-3LTNL with decreasing concentrations of *Xba* I. The linearised vector was then run on a gel to separate any plasmids that had been cut at both *Xba* I sites and the 7.6 kb single-cut vector isolated from the gel using a QIAEX II kit. The cut ends of the vector were blunt ended as described in section 2.1.11.9 and contaminating enzyme and dNTPs removed by phenol:chloroform:isoamyl alcohol extraction and ethanol precipitation. The linearised vector was then resuspended in TE and re-ligated using the previously described method. Five µl of the ligation mixture were used to transform electrocompetent XLI Blue *E. coli*. This process resulted in the generation of 3 different populations of plasmids featuring the destruction of either the 5' or 3'*Xba* I sites or the original configuration in which both *Xba* I were present. Restriction digestion mapping with *Xba* I and *Xho* I was used to distinguish between these populations.

4.1.5 PREPARATION OF 3' HOMOLOGY ARM

The initial step in the construction of the 3' homology arm was to sub-clone the region of the ET_B receptor gene spanning from the *Hpa* I site in intron 3 to the first 54 bp of exon 5 into the pBluescript® II KS+ vector (illustrated in Figure 4.3). For the short homology arm of pλPW(NoDT), this fragment was subsequently sub-cloned into the 3' region of the modified pλP2-3LTNL plasmid linearised with *Xba* I and *Not* I (illustrated in Figure 4.5). For pλPW, the region downstream of the *Bse* RI site in intron 4 was replaced with a diphtheria toxin gene cassette, producing the plasmid pλP4-dt. The cassette was isolated from the plasmid pCAGGS-dt (illustrated in Figure 2.6) and sub-cloned into the shuttle vector pSP72poly1 (Figure 2.7). The shuttle vector was used to provide additional restriction sites in the polylinker region to facilitate the later sub-cloning of pλP4-dt into the pλP2-3LTNL construct (Figure 4.5).

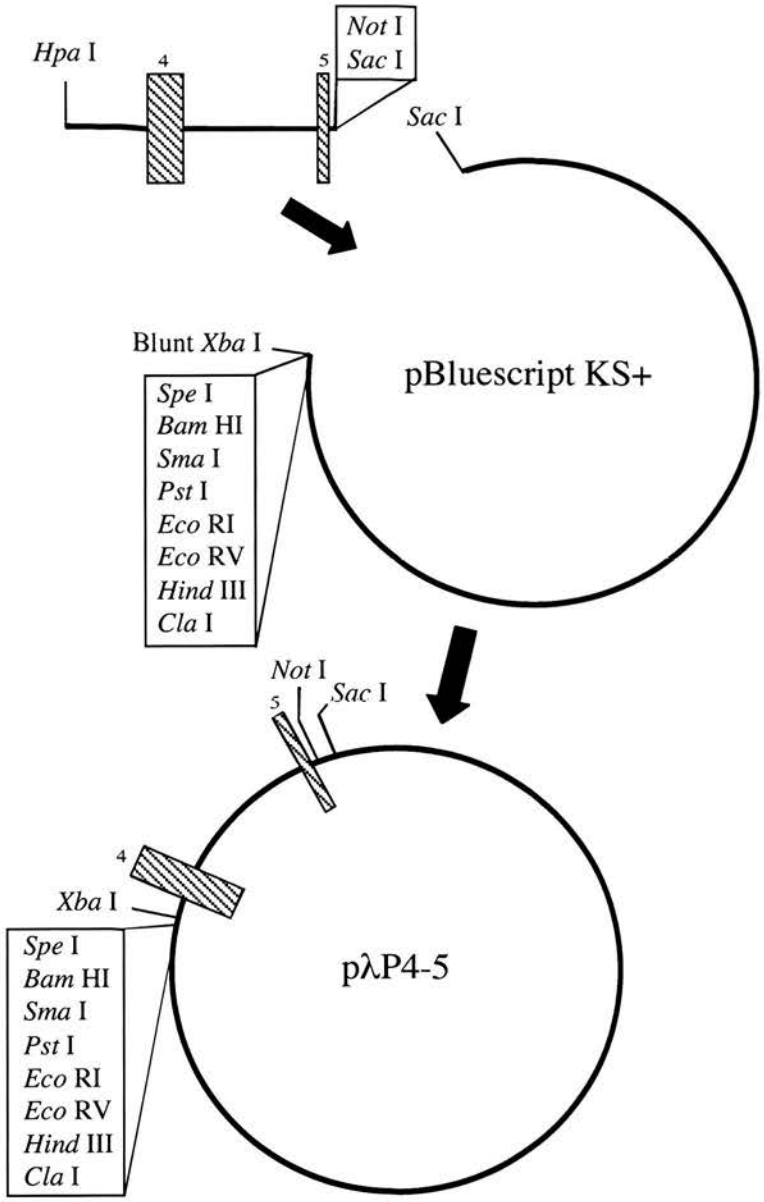

Figure 4.3

The *Hpa* I-*Sac* I fragment of pλP was isolated and ligated to a pBluescript vector linearised with *Xba* I, blunt-ended and then cut with *Sac* I to produce the plasmid pλP4-5. Shaded rectangles, exons.

4.1.5.1 *Preparation of pλP4-5*

The 2.0 kb *Hpa* I-*Sac* I fragment of pλP was isolated by restriction digestion, gel electrophoresis and use of a QIAEX II kit as described previously. The pBluescript® KS+ vector was linearised by *Xba* I restriction digestion followed by blunt ending of the cut ends using Klenow enzyme as described in section 2.1.11.9. The linearized vector was then cut with *Sac* I before extraction with phenol:chloroform:isoamyl alcohol, ethanol precipitation and resuspension in TE. XLI Blue *E. coli* transformed by electroporation with 5 μl of ligation mixture were screened for the presence of the insert by hybridisation with a PCR-prepared radio-labelled probe. The primers INT3F and 417R were used to amplify the 895 bp region spanning from intron 3 to exon 4 of the ET_B receptor gene. The probe was gel-purified using a QIAEX II kit and labelled with ^{32}P dCTP as described in section 2.1.11.17. Hybridisation was performed overnight at 68°C on colony lifts of transformed cells prepared as described in section 2.1.11.16. Positive colonies were picked, grown overnight and plasmid DNA isolated by alkaline lysis. Plasmids were mapped by restriction digestion with *BamH* I, *Xba* I and *Eco* RI to confirm the presence and orientation of the *Hpa* I-*Sac* I fragment. The results were subsequently confirmed by direct sequencing of the insert. The resultant plasmid was termed pλP4-5. Large-scale preparation of pλP4-5 was performed using a Qiagen Midi-prep kit as previously described.

4.1.5.2 *Isolation of the diphtheria toxin gene cassette from pCAGGS-dt*

The plasmid pCAGGS-dt (Figure 2.6) contains the diphtheria toxin gene under the transcriptional regulation of the chicken actin gene promoter region and a rabbit β-globin polyadenylation signal. The 2857 bp fragment containing these elements was isolated by restriction digestion with *Spe* I, *Hind* III and *Bam*H I, followed by gel electrophoresis and use of a QIAEX II kit as previously described. Subsequent cloning steps for the construction of pλPW required preservation of the 3' *Not* I site. In order to achieve this, the *Spe* I-*Hind* III fragment of pCAGGS-dt was ligated into a pSP72poly 1 plasmid (illustrated in Figure 2.7) that had been linearised by overnight restriction

digestion with *Xba* I and *Hind* III. pSP72poly 1 contains a *Not* I site in the polylinker region 3' to the *Hind* III site and an *Xho* I site 5' to the *Xba* I site destroyed during this ligation step. This shuttle plasmid was named pCAGGS-dt in pSP72poly 1. Following electroporation of the ligation mix, the presence and orientation of the CAGGS-dt insert was confirmed by restriction digestion mapping with the enzymes *Xho* I and *Not* I.

4.1.5.3 *Preparation of pλP4-dt*

The preparation of pλP4-dt is illustrated in Figure 4.4. Five μg of pλP4-5 were digested overnight with 10 units of *Bse*R I. The enzyme was heat inactivated and the cut ends of the plasmid blunt ended using Klenow enzyme as previously described. The mixture was phenol:chloroform:isoamyl alcohol extracted, ethanol precipitated and resuspended in TE. The linearised plasmid was then further digested with 10 units of *Not* I to remove the 300 bp region between the *Bse*R I site and the *Not* I site in the plasmid polylinker region. The resultant fragments were separated by gel electrophoresis and the 4.1 kb linearised vector fragment isolated using a QIAEX II kit. To produce compatible ends for ligation, CAGGS-dt in pSP72poly 1 was cut with *Xho* I and blunt-ended as previously described. This was followed by further digestion with *Not* I and *Pvu* I. The *Xho* I-*Not* I fragment of CAGGS-dt in pSP72poly 1 contains the diphtheria toxin gene with associated promoter and polyadenylation sequences. There is a single *Pvu* I site within the vector region of CAGGS-dt in pSP72poly 1. The inclusion of a *Pvu* I digestion step produced additional linearised vector fragments with cut ends that were incompatible with subsequent cloning steps. This technique was utilised to circumvent the requirement for gel isolation of the *Xho* I-*Not* I fragment. The linearised pλP4-5 vector and diphtheria toxin gene cassette were then ligated as described in section 2.1.11.8 and 5 μl of ligation mix used to transform 40 μl of XLI Blue *E. coli* by electroporation. Colonies were picked, grown overnight and plasmid DNA prepared by the alkaline lysis method. The presence and orientation of the inserted diphtheria toxin gene cassette were confirmed by restriction digestion mapping with the enzymes *Spe* I and *Not* I.

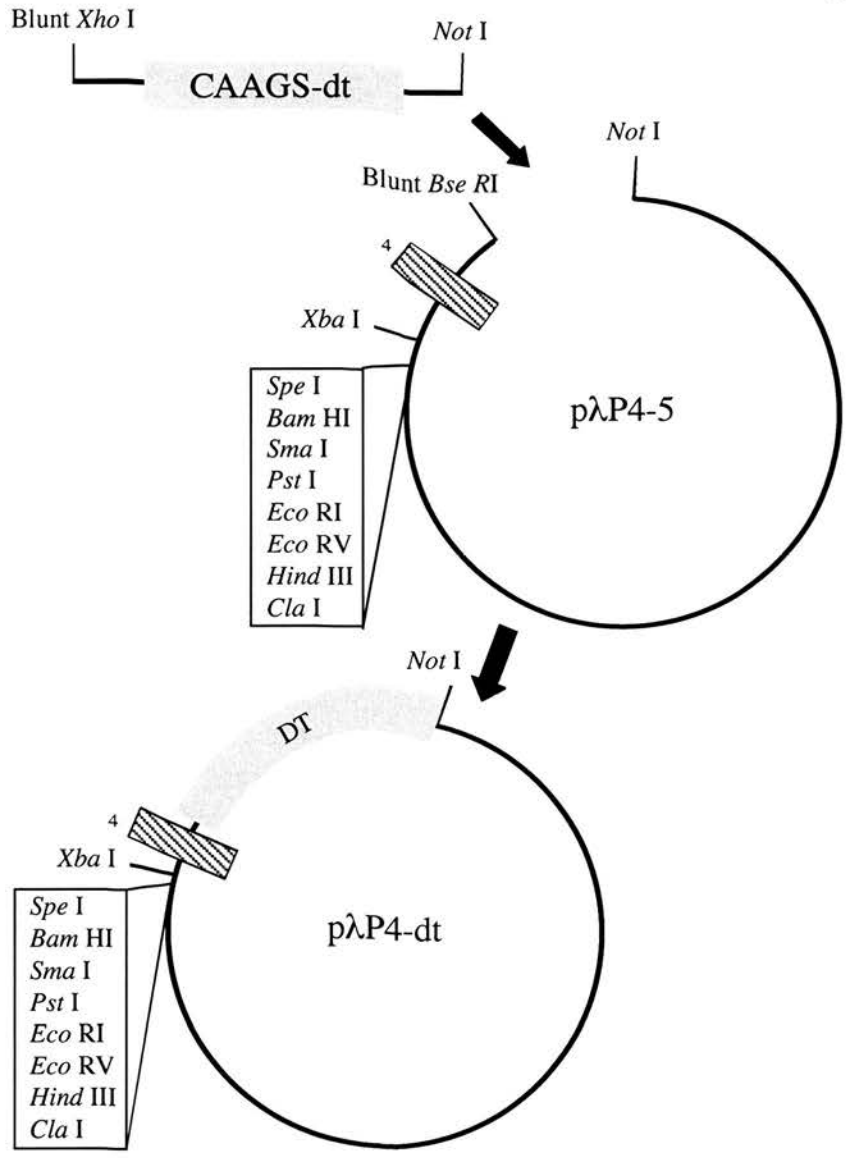

Figure 4.4

CAAGS-dt in pSP72 poly 1 was digested with *Xho* I and blunt ended. The *Xho* I-*Not* I fragment was isolated and ligated to a pλP4-5 vector that had been linearised by restriction digestion with *Bse* RI, blunt ended and then further digested with *Not* I. The resultant plasmid was termed pλP4-dt. Shaded rectangles, exons.

4.1.5.4 *Preparation of pλP2-3LTNL4-dt*

Five μg of the construct pλP2-3LTNL were linearised in the 3' polylinker region by restriction digestion with *Xba* I and *Not* I. The 4.8 kb *Spe* I-*Not* I fragment of pλP4-dt was prepared by restriction digestion of 5 μg of pλP4-dt with *Spe* I, *Not* I and *Pvu* I. Restriction digestion with *Pvu* I was included to avoid the requirement for gel isolation of the insert fragment as described earlier. This process is illustrated in Figure 4.5. Ligation of the vector and insert was performed as previously described and 40 μl of XLI Blue *E. coli* transformed by electroporation. Colonies were screened by plasmid miniprep and *Cla* I and *Not* I digestion. Large-scale preparation of pλP2-3LTNL4-dt was undertaken using a Qiagen Midi-prep kit as previously described.

4.1.5.5 *Preparation of pλP2-5LTNL*

The 3' homology arm of pλPW(NoDT) was prepared by restriction digestion of 5 μg of pλP4-5 with *Spe* I, *Not* I and *Pvu* I. The ~2.0 kb *Spe* I-*Not* I fragment was then ligated with the vector pλP2-3LTNL linearised in the 3' polylinker region by restriction digestion with *Xba* I and *Not* I. This process is illustrated in Figure 4.5. Ligation was performed as previously described and 5 μl of the ligation mix were used to transform XLI Blue *E. coli* by electroporation. Plasmid DNA isolated from colonies by alkaline lysis miniprep were screened by restriction digestion mapping with the enzymes *Cla* I and *Not* I. The plasmid was subsequently prepared on a large scale using a Qiagen Midi-prep kit as previously described.

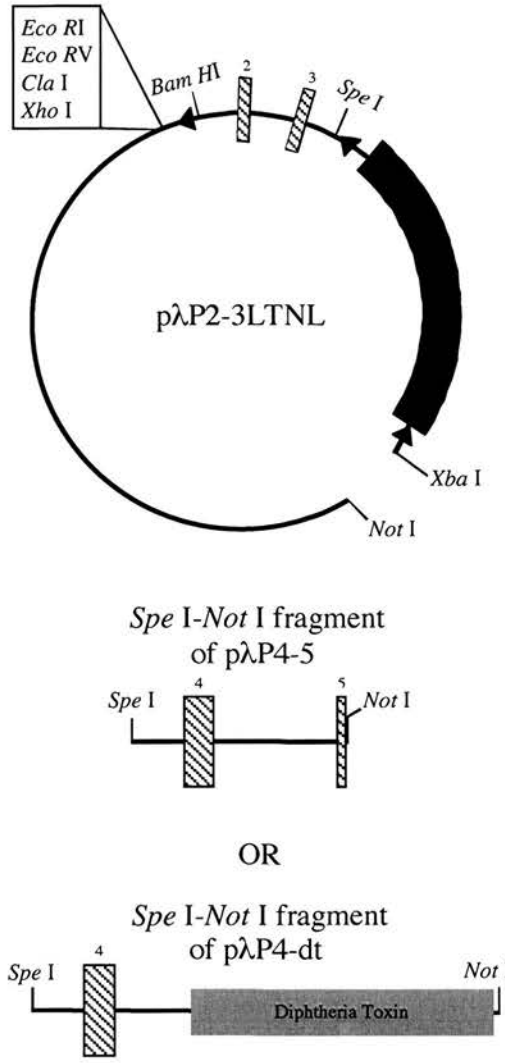

Figure 4.5

The vector pλP2-3LTNL was linearised by restriction digestion with *Xba* I and *Not* I and ligated to the *Spe* I-*Not* I fragment of either pλP4-5 (for pλPW(NoDT)) or pλP4-dt (for pλPW). This process destroyed the *Spe* I/*Xba* I site but preserved the 3' *Not* I site. Black triangle, loxP site; black rectangle, LTNL selection cassette; shaded rectangles, exons.

4.1.6 PREPARATION OF 5' HOMOLOGY ARM

The 5' polylinker region of pλP2-5LTNL and pλP2-3LTNL4-dt are identical and contain *Xho* I and *Cla* I sites orientated as illustrated in Figure 4.6. The same cloning strategy for the addition of the long 5' homology arm was, therefore, utilised in the preparation of pλPW(NoDT) and pλPW. To facilitate cloning, the plasmid pλP (Figure 2.9) was modified by the addition of an *Xho* I linker into the 5' polylinker region adjacent to intron 1 to produce pλPXho (Figure 2.10). A native *Nae* I site located 1454 bp upstream of exon 2 in pλP was used in conjunction with the *Xho* I site to remove a 11911 bp fragment of intron 1 from pλP for use in subsequent cloning steps (illustrated in Figure 2.10).

4.1.6.1 *Addition of a Xho I linker site to pλP*

Because of a paucity of unique restriction sites within intron 1 of the ET_B receptor gene, an *Xho* I site was introduced into pλP to facilitate cloning of the 5' homology arm. The primer XHO I (CCTCGAGGGGCC) was designed to include both an *Xho* I site and termini that were compatible with *Apa* I-cut vector termini. The 5' termini of 2 μg of this primer were phosphorylated by incubation with 2 units of polynucleotide kinase enzyme (PNK), 1 x PNK buffer (50mM Tris-HCl pH 7.6, 10mM $MgCl_2$, 5mM DTT, 0.1mM spermidine and 0.1mM EDTA) and 1mM ATP at 37°C for 60 minutes. The enzyme was heat inactivated and the mixture allowed to cool slowly to room temperature to facilitate annealing of linkers. pλP was then linearised at the *Apa* I site within the polylinker region adjacent to intron 1. Following dephosphorylation, linearised pλP was phenol:chloroform:isoamyl alcohol extracted, ethanol precipitated and resuspended in TE. 0.5 μg of pλP were then ligated with 2.0 μg of phosphorylated XHO I linkers as previously described with the addition of 1mM ATP to the ligation reaction. Five μl of the ligation mix were used to transform 40 μl of DH10B *E. coli*.. Plasmid DNA was isolated from transformed colonies by the alkaline lysis method and screened by restriction digestion mapping with the enzymes *Xho* I and *Sal* I.

4.1.6.2 *Preparation of pλPW and pλPW(NoDT)*

The preparation of pλPW and pλPW(NoDT) is illustrated in Figure 4.6 and Figure 4.7, respectively. Five μg of pλP2-3LTNL4-dt and pλP2-5LTNL were linearised by digestion with *Cla* I. The vectors were then blunt-ended using CAIP as previously described. Following phenol:chloroform:isoamylalcohol extraction, ethanol precipitation and resuspension in TE, the linearised vectors were cut with *Xho* I. The 5' long homology arm was prepared by overnight digestion of 10 μg of pλPXho with 20 units of Turbo™ *Nae* I (Promega, Southhampton, UK; Product number R7321). Turbo™ *Nae* I buffer contains a non-cleavable effector sequence that facilitates the efficient digestion of slow and resistant sites. Preliminary attempts at restriction digestion of pλPXho without this buffer had demonstrated that 1 of the 2 *Nae* I sites was resistant to cleavage, despite overnight incubation with a tenfold excess of the enzyme. Following digestion, the reaction mixture was extracted with phenol:chloroform:isoamylalcohol, precipitated with ethanol and resuspended in TE. The plasmid was then digested with *Xho* I and the resultant ~11.9 kb *Xho* I-*Nae* I fragment separated by gel electrophoresis. The fragment was recovered using a QIAEX II kit and ligated to the pλP2-3LTNL4-dt and pλP2-5LTNL vectors as previously described. Five μl of ligation mixture were used to transform 40 μl of DH10B *E. coli* and plasmid DNA was isolated from colonies using the alkaline lysis method. Plasmids were screened for the presence and orientation of the *Xho* I-*Nae* I insert by restriction digestion mapping with *Xho* I and *Sal* I. Positive colonies were subsequently restriction digest mapped in greater detail and sequenced to confirm the presence of each element of the completed construct.

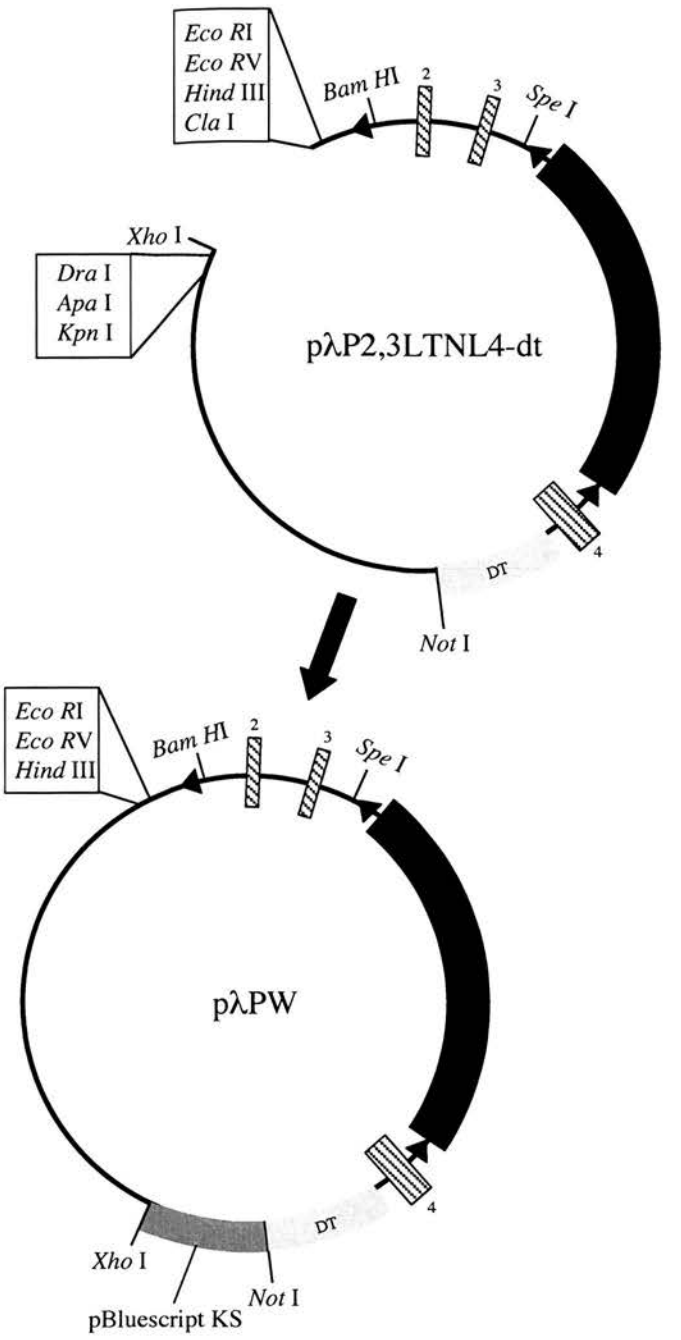

Figure 4.6

The *Xho* I-*Nae* I (blunt) fragment of pλP*Xho* was sub-cloned into the pλP4-dt vector to complete the targeting construct pλPW. Black triangle, loxP site; black rectangle, LTNL selection cassette; shaded rectangles, exons.

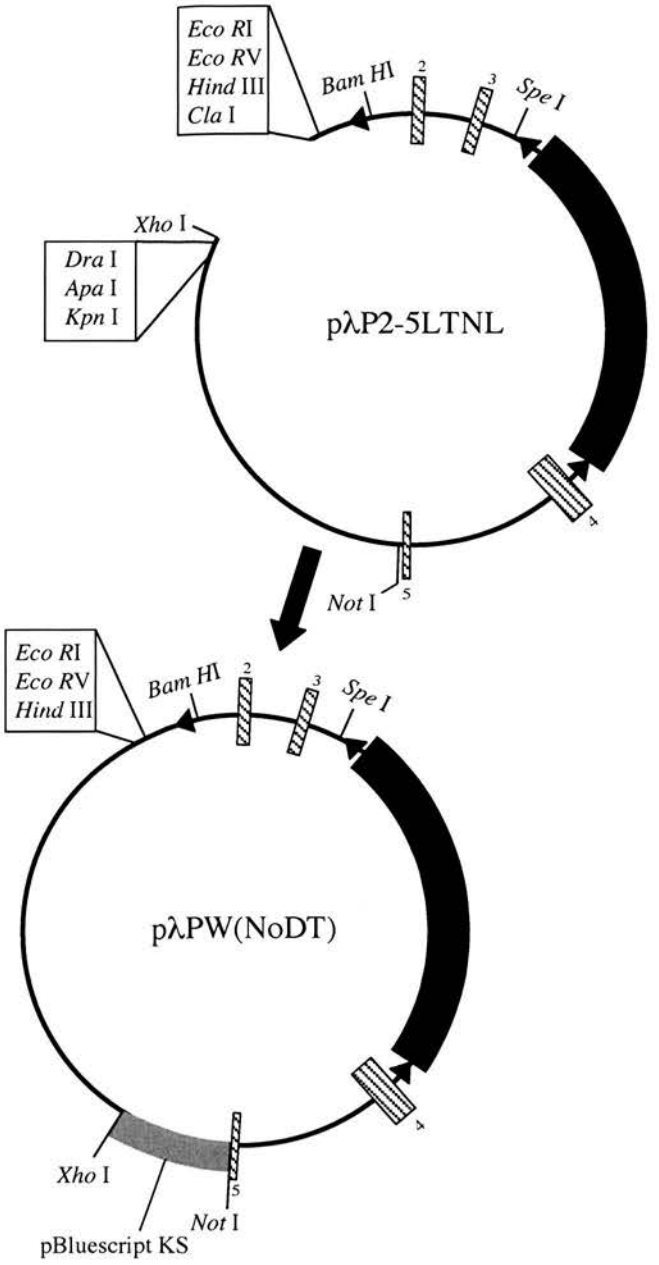

Figure 4.7

The *Xho* I-*Nae* I (blunt) fragment of pλP*Xho* was sub-cloned into the pλP2-5LTNL vector to complete the targeting construct pλPW(NoDT). Black triangle, loxP site; black rectangle, LTNL selection cassette; shaded rectangles, exons.

4.1.7 RESULTS

4.1.7.1 *Preparation of pλP2-3*

The results of PCR with the primers M230F/584R are illustrated in Figure 4.8. Following electroporation, 30 colonies were obtained from 150 μl of ligation mixture. Two colonies were obtained from the equivalent negative control plate. Plasmid DNA was screened by digestion with *Bam*H I. Successful incorporation of the PCR product into the vector would be expected to produce an additional band of 956 bp. A single plasmid (number 21) produced the expected pattern and was termed pλP2-3. These results are illustrated in Figure 4.9.

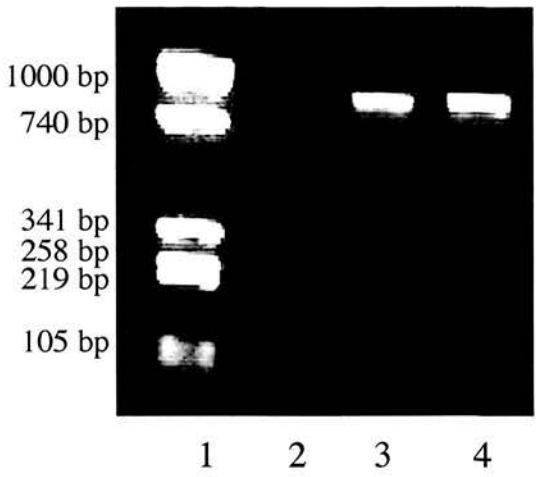

Figure 4.8

PCR amplification of 129 ES cell genomic DNA using primers M230F and 584R and *Pfu* DNA polymerase. Lane 1, pBluescript/*Sau* 3AI DNA; Lane 2, negative control (No DNA); Lanes 3 and 4, 956bp PCR product.

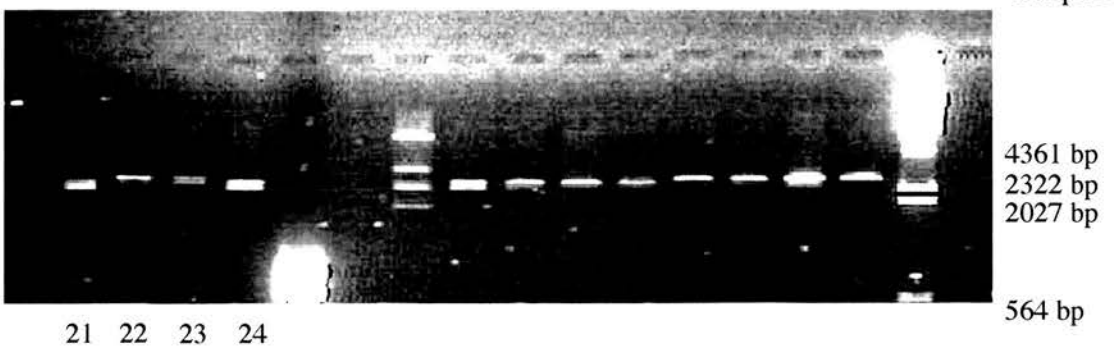

Figure 4.9

BamH I digestion of plasmid DNA following electroporation of M230F/584R PCR product/LoxP^{2}ROSA vector ligation mix. Lane 21 demonstrates an additional 956 bp band consistent with successful cloning of the PCR product.

4.1.7.2 *Further analysis of pλP2-3 by restriction digestion mapping*

pλP2-3 was further characterised by restriction digestion mapping with the enzymes *Xho* I, *Cla* I, *Xba* I and *Bam*H I. Double digests with *Xho* I and *Cla* I, and *Xba* I and *Cla* I produced identical bands of 956 bp (Figure 4.10) corresponding to the incorporation of the PCR product into the polylinker region of LOXP^{2}ROSA. Because of the short insert size, orientation of the insert fragment was determined by sequencing alone.

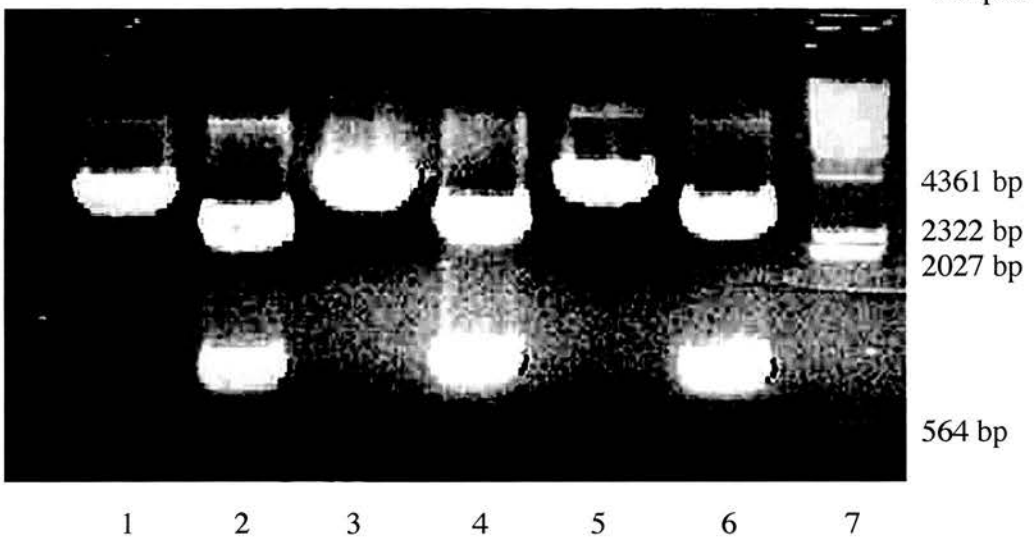

Figure 4.10

Restriction digestion mapping of pλP2-3 demonstrating the presence of *BamH* I sites flanking the 956 bp M230F/584R insert. Lane 1, *Xho* I; Lane 2 *Xho* I + *Xba* I; Lane 3, *Cla* I; Lane 4, *Cla* I + *Xba* I; Lane 5, *Xba* I; Lane 6, *BamH* I; Lane 7, Lamda DNA/*Hind* III.

4.1.7.3 *Direct sequencing of pλP2-3*

Alignment of the pλP2-3 sequence with the recently published mouse ET_B receptor sequence is illustrated in Figure 4.11 and Figure 4.12.

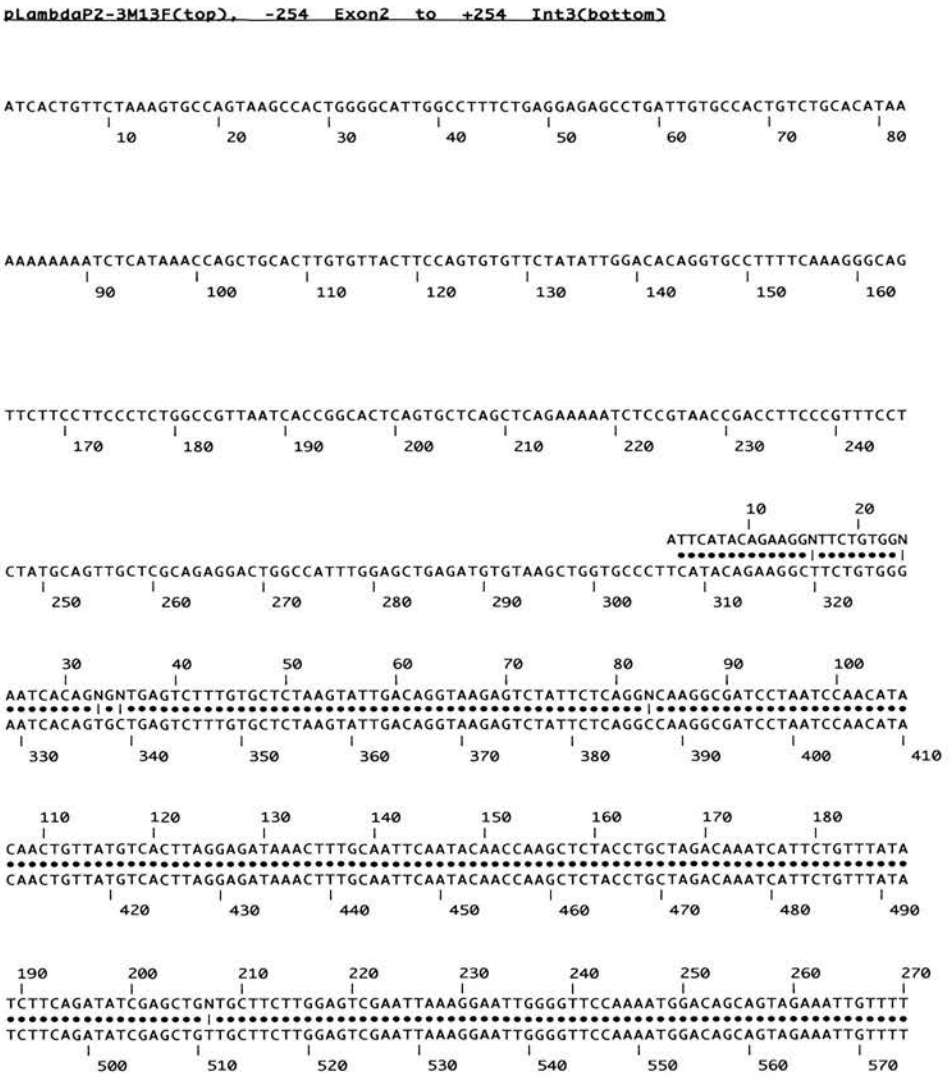

Figure 4.11

Sequence alignment of the plasmid pλP2-3 sequenced with the M13F primer (top) with the published sequence of the ET_B receptor gene locus from 254bp upstream of exon 2 to 254bp downstream of exon 3 (bottom).

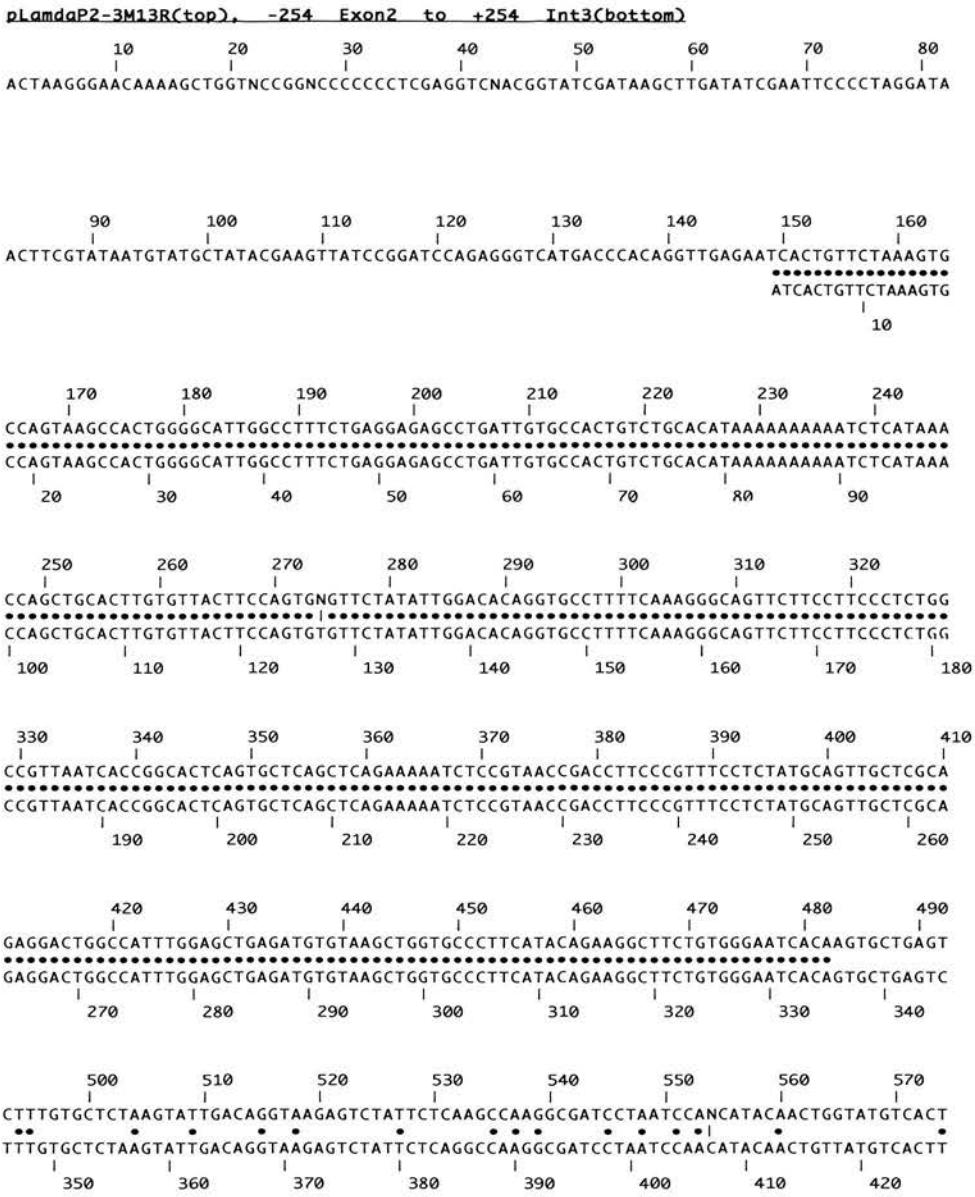

Figure 4.12

Sequence alignment of the plasmid pλP2-3 sequenced with the M13R primer (top) with the published sequence of the ET_B receptor gene locus from 254bp upstream of exon 2 to 254bp downstream of exon 3 (bottom).

4.1.7.4 *Preparation of pλP2-3LTNL*

The 150 μl ligation and negative control plates yielded 123 and 76 colonies respectively. Successful incorporation of the LTNL *Xba* I fragment into pλP2-3 was identified by the presence of an additional 3.8 kb band following digestion with *Xba* I (data not shown). Insert orientation was determined by sequencing and further restriction digestion mapping.

4.1.7.5 *Destruction of the 5' Xba I site of PλP2-3LTNL*

Colonies in which the 5' *Xba* I site was destroyed produced fragments of 4.5 kb and 3.0 kb. Destruction of the 3' *Xba* I site resulted in fragments of 800 bp and 6.8 kb. Preservation of both *Xba* I sites resulted in fragments of 800 bp, 3.8 kb and 3.0 kb. Plasmid numbers 8 and 25 demonstrated digestion patterns compatible with destruction of the 5' *Xba* I site and were selected for further mapping by restriction digestion and sequencing. The results are illustrated in Figure 4.13.

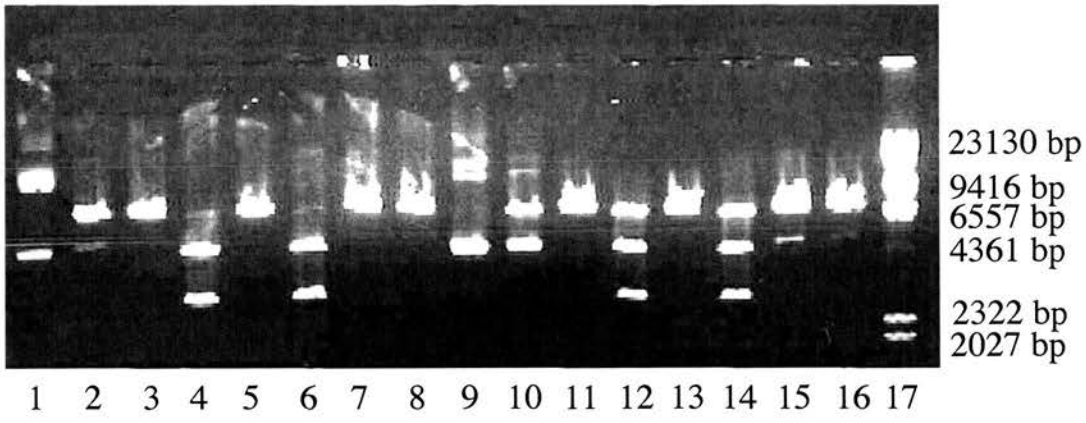

Figure 4.13

Restriction digestion analysis of 2 clones of pλP2-3LTNL following destruction of the 5' *Xba* I site. Lanes 1-8, Clone 8. Lanes 9-16, Clone 25. Lanes 1 and 9, uncut; Lanes 2 and 10, *Xba* I; Lanes 3 and 11, *Xho* I; Lanes 4 and 12, *Xba* I and *Xho* I; Lanes 5 and 13, *Cla* I; Lanes 6 and 14, *Cla* I and *Xba* I; Lanes 7 and 15, *Not* I; Lanes 8 and 16, *Not* I and *Xba* I. Lane 17, Lamda/*Hind* III DNA.

4.1.7.6 *Preparation of pλP4-5*

Multiple colonies containing the sub-cloned *Hpa* I-*Sac* I fragment of pλP were identified following hybridisation with the radiolabelled INT3F/417R probe. Plasmid DNA insert orientation was determined in selected colonies by restriction digestion with *Bam HI*, *Eco RI* and *Xba* I. The results are illustrated in Figure 4.14. Ligation of the *Hpa* I-cut end to the blunt-ended *Xba* I site of the pBluescript vector resulted in the formation of a new *Xba* I site, but this did not interfere with subsequent cloning steps.

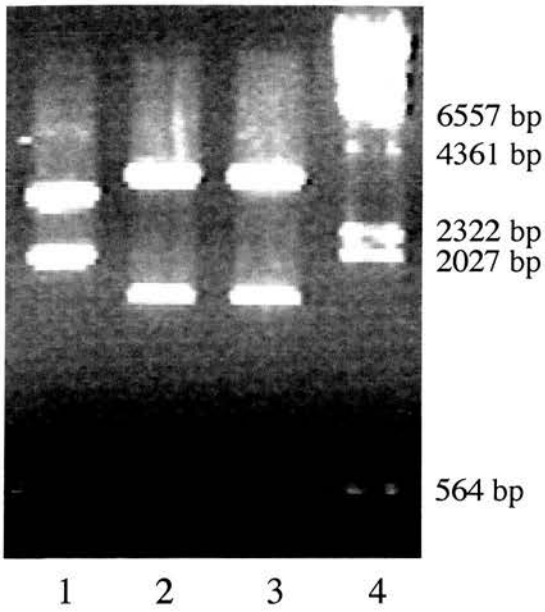

Figure 4.14

Restriction digestion analysis of pλP4-5. Lane 1, *Bam HI*; Lane 2, *Eco RI*, Lane 3, *Xba* I; Lane 4, Lambda/*Hind* III DNA.

4.1.7.7 *Preparation of pCAGGS-dt in pSP72 poly1*

Plasmid DNA was screened for the presence of the 2857 bp *Spe* I-*Hind* III fragment of pCAGGS-dt by restriction digestion with *Xho* I and *Not* I. The results are illustrated in Figure 4.15. Lanes 3, 6, 10, 11 and 14 demonstrate bands of ~2.8 kb (insert) and ~2.5 kb (vector) consistent with successful ligation of the diphtheria toxin gene cassette into the shuttle vector.

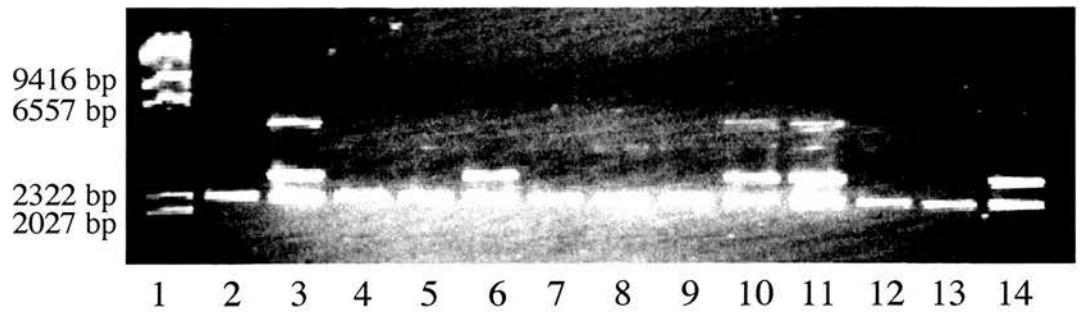

Figure 4.15

Restriction digestion analysis of plasmid DNA with *Xho* I and *Not* I following ligation of the *Spe* I-*Hind* III fragment of pCAGGs to pSP72 poly1 cut with *Xba* I and *Hind* III. Lane 1, Lamda/*Hind* III DNA; Lanes 3, 6, 10, 11 and 14 demonstrate an additional band of ~2.8 kb consistent with successful ligation. These plasmids were termed pCAGGs-DT in pSP72poly1.

4.1.7.8 *Preparation of pλP4-dt*

Correctly orientated inserts within the plasmids were predicted to produced bands of 3.0 kb (vector) and 4.8 kb (insert) following restriction digestion with *Spe* I and *Not* I. Lanes 2-10, 12-13, 16-17 and 19-25 demonstrate successful ligation and the resulting plasmid was termed pλP4-dt (illustrated in Figure 4.16).

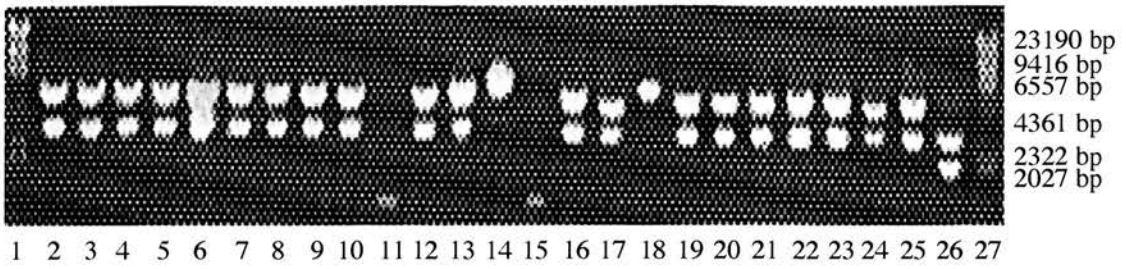

Figure 4.16

Restriction digestion analysis of plasmid DNA with *Spe* I and *Not* I following ligation of pλP4-5 cut with *Not* I and *Bse* RI (blunt) to pCAGGs-DT cut with *Xho* I (blunt), *Not* I and *Pvu* I. Lanes 1 and 27, Lambda/*Hind* III DNA; Lanes 2-10, 12-13, 16-17 and 19-25 demonstrate successful ligation and the resulting plasmid was termed pλP4-dt. Lane 26, pλP4-5 cut with *Spe* I and *Not* I.

4.1.7.9 *Preparation of pλP2-3LTNL4-dt*

Sub-cloning of the *Spe* I-*Not* I fragment of pλP4-dt into pλP2-3LTNL resulted in destruction of the 5' *Xba* I/*Spe* I sites and preservation of the 3' *Not I* site. Plasmids in which the *Spe* I-*Not* I fragment was successfully ligated produced bands of 9.1 kb (insert) and 3.0 kb (vector) when digested with *Cla* I and *Not* I. In contrast, control plasmids produced bands of 4.3 kb (*Cla* I-*Not* I fragment of pλP2-3LTNL) and 3.0 kb (vector). These results are illustrated in Figure 4.17.

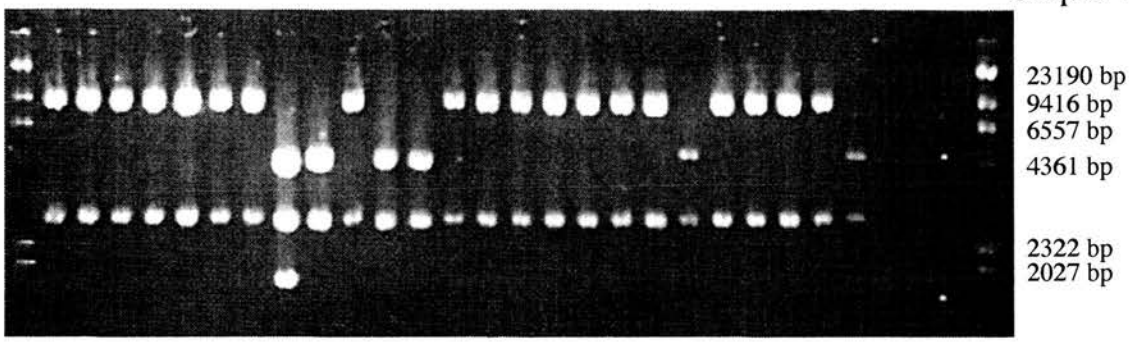

Figure 4.17

Restriction digestion analysis of plasmid DNA with *Not* I and *Cla* I following ligation of pλP2-3LTNL cut with *Xba* I and *Not* I to pλP4-dt cut with *Not* I, *Spe* I and *Pvu* I (lanes 1-24). Lane 25, pλP2-3LTNL cut with *Not* I and *Cla* I. Clones 1-7, 10, 13-19 and 21-24 demonstrated successful ligation and were termed pλP2,3LTNL4-dt.

4.1.7.10 *Preparation of pλP2-5LTNL*

Plasmids with the *Spe* I-*Not* I fragment of pλP4-5 successfully inserted into the pλP2-3LTNL vector produced bands of 6.3 kb and 3.0 kb when digested with *Cla* I and *Not* I (illustrated in Figure 4.18).

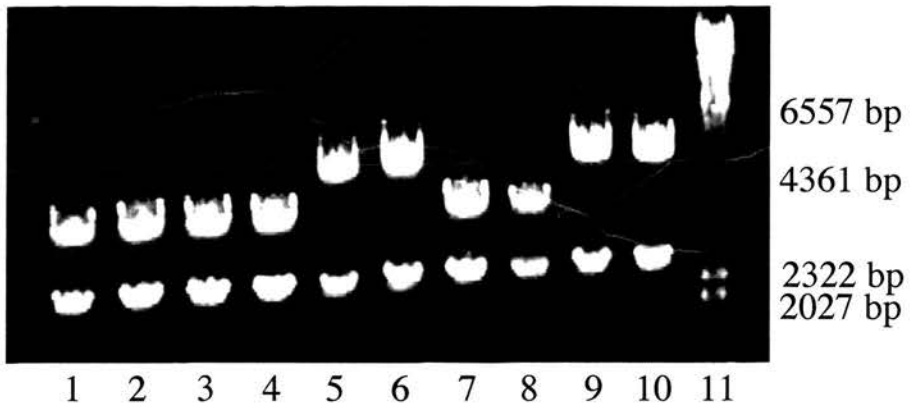

Figure 4.18

Restriction digestion analysis of plasmid DNA with *Cla* I and *Not* I following ligation of pλP2-3LTNL cut with *Xba* I and *Not* I to pλP4-5 cut with *Spe* I, *Not* I and *Pvu* I. Clones 5,6, 9 and 10 demonstrate bands of 3.0 kb and 6.3 kb consistent with successful ligation. These clones were named pλP2-5LTNL. Lane 11, Lamda/*Hind* III DNA.

4.1.7.11 *Addition of Xho I linker site to pλP*

Successful incorporation of the *Xho* I linker site into the polylinker of pλP was evidenced by the appearance of bands measuring ~7.2 kb and ~8.5 kb following restriction digestion with *Xho* I and *Sal* I. In contrast, digestion of pλP resulted in a single band of ~15.7 kb. These results are illustrated in Figure 4.19 and Figure 4.20.

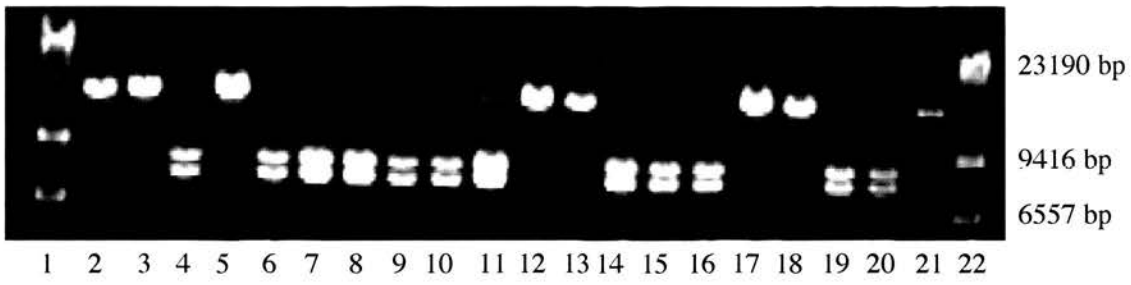

Figure 4.19

Restriction digestion analysis of plasmid DNA with *Xho* I and *Sal* I following addition of *Xho* I linker into the *Apa* I site of pλP. Lanes 1 and 22, Lambda/*Hind* III DNA; Lanes 4, 6 11, 14-16 and 19-20 demonstrate successful insertion of linker and were termed pλPXho. Lane 21, pλP digested with *Xho* I and *Sal* I.

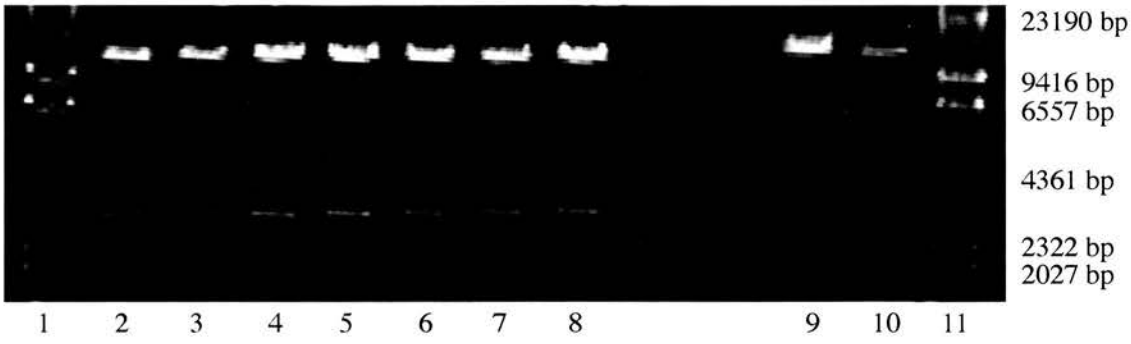

Figure 4.20

Restriction digestion analysis of pλPXho. Lanes 1 and 11, Lambda/*Hind* III DNA; Lanes 2-8 confirm successful ligation with liberation of ~3.0 kb band following digestion with *Xho* I and *Not* I; Lane 9, undigested DNA; Lane 10, pλP digested with *Xho* I and *Not* I.

4.1.7.12 *Preparation of pλPW and pλPW(NoDT)*

Representative gels of restriction digestion mapping exercises are illustrated in Figure 4.21 and Figure 4.22.

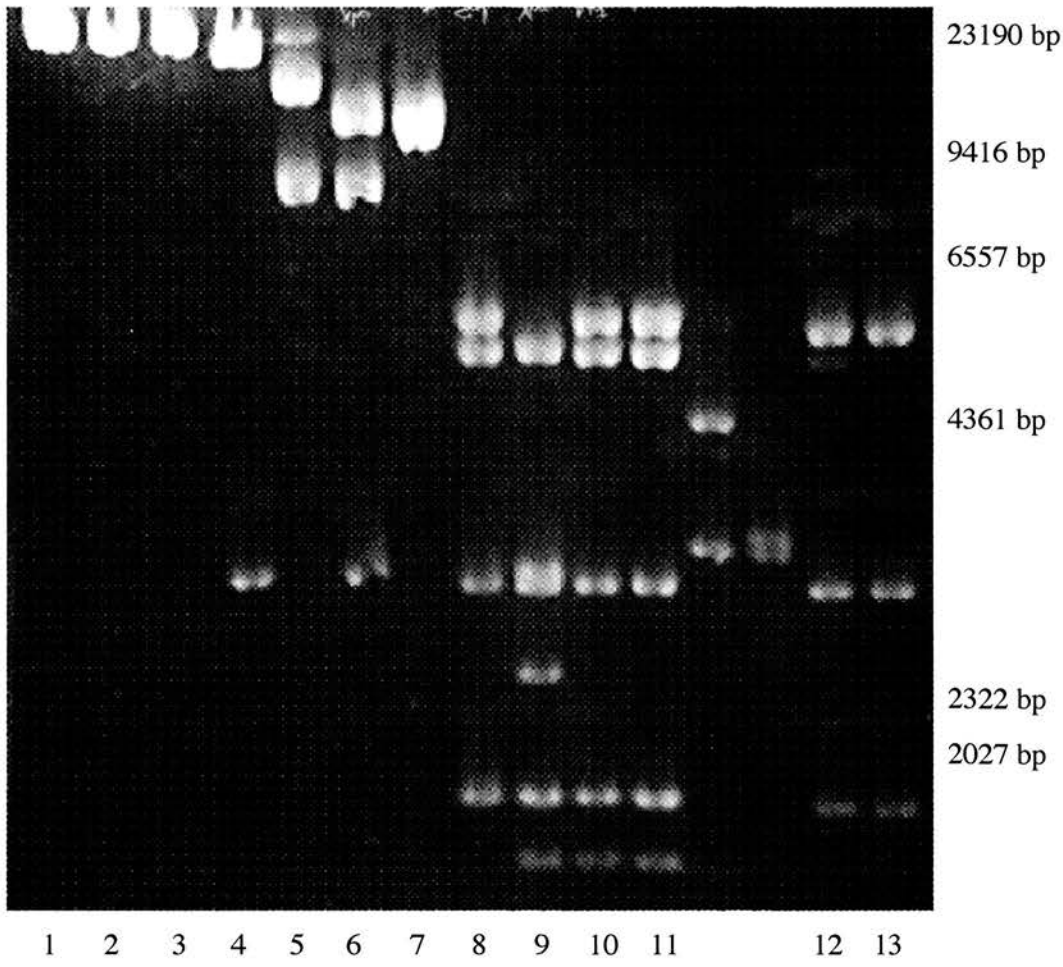

Figure 4.21

Restriction digestion analysis of pλPW. Lane 1, *Not* I; Lane 2, *Xho* I; Lane 3, *Sal* I; Lane 4, *Xho* I and *Not* I; Lane 5, *Xho* I and *Sal* I; Lane 6, *Xho* I, *Sal* I and *Not* I; Lane 7, *Not* I and *Sal* I; Lane 8, *Sal* I and *Hind* III; Lane 9, *Xho* I and *Hind* III; Lane 10, *Not* I and

Hind III; Lane 11, *Hind* III; Lane 12, pλP2-5LTNL and *Hind* III; Lane 13, pλP2-5LTNL, *Sal* I and *Hind* III.

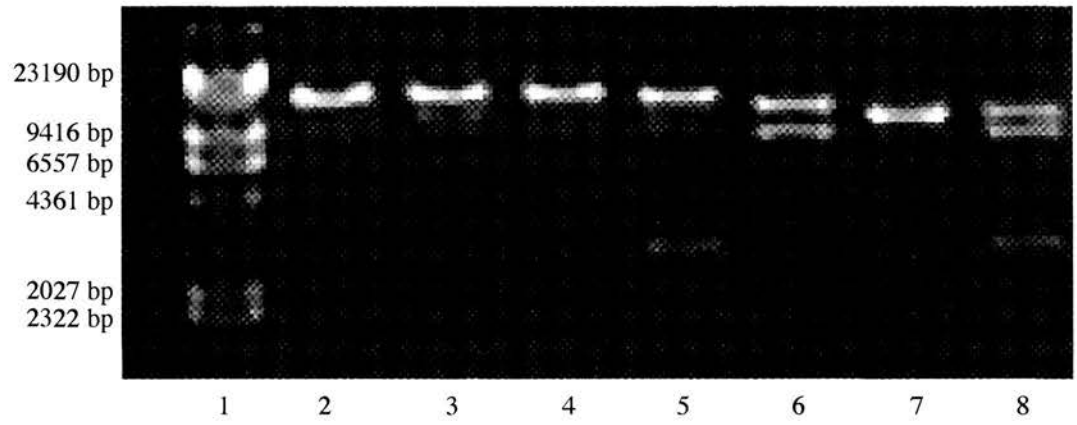

Figure 4.22

Restriction digestion analysis of pλPW. Lane 1, Lamda/Hind III; Lane 2, Xho I; Lane 3, *Not* I; Lane 4, *Sal* I; Lane 5, *Xho* I and *Not* I; Lane 6, *Xho* I and *Sal* I; Lane 7, *Sal* I and *Not* I; Lane 8, *Sal* I, *Not* I and *Xho* I.

4.1.8 DISCUSSION

This chapter has described the construction of the targeting vectors pλPW and pλPW(NoDT). These vectors were designed to facilitate homologous recombination within the mouse ET_B receptor gene locus in ES cells, resulting in the introduction of loxP sites flanking exons 2 and 3. *In vivo* Cre-mediated excision of exons 2 and 3 and the intervening intronic region was specifically chosen to inhibit ET_B receptor expression because this region contains the only known site for the generation of splice variants (Shyamala *et al.*, 1993). Although never demonstrated in the mouse, alternative splicing of ET_B receptor RNA has been observed in human brain, lung and heart. I, therefore, adopted a strategy that minimised the potential for continued expression of functional splice variants following recombination events within the ET_B receptor gene

locus. Recently, a novel mutation of the ET_B receptor gene has been identified in mice wherein a 318 nucleotide deletion spanning exons 2 and 3 results in the absence of functional ET_B receptors. These mice demonstrate a phenotype similar to Waardenberg syndrome type 4 (audio-pigmentary defects and Hirschsprung's disease) and have been proposed as a murine model of this syndrome (Matsushima *et al.*, 2002).

Successful homologous recombination is dependent on a number of factors (Capecchi, 1989), the most important of which is the length of homology between the vector and targeted locus (Deng and Capecchi, 1992). The presence of a large region of intron 1 in the plasmid pλP permitted the design of a targeting vector with a 5' homology arm of ~11.9 kb. The shorter 3' homology arm was in excess of 2 kb. The total region of homology was, therefore, ~14 kb, close to the size at which the rate of recombination saturates (Deng and Capecchi, 1992). In contrast, the non-homologous LTNL selection cassette and loxP sites were less than 3.9 kb in length. Targeting frequency is also increased through the use of isogenic vector DNA (te Riele *et al.*, 1992). With the exception of a 956 bp region spanning exons 2 and 3, all elements of the targeting vectors were constructed from 129/SV genomic DNA. The use of long homology arms was designed to maximise the frequency of homologous recombination events and hence minimise the requirement for ES cell colony screening. However, this design introduced several complicating factors. Firstly, there was a paucity of unique restriction enzyme recognition sites within intron 1. This necessitated the introduction of a linker region into the 5' polylinker region of pλP to facilitate cloning of the 5' arm. In addition, it was necessary to delete the region of intron 1 downstream of the *Nae* I site. I predicted that the deletion of this ~1.1 kb region would not adversely affect gene transcription since it contained no known gene regulatory elements. Currently, the only region of intron 1 known to regulate transcription lays at the exon 1/intron 1 boundary. A 301 bp deletion of this region results in the null sl mutation in mice and rats (Hosoda *et al.*, 1994). Alternatively, the insertion of a retroposon in this area results in down regulation of ET_B receptor expression by ~75% (Ohuchi *et al.*, 1999). In our construct, the inclusion of the region 288 bp immediately upstream of exon 2 and the region 155

bp downstream of exon 3, was specifically designed to maintain the presence of any potential splice acceptor and donor sites that are normally located within 100 bp of exon/intron boundaries. The use of a very long 5' homology arm also presented difficulties for the design of 5' external probes for southern blot analysis of targeted ES cell clones. Very little sequence data were available for the remaining intronic and upstream regulatory regions of the ET_B receptor gene at the time of targeting vector design. Hence, the identification of suitable restriction sites that might be utilised to differentiate targeted and wild type clones was problematic. The size of the 5' homology arm also dictated that the restriction fragments of wild type and targeted loci identified by an external probe would be lengthy and, therefore, more difficult to resolve by simple gel electrophoresis. To overcome these difficulties, a PCR-based screening strategy based around the shorter 3' homology arm to identify homologously targeted clones was designed (described in chapter 5). Clones identified in this way were then further screened by southern blot.

Our targeting vector utilised the commonly used neomycin resistance gene cassette as a positive selection marker. However, several groups have reported concerns that the promoters used in such selection cassettes may interfere with the normal expression of targeted and neighbouring genes (reviewed by (Muller, 1999). I, therefore, flanked the selection cassette with an additional loxP site to facilitate the removal of the cassette following identification of targeted clones. This was designed such that the remaining loxP following a recombination event would be positioned downstream of exon 3, thereby facilitating later *in vivo* Cre-mediated excision of exons 2 and 3. The inclusion of a thymidine kinase gene within the cassette additionally permitted the selection against clones retaining the cassette following Cre-mediated excision.

The vector pλPW contained a diphtheria toxin gene cassette at its 3' end. This was intended to negatively select against clones have undergone random vector integration events and to positively select for clones featuring homologous recombination events. This 'positive/negative' strategy has previously been shown to

enrich for homologous recombination events up to 10 fold within targeted clones (Yagi *et al.*, 1990).

Alternative strategies for the construction of the targeting vectors might have utilised the introduction of synthetic loxP linker sites into the intronic regions at convenient restriction enzyme recognition sites. The long and short homology arms might also have been synthesised by PCR using a high fidelity proof-reading DNA polymerase. Although possible, difficulties with accurately amplifying large fragments of DNA by PCR are often encountered. This strategy is, therefore, used more commonly to generate shorter homology arms, albeit with a consequent decrease in targeting efficiency. Lower rates of targeting efficiency are acceptable if screening procedures are rapid enough to facilitate the screening of large numbers of colonies. However, preliminary experiments within our lab had revealed that isolation of ES cell DNA from 96 well plates often did not provide sufficient quantity of DNA for effective screening. It was, therefore, necessary to expand ES cell colonies into 24 well plates prior to DNA isolation. The increased workload that this entailed favoured strategies that maximised targeting efficiency. The influence of homology arm length upon the efficiency of homologous recombination at the ET_B gene locus has recently been exemplified. Our group has undertaken further targeting of this gene with a β-galactosidase gene construct. The 5' homology arm used for this construct consisted of only the final 5 kb of intron 1. Targeting efficiency of this construct was somewhat poorer at ~0.3% (A. Gordon, University of Edinburgh, personal communication).

The use of conventional cloning techniques in the construction of the targeting vectors pλPW and pλPW(NoDT) thus provided a relatively simple, time efficient strategy. The rapid identification and cloning of the plasmid pλP ensured that all genomic elements of the constructs could be isolated without significant concerns regarding the introduction of mutations, since novel mutations in regions distant from ligation sites are a comparatively rare event.

5 Chapter 5

5.1 TARGETING OF THE ET_B RECEPTOR GENE ALLELE AND GERMLINE TRANSMISSION OF THE FLOXED ET_B RECEPTOR ALLELE

5.1.1 INTRODUCTION

This chapter will describe the targeting of the ET_B receptor gene in ES cells with the constructs pλPW and pλPW(NoDT). The strategy for the identification of ES cell clones having undergone homologous recombination events and their subsequent genetic manipulation to remove selection markers prior to blastocyst injection will also be described. Finally, the generation of chimaeric mice and the genotyping strategy adopted for the identification of the targeted allele in their offspring will be outlined.

Following electroporation of the targeting construct, recombination events within the ES cell genome result in the introduction of a selectable genetic marker. Surviving ES cell colonies must then be screened to differentiate those cells featuring the desired homologous integration event from those in which the targeting vector has randomly inserted into the genome. For the purpose of these experiments, normal expression of ET_B receptors in the absence of Cre-mediated recombination events within the ET_B receptor gene locus was required. Following identification of homologously targeted ES cell clones, I therefore removed the neomycin resistance/thymidine kinase selection cassette to prevent interference of this exogenous DNA with the transcription of the targeted and neighbouring genes. The cassette was removed through the transient expression of Cre recombinase. Clones in which the thymidine kinase gene was retained were sensitive to subsequent negative selection with gancyclovir. Further screening was then undertaken to identify clones featuring loxP sites flanking ('floxing') exons 2 and 3 of the ET_B locus. These clones were then expanded and injected into blastocysts from a donor strain of mice to produce chimaeric pups. The screening strategy adopted to identify clones following each of these manipulations will now be described.

5.1.1.1 *Screening strategies for the detection of homologous recombination events in ES cells*

Southern analysis of targeted clones is generally regarded as the gold standard for the detection of recombination events, but is time consuming and labour intensive. Defined restriction sites must also be identified within the targeted and flanking regions to permit size differentiation of restriction fragments from targeted and non-targeted alleles. Because little detailed sequence data were available from the flanking regions at the time of the experiment, I adopted a PCR-based strategy for initial screening of G418-resistant ES cell colonies, followed by Southern analysis of positive clones. In this approach, one PCR primer is common to both mutant and wild-type alleles, one primer is specific to the mutant allele and one primer is specific to the wild type allele (Mantamadiotis *et al.*, 1998). This approach is described below.

5.1.1.2 *PCR screening strategy for the detection of recombination events in ES cells*

Genomic DNA prepared from each clone was amplified with 3 separate primer pairs. The location of regions of the ET_B receptor gene and targeting construct complementary to the 3 primer pairs and the position of the 3' southern blot probe are illustrated in Figure 5.1 and Figure 5.2. LTNLF (GCCTCTGTTCCACATACACTTCATTC) and 417R (GTAGAAACTGAACAGCCACCAATC) are complementary to unique sequences within the targeting vector and amplify a 1420 bp region between the selection cassette and exon 4. The primers Exon 5R (TGAGGTGAAGGGGAAGCCAACAGAGA) and 5to4R (GAACAGCTGCCACGTCTC) are complementary to sequences of the ET_B receptor locus downstream of the 3' homology arm. Successful amplification of a genomic fragment using the LTNLF primer paired with either Exon 5R (for ES cells targeted with pλPW; 2104 bp) or 5to4R (for ES cells targeted with pλPW(NoDT); 2204 bp) is only possible in clones having undergone a homologous recombination event. The external primer 5to4R was utilised instead of Exon 5R to screen ES cells targeted with pλPW(NoDT) as this targeting vector contains sequences complementary to the Exon

5R primer. A positive control (78F (TTTGGGTGGTCTCTGTGGTTCTGG) paired with either Exon 5R or 5to4R) was also included for each clone. This primer pair amplifies either a 2313 bp (78F/Exon 5R) or a 2413 bp (78F/5to4R) genomic region of the non-targeted wild-type ET_B allele. Amplification with all 3 primer pairs was a pre-requisite for clone selection.

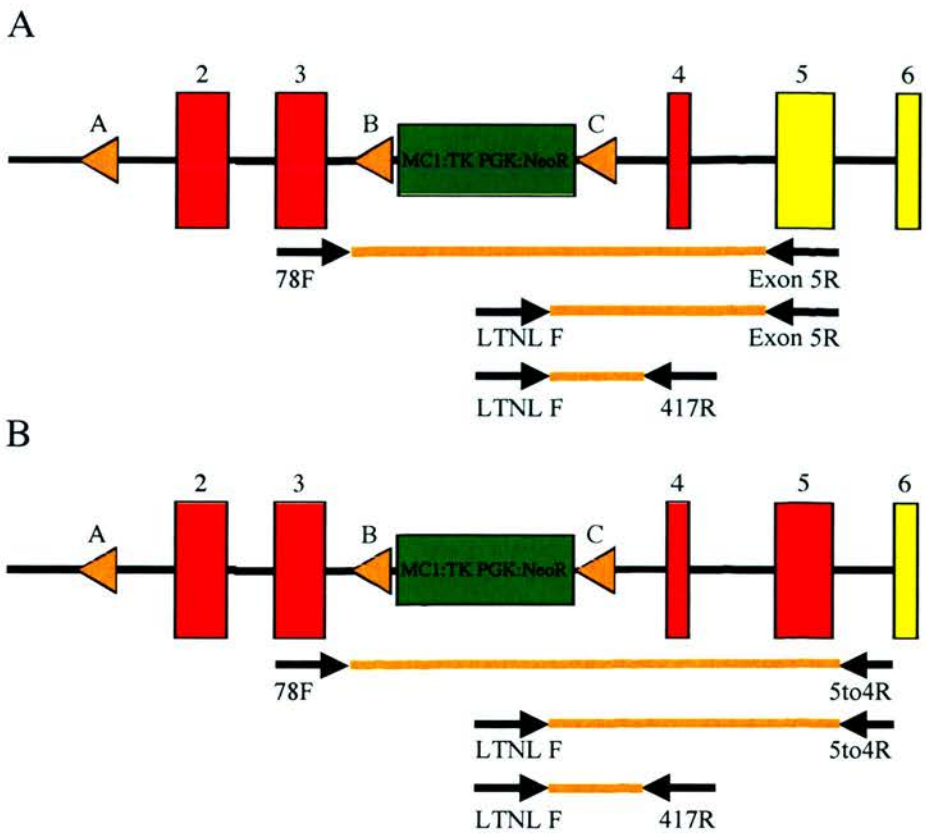

Figure 5.1

Panel A: PCR screening strategy for identification of homologous recombination events following targeting with the pλPW construct.

Panel B: PCR screening strategy for identification of homologous recombination events following targeting with the pλPW(NoDT) construct. Red rectangles, exons present within the targeting construct; Yellow rectangles, exons external to the targeted region; Orange triangles, loxP sites; Green rectangle, selection marker (MC1:Thymidine Kinase and PGK:Neomycin phosphotransferase).

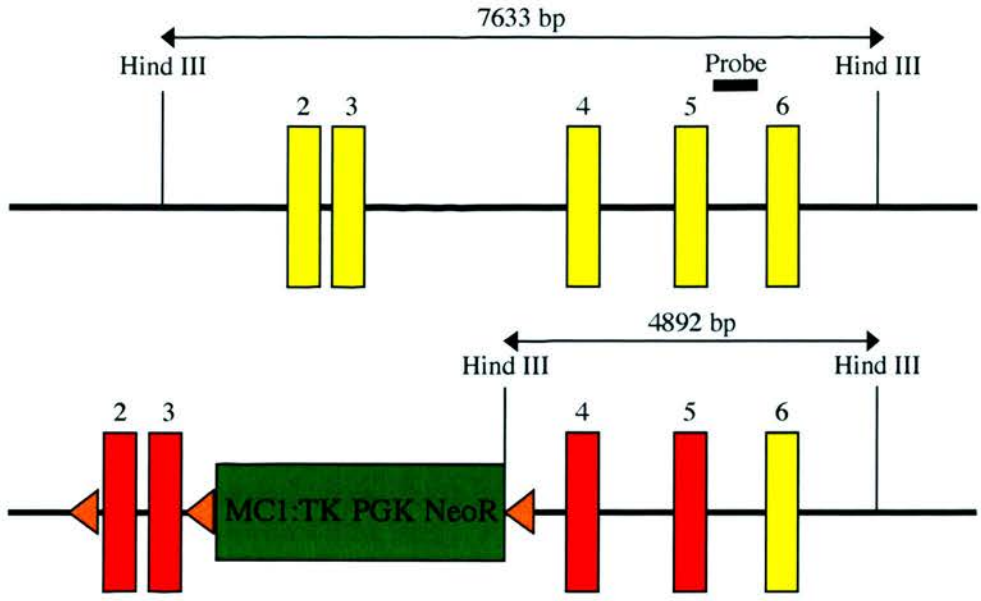

Figure 5.2

Southern blot screening strategy for the detection of 3' homologous recombination events following targeting with the constructs pλPW and pλPW(NoDT). Successful targeting resulted in the introduction of a *Hind* III site within intron 3. Genomic DNA was screened following *Hind* III digestion with a PCR-generated probe external to the region of homology. Red rectangles, exons present within the targeting construct; Yellow rectangles, exons external to the targeted region; Orange triangles, loxP sites; Green rectangle, selection marker (MC1:Thymidine Kinase and PGK:Neomycin phosphotransferase).

5.1.1.3 *Southern blot screening strategy for the detection of 3' recombination events*

Clones in which homologous recombination events were detected by PCR were further analysed for 3' recombination events by Southern blotting. The strategy for Southern blotting is illustrated in Figure 5.2. Targeted clones contain an additional *Hind* III site at the 3' end of the LTNL selection cassette. Restriction digestion with *Hind* III will produce bands of 4892 bp and 7633 bp in targeted and non-targeted alleles, respectively.

Restriction fragments were detected by hybridisation with a PCR-generated probe external to the 3' region of homology, complementary to intron 5.

5.1.1.4 *Screening strategy to identify recombination-mediated removal of the selection cassette from homologously targeted ES cell clones*

G418-resistant clones selected by PCR and 3' southern blotting in the first round of screening were transiently transfected with a Cre recombinase-expression plasmid (Araki *et al.*, 1995) under a chicken beta actin promoter that was kept in circular form to prevent genomic integration. This resulted in the initiation of recombination events within the targeted allele between the 3 loxP sites with consequent removal of either the selection cassette, exons 2 and 3, or the entire region between the 5' and 3' loxP sites. The potential patterns of recombination are illustrated in Figure 5.3. Gancyclovir was then utilised to negatively select against the presence of the thymidine kinase gene. Clones retaining this gene are able to efficiently activate gancyclovir to the triphosphate state with consequent inhibition of DNA replication. DNA from gancyclovir-resistant clones was screened by PCR to confirm both the presence of the loxP site downstream of exon 3 and the absence of the selection cassette. The presence of the loxP site and associated polylinker sequence downstream of exon 3 in the targeted allele results in a net gain of 50bp compared to the wild type allele. The primers 78F and 681R (AGCCATAAAGTCACAGCCATTC) amplify this region (illustrated in Figure 2.1), producing bands of 380 bp and 430 bp with the wild type and floxed allele, respectively. The pattern of recombination events following transient transfection with Cre recombinase was also used to confirm the functional presence of the 5' loxP site upstream of exon 2 and hence of a successful 5' homologous recombination event. Clones were selected only if potential patterns of recombination involving all 3 loxP sites were demonstrated.

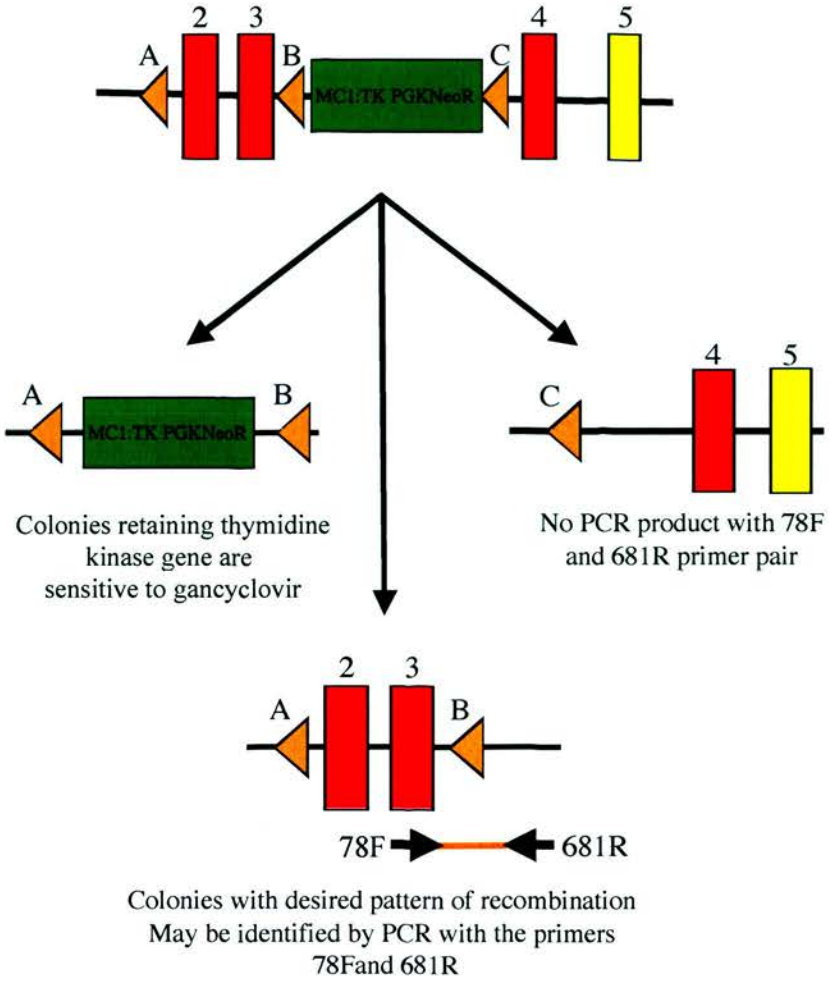

Figure 5.3

PCR screening of targeted clones following transient transfection with the Cre recombinase-expression plasmid pMC-Cre and selection with gancyclovir. Clones featuring recombination events between loxP sites at positions A and B retain the selection cassette and are sensitive to negative selection with gancyclovir. Recombination between loxP sites B and C may be identified by PCR amplification with the primers 78F and 681R. Bands of 380 bp (wild type allele) and 430 bp (targeted allele) are observed. Clones featuring recombination between loxP sites A and C are only able to amplify DNA from the non-targeted wild type allele since this recombination event removes exon 3 from the targeted allele. Functional evidence of the presence of the 5' loxP site in a parent clone rests, therefore, on the production of

recombination patterns compatible with each of these scenarios in colonies derived from a single parent clone.

5.1.1.5 *Screening strategy for the analysis of 5' recombination events in gancyclovir-resistant clones*

Clones selected in this manner were subsequently analysed to confirm a 5' recombination event by further PCR screening and direct sequencing. The primers 81R (CTTAGAGCACAAAGACTCAGCAC) and 454F are complementary to regions within intron 1 flanking the 5' loxP site (illustrated in Figure 2.2). Each targeted allele features a net deletion of 1105 bp in this region (spanning from the *Nae* I site to 288 bp upstream of exon 2). This size differential was utilised to confirm 5' homologous recombination events and PCR products generated during each of the screening reactions were subsequently isolated and directly sequenced. The PCR primers 78F/681R and 454F/681R were used for sequencing of the 3' and 5' loxP sites, respectively.

5.1.1.6 *Generation of homozygous 'floxed' ET_B receptor mice*

The ability of ES cells to contribute to the formation of all cell lineages, including gametes, was exploited through the *in vitro* injection of targeted ES cells into developing wild type blastocysts. Chimaeric blastocysts, comprised of both wild type and targeted cells, are re-implanted into the uterus of pseudopregnant mice and allowed to develop into chimaeric pups. In a proportion of such mice, targeted ES cells will contribute to the formation of germ cells. The targeted allele may, therefore, be inherited by the offspring of the chimaera. Through intercross of these offspring, mice homozygous for the targeted allele may be generated. These mice were termed 'floxed ET_B receptor mice'.

5.1.2 METHODS

5.1.2.1 *Electroporation of ES cells*

Seventy five μg of the pλPW targeting vector were cut overnight with either 10 units of *Xho* I or a combination of 10 units each of *Not* I and *Xho* I. pλPW(NoDT) was cut with 10 units of *Xho* I alone. ES cells and linearised targeting vector were prepared for electroporation as described in 2.1.13.7.

5.1.2.2 *Selection of G418-resistant ES cell colonies*

Twenty four hours post-electroporation, cells were washed twice and the media replaced with ES cell media supplemented with 200 μg/ml G418 (Boehringer Maanheim, Germany; Product number 1464981). Selection was continued for 7 days.

5.1.2.3 *Picking of G418-resistant ES cell colonies*

Following G418 selection, cultures were washed twice and covered with 7 ml of PBS. Individual colonies were picked by simultaneous scraping and aspiration with a P20 pipette. Cells were aspirated along with 20 μl of PBS and transferred to a round-bottomed 96 well plate containing 20 μl of TVP in each well. Plates were then incubated at 37°C for 2 minutes to dissociate cells. Cells were transferred to the corresponding well of a second round-bottomed gelatinised 96 well plate containing 150 μl of pre-warmed ES cell media supplemented with G418 (200 μg/ml) per well. Media was changed every two days and when an individual well reached confluence, cells were passaged onto a 24 well plate and diluted with 2ml of media. Following passage, each clone was ascribed a unique identification number that was maintained throughout all subsequent experiments. Individual wells were grown to confluence and then split 1:2 onto replica 24 well plates, termed 'DNA' and 'freezing'. Both the 'DNA' and the 'freezing' plates were grown to confluence with G418 (200 μg/ml) selection maintained at all times.

5.1.2.4 *PCR screening of G418-resistant ES cell colonies following targeting with pλPW or pλPW(NoDT)*

Genomic DNA was isolated from ES cell colonies as described in section 2.1.13.6. PCR reactions were performed using the Expand™ system and the primer pairs LTNLF/417R, LTNLF/Exon 5R or 5to4R and 78F/Exon 5R or 5to4R. Reaction mixtures were prepared as described in section 2.1.13.11. Cycling parameters were 92°C for 2 minutes, 10 cycles of 92°C for 10 seconds, 60°C for 30 seconds and 68°C for 3 minutes, followed by 20 cycles of 92°C for 10 seconds, 60°C for 30 seconds and 68°C for 3 minutes plus an additional extension period of 20 seconds per cycle. A final extension period of 68°C for 7 minutes completed the programme. During the second round of screening a simplified PCR programme was utilised: 92°C for 2 minutes, 30 cycles of 92°C for 30 seconds, 60°C for 30 seconds and 68°C for 2 minutes, followed by a 10 minute final extension period at 68°C. This protocol was found to amplify the desired regions without a decrease in detection sensitivity.

5.1.2.5 *3' Southern blot of clones identified by PCR screen*

A probe complementary to intron 5 was generated by PCR using the primers 32F/359R and a genomic DNA template as described in section 3.1.2.1. The probe was purified and radiolabelled as previously described. Five μg of genomic DNA from the homologously targeted clones 3B3, 9D3 and 4B2, from the non-homologously targeted clones 2D1 and 6D3, and from non-targeted E14 ES cells were digested overnight with 10 units of *Hind* III. Samples were checked for complete digestion of DNA and then the entire sample was separated by gel electrophoresis. Southern blotting and hybridisation was performed as described in section 2.1.11.18.

5.1.2.6 *Transient transfection of targeted clones with pMC-Cre*

Homologously targeted clones identified in the previous round of screening were electroporated with either 50 μg of pMC-Cre or vehicle using the electroporation protocol described in section 2.1.13.8. Cells were grown to confluence without G418

selection then counted and seeded onto 1% geletin-coated petri-dishes (10^2-10^5 cells/plate). Negative selection with 2.5μM gancyclovir was maintained for 4-5 days. Surviving clones were picked onto 96 well plates as previously described then grown to confluence in 24 well plates before splitting onto 'freezing' and 'DNA' plates.

5.1.2.7 *PCR screening of gancyclovir-resistant clones for the presence of the 3' loxP site*

Recombination-mediated removal of the LTNL selection cassette was identified by screening genomic DNA by PCR using the primers 78F and 681R and the following cycling parameters: 92°C for 5 minutes, 30 cycles of 92°C for 30 seconds, 60°C for 30 seconds and 68°C for 2 minutes, followed by final extension at 68°C for 10 minutes. Reaction mixtures were prepared as described in section 2.1.13.11. PCR products from wild type and targeted alleles differed in size by 50 bp and were separated by gel electrophoresis using a 2% agarose gel. For clones used for blastocyst injection, PCR products were isolated from the gel as previously described and sequenced using the primers 78F and 681R. Sequencing was performed as described in section 2.1.11.4.

5.1.2.8 *PCR screening of gancyclovir-resistant clones for the presence of the 5' loxP site*

5' recombination events were detected by screening genomic DNA by PCR using the primers 454F and 81R. The targeted allele features a deletion of an 1166 bp segment of intron 1, spanning from the *Nae* I site 1454 bp upstream of exon 2 to a site 288 bp upstream of the exon 2. Sixty one bp were added to the 5' region (loxP site and associated polylinker regions) during vector construction, resulting in a net deletion of 1105 bp from the floxed allele. The primers were thus predicted to amplify bands of ~500bp and ~1600bp in targeted and wild type alleles, respectively. The following cycling parameters were utilised: 92°C for 5 minutes, 30 cycles of 92°C for 30 seconds, 50°C for 30 seconds and 68°C for 2 minutes, followed by final extension at 68°C for 10 minutes. Reaction mixtures were prepared as described in section 2.1.13.11. PCR

products generated were isolated by gel electrophoresis and recovered using a QIAEX II™ kit as described in section 2.1.11.7 for sequencing.

5.1.2.9 *Generation of chimaeric mice*

ES cell clones 3B3 (2B5), 9D3 (1B1) and 2D2 (1C1) were prepared and injected into blastocysts as described in section 2.1.13.9. Chimaeric male offspring were mated with white BKW strain mice and the progeny screened for germline transmission of the targeted allele by coat colour. Black mice carry a full complement of C57BL/6 chromosomes derived from the parent blastocyst and do not, therefore, carry the targeted mutation. In contrast, sandy coloured pups inherit a complement of chromosomes derived from 129/SV ES cells and hence posses a 1 in 2 chance of carrying the targeted mutation. The presence of the 3' loxP site in tail tip DNA from sandy coloured pups was detected by PCR using the primers 78F and 681R as previously described.

5.1.3 RESULTS

5.1.3.1 *PCR screen of G418-resistant ES cell colonies following targeting with pλPW*

155 colonies were picked and screened. A representative PCR screen is illustrated in Figure 5.4. Clone number 84 (9D3) produced bands with each of the 3 primer pairs, suggesting a homologous recombination event following targeting with pλPW. Negative control reactions using wild type ES cell DNA template produced bands only with the 78F/Exon 5R primer pair, as predicted. 4/155 colonies were identified as having undergone homologous recombination events, giving a targeting efficiency of 2.5%. Positive clones were defrosted, grown to confluence and split to provide an extra plate from which further DNA samples were isolated. Of the 4 clones, 1 failed to grow following defrosting and 2 others no longer tested positive for the homologous recombination event when PCR screening was repeated. A single clone (9D3) remained positive with all 3 primer pairs following defrosting and expansion.

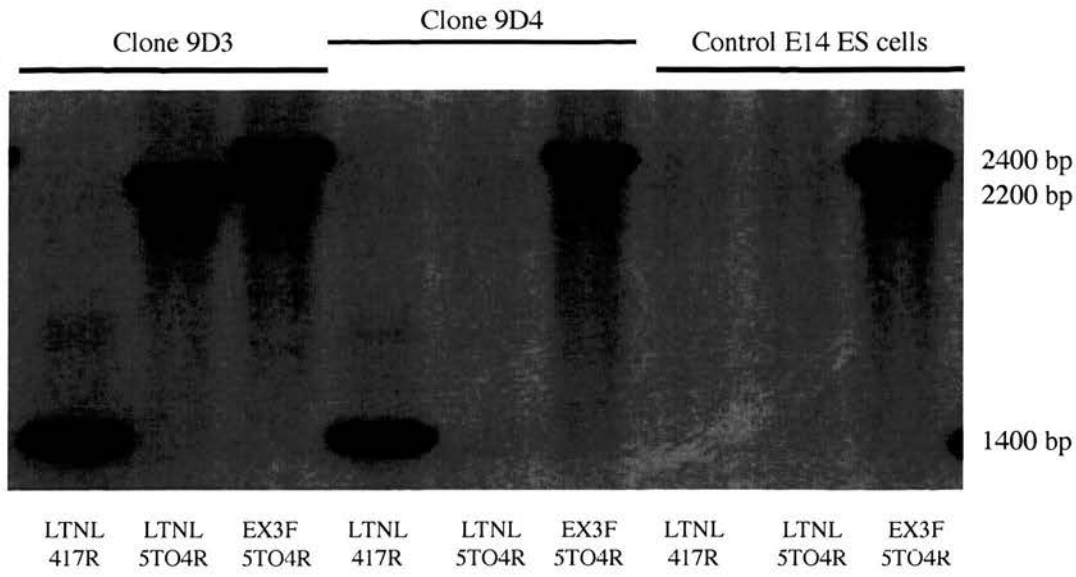

Figure 5.4

Representative primary PCR screen of targeted ES cell clones (9D3 and 9D4) and non-targeted control E14 ES cells. Each of the 3 primer pairs amplified specific regions of the ET_B receptor locus in clone 9D3, indicating a homologous recombination event. Clone 9D4 demonstrates non-homologous integration of the targeting construct. E14 ES cells produce PCR bands only with the primer pair complimentary to the wild type allele. This genotyping strategy is illustrated in Figure 5.1.

5.1.3.2 *PCR screen of G418-resitant ES cell colonies following targeting with either pλPW or pλPW(NoDT)*

Because only a single homologously targeted clone survived following targeting with pλPW, targeting was repeated using pλPW and pλPW(NoDT). This permitted examination of the effects upon targeting efficiency of both the inclusion of the diphtheria toxin gene and of the site of vector linearization. Following G418 selection, the number of surviving ES cell colonies was of the rank order pλPW(NoDT)>pλPW (*Xho* I+*Not* I-cut)> pλPW (*Xho* I-cut). 307/ 400 colonies picked survived, of which 97 were screened by PCR as previously described. The frequency of homologous recombination events using each of the targeting constructs is shown in Table 5.1.

Targeting efficiency was of the rank order pλPW(NoDT)>pλPW (*Xho* I+*Not* I-cut)> pλPW (*Xho* I-cut). Overall targeting efficiency was 6.18% in the 97 clones screened.

TARGETING **CONSTRUCT**	**NUMBER OF HOMOLOGOUS RECOBINATION EVENTS/NON-HOMOLGOUS EVENTS**	**TARGETING EFFICIENCY %**
pλPW(NoDT)	5/53	9.43
pλPW *Xho* I+*Not* I-cut	1/26	3.84
pλPW *Xho* I-cut	0/18	0
TOTAL	**6/97**	**6.18**

Table 5.1

The six clones identified were 1B1, 1C1, 2D2, 3B3, 3C3 and 4B2. Of these, 2D2 and 3B3 were defrosted and re-grown. Each clone remained positive with all 3 primer pairs when PCR screening was repeated. Transient transfection with pMC-Cre was undertaken in clones 9D3 (identified from the first targeting screen), 2D2 and 3B3.

5.1.3.3 *3' Southern blot of homologously targeted clones identified by PCR screen*

The results of Southern blotting of genomic DNA following *Hind* III digestion are illustrated in Figure 5.5. Clones 3B3, 4B2 and 9D3, identified by PCR as having undergone homologous recombination reactions, demonstrate bands of ~4.9 kb (targeted allele) and ~7.6 kb (wild type allele). Non-targeted ES cells and the non-homologously targeted clones 2D1 and 6D3 demonstrate a single band of ~7.6 kb only.

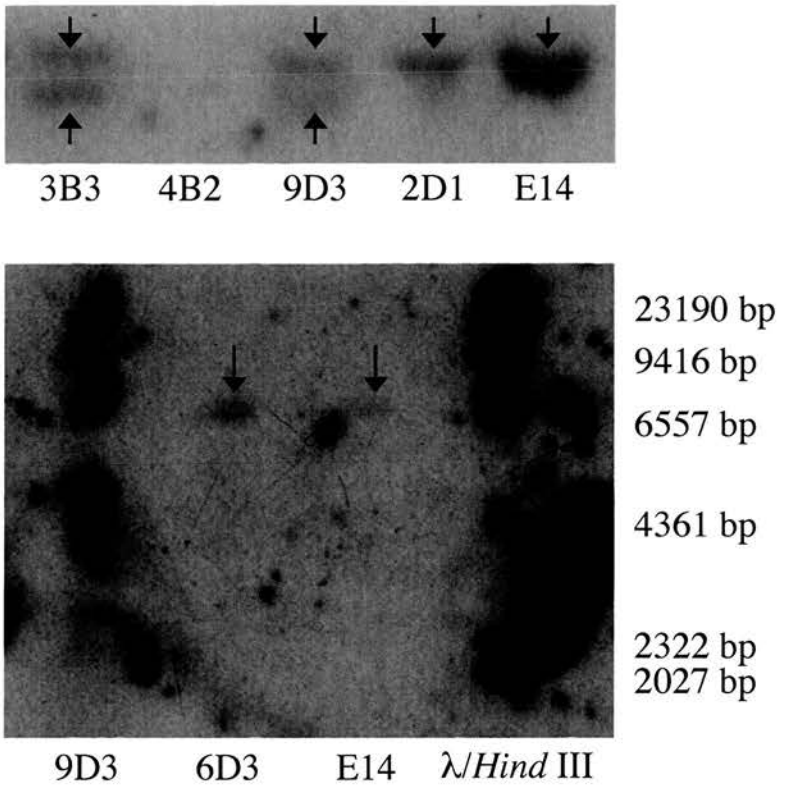

Figure 5.5

3' Southern blot of homologously targeted (9D3, 3B3, 4B2), non-homologously targeted (2D1, 6D3) and wild type E14 ES cell genomic DNA following *Hind* III restriction digestion. A PCR-generated external probe (32F/359R) complementary to intron 5 was utilised to detect restriction fragments in each case. The upper panel demonstrates a ~4.9 kb fragment in addition to the wild type ~7.6 kb band in homologously targeted clones. The Southern blot was repeated (lower panel) following a prolonged period of electrophoresis to improve separation of bands and permit accurate sizing.

5.1.3.4 *Gancyclovir selection of clones following transient transfection with pMC-Cre*

All clones electroporated without pMC-Cre died under gancyclovir selection, but propagated normally in the absence of gancyclovir. Survival in clones transiently

transfected with pMC-Cre was dependent upon the initial seeding density and the efficiency of recombination-mediated removal of the selection cassette. Clone survival on plates seeded with 10^2, 10^3 and $>10^3$ cells was ~10%, ~20% and 0%, respectively.

5.1.3.5 *PCR screen of gancyclovir-resistant clones for removal of the LTNL selection cassette and presence of the 3' loxP site*

The number of gancyclovir-resistant colonies picked following transfection of heterologously targeted clones with pMC-Cre is illustrated in Table 5.2 along with the relative proportion of colonies in which the desired recombination event was detected by PCR screening with the primers 78F and 681R.

PARENT CLONE	NO. COLONIES PICKED	NO. OF SURVIVING COLONIES	NO. POSITIVE WITH 78F/681R PRIMERS	% POSITIVE WITH 78F/681R PRIMERS
9D3	150	95	3	3.15
2D2	48	36	3	8.33
3B3	96	62	5	8.06
TOTAL	**294**	**193**	**11**	**5.70**

Table 5.2

A typical genotyping reaction is illustrated in Figure 5.6. Targeted and wild type alleles were identified as 430bp and 380 bp bands, respectively. From the 11 clones identified, 3 were selected for further analysis of 5' recombination events. 3B3 (2B5), 9D3 (1B1) and 2D2 (1C1) were defrosted and screening for the 3' loxP site repeated. All clones produced identical results on repeat screening.

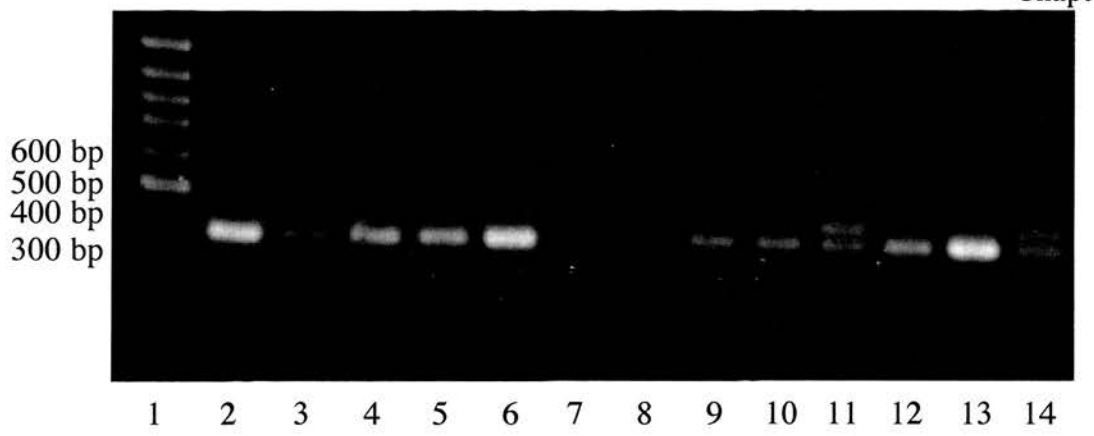

Figure 5.6

PCR screening for the presence of the 3' LoxP site. The primers 78F and 681R were utilised to screen targeted ES cells (clone 3B3) following transient transfection with the pMC-Cre plasmid. Lanc 1, DNA size marker; Lanes 11 and 14 demonstrate an additional band of 430 bp, consistent with Cre recombinase-mediated removal of the LTNL selection cassette and preservation of the 3' LoxP site. The PCR products amplified from the targeted and wild type alleles were of similar intensity, suggesting similar DNA concentrations. PCR products were isolated and sequenced to confirm the sequence of the 3' LoxP site and wild type alleles.

5.1.3.6 *PCR screen of gancyclovir-resistant clones for the presence of the 5' loxP site*

3B3 (2B5), 9D3 (1B1) and 2D2 (1C1) were screened by PCR for evidence of 5' recombination events using the primers 454F and 81R. Amplification of the targeted and wild type allele produced bands of 500bp and 1600bp, respectively in all clones (illustrated in Figure 5.7).

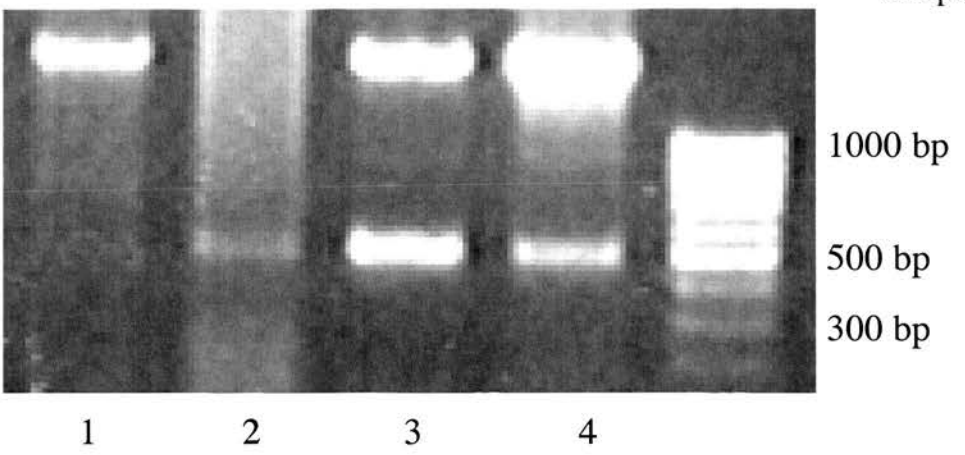

Figure 5.7

PCR screening to confirm the presence of the 5' LoxP site. The primers 454F and 81R were used to screen ES cell DNA following Cre recombinase-mediated removal of the LTNL selection cassette. Lane 1, non-targeted E14 ES cell DNA; Lane 2, insufficient template DNA; Lane 3, clone 3B3; Lane 4, clone 9D3. DNA from targeted clones 3B3 and 9D3 demonstrate the presence of both wild type (~1600 bp) and targeted (500 bp) ET_B receptor alleles, confirming 5' recombination of the targeting construct within the ET_B receptor gene. PCR products were isolated and sequenced to confirm the sequence of the 5' LoxP site.

5.1.3.7 *Sequence of 5' and 3' loxP sites*

The 5' loxP site upstream of exon 2 and the 3' loxP site downstream of exon 3 contained no additional mutations in the clones 3B3 (2B5), 9D3 (1B1) and 2D2 (1C1). Sequence data for 3B3 (2B5) are illustrated in Figure 5.8 and Figure 5.9.

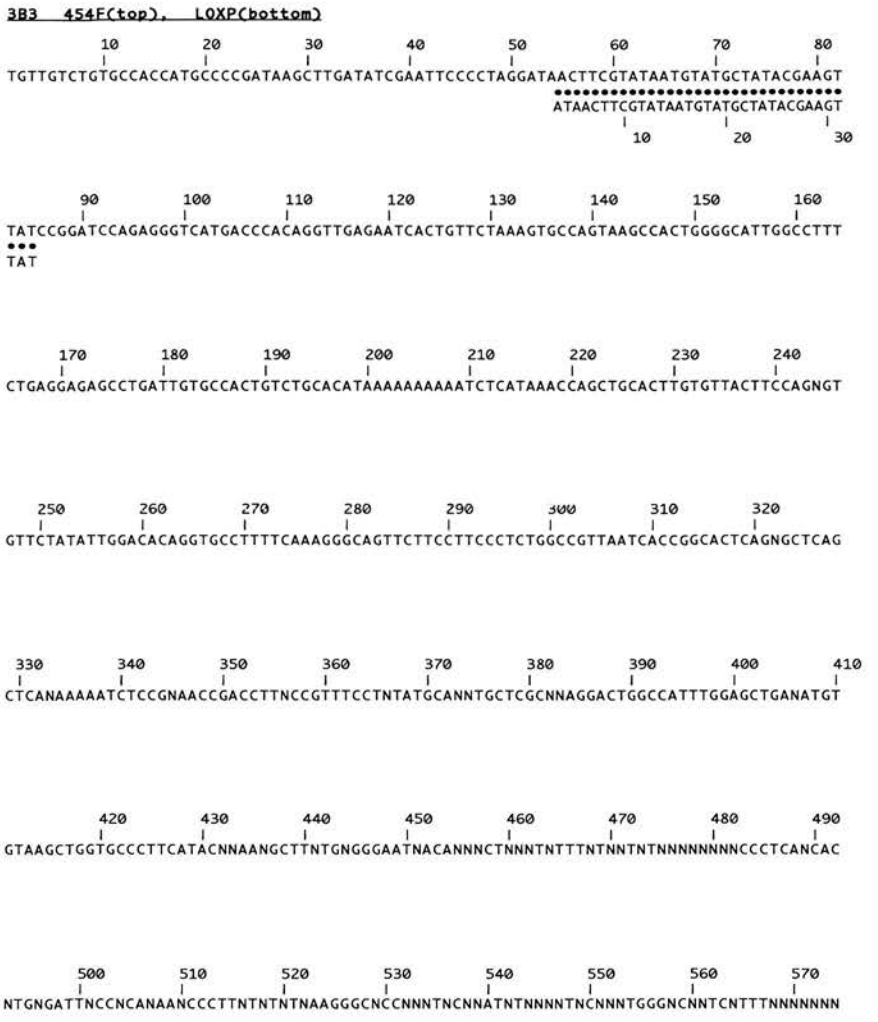

Figure 5.8

Sequence alignment of genomic DNA isolated from the clone 3B3 (2B5) and sequenced with the 454F primer (top) with the loxP site sequence (bottom). The 5' loxP site contained no mutations.

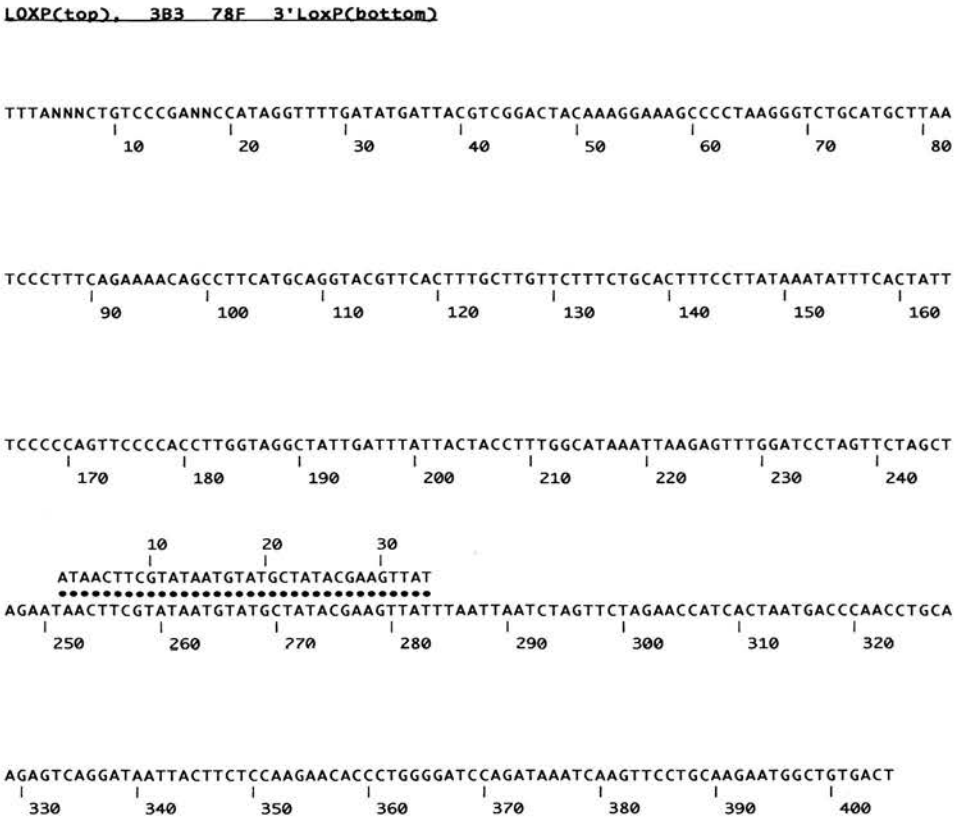

Figure 5.9

Sequence alignment of genomic DNA isolated from the clone 3B3 (2B5) and sequenced with the 78F primer (bottom) with the loxP site sequence (top). The 3' loxP site contained no mutations.

5.1.3.8 *Generation of chimaeric mice and analysis of progeny*

Six chimaeras were derived from clone 9D3 (1B1), 4 from 2D2 (1C1) and 3 from 3B3 (2B5). All chimaeras were male with the exception of a single female derived from clone 9D3 (1C1). This sex bias reflects the use of XY karyotype ES cells. Female chimaeric mice are often infertile (Bronson *et al.*, 1995) and were not used further. Three distinct coat colours were observed in the F_1 progeny. Black mice and dark brown mice were found not to carry the targeted mutation, as predicted. The presence of the 3' loxP site was identified in sandy coloured pups by PCR screening of tail-tip DNA with the primers 78F and 681R as previously described. Mice heterozygous for the targeted allele produced bands of 380 bp and 430 bp from wild type and targeted alleles, respectively. Mice heterozygous for the targeted allele were subsequently intercrossed to produce homozygous floxed ET_B receptor mice. Homozygous floxed offspring were produced in the expected Medelian frequency (1/4 of pups) from these intercrosses. A representative PCR genotype screen following intercross of F1 mice is illustrated in Figure 5.10.

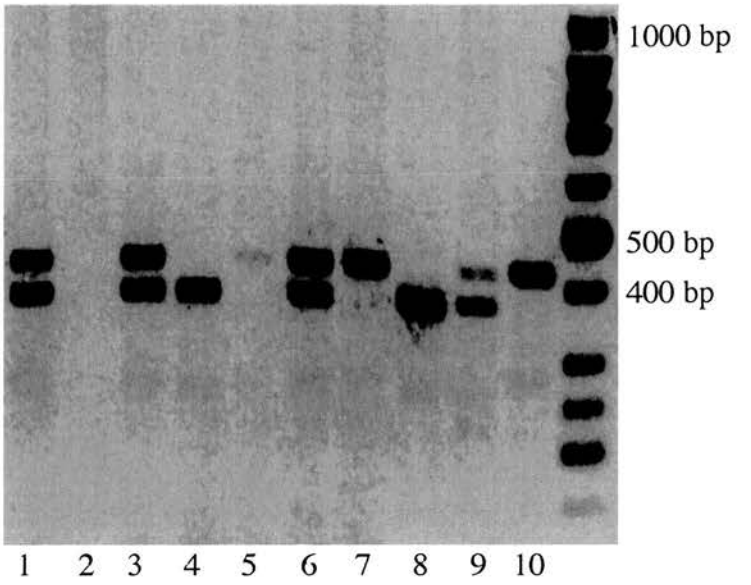

Figure 5.10

PCR genotyping with the primers 78F and 681R of an F1 intercross of Flox/W mice. Floxed ET_B receptor allele 430 bp; Wild type ET_B receptor allele 380 bp. Lane 1 Flox/W; Lane 2 No DNA; Lane 3 Flox/W; Lane 4 W/W; Lane 5 Flox/Flox; Lane 6 Flox/W; Lane 7 Flox/Flox; Lane 8 W/W; Lane 9 Flox/W; Lane 10 Flox/Flox. Flox = targeted ET_B receptor allele; W = wild type ET_B receptor allele.

5.1.4 DISCUSSION

This chapter has described the targeting of ES cells with pλPW and pλPW(NoDT) and the subsequent generation of mice homozygous for the floxed ET_B receptor allele. Identification of homologous recombination events following transformation of ES cells is typically achieved by Southern blot hybridisation. Such screening strategies involve the identification of homologous recombination events in both the 3' and 5' homology arms through the use of probes external to homology regions present within the targeting construct. An alternative approach is to use a PCR-based strategy based on 3 primers (Mantamadiotis *et al.*, 1998), as previously described. The successful amplification of a genomic fragment between the common primer and specific mutant allele primer is then dependent upon a homologous recombination event at the target locus. Although prone

to false positive results, this method is often utilised to quickly screen large numbers of G418 resistant clones that may subsequently be analysed in greater detail by Southern blot. In addition, PCR offers advantages over Southern blotting for detection of loxP sites within the mutant allele following removal of the selection marker, when the size differential between wild type and mutant alleles is small. In our assay, the floxed allele featured an additional 50 bp consisting of the 3' loxP site and associated polylinker region. Because of the similar size of PCR products amplified from targeted and wild type alleles in this reaction, the amplification rate is likely to be similar from each allele. PCR screening thus provides an additional method of quickly detecting the random insertion of multiple copies of the targeting construct by analysis of the signal intensity of the PCR product (Mantamadiotis *et al.*, 1998). In our screen, both the wild type and floxed allele produced bands of equal intensity, suggesting that only a single copy of the targeting construct was integrated into the ET_B receptor allele.

Southern blotting to confirm homologous recombination of the 5' arm of either pλPW or pλPW(NoDT) was problematic due to the large size of the homology arm and lack of available sequence data from flanking regions at the time of the experiment. These factors limited the availability and identification of unique restriction enzyme recognition sites within and external to the targeting construct. For this reason, confirmation of 5' recombination events was determined by PCR amplification and direct sequencing of the 5' loxP site in candidate clones following removal of the selection cassette. Functional evidence of the presence of the 5' loxP site (and hence, of 5' recombination events) was also provided by the pattern of Cre-mediated recombination following transient transfection of targeted clones with pMC-Cre. All clones selected demonstrated patterns of recombination that involved both the 5' and 3' loxP sites.

In order to screen targeted ES cell colonies for homologous recombination events, it is imperative that the screening technique utilised is of sufficient sensitivity to detect a single recombination event within a single genome equivalent. The detection sensitivity of our PCR-based screening method was assessed using a mouse genomic

DNA template spiked with a plasmid DNA template homologous to the ET_B locus at a concentration equivalent to a single copy per single genome (data not shown). Our results demonstrated that the PCR reactions utilised were of sufficient sensitivity to detect a single homologous targeting event within a single genome equivalent.

A number of homologously targeted clones identified during the first round of screening did not subsequently test positive following defrosting and expansion. Although not investigated thoroughly, it is likely that such clones were a heterogeneous population of homologously and non-homologously targeted cells prior to freezing. The presence of the selection cassette within the ET_B receptor gene locus may have conferred a selective growth disadvantage in homologously targeted cells. Hence, when the colony was expanded further, homologously targeted cells were overgrown by non-homologously targeted cells. In the presence of large quantities of non-homologously targeted cells, competition for PCR substrate may have then decreased the detection sensitivity of the screening reaction.

This finding necessitated a second round of targeting and permitted investigation of the effects upon targeting efficiency of the inclusion of the diphtheria toxin gene cassette and of the site of vector linearization. Previous studies (Yagi *et al.*, 1990) have demonstrated up to 10-fold enrichment of ES cells featuring homologous recombination events following gene targeting with vectors containing a diphtheria toxin gene cassette. Fewer colonies survived following targeting with pλPW cut with *Xho* I compared to those targeted with pλPW cut with *Xho* I and *Not* I, or pλPW(NoDT). From this, I predicted that the inclusion of the diphtheria toxin gene, and its 'protection' through retention of the pBluescript vector at the 3' end of the targeting construct, had decreased survival of clones following non-homologous recombination events. However, the relative proportion of homologous recombination events (2.5% and 3.4% in clones targeted with pλPW vs. 9.4% in those targeted with pλPW(NoDT)) was not increased by the presence of the diphtheria toxin gene. The reasons underlying this observation were not investigated further but did reflect the subsequent experience of other groups within our institute (Dr Andrew Smith, University of Edinburgh, personal communication).

This finding may represent insufficient transcription of the diphtheria toxin gene cassette in non-homologously targeted clones, possibly through gene silencing by methylation. Gene expression may also be compromised by events occurring during the recombination process itself. It is well recognised that host DNA modifying enzymes may degrade the linear ends of targeting constructs. Removal of the pBluescript vector from pλPW by digestion with both *Xho* I and *Not* I exposed the 3' end of the diphtheria toxin gene to such events. However, I observed no increase in the efficiency of homologous recombination in clones targeted with constructs in which the 3' end of the diphtheria toxin gene was protected by the pBluescript vector. Despite the apparent absence of effect of inclusion of the diphtheria toxin gene, the targeting efficiencies observed may not reflect true values, since less than one third of the total G418-resistant colonies harvested were screened. The first 97 samples screened yielded sufficient numbers of homologously targeted clones to obviate the need for further screening and time constraints prevented further analysis.

Following initial screening for 3' recombination events, colonies were transiently exposed to Cre recombinase to catalyse recombination reactions between loxP sites. Gancyclovir was used to negatively select against clones in which the selection cassette had been retained. Clone survival was dependent upon both the efficiency of recombination-mediated removal of the selection cassette and on initial seeding density. All colonies transfected with pMC-Cre and seeded at densities of $>10^3$ cells/plate were killed. This may represent a 'bystander' effect, wherein individual colonies in close contact with one another die as a result of activation of gancyclovir to the triphosphate state in adjacent colonies in which the thymidine kinase gene is retained. In plates seeded with 10^2 and 10^3 cells, ~ 20% of cells survived gancyclovir selection. This suggests that recombination events between the loxP sites flanking exons 2 and 3 occurred more frequently than those involving the loxP site flanking the selection cassette. This is likely to result from the shorter distance between these 2 sites.

Blastocyst injection of the selected clones produced chimeras in each case. However, germline transmission was only achieved from chimeras originally derived

from the 3B3 (2B5) clone. The reasons underlying this are not clear, but may relate to the degree of differentiation of the ES cells injected into the blastocyst. Although morphologically identical, I cannot discount the possibility that the clones in which germline transmission was not observed were more differentiated than the 3B3 (2B5) clone. Clones differentiated beyond a certain stage may lose the ability to contribute to the germ cell lineage and hence chimeras generated from such clones will not transmit the targeted allele. The F1 offspring of chimaeric mice in whom the floxed ET_B receptor allele was present demonstrated normal growth and fertility. The floxed allele was stably transmitted in the predicted Medelian frequency throughout subsequent intercrosses, permitting the breeding of homozygous floxed ET_B receptor mice (Flox/Flox -/-). Intercross of homozygous floxed mice produced no piebald offspring, indicating that sufficient ET_B receptor expression was maintained from transcription of the targeted allele to permit normal embryogenesis.

This chapter has described the generation of homozygous floxed ET_B receptor mice through targeting of the ET_B receptor allele in ES cells. PCR screening for homologous recombination events in ES cells and for loxP sites following removal of the selection cassette is a reliable and effective method for genotyping ES cells and mice. Additionally, PCR screening permits the assessment of copy number differences between clones when the PCR products are of similar size.

6 Chapter 6

6.1 REDUCED ^{125}I ET-1 BINDING TO ENDOTHELIAL CELLS FROM FLOX/FLOX TIE2 MICE

6.1.1 INTRODUCTION

The study of gene function through the use of animal models of gene-inactivation and gene over-expression has revealed many novel insights. However, many genes have non-redundant roles during embryogenesis in addition to their function during adult life. Whole animal knockout of such genes results in a lethal phenotype, precluding study of gene function in the adult animal. Binary transgenic systems provide a mechanism by which gene expression is dependent upon two interacting elements and may be utilised to circumvent such problems. The Cre/loxP system (Orban *et al.*, 1992, Sauer and Henderson, 1989) is the best characterised of these and may be utilised to spatially regulate mammalian gene expression *in vivo*. LoxP sites introduced into the genome using standard gene targeting techniques undergo recombination only when Cre recombinase transgenes are co-expressed within a cell. Cell type-specific expression of the Cre recombinase transgene thus limits recombination events to the cell type or tissue of interest. In addition to avoiding the lethal phenotype associated with whole knockouts, this approach may be used to examine the effects of gene-inactivation in an individual cell type *in vivo* without the confounding effects of gene-inactivation in other tissues. Biological questions may, therefore, be addressed with an exquisite accuracy not possible with conventional gene knockout or pharmacological approaches.

6.1.1.1 *Endothelial cell specific knockout of the ET_B receptor*

Selective deletion of genes from vascular ECs became possible following the identification of promoter and enhancer elements that limit Cre transgene expression to this cell type (Schlaeger *et al.*, 1997). The murine Tie2 gene encodes a tyrosine kinase receptor for angiopoietin I, an angiogenic factor required for normal vascular

development (Suri *et al.*, 1996). The Tie2Cre transgene mirrors endogenous expression of this receptor (Kisanuki *et al.*, 2001) and consists of the 2.1 kb promoter region of the Tie2 gene, a Cre recombinase cDNA with a metallothionine poly A signal, and a 10.1 kb enhancer fragment of the Tie2 gene. Crosses of Tie2Cre transgenic mice with both *lacZ* (Kisanuki *et al.*, 2001) and GFP (Constien *et al.*, 2001) floxed reporter mice have demonstrated that recombination events in F1 offspring are limited to ECs and to cells of the haematopoietic lineage. Recently however, recombination events have also been noted in the germ cells of female mice featuring a floxed allele and the Tie2 Cre transgene (Constien *et al.*, 2001, Koni *et al.*, 2001). This has necessitated the use of selective breeding strategies to maintain the EC-specificity of recombination events.

To achieve EC-specific down-regulation of the ET_B receptor, I have crossed mice homozygous for the floxed ET_B allele with Tie2Cre transgenic mice (a kind gift of Professor M. Yanagisawa, University of Texas). Male F1 mice heterozygous for both the floxed ET_B allele and the Tie2Cre transgene were then crossed with homozygous and heterozygous female floxed ET_B receptor mice. This breeding strategy provided littermates of each genotype (Flox/Flox Tie2, Flox/Flox -/-, W/W Tie2 and W/W -/-) and minimised the variation in genetic background between experimental animals. This breeding strategy is illustrated in Figure 6.1. In addition, a number of F2 intercrosses of Flox/Flox Tie2 mice were established to generate mice homozygous for the recombined ET_B receptor allele. To assess the extent of recombination within the ET_B receptor locus and subsequent down-regulation of ET_B receptor expression in EC-specific knockout mice, pulmonary EC were isolated and ^{125}I-ET-1 binding measured in the presence or absence of an ET_A receptor antagonist. The ET_B receptor is hypothesised to act as a clearance receptor for circulating ET-1 (Fukuroda *et al.*, 1994). Plasma ET-1concentration was, therefore, also measured in EC-specific ET_B receptor knockout mice to assess the effect upon circulating ET-1 concentration.

Breeding Strategy for experimental animals

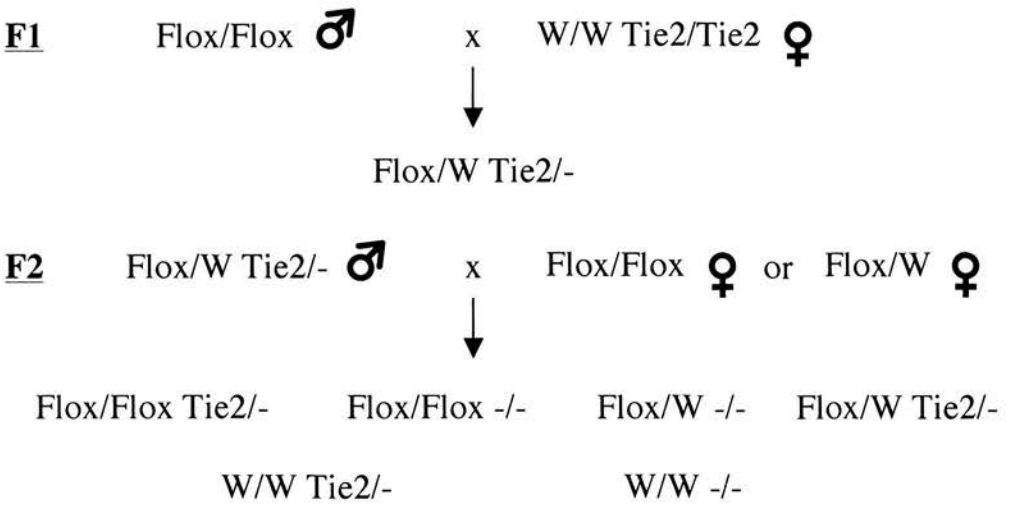

Breeding Strategy for piebald animals

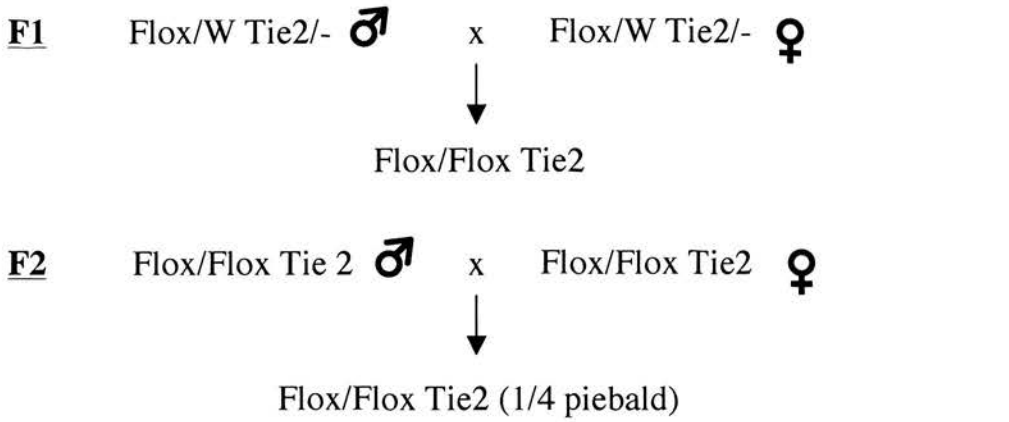

Figure 6.1

Schematic of breeding strategy used to produce EC-specific ET_B receptor knockout mice (Flox/Flox Tie2), wild type and single transgenic control animals (upper panel). Recombination events within germ cells of female mice featuring a floxed allele and the Tie2 transgene were exploited to generate piebald mice homozygous for the recombined allele (lower panel).

6.1.2 METHODS

6.1.2.1 *Genotyping of founder and offspring mice*

Tail DNA was isolated from mice as described in section 2.1.13.10. Genotyping was performed by PCR analysis using the primers 454F (TCAGTTGTAATGAGACACAGAC) and 681R (AGCCATAAAGTCACAGCCATTC) and an amplification protocol identical to that described in section 2.1.13.11. These primers are complementary to regions flanking the targeted allele. In the wild type allele this primer pair amplifies the 2197 bp region spanning from 1496 bp upstream of exon 2 to intron 3. The targeted allele features a deletion of a 1166 bp segment of intron 1, spanning from the *Nae* I site 1454 bp upstream of exon 2 to a site 288 bp upstream of exon 2 (illustrated in Figure 6.2). Sixty one bp were added to the 5' region and 50 bp to the 3' region (loxP sites and associated polylinker regions) during vector construction, resulting in a net deletion of 1055 bp from the floxed allele. Thus, wild type and floxed ET_B receptor alleles produce bands of 2197 bp and 1142 bp respectively, when amplified with these primers. Tail DNA also contains a small proportion of DNA from EC of the tail vasculature. Recombination events within the floxed EC ET_B receptor gene result in the deletion of a further 956 bp and the appearance of a 186 bp PCR band. This genotyping strategy is illustrated in Figure 6.2. Representative samples of PCR products from wild type, floxed and recombined alleles were directly sequenced to confirm specific amplification of the ET_B receptor gene.

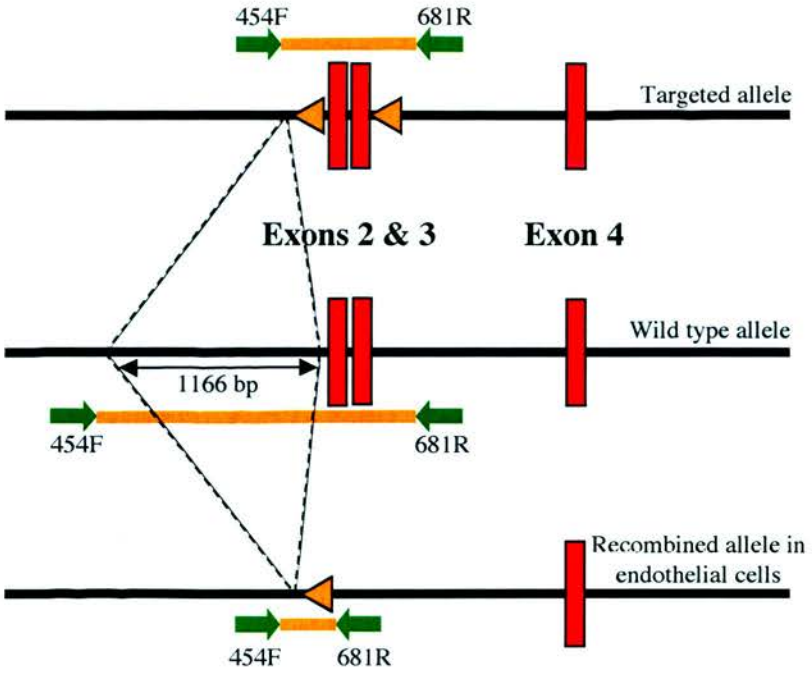

Figure 6.2

PCR-based genotyping strategy. PCR products of 2197 bp, 1092 bp and 186 bp are amplified from wild type, floxed and recombined alleles, respectively.

6.1.2.2 *Genotyping for the Tie2Cre transgene*

Offspring of Flox/Flox -/- and W/W Tie2/Tie2 crosses and subsequent offspring were genotyped for the presence of the Tie2Cre transgene by PCR of tail tip DNA as previously described (Kisanuki *et al.*, 2001). The primers Tie2 98F (CGCATAACCAGTGAAACAGCATTGC) and Tie2 101R (CCCTGTGCTCAGACAGAAATGAGA) are complimentary to regions with the Cre coding region and Tie2 promoter region, respectively. DNA was amplified for 35 cycles using the following programme: 94°C for 1 minute, 60°C for 1.5 minutes, 72°C for 2 minutes. Successful amplification of a ~900 bp fragment confirmed the presence of the Tie2Cre transgene.

6.1.2.3 *Isolation of pulmonary endothelial cell-enriched populations from murine lung tissue*

Enriched populations of pulmonary endothelial cells were prepared as described in section 2.1.17.1 according to the general method previously described by Dong (Dong *et al.*, 1997). A 100 µl aliquot of the suspension was taken for Bradford measurement of protein concentration (Bradford, 1976) and a 700 µl aliquot used for subsequent binding experiments.

6.1.2.4 *Pulmonary endothelial cell ^{125}I ET-1 binding*

0.5 µCi of ^{125}I ET-1 (Amersham Pharmacia Biotech UK Ltd, Little Chalfont, UK; Product number IM223) were diluted in 2 ml of HEPES-Ringer/0.2% BSA buffer and 100 µl (5×10^4 cpm) of the resultant solution added to 700 µl of cell suspension. The suspension was then diluted to a final volume of 1ml by the addition of a further 200 µl of HEPES-Ringer/0.2% BSA buffer. Unlabelled ET-1 (final concentration 3×10^{-9}M), A192621 (a selective ET_B receptor- antagonist; final concentration 3×10^{-7}M) or A-147627 (a selective ET_A receptor antagonist; final concentration 3×10^{-7}M) was then added and the mixtures incubated for 90 minutes at room temperature. GSL I-B4-coated magnetic beads were prepared as described in section 2.1.17.2. Approximately 10^7 beads were added and the suspension incubated for a further 30 minutes with gentle mixing at 4°C to bind ECs. Bound cells were recovered with a magnetic particle concentrator and washed twice with ice-cold PBS/0.2% BSA solution. ^{125}I ET-1 binding was measured in a γ-counter over a 60 second period and expressed as cpm/50µg membrane protein. Binding in the presence of ET-1 was used as an index of non-specific binding, whilst binding in the presence of A-147627 represented specific ET_B receptor binding.

6.1.2.5 *Measurement of plasma ET-1*

The low plasma concentration of ET-1 precludes direct measurement by radioimmunoassay (RIA). ET-1 was, therefore, extracted from plasma using the previously described acetic acid extraction technique (Rolinski *et al.*, 1994). Briefly, 1

ml of mouse plasma was mixed with 1 ml of 20% acetic acid and applied to a Varian C18 Bond Elute column (Varian Inc., Lexington, USA). Columns were washed with 10% acetic acid and ethyl acetate. ET-1 was eluted in 1.5 ml of elution buffer (1 volume of 0.05M NH_4HCO_3 in 4 volumes of methanol) and the sample concentrated by evaporating to dryness under nitrogen followed by resuspension in 100 µl of RIA buffer (3.853 g NaH_2PO_4, 18.07 g Na_2HPO_4, 2.927 g NaCl, 1 g BSA, 1 ml Triton X-100 and 100 mg sodium azide in 1000 ml deionised H_2O, pH 7.4). RIA was performed on the concentrated sample using a Peninsula Laboratory kit for determination of plasma ET-1 (Peninsula Laboratories Europe Ltd., St. Helens, UK). In short, 100 µl of standard, sample or control was incubated overnight with a rabbit anti-mouse ET-1 antibody. The following day a known concentration of ^{125}I ET-1 (Peninsula Laboratories, product number Y6901) was added and the tubes incubated for a further 16 hours. On day 3, the immune complexes were precipitated with Amerlex™ donkey anti-rabbit antibody. The precipitates were counted in a γ counter, a standard curve constructed and the unknown values read from the curve. All measurements of plasma [ET-1] were performed by Neil Johnston (Department of Clinical Pharmacology, University of Edinburgh).

6.1.3 RESULTS

6.1.3.1 *Genotyping of offspring*

A typical genotyping PCR reaction for the ET_B receptor gene allele is illustrated in Figure 6.3 and for the Tie2 transgene in Figure 6.4. Heterozygous mice (Flox/W Tie2) demonstrate 3 bands: A 2197 bp band amplified from the wild type allele, a 1142 bp band amplified from the non-recombined floxed allele, and a 186 bp band amplified from recombined floxed alleles present within a sub-population of tail-derived cells. Flox/Flox Tie2 mice exhibit bands of 1142 bp and 186 bp (floxed allele and recombined allele) whilst Flox/Flox -/- mice exhibit only the 1142 bp band. A single band of 2197 bp was amplified from homozygous wild type mice. Piebald offspring were produced with the predicted Medelian frequency (1/4 of offspring) by some F2 intercrosses and demonstrated only the 186 bp recombined allele band (Figure 6.5). The presence of the

Tie2 Cre transgene was confirmed by the amplification of a ~900 bp band in a separate PCR reaction.

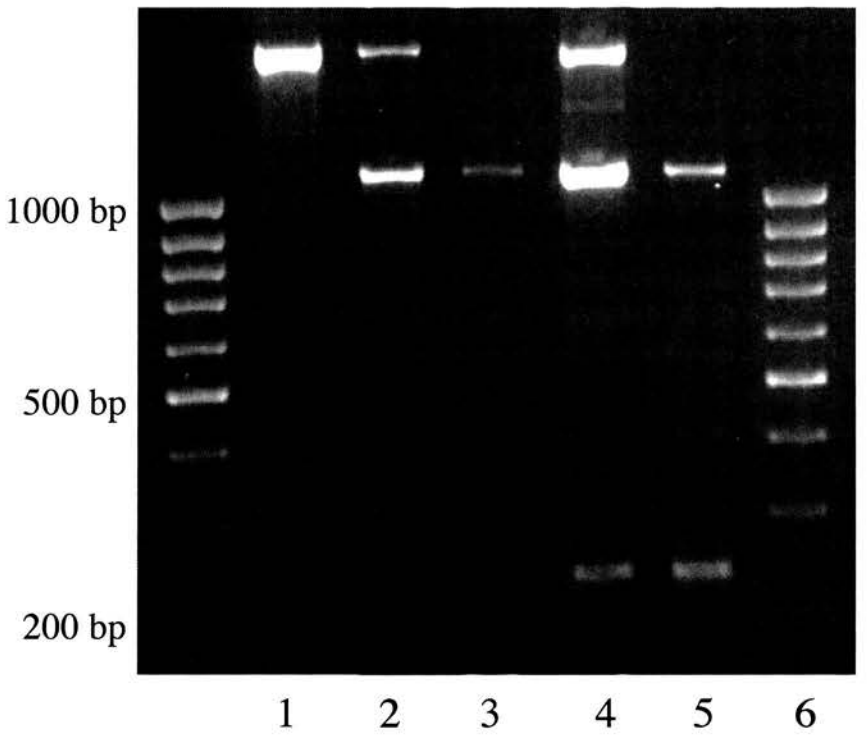

Figure 6.3

Representative genotyping PCR for the ET_B receptor allele using the primers 454F and 681R and tail tip DNA as template. Lane 1 W/W -/-, Lane 2 Flox/W -/-, Lane 3 Flox/Flox -/-, Lane 4 Flox/W Tie2, Lane 5 Flox/Flox Tie2, Lane 6 Size markers.

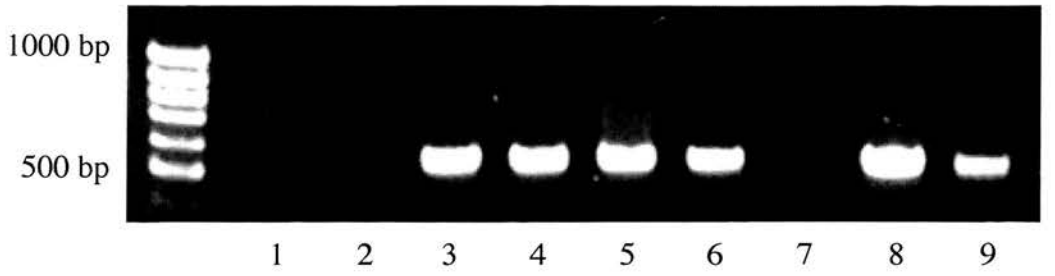

Figure 6.4

Representative PCR products obtained using the primers Tie2 98F and Tie2 101R to detect the presence of the Tie2-Cre transgene in a tail tip DNA template. Lanes 1, 2, 7, transgene absent; Lanes 3-6, 8, transgene present; Lane 9, control DNA from W/W Tie2/Tie2 mouse.

6.1.3.2 *Genotype and phenotype of piebald mice*

Two of the 3 F2 Flox/Flox Tie2 breeding pairs produced offspring with a piebald appearance in 1/4 of the pups. Piebald offspring were of normal size at birth, but failed to thrive thereafter and died shortly after weaning from intestinal obstruction (illustrated in Figure 6.5). Littermates of piebald mice were of normal pigmentation and demonstrated normal growth and development. Evidence of the recombined allele was seen in addition to the floxed allele on PCR genotyping of littermates.

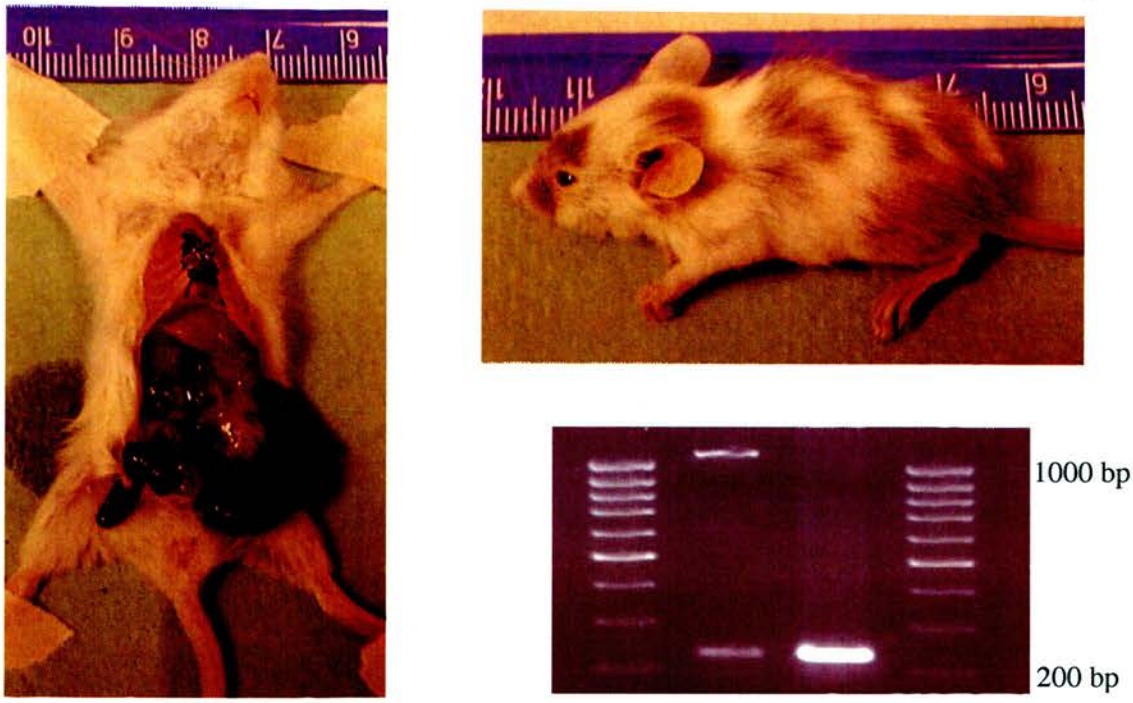

Figure 6.5

F2 intercross of Flox/Flox Tie2 mice results in offspring with piebald appearance and intestinal obstruction consistent with complete knockout of ET_B receptor expression. PCR genotyping with the primers 454F/681R demonstrates only the recombined allele in piebald mice. An EC-specific ET_B receptor knockout genotype (Flox/Flox Tie2/-) is illustrated for comparison.

6.1.3.3 *Pulmonary EC ^{125}I ET-1 binding*

^{125}I ET-1 binding was significantly decreased in Flox/Flox Tie2 pulmonary EC compared with wild type controls following incubation with 3 x 10^{-7}M A147627 (cpm/50 μg membrane protein ± SEM; Flox/Flox Tie2 581 ± 67; W/W -/- 3175 ± 268; $p<0.001$; n = 3 in both groups). Total ^{125}I ET-1 binding and ^{125}I ET-1 binding following incubation with 3 x 10^{-7}M A192621 did not differ significantly between Flox/Flox Tie2 and W/W -/- pulmonary EC (total binding Flox/Flox Tie2, 6783 ± 1507; W/W -/-, 8224 ± 2880; $p = 0.68$. Binding in presence of A192621 Flox/Flox Tie2, 4023 ± 806; W/W -/-

, 3445 ± 522; $p = 0.58$; n = 3 in each group). These results are illustrated in Figure 6.6. Binding studies were not performed in piebald mice because of the limited availability of experimental subjects.

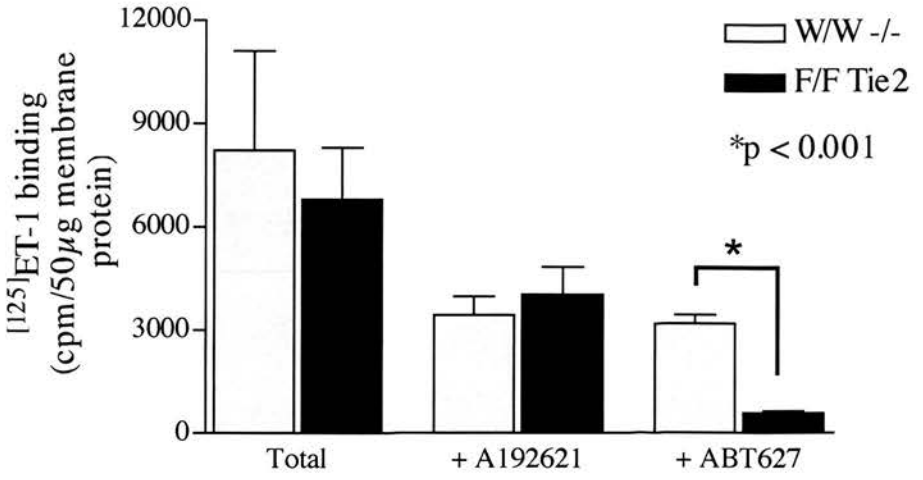

Figure 6.6

^{125}I ET-1 binding of isolated pulmonary EC. Binding in the presence of the selective ET_A receptor antagonist ABT627 (3 x 10^{-7}M) was significantly decreased in Flox/Flox Tie2 cells compared to W/W -/- cells ($p<0.001$). Total ^{125}I ET-1 binding and binding in the presence of the selective ET_B receptor antagonist A192621 (3 x 10^{-7}M) did not differ significantly between groups (n = 3 in all groups).

6.1.3.4 *Plasma ET-1 concentration*

Plasma ET-1 concentration was significantly increased in Flox/Flox Tie2 mice compared with controls (mean plasma [ET-1] pg/ml ± SEM; Flox/Flox Tie2 12.40 ± 2.95; W/W -/- 2.94 ± 0.83; W/W Tie2 2.95 ± 0.85; Flox/Flox -/- 4.05 ± 0.54; $p < 0.001$; n = 6 in each group) This result is illustrated in Figure 6.7. The limited number and small size of piebald mice prevented analysis of plasma [ET-1] in this genotype.

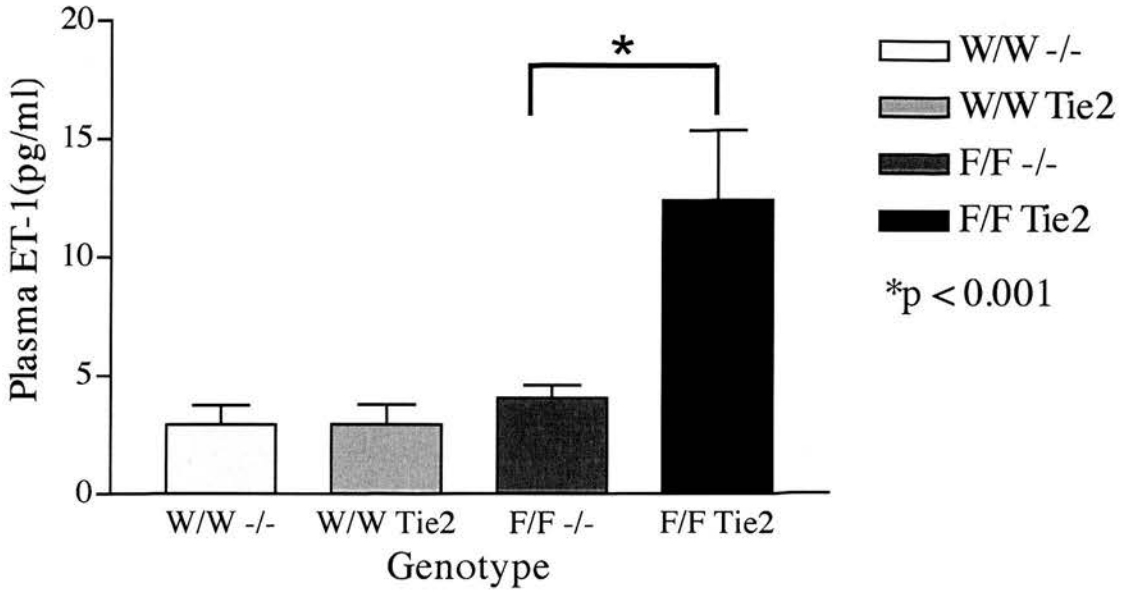

Figure 6.7

Plasma ET-1 concentration is increased in Flox/Flox Tie2 mice compared to wild type and single transgenic littermate controls (mean plasma [ET-1] pg/ml ± SEM; Flox/Flox Tie2 12.40 ± 2.95; W/W -/- 2.94 ± 0.83; W/W Tie2 2.95 ± 0.85; Flox/Flox -/- 4.05 ± 0.54; $p < 0.001$; n = 6 in each group).

6.1.4 DISCUSSION

In order to examine the role of the EC ET_B receptor in cardiovascular homeostasis *in vivo*, I have developed the Flox/Flox Tie2 mouse model in which expression of the ET_B receptor is selectively down regulated in EC. EC-specific knockout was achieved by intercross of 2 separate mouse strains. Floxed ET_B receptor mice feature loxP sites flanking exons 2 and 3 of the ET_B receptor gene. These mice were bred to transgenic mice in which the expression of a Cre recombinase transgene was restricted to EC through the use of Tie2 promoter/enhancer elements. Thus, only EC contain loxP sites

and co-express the Cre recombinase enzyme, thereby limiting recombination events to this cell type.

I developed a PCR-based method of rapidly genotyping tail tip DNA from EC-specific ET_B receptor knockout mice. This method was able to identify wild type, floxed and recombined alleles from a single PCR reaction. Previous PCR methods developed in our laboratory to genotype floxed ET_B receptor ES cells and floxed ET_B receptor mice were unable to identify the recombined allele because the primers used (78F/681R) flanked only the 3' loxP site of the targeted allele. Following cross breeding of floxed ET_B receptor mice with Tie2Cre mice, recombination events would be predicted to occur within the floxed allele of ECs, removing the region between the 5' and 3' loxP sites, including the region complimentary to the 78F primer. Hence, a second primer pair (454F/681R), complimentary to sequences flanking the 5' and 3' loxP sites, was designed. Tail tip DNA will contain a small proportion of DNA derived from EC of the tail vessels. The recombined allele was easily detected by PCR in mice homozygous for the floxed allele and the Tie2 transgene and direct sequencing of this PCR product confirmed the predicted post-recombination sequence. In mice heterozygous for the floxed and wild type alleles (Flox/W Tie2), the recombined allele was fainter, presumably reflecting the lower concentration of DNA template. However, in the context of evidence for continued presence of both a floxed and a wild type allele, the additional presence of the recombined allele provides good evidence that a sub-population of cells from the tail had undergone recombination events. Tissue staining of reporter mouse strains bearing the Tie2Cre allele (Constien *et al.*, 2001, Kisanuki *et al.*, 2001) indicate that this subpopulation is likely to represent EC and I have confirmed, through binding studies, that ET_B receptor expression is down-regulated in pulmonary EC. However, I have been unable to isolate sufficiently pure populations of EC from tail or lung samples to conclusively demonstrate that the recombined allele is exclusively present in EC. Isolation of tissue that does not contain either ECs or cells of the haematopoietic lineage, in order to demonstrate the absence of recombination events in non-EC, has also proven difficult.

To assess the extent of functional ET_B receptor down-regulation in EC through Cre/loxP-mediated recombination, I have performed a combination of binding and functional pharmacological studies (described in chapter 7). EC ET_B receptor-specific binding was assessed using ^{125}I ET-1 in EC-enriched cell populations following incubation with the selective ET_A receptor antagonist A147627. ^{125}I ET-1 binding in EC-enriched populations from Flox/Flox Tie2 mice was decreased by ~80% compared to wild type ECs. This represents an at least 80% reduction in EC ET_B receptor expression, since some of the remaining ^{125}I ET-1 binding may be mediated by ET_B receptors on contaminating SMC. Contamination of enriched EC populations with SMC was assessed by measurement of both total ^{125}I ET-1 binding and binding in the presence of the selective ET_B receptor antagonist A192621. Unlike EC, SMC express both ET_A and ET_B receptors and would be expected to bind significant quantities of ET-1 in the presence of A192621. Total ^{125}I-ET-1 binding was decreased in Flox/Flox Tie2 preparations, but this difference did not reach significance. In the presence of A192621 ^{125}I-ET-1 binding was still present, but there was no significant difference in binding between wild type and Flox/Flox Tie2 EC populations. Taken together, these results confirm SMC contamination of enriched EC populations and suggest that the extent of contamination was comparable between groups. It is likely, therefore, that a significant portion of residual ET_B receptor-dependent binding observed in the Flox/Flox Tie2 group is derived from contaminating SMC in which normal ET_B receptor expression is maintained. I have not isolated SMC-enriched populations to directly assess ^{125}I ET-1 binding in Flox/Flox Tie2 and wild type mice. However, there were no abnormalities of pigmentation or gut development and SMC ET_B receptor-mediated tracheal contraction was maintained in Flox/Flox Tie2 mice (described in chapter 7), suggesting that expression of non-EC ET_B receptors was sufficient to maintain normal physiological responses. The results of these experiments have, therefore, demonstrated that Cre/loxP recombination within the ET_B receptor locus is sufficient to down regulate functional ET_B receptor expression by greater than 80% *in vivo*. This finding strongly suggests that the floxed ET_B receptor mouse is a useful tool for assessing the functional consequences of cell type-specific ET_B receptor down regulation.

Attempts to further assess the degree of ET_B receptor down-regulation by visualisation of tissue staining with ET_B receptor antibodies were unsuccessful (data not shown). No commercially available antibody was able to reliably reproduce the pattern of ET_B receptor expression seen in 'knock-in' ET_B–lacZ reporter mice (Adele Gordon, University of Edinburgh, personal communication). Furthermore, attempts to quantify ET_B receptor protein concentration from preparations of pulmonary, aortic and renal tissue by western blot analysis using commercial antibodies also lacked specificity.

EC-specific ET_B receptor knockout mice demonstrate a ~4 fold increase in plasma ET-1. The ET_B receptor has been proposed as a clearance receptor for ET-1 (Fukuroda *et al.*, 1994) and my data suggests that EC ET_B receptors contribute importantly to this process. Clearance of ET-1 occurs predominantly in the lung and liver (Fukuroda *et al.*, 1994). The relative importance of non-EC ET_B receptor-mediated clearance may be examined with further tissue-specific ET_B receptor knockout models. An alternative hypothesis is that deletion of ET_B receptors could result in an increase in the production of ET-1. ET-1 production has not been studied in other models of ET_B receptor deficiency (Berthiaume *et al.*, 2000, Gariepy *et al.*, 2000), although in the rescued rat model (Gariepy *et al.*, 2000), ET_B genotype was the only significant independent variable found to correlate with plasma [ET-1]. On the other hand, clearance of ^{125}I ET-1has been shown to be impaired in heterozygous ET_B receptor knockout mice (Berthiaume *et al.*, 2000). It is likely, therefore, that the increase of plasma [ET-1] in our model represents defective clearance, rather than significantly increased production.

Tie2Cre transgenic mice represent a novel genetic tool for the analyses of the EC-lineage and for EC-specific gene targeting (Kisanuki *et al.*, 2001). However, several groups have recently reported Cre-mediated recombination events in the germline of female mice expressing both the Tie2 Cre transgene and a floxed allele (Constien *et al.*, 2001, Koni *et al.*, 2001). This process results in the presence of a recombined maternally-derived allele in all cells of the developing embryo. The mechanism underlying the loss of spatial regulation of Cre recombinase expression in germ cells is

currently unknown, but may result from demethylation events that occur during gametogenesis. I utilised the phenomenon of germ cell recombination to deliberately generate mice that were homozygous for the recombined ET_B receptor allele in all cell types to test the hypothesis that exons 2 and 3 of the ET_B receptor gene were necessary for functional ET_B receptor expression. Theoretically, expression of functional ET_B receptors may have been maintained in these mice despite recombination-mediated removal of these coding regions. This may occur through the expression of truncated yet functional ET_B receptor protein or through 'skipping' of the mutated region by aberrant splicing (reviewed by (Muller, 1999). Splice variants of human, but not murine, ET_B receptor RNA have been demonstrated (Shyamala *et al.*, 1993). However, the appearance of the piebald lethal phenotype in mice homozygous for the recombined allele confirmed that deletion of exons 2 and 3 via Cre-loxP-mediated recombination is sufficient to prevent normal ET_B receptor function. Since completion of these experiments, a novel deletion mutation spanning exons 2 and 3 has been identified in ET_B receptor-deficient mice (Matsushima *et al.*, 2002). The demonstration of the piebald phenotype in F2 offspring does not, however, imply 100% efficiency of Cre-mediated recombination events within EC of Flox/Flox Tie2 mice. All piebalds were derived from gametes in which a single recombination event during gametogenesis resulted in the formation of a null ET_B receptor allele. However, the results of my binding studies would suggest that Cre-mediated recombination is sufficient to down-regulate ET_B expression by >80%.

The frequency of germ cell recombination events appears variable. I have intercrossed F2 Flox/Flox Tie2 mice (pair 55, data not shown) and observed no evidence of the piebald phenotype in the offspring, suggesting that there was no germ cell recombination in this pairing. In other F2 intercrosses, piebald mice have been produced in the expected Medelian 1:4 ratio. The precise timing of possible germ cell recombination events has also not been determined. I have observed offspring of Flox/W Tie2 female mice which are heterozygous for the recombined allele but do not possess

the Tie2 transgene. This would suggest that recombination events occur during gametogenesis prior to segregation of the floxed allele and Tie2 transgene.

The phenomenon of germ cell recombination secondary to loss of normal spatial regulation of transgene expression does not appear to be limited solely to the Tie2Cre transgene. The VSMC-specific Cre transgene (smooth muscle-myosin heavy chain (SM-MHC)-Cre) has also been shown to initiate recombination events in female germ cells (Professor Gary Owens, personal communication). It has been proposed that this may occur secondary to transplacental transfer of Cre recombinase from uterine SMC into the developing embryo during early gestation. Were a similar mechanism of transplacental transfer of EC-derived Cre responsible for this phenomenon, I might expect that all offspring homozygous for the floxed allele would be piebald. In fact, I noted several offspring from F2 intercrosses featuring non-recombined floxed alleles. Germ cell recombination is also observed in the offspring of male mice carrying both a floxed allele and the inner medullary collecting duct-specific Cre transgene, Aquaporin2-Cre (AQ2Cre). However, in these animals, GFP reporter mice have demonstrated that this transgene is also expressed in the testis of adult animals (D. Kohan, University of Utah, personal communication), suggesting that this process may reflect the normal spatial pattern of AQ2 promoter activity, rather than dysregulation during gametogenesis.

Germ cell recombination events may be utilised to maximise the likelihood of complete knockout of gene expression in EC (Constien *et al.*, 2001). F2 offspring will feature a single null allele in all cells, with conditional knockout of the remaining allele in EC only. This strategy may be utilised when complete loss of expression is required to produce the desired phenotype. However, care must be taken to ensure that homozygous knockout of the gene in other cells does not influence the phenotypical trait under investigation. Data from heterozygous ET_B receptor knockout mice suggests that blood pressure is increased and clearance of ET-1 is impaired (Berthiaume *et al.*, 2000, Berthiaume *et al.*, 2000, Berthiaume *et al.*, 1998) following deletion of a single allele. For this reason, I specifically undertook breeding strategies that minimised the potential for heterozygous knockout of the ET_B receptor in the offspring.

This chapter has described the generation and genotyping of Flox/Flox Tie2 mice and demonstrated significant down-regulation of ET_B receptor-dependent ET-1 binding in pulmonary EC from these animals. Plasma ET-1 concentration is increased in Flox/Flox Tie2 mice, consistent with the proposed 'clearance receptor' role for the ET_B receptor.

7 Chapter 7

7.1 ENDOTHELIAL CELL SPECIFIC KNOCKOUT OF THE MOUSE ET_B RECEPTOR RESULTS IN SALT-INSENSITIVE HYPERTENSION AND IMPAIRED VASODILATATION TO ET_B RECEPTOR AGONISTS AND ACETYLCHOLINE

7.1.1 INTRODUCTION

The importance of ET_B receptors in the regulation of blood pressure and the molecular and cellular mechanisms through which such regulation may occur, remains controversial. Renal tubular, vascular and central nervous system ET_B receptors have been implicated in cardiovascular homeostasis (Gariepy *et al.*, 2000, Mosqueda-Garcia *et al.*, 1993, Strachan *et al.*, 1999). The aim of this study was to determine whether endogenous EC ET_B receptor signalling contributed significantly to vascular tone in the mouse and, if so, whether this effect was important for the determination of blood pressure. Renal tubular ET_B receptors have been proposed as important regulators of natriuretic pathways under conditions of high salt (Gariepy *et al.*, 2000). The contribution of EC ET_B receptors expressed in the vasa recta of the renal medulla to this process was also investigated. Previously available loss of function models feature down-regulation of ET_B receptor expression in all tissues concurrently. The relative importance of vascular EC ET_B receptors in the control of blood pressure and natriuresis in the mouse has not, therefore, been assessed without the confounding influence of simultaneous loss of renal tubular and VSMC ET_B receptor signalling. Selective ET_B receptor antagonists are also unable to block EC ET_B receptors *in vivo* without concurrent blockade of ET_B receptors in other cell types. Cell type-specific down-regulation of ET_B receptor expression, therefore, provides a unique and powerful method by which to examine the relative contribution of ET_B receptor signalling in a single cell type to the regulation of complex physiological systems such as the control of blood pressure, natriuresis or endothelial function.

ET_B receptors are expressed on both ECs and VSMCs of the vasculature (Gray *et al.*, 2000). EC ET_B receptors mediate vasodilatation (Takayanagi *et al.*, 1991) through signal transduction mechanisms that result in the release of NO (Namiki *et al.*, 1992) and/or dilator prostagladins. In contrast, activation of VSMC ET_B receptors initiates a complex cascade of events resulting in a rise in $[Ca^{2+}]_i$, and ultimately, cellular contraction (Sumner *et al.*, 1992). In a given vessel or vascular bed, it is hypothesised that the balance between endogenous activation of vasoconstrictor VSMC ET_B receptors and vasodilator EC ET_B receptors will determine the overall response of the vessel to ET_B receptor agonists, including ET-1and S6c. This balance may differ between vascular beds, providing a potential mechanism for the differential regulation of vessel tone and hence, blood flow. In humans, the net effect of endogenous ET_B receptor activation in the forearm circulation is one of vasodilatation (Verhaar *et al.*, 1998) and the results of these local studies have since been confirmed in the systemic circulation (Strachan *et al.*, 1999). Studies of localised vascular circuits *in vivo* have not been performed in the mouse. However, in the rescued ET_B receptor-deficient rat, pulmonary artery pressure (PAP) and total pulmonary resistance are increased, suggesting that in the rodent vascular ET_B receptors also exert a net vasodilator effect (Ivy *et al.*, 2001).

The phenotypical effects of alterations in vascular gene expression may be assessed using the technique of small vessel myography (Mulvany and Halpern, 1976, Mulvany *et al.*, 1978). This technique permits investigation of the mechanical, morphological and pharmacological properties of vessels *in vitro*. The response to the highly selective ET_B receptor agonist S6c of aortic and tracheal rings isolated from mice featuring down regulation of EC ET_B receptor expression (Flox/Flox Tie2) were compared to those of wild type and single transgenic littermates. To demonstrate that S6c-evoked responses were due to activation of ET_B receptors, comparison was made with vessel rings from the same animals following pre-incubation with the selective ET_B receptor antagonist A192621 (Douglas, 1997) at a dose previously shown to inhibit ET_B receptor-mediated tracheal constriction (Hay *et al.*, 2001). Endothelial function was assessed by measurement of the vasodilator response to ACh and the influence of acute

blockade of NOS activity upon NE-induced vasoconstriction was studied. Endothelium-independent vasodilatation to the diazeniumdiolate NO donor deta/NO was measured to ensure that any changes in vasodilatation were not due to alteration of the sensitivity of VSMC to NO. This compound was specifically chosen because, unlike sodium nitroprusside, it decomposes spontaneously to generate NO (Horstmann *et al.*, 2002) requiring no prior metabolism. The long duration of action additionally permitted the construction of stable concentration response curves (De Vriese *et al.*, 2002).

In order to accurately assess the specific role of the EC ET_B receptor in the regulation of vascular tone and blood pressure, preservation of SMC and other non-EC ET_B receptor signalling was required. In the trachea, both ET_A and SMC ET_B receptors mediate bronchoconstriction (Henry, 1993). ET_B receptor-mediated bronchoconstriction occurs through direct activation of airway SMC and through augmentation of cholinergic nerve-mediated responses (Carr *et al.*, 1997). Bronchoconstriction in response to selective ET_B receptor agonists was measured, therefore, to provide evidence of the functional preservation of SMC ET_B receptor signalling and hence, of the cell-specificity of recombination events.

7.1.2 METHODS

7.1.2.1 *In vivo measurement of blood pressure*

Male mice were fed either a standard chow diet (0.8% Na^+ content) or high salt diet (7.6% Na^+ content) for a minimum of 21 days following weaning. Mean arterial pressure (MAP) was measured via an indwelling carotid cannula under conscious unrestrained conditions in 8-12 week old mice as described in section 2.1.16. Measurements were performed in a quiet room on days 2 and 3 post-surgery to permit adequate recovery and minimise the post-surgical stress response. Blood pressure was recorded continuously for 90 minutes using a pressure transducer. The first 30 minutes of each recording was disregarded to minimise the effects of acute stress when connecting the transducer.

7.1.2.2 *In vitro vascular responses of aortic and tracheal rings*

Experiments were performed on segments of aorta and trachea isolated as described in section 2.1.15.1 from adult mice age 8-10 weeks (24.2-37.4 g). Vessels were mounted in wire myograph chambers as described in section 2.1.15.2 and incubated with 6 ml of fresh PSS solution at 37°C constantly bubbled with 95%/5% O_2/CO_2. Aortic and tracheal rings underwent a KPSS 'wake-up' protocol as described in section 2.1.15.3. In aortic preparations, a single pre-constriction with 3 x 10^{-7}M NE followed by relaxation with 10^{-6}M ACh was also performed. In order to eliminate any effects related to changes in vessel tension during the course of the experiments, a baseline tension of 1.5 g (7.36 mN) for aortic rings and 0.5 g (2.45 mN) for tracheal rings was restored prior to the construction of each dose response curve.

7.1.2.3 *Isolated aortic rings*

Cumulative additions of NE in half-log increments (10^{-8}M-3x10^{-6}M) were made allowing the maximal response to each dose to plateau prior to subsequent additions. From this data, the dose of NE required to produce 80% of the maximal NE-induced contraction (EC_{80}) was calculated. Following a 10 minute washout period with PSS, rings were pre-constricted to their EC_{80} with NE and a concentration response curve to cumulative half-log increments of ACh constructed (10^{-9}M-3x10^{-6}M). Relaxation in response to ACh was expressed as a percentage of the EC_{80} tension. Vessels then underwent one of the following 3 protocols: In the first protocol, a further preconstruction with EC_{80} was followed by construction of a cumulative concentration response curve to half log increments of deta/NO (10^{-7}M-3x10^{-4}M) to assess endothelium-independent vasodilatation. In the second and third protocols, vessels were incubated with either 10^{-7}M A192621 or vehicle (DMSO; 1:1000 dilution) for 20 minutes. To examine the effect of EC-specific ET_B receptor down regulation upon responses to ET_B receptor-selective agonists, pre-constriction with EC_{80} NE was performed, followed by addition of 10^{-7}M S6c. Vasodilatation was calculated as a percentage of the EC_{80} tension. In the third protocol, incubation with A192621 or vehicle

was followed by construction of a second ACh concentration response curve. Rings were then incubated with the NOS inhibitor L-NAME (10^{-4}M) for 30 minutes and the NE concentration response curve repeated. At the end of the experiment, aortic rings were contracted with KPSS to assess the viability of the preparation and provide a reference contraction for analysis of the NE concentration response curve. These protocols are illustrated in Figure 7.1, Figure 7.2 and Figure 7.3. Data from vessels were rejected if the EC_{80} pre-constriction exceeded ≥140% of the maximal NE-induced contraction or if they failed to dilate by ≥50% in response to ACh. A failure to dilate by >50% was taken as evidence of significant endothelial damage during vessel mounting.

7.1.2.4 *Tracheal rings*

The standard 'wake-up' protocol described in section 2.1.15.3 was followed by construction of a concentration response curve with half log increments of carbachol (10^{-8}M-$3x10^{-5}$M). Responses were allowed to plateau prior to addition of subsequent doses. Rings were then washed for 20 minutes in PSS prior to incubation for 20 minutes with either 10^{-7}M A192621 or vehicle. A cumulative concentration response curve to half-log increments of S6c was then constructed (10^{-11}M-10^{-7}M) and the rings washed prior to a final contraction with KPSS. All contractile responses were compared to a final KPSS reference contraction for data analysis. This protocol is illustrated in Figure 7.4.

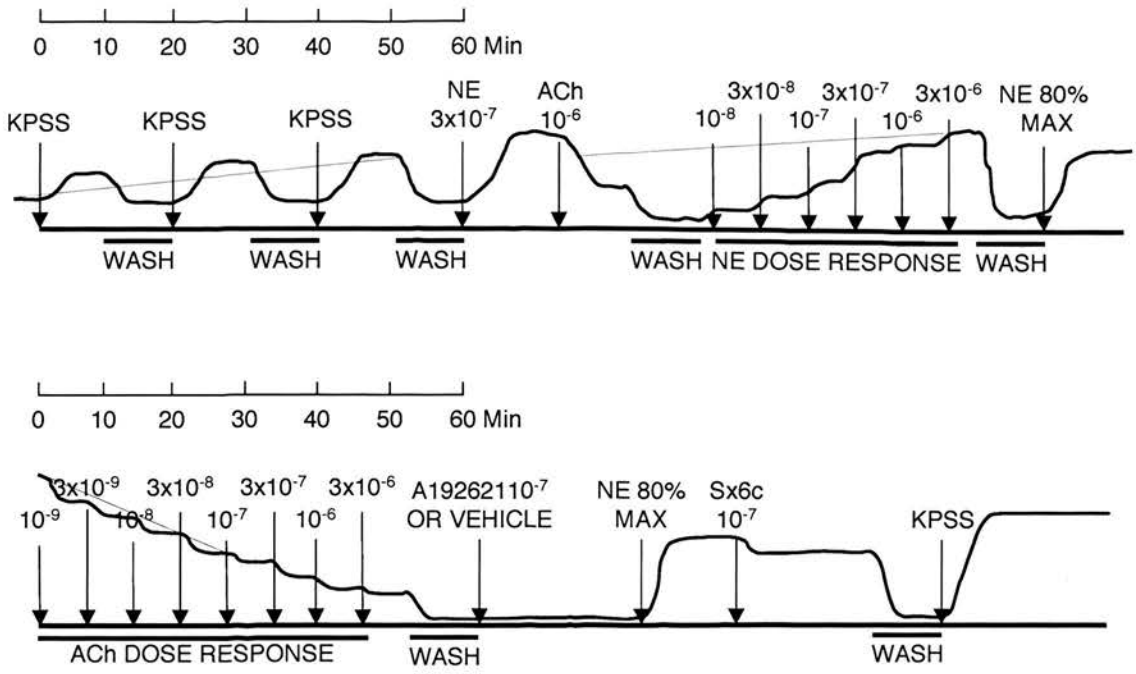

Figure 7.1

Protocol 1: *In vitro* wire myograph protocol for the assessment of responses of aortic rings to nor-epinephrine (NE), acetylcholine (ACh) and the selective ET_B receptor agonist S6c.

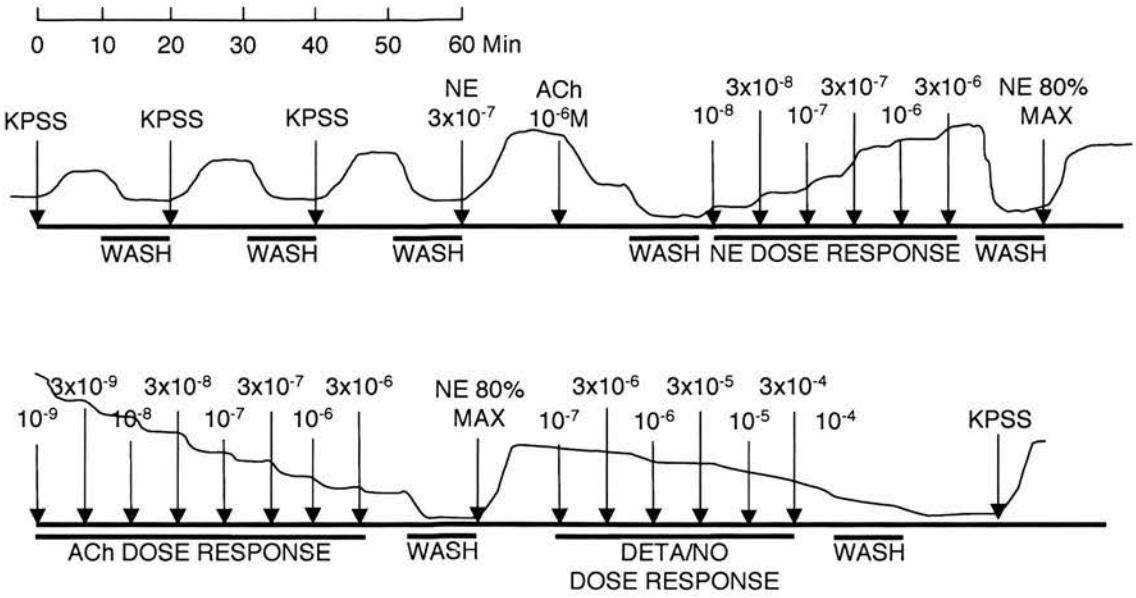

Figure 7.2

Protocol 2: *In vitro* wire myograph protocol for the assessment of responses of aortic rings to NE, ACh and the endothelium-independent NO donor deta/NO.

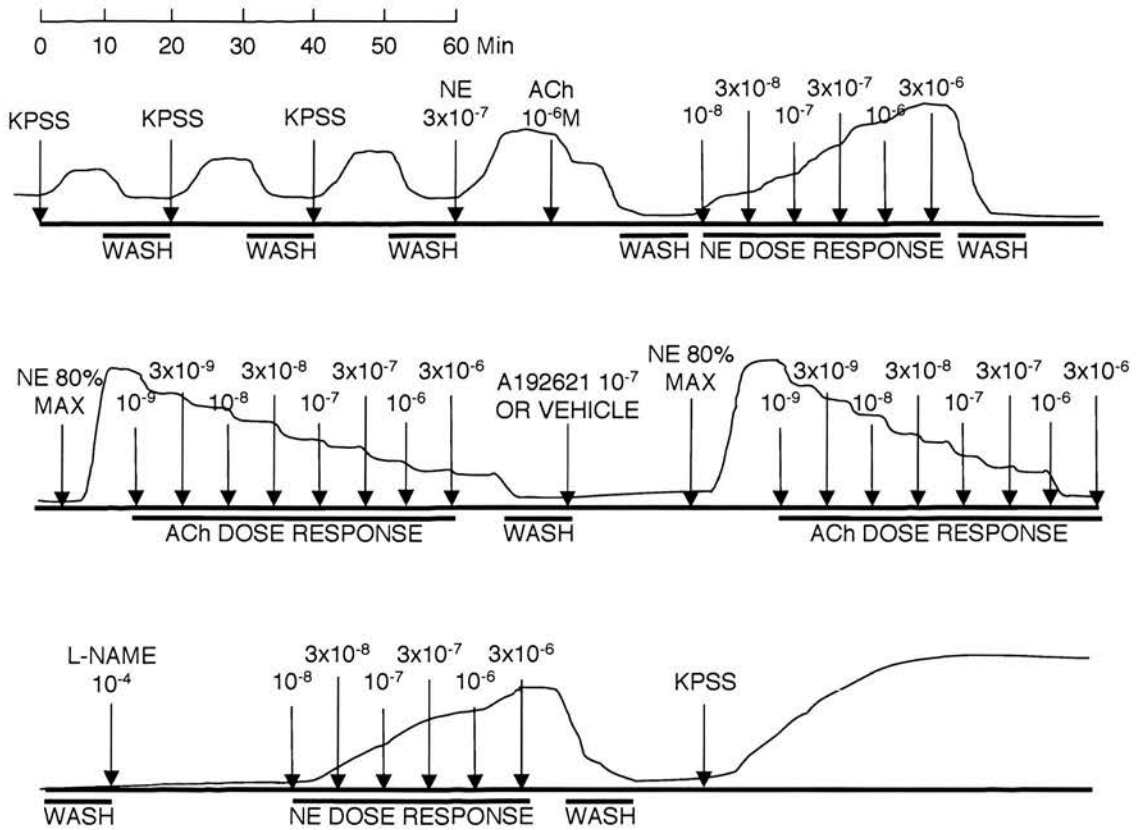

Figure 7.3

Protocol 3: *In vitro* wire myograph protocol for the assessment of the responses of aortic rings to ACh following selective ET_B receptor antagonism and to NE following inhibition of NOS with L-NAME.

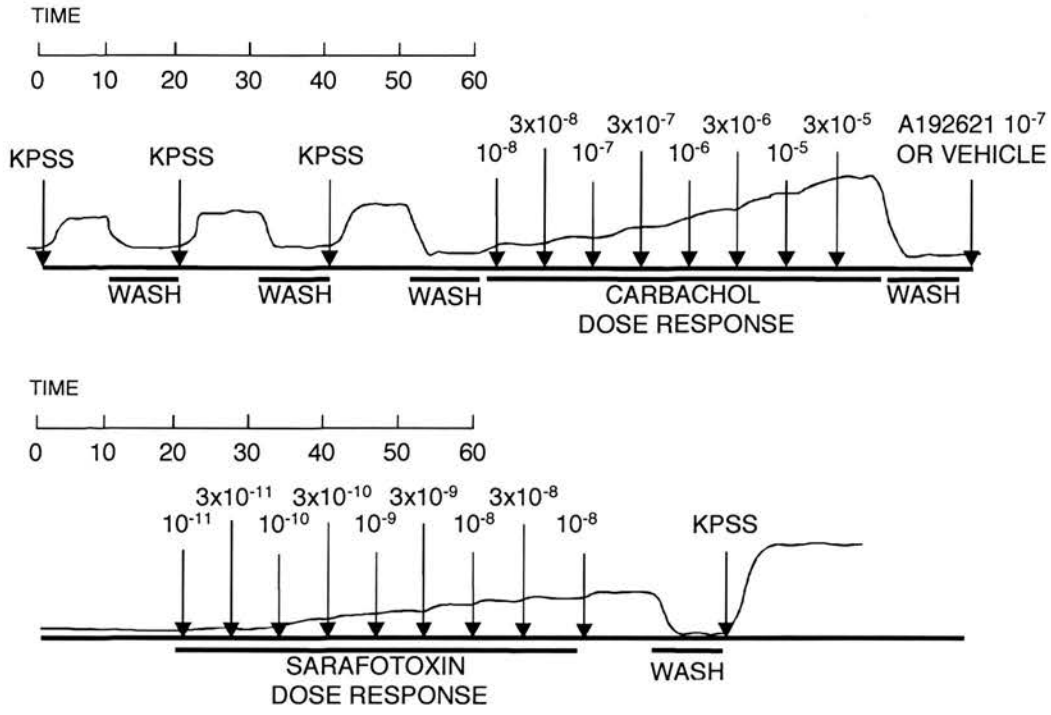

Figure 7.4

In vitro wire myograph protocol for the assessment of tracheal contraction in response to carbachol and the selective ET_B receptor agonist S6c.

7.1.2.5 *Analysis of results*

P values for MAP were derived using 2 factor analysis of variance (ANOVA) with Bonferroni post-test analysis. S6c-induced vasodilatation was compared using repeated measures ANOVA with Dunnett's Multiple Comparison post-test analysis. *P* values for concentration response curves were obtained by 2 factor ANOVA. A probability value of $p<0.05$ was considered statistically significant. Geometric mean log EC_{50} values were calculated from linear regression analyses of data sets. All analysis was performed using Graphpad Prism 3.0 software (Macintosh version).

7.1.3 RESULTS

7.1.3.1 *In vivo blood pressure*

Mean arterial pressure was significantly elevated in Flox/Flox Tie2 compared with control mice when fed either a normal or high salt diet (MAP ± SEM; Flox/Flox Tie2 137.2 ± 6.4 (n = 5); W/W -/- 113.7 ± 4.7 (n = 6; $p<0.05$). Pre-treatment with a high salt diet for 3 weeks did not significantly increase blood pressure in either wild type or Flox/Flox Tie2 mice above that observed on a normal salt diet (High salt diet; Flox/Flox Tie2 141.0 ± 6.7 (n = 5); W/W -/- 118.3 ± 5.0 (n = 4; $p=0.48$ compared to normal salt diet). These results are illustrated in Figure 7.5.

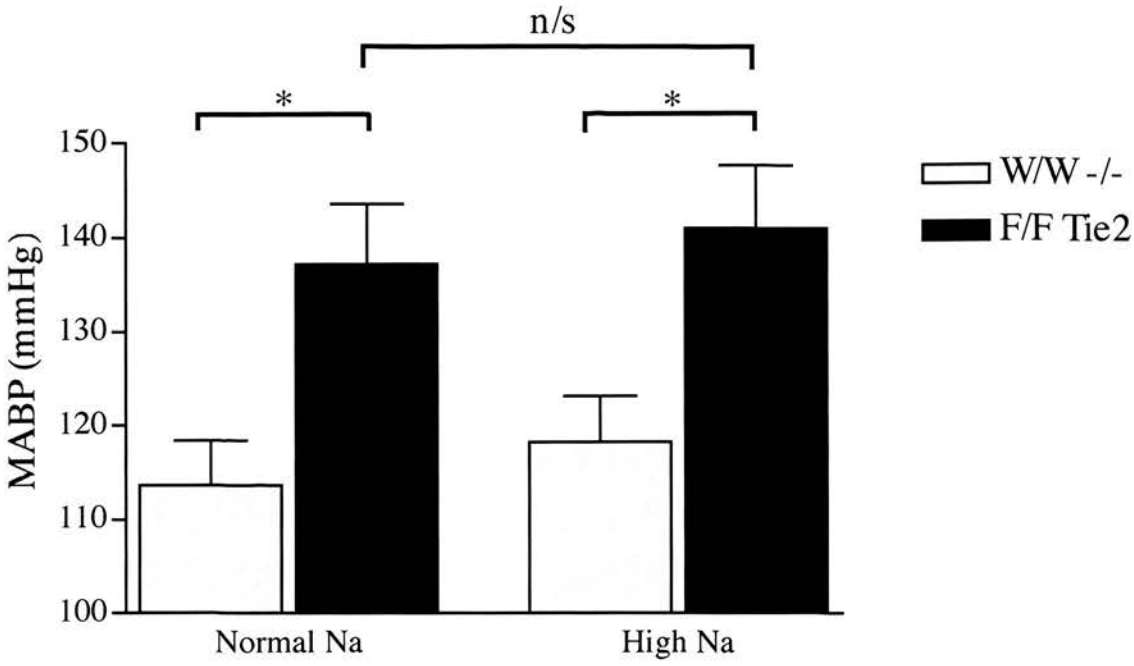

Figure 7.5

MABP measured via in-dwelling carotid cannula in mice under conscious unrestrained conditions. Mice were fed a standard (0.8% NaCl) or high salt (0.76% NaCl) chow diet from weaning for a minimum of 21 days prior to BP measurement. MABP was measured on days 2 and 3 post-surgery. MABP was significantly increased in Flox/Flox Tie2 mice compared to wild type controls on both a normal and high salt diet. High salt diet had no significant additional effect upon MABP (MABP mmHg ± SEM; 0.8% NaCl diet Flox/Flox Tie2, 137.2 ± 6.4 (n = 5); W/W -/-, 113.7 ± 4.7 (n = 6; $p<0.05$); 7.6% NaCl diet Flox/Flox Tie2, 141.0 ± 6.7 (n = 5); W/W -/-, 118.3 ± 5.0 (n = 4; $p=0.48$ compared to normal salt diet).

7.1.3.2 *Aortic vasoconstriction to NE*

NE produced concentration-dependent contraction of aortic rings in all groups. NE-induced contraction did not differ between groups ($logEC_{50}$ ± SEM: Flox/Flox Tie2, 7.32 ± 0.15; W/W -/-, 7.43 ± 0.22; W/W Tie2, 7.36 ± 0.19; Flox/Flox -/-, 7.40 ± 0.21; *p*

=0.50; E_{Max} ± SEM; Flox/Flox Tie2, 76.09 ± 5.78; W/W -/-, 85.66 ± 9.50; W/W Tie2, 63.80 ± 6.23; Flox/Flox 69.47 ± 7.25; p = 0.19; n = 16 in each group). These results are illustrated in Figure 7.6.

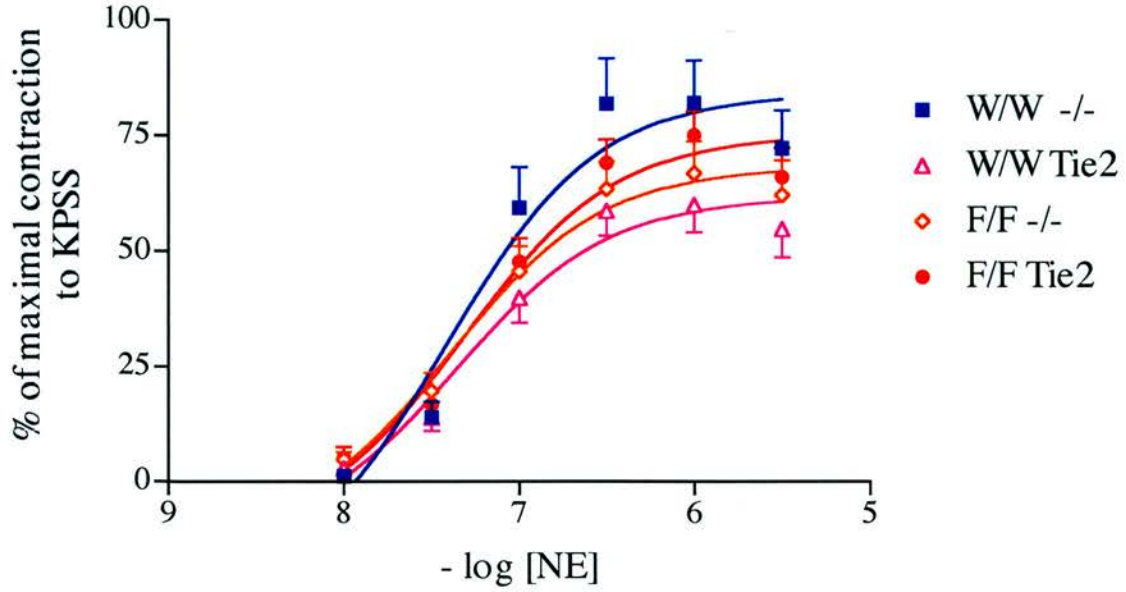

Figure 7.6

Contraction of aortic rings in response to NE. LogEC_{50} ± SEM: Flox/Flox Tie2, 7.32 ± 0.15; W/W -/-, 7.43 ± 0.22; W/W Tie2, 7.36 ± 0.19; Flox/Flox -/-, 7.40 ± 0.21; E_{Max} ± SEM; Flox/Flox Tie2, 76.09 ± 5.78; W/W -/-, 85.66 ± 9.50; W/W Tie2, 63.80 ± 6.23; Flox/Flox 69.47 ± 7.25; n = 16 in each group). There were no significant differences between groups.

7.1.3.3 *Aortic vasodilatation to ACh*

ACh-induced concentration-dependent relaxation of aortic rings in all groups. There was a significant rightwards shift of the concentration-response curve in aortic rings from Flox/Flox Tie2 mice ($logEC_{50}$ ± SEM: Flox/Flox Tie2, 6.76 ± 0.08; W/W -/- 6.87 ± 0.10; W/W Tie2 7.04 ± 0.07; Flox/Flox -/- 6.82 ± 0.09; $p<0.011$); There was a trend towards a decreased maximal ACh-induced relaxation in Flox/Flox Tie2 rings that did not reach statistical significance (E_{Max} ± SEM: Flox/Flox Tie2, 70.29 ± 3.44; W/W -/-, 75.19 ± 3.41; W/W Tie2, 79.67 ± 2.82; F/F -/-, 82.08 ± 3.64; $p=0.07$; n = 16 in each group). These results are illustrated in Figure 7.7.

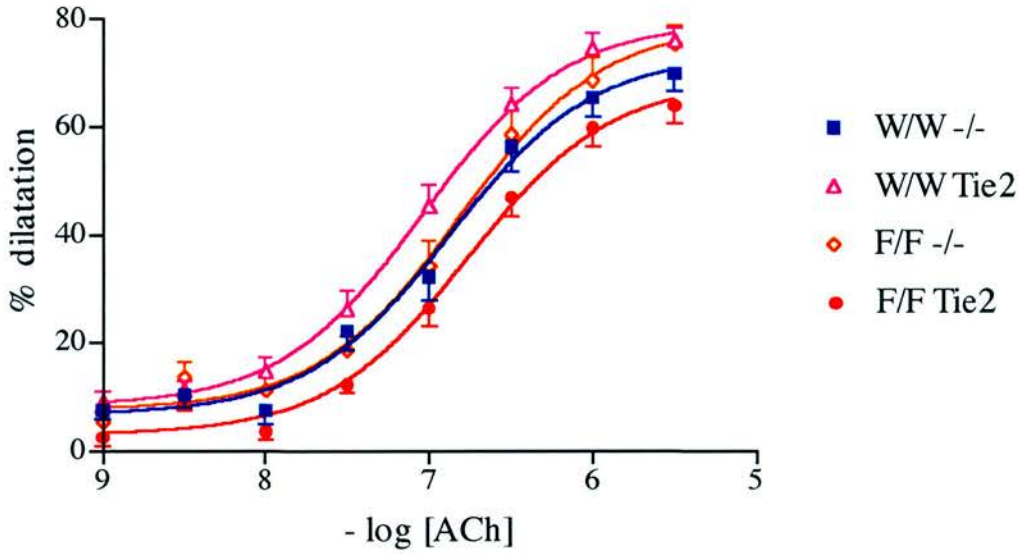

Figure 7.7

Aortic vasodilatation in response to ACh. ACh-induced vasodilatation was significantly impaired in Flox/Flox Tie2 aortic rings compared to control vessels ($LogEC_{50}$ ± SEM: Flox/Flox Tie2, 6.76 ± 0.08; W/W -/-, 6.87 ± 0.10; W/W Tie2, 7.04 ± 0.07; Flox/Flox -/- 6.82 ± 0.09; $p<0.011$; n = 16 in each group).

7.1.3.4 *Effect of acute ET_B receptor inhibition upon aortic vasodilatation to ACh*

Prior incubation with A192621 significantly inhibited ACh-induced vasodilatation in aortic rings from W/W -/- mice but not Flox/Flox Tie2 mice ($logEC_{50}$ ± SEM; W/W -/-, 6.76 ± 0.06; W/W -/- with A192621, 6.38 ± 0.08; $p<0.001$; Flox/Flox Tie2, 6.30 ± 0.04; Flox/Flox Tie2 with A192621 6.33 ± 0.06; $p>0.05$; E_{Max} ± SEM; W/W -/-, 90.30 ± 3.05; W/W -/- with A192621, 73.11 ± 3.22; $p<0.001$; Flox/Flox Tie2, 76.84 ± 2.86; Flox/Flox Tie2 with A192621, 72.86 ± 2.50; $p>0.05$; n = 6 in each group). These results are illustrated in Figure 7.8.

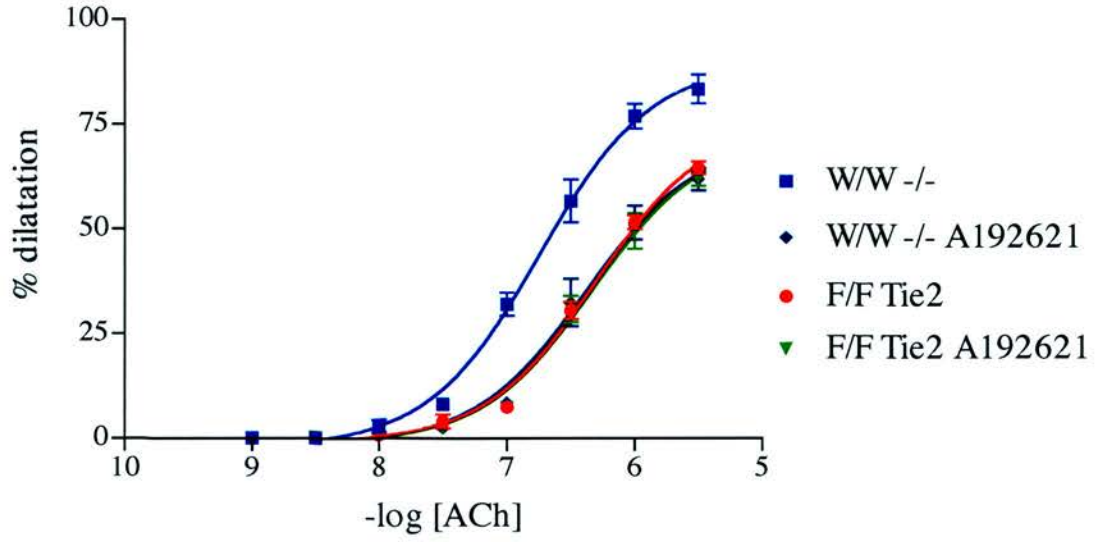

Figure 7.8

Aortic vasodilatation in response to ACh following incubation with either the selective ET_B receptor antagonist A192621 (10^{-7}M) or vehicle. Prior incubation with A192621 significantly inhibited ACh-induced vasodilatation in aortic rings from W/W -/- mice but not Flox/Flox Tie2 mice ($logEC_{50}$ ± SEM; W/W -/-, 6.76 ± 0.06; W/W -/- with A192621, 6.38 ± 0.08; $p<0.001$; Flox/Flox Tie2, 6.30 ± 0.04; Flox/Flox Tie2 with A192621 6.33 ± 0.06; $p>0.05$; n = 6 in each group).

7.1.3.5 *Aortic vasodilatation to deta/NO*

The endothelium-independent NO donor, deta/NO, produced concentration-dependent relaxation of aortic rings preconstricted to EC_{80} with NE. There was no significant difference in deta/NO-induced vasodilatation between wild type and Flox/Flox Tie2 mice ($logEC_{50}$ ± SEM: Flox/Flox Tie2, 5.46 ± 0.09; W/W -/-, 5.51 ± 0.07; n = 6 in each group; $p>0.05$). These results are illustrated in Figure 7.9.

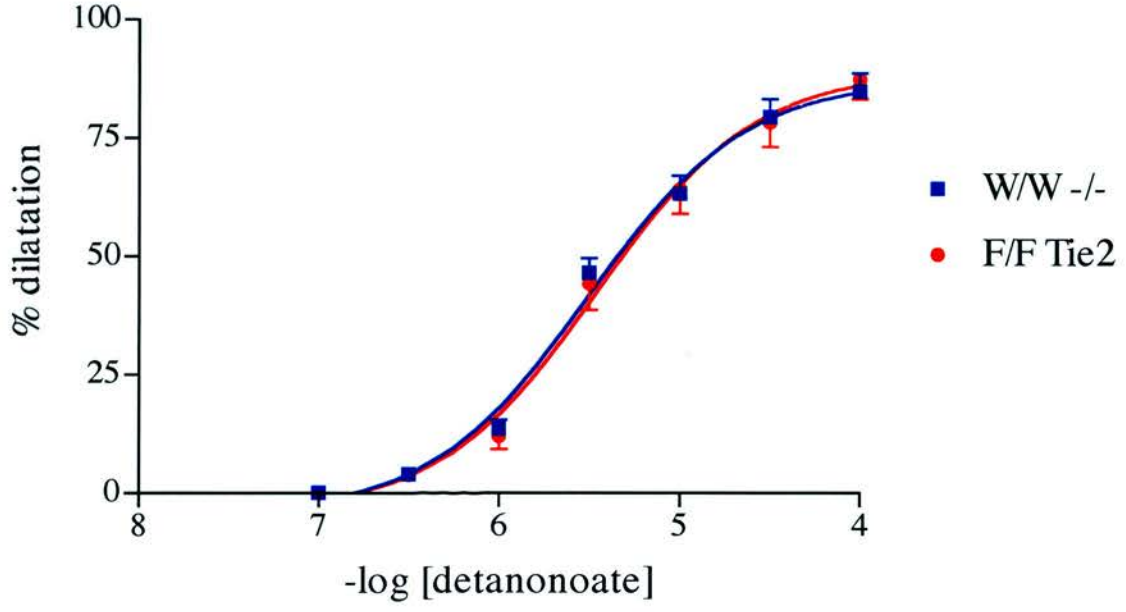

Figure 7.9

Vasodilatation of aortic rings in response to Deta/NO. There was no significant difference in endothelium-independent vasodilatation between aortae of wild type and Flox/Flox Tie2 mice ($LogEC_{50}$ ± SEM: Flox/Flox Tie2 5.46 ± 0.09; W/W -/- 5.51 ± 0.07; n = 6 in each group; $p>0.05$).

7.1.3.6 *Aortic vasoconstriction to NE following inhibition of NOS*

NE-induced contraction of aortic rings was increased following inhibition of NOS with L-NAME in W/W -/- ($p<0.001$) and Flox/Flox Tie2 ($p<0.01$) mice. Contraction following L-NAME was increased to a greater extent in W/W -/- aortic rings compared to Flox/Flox Tie2 aortic rings ($logEC_{50}$ ± SEM; W/W -/-, 7.15 ± 0.15; W/W -/- with L-NAME, 8.15 ± 0.06; Flox/Flox Tie2, 7.47 ± 0.06; Flox/Flox Tie2 with L-NAME, 7.87 ± 0.07; n = 6 in each group). These results are illustrated in Figure 7.10 and Figure 7.11, respectively.

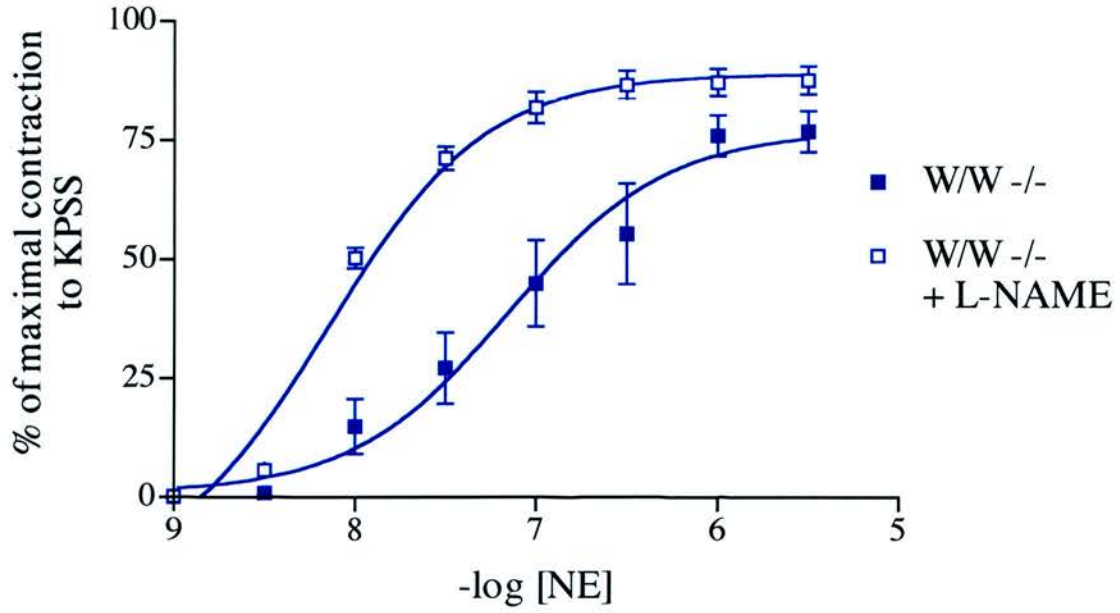

Figure 7.10

Contraction of aortic rings in response to NE following incubation with L-NAME (10^{-4}M) was significantly increased compared to incubation with vehicle ($LogEC_{50}$ ± SEM; W/W -/- 7.15 ± 0.15; W/W -/- with L-NAME 8.15 ± 0.06; n = 6 in each group; $p<0.001$).

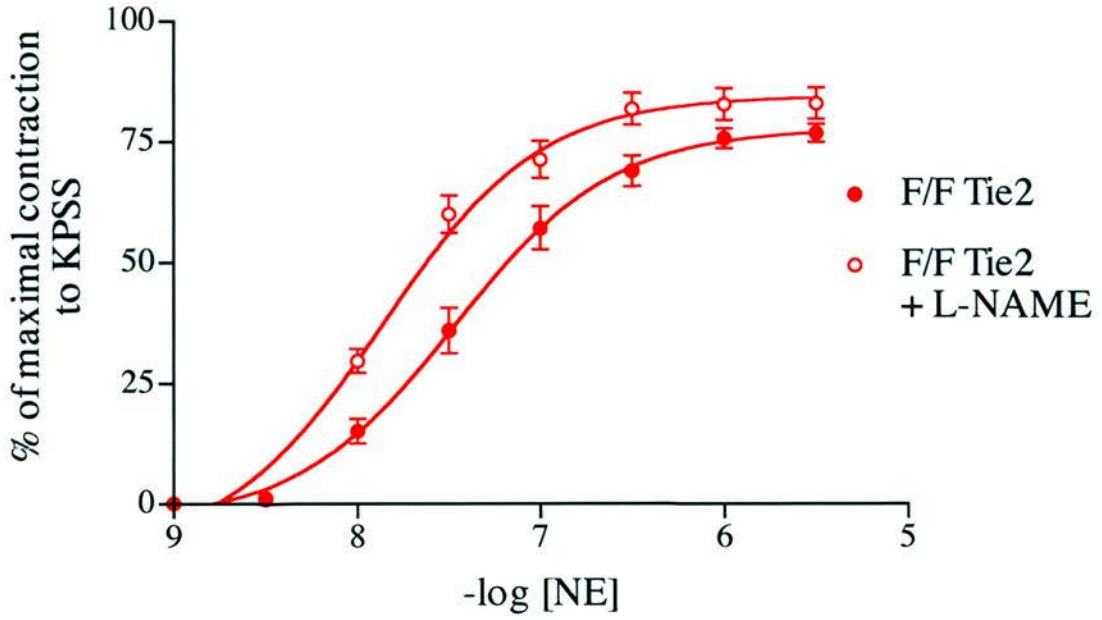

Figure 7.11

Contraction of aortic rings in response to NE following incubation with L-NAME (10^{-4}M) was significantly increased compared to incubation with vehicle ($LogEC_{50}$ ± SEM; Flox/Flox Tie2 7.47 ± 0.06; Flox/Flox Tie2 with L-NAME 7.87 ± 0.07; n = 6 in each group; $p<0.05$).

7.1.3.7 *Aortic vasodilatation to S6c*

The vasodilator response to 10^{-7}M S6c was significantly attenuated in Flox/Flox Tie2 mice compared to W/W -/-, W/W Tie2 and Flox/Flox -/- littermates (mean % dilatation ± SEM; Flox/Flox Tie2, 6.38 ± 1.78; W/W -/-, 16.69 ± 1.30; W/W Tie2, 20.42 ± 3.77; Flox/Flox -/-, 16.73 ± 2.81; $p<0.05$, n = 10 in each group). Following incubation with A192621, aortic rings from control animals demonstrated no significant differences in S6c-induced vasodilatation compared to Flox/Flox Tie2 aortic rings incubated with vehicle (W/W -/- with A192621, 5.69 ± 3.17; W/W Tie2 with A192621, 3.17 ± 3.30; Flox/Flox -/- with A192621, 4.44 ± 2.49; $p>0.05$, n = 10 in each group). Prior incubation with A192621 significantly inhibited the vasodilator response of W/W -/-, W/W Tie2

and Flox/Flox -/- vessels (p <0.05), but not Flox/Flox Tie2 vessels (Flox/Flox Tie2 with A192621 13.78 ± 2.89; p >0.05). These results are illustrated in Figure 7.12.

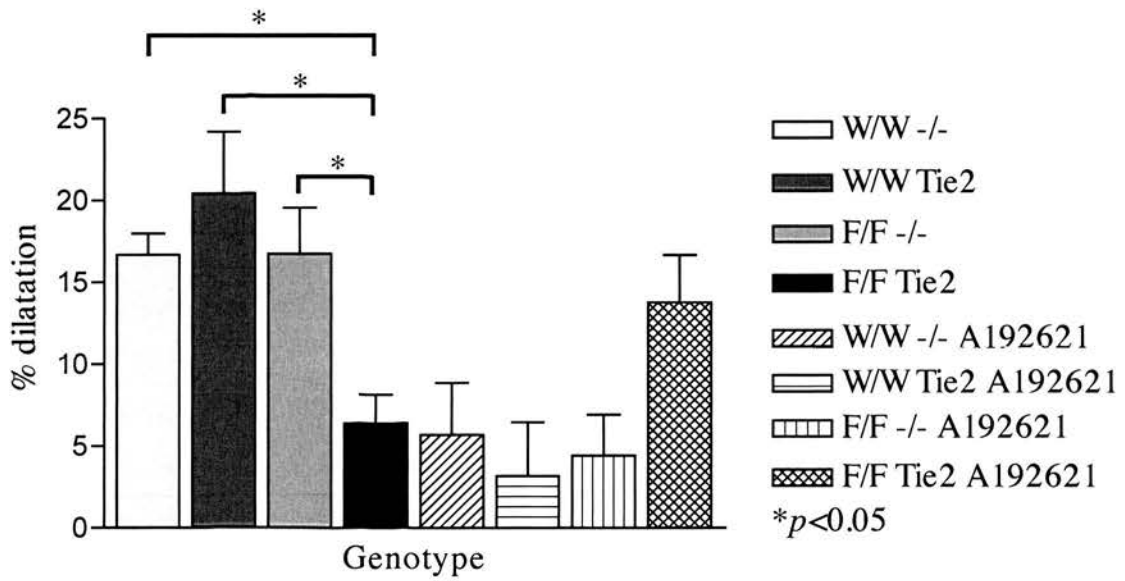

Figure 7.12

In vitro S6c-induced vasodilatation of aortic rings. Dilatation in response to S6c (as a percentage of NE_{80}) was significantly impaired in aortae from Flox/Flox Tie2 mice (mean % dilatation ± SEM; Flox/Flox Tie2, 6.38 ± 1.78; W/W -/-, 16.69 ± 1.30; W/W Tie2, 20.42 ± 3.77; Flox/Flox -/-, 16.73 ± 2.81; p<0.05, n = 10 in each group). Following incubation with the selective ET_B receptor antagonist A192621, S6c-induced vasodilatation of aortae from W/W -/-, W/W Tie2 and Flox/Flox -/- mice did not differ significantly from untreated Flox/Flox Tie2 aortae (W/W -/- with A192621, 5.69 ± 3.17; W/W Tie2 with A192621, 3.17 ± 3.30; Flox/Flox -/- with A192621, 4.44 ± 2.49; p > 0.05; n = 10 in each group).

7.1.3.8 *Tracheal constriction to S6c*

With the exception of piebald mice, tracheal rings isolated from each genotype of mice demonstrated dose dependent contraction in response to S6c (illustrated in Figure 7.13). There was no significant difference in the response of Flox/Flox Tie2 tracheas compared to tracheas isolated from W/W -/- or W/W Tie2 mice (E_{Max} ± SEM; W/W -/-, 20.07 ± 2.88; W/W Tie2, 15.73 ± 2.05; Flox/Flox -/-, 10.67 ± 2.17; Flox/Flox Tie2, 18.74 ± 2.24; $LogEC_{50}$ ± SEM; W/W -/-, 9.54 ± 0.42; W/W Tie2, 9.10 ± 0.30; Flox/Flox -/-, 9.23 ± 0.47; Flox/Flox Tie2, 9.22 ± 0.29; $p>0.05$ in all groups; n = 16 in each group). In contrast, tracheas from piebald mice demonstrated no contractile response to S6c (E_{Max} - 0.84 ± 0.44; n = 4). Prior incubation with A192621 significantly attenuated the S6c-induced contractile response of tracheas from all genotypes (E_{Max} in the presence of A192621 ± SEM; W/W -/-, 5.36 ± 1.92; W/W Tie2, 2.95 ± 0.76; Flox/Flox -/-, 0.17 ± 0.49; Flox/Flox Tie2, 3.23 ± 1.25; n = 16 in each group; $p<0.001$).

7.1.3.9 *Tracheal constriction to carbachol*

Maximal carbachol-induced tracheal contraction was significantly impaired in Flox/Flox Tie2 and piebald mice (E_{Max} ± SEM; W/W -/- 190.1 ± 7.90; W/W Tie2, 192.4 ± 7.88; Flox/Flox -/-, 188.6 ± 5.41; Flox/Flox Tie2, 153.5 ± 3.72; piebald, 146.7 ± 8.26. ($p<0.005$; n = 16 in all groups except piebald (n = 8). These results are illustrated in Figure 7.14.

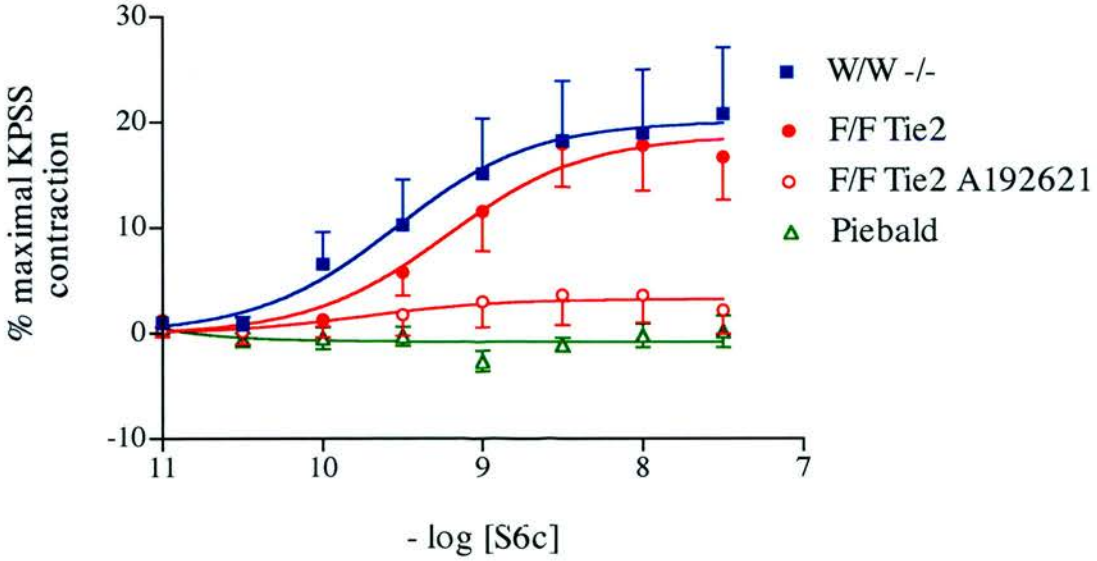

Figure 7.13

In vitro S6c-induced constriction of tracheal rings. S6c-induced tracheal constriction in Flox/Flox Tie2 mice did not differ significantly from W/W -/- and W/W Tie2 controls (maximal contraction expressed as % of maximal contraction with KPSS ± SEM; W/W -/-, 20.07 ± 2.88; W/W Tie2, 15.73 ± 2.05; Flox/Flox -/-, 10.67 ± 2.17; Flox/Flox Tie2, 18.74 ± 2.24; n = 16 in each group, $p>0.05$). S6c-induced constriction was significantly impaired in piebald mice and following incubation of tracheal rings from other genotypes with A192621 (piebald, –0.84 ± 0.44; W/W -/- with A192621, 5.36 ± 1.92; W/W Tie2 with A192621, 2.95 ± 0.76; Flox/Flox -/- with A192621, 0.17 ± 0.49; Flox/Flox Tie2 with A192621, 3.23 ± 1.25; $p<0.001$; n = 16 in each group except piebald (n = 4); data not plotted for W/W Tie2 and Flox/Flox -/-).

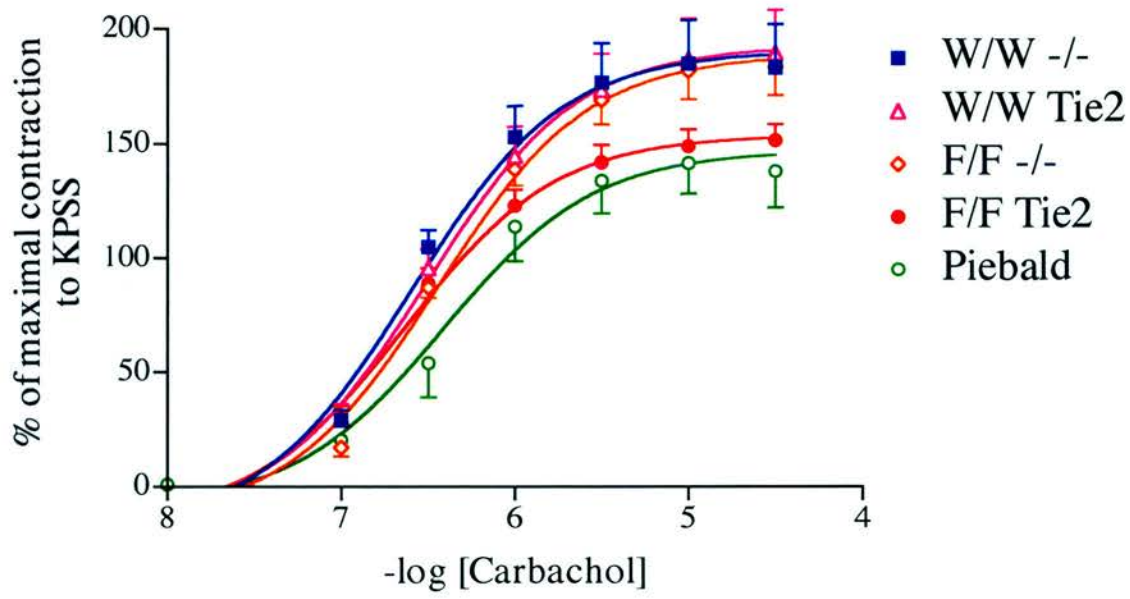

Figure 7.14

In vitro carbachol-induced constriction of tracheal rings. Maximal carbachol-induced tracheal contraction (as percentage of KPSS-induced contraction) was significantly impaired in Flox/Flox Tie2 and piebald mice (E_{Max} ± SEM; W/W -/- 190.1 ± 7.90; W/W Tie2 192.4 ± 7.88; Flox/Flox -/- 188.6 ± 5.41; Flox/Flox Tie2 153.5 ± 3.72; piebald 146.7 ± 8.26; $p < 0.005$; n = 16 in all groups except piebald (n = 8)).

7.1.4 DISCUSSION

I have examined resting blood pressure and the *in vitro* vascular and tracheal responses of mice featuring EC-specific down-regulation of ET_B receptor expression. EC-specific down-regulation of ET_B receptor expression results in hypertension in mice that is unaffected by increasing dietary salt. Previous models of ET_B receptor deficiency (Berthiaume *et al.*, 2000, Gariepy *et al.*, 2000, Murakoshi *et al.*, 2002, Ohuchi *et al.*, 1999) and pharmacological ET_B receptor blockade (Giardina *et al.*, 2001, Pollock, 2001, Pollock and Pollock, 2001, Wessale *et al.*, 2002) also demonstrate hypertension. In each of these models under conditions of normal salt, the increase in blood pressure tends to be relatively modest. The degree of hypertension observed in our EC-specific ET_B

receptor-deficient mice (MAP ~140 mmHg) is similar to that of rats treated with A192621 (MAP ~144 mmHg) (Giardina *et al.*, 2001), but greater than that observed in the rescued ET_B receptor-knockout rat (MAP ~125 mmHg) (Gariepy *et al.*, 2000) and mouse (MAP ~123 mmHg (Murakoshi *et al.*, 2002). When these models were exposed to high salt, blood pressure became further elevated (MAP ~170 mmHg). This response may result from loss of normal ET_B receptor-mediated inhibition of ENaC activity in the distal nephron, with consequent inappropriate reabsorbtion of sodium (Gariepy *et al.*, 2000). The results of my studies suggest that the EC ET_B receptor exerts a tonic hypotensive effect under normal and salt-loaded conditions but that preservation of distal tubular ET_B receptor signalling is protective against salt-induced hypertension. The response of Flox/Flox Tie2 mice to complete ET_B receptor blockade following high salt diet and the effect of addition of ENaC-selective doses of amiloride may now be examined to determine the precise contribution of distal tubular ET_B receptor signalling to salt sensitivity. Using the floxed ET_B receptor mouse developed for this study, distal tubular cell-specific knockout of the ET_B receptor is also now possible through crosses with AQ2Cre transgenic mice (Nelson *et al.*, 1998). Blood pressure under normal salt and high salt conditions in these animals will help to further define the importance of distal tubular ET_B receptors in the response to salt.

A loss of endothelium-dependent ET_B receptor-mediated vasorelaxant pathways may also contribute to salt-sensitive increases in blood pressure. Previous groups have demonstrated that these pathways are upregulated during high salt conditions (Giardina *et al.*, 2001). In my study, blood pressure was slightly increased in Flox/Flox Tie2 mice following a high salt diet. A similar increase was also observed in wild type mice on a high salt diet. It is unclear, therefore, whether the small blood pressure difference represents a non-specific response to high salt or was directly related to loss of EC ET_B receptor-dependent vasorelaxant pathways in Flox/Flox Tie2 mice. Loss of ET_B receptor-dependent vasodilatation may affect blood pressure through alteration of peripheral vascular resistance or through changes in sodium handling within the kidney. ET-1 activates ET_B receptors in the renal medulla increasing medullary blood flow

(Gurbanov *et al.*, 1996) and promoting natriuresis. This effect is mediated via the release of NO (Hoffman *et al.*, 2000) and ET_B receptor-dependent medullary vasodilatation appears to be particularly important under high salt conditions (Pollock *et al.*, 2000, Pollock and Pollock, 2001, Vassileva *et al.*, 2003). Specifically, the medullary ET_B receptor is thought to regulate the relationship between perfusion pressure and natriuresis during high salt conditions (Vassileva *et al.*, 2003). I have demonstrated that EC-specific ET_B receptor down-regulation does not result in significant salt sensitivity. However, whether the pressure-natriuresis-diuresis relationship remains normal following loss of medullary vasa recta EC ET_B receptors is unknown. EC-specific mice also exhibit increased plasma ET-1 concentration. The relative contribution of ET_A receptor-mediated responses to the hypertensive phenotype will provide an interesting avenue of further investigation. Whilst our results suggest that the EC ET_B receptor mediates a tonic hypotensive effect under normal and high salt conditions, measurement of MAP in single transgenic littermates is also required to ensure that the observed blood pressure effect is not due to either the presence of the Tie2Cre transgene or genetic manipulation of the ET_B receptor gene locus itself.

Aortic rings from EC-specific ET_B receptor knockout mice demonstrate impaired vasodilatation in response to S6c. S6c-induced vasodilatation in wild type mice is significantly inhibited by the selective ET_B receptor antagonist A192621, suggesting that this response is ET_B receptor-dependent. Taken together, these results imply the functional absence of vasodilator EC ET_B receptors in Flox/Flox Tie2 mice. Vasodilatation following ET_B receptor activation is likely to be endothelium-dependent and mediated through the generation of NO and/or dilator prostaglandins (Ohuchi *et al.*, 1999) (Giardina *et al.*, 2001). Studies in humans demonstrate that ET_B receptor-mediated vasodilatation in the forearm is dependent upon the release of NO and that inhibition of prostaglandin synthesis has little effect (Verhaar *et al.*, 1998). In the mouse the evidence is less clear. The increase in blood pressure following acute ET_B receptor blockade in wild type mice may be attenuated by pre-treatment with indometacin but not NG-monomethyl-L-arginine (Ohuchi *et al.*, 1999), suggesting that tonic ET_B receptor-

mediated vasodilatation depends upon the release of dilator prostaglandins. ET_B receptor-dependent vascular NO release may also be important, however, since rescued ET_B receptor knockout mice are hypertensive and fail to increase vascular tissue NO_x levels following carotid artery ligation (Murakoshi *et al.*, 2002). The difference in these observations may represent strain-specific differences, or differences between the vascular beds studied. However, the results of my study also suggest that loss of ET_B receptor signaling results in a decrease in NO bioavailability. I examined *in vitro* endothelium-dependent and endothelium-independent vasodilatation in aortic rings and found that Flox/Flox Tie2 mice exhibit impaired ACh-induced vasodilatation compared to wild type littermates. Impaired vasodilatation in response to ACh is a recognised marker of endothelial dysfunction (Haynes and Webb, 1998) and may be secondary to a decrease in EC-derived NO .To examine whether EC-specific ET_B receptor knockout mice have decreased bioavailability of NO as a result of loss of endogenous ET_B receptor signaling, I examined contraction of aortic rings before and following inhibition of NOS with L-NAME. In wild type vessels, inhibition of NO synthesis resulted in a marked potentiation of NE-induced vasoconstriction. In contrast, the increase following NOS inhibition in Flox/Flox Tie2 mice was much smaller, suggesting that in these mice NO contributes to resting vascular tone to a lesser extent. In addition, vasodilatation to ACh was inhibited in wild type vessels following acute pharmacological antagonism of ET_B receptors. This is likely to be a result of EC ET_B receptor blockade since pharmacological ET_B receptor antagonists had no additional effect upon ACh-induced vasodilatation in Flox/Flox Tie2 mice, in which VSMC ET_B receptor signalling is maintained. Endothelium-independent vasodilatation, as assessed by vasodilatation in response to deta/NO, did not, however, differ between wild type and Flox/Flox Tie2 mice. This implies that the sensitivity of VSMC to NO did not differ between genotypes. Taken together, these results suggest that the basal release of NO from the aortic endothelium is decreased as a result of EC-specific ET_B receptor down regulation. The increased blood pressure observed in EC-specific ET_B receptor knockout mice may also have contributed to endothelial dysfunction through non-ET_B receptor-dependent mechanisms. However, Ryan and colleagues (Ryan *et al.*, 2002) recently reported no

correlation between endothelial function and blood pressure in a variety of commonly used experimental mouse strains. Of note in their study was the finding that strains with markedly impaired aortic responses to ACh (e.g. 129X1/SV) were found not to have generalised endothelial dysfunction when vasodilatation to other endothelium-dependent dilators was assessed. Significant differences in ACh response between resistance and conductance vessels within individual strains were also seen. To examine resistance vessel function, I performed pilot studies in mesenteric arterioles at the start of phenotyping but trauma to the endothelium during mounting of these small vessels resulted in marked variation in endothelium-dependent vasodilatation within a single genotype. Hence, the aorta was utilised for all subsequent studies. It is thus currently unclear whether our findings represent generalised endothelial dysfunction, or rather a specific impairment of ACh signalling in the aorta. Such a phenomenon might occur were the ET_B receptors to exert a permissive influence upon muscarinic receptor signalling. Interestingly, I have observed impaired contractile responses of tracheal rings to the cholinergic agonist carbachol in EC-specific and complete (piebald) ET_B receptor knockout mice. The mechanism underlying this response is unclear, but may point to a specific interaction between the ET_B receptor and muscarinic receptors. At present, I cannot discount the possibility that genes that influence muscarinic receptor signalling have not preferentially segregated with the modified ET_B receptor gene. Thus, despite the use of littermates as controls, small differences in genetic background may still have influenced blood pressure and vascular responses.

Several mechanisms may underlie the decrease in NO bioavailability observed following EC-specific ET_B receptor down-regulation. Normally ET-1, via activation of the EC ET_B receptor, induces expression of eNOS protein, eNOS mRNA and production of nitrite species (Zhang *et al.*, 1999). Thus, despite an increase in ET-1 concentration in Flox/Flox Tie2 mice, loss of EC ET_B receptor signalling may result in down-regulation of eNOS expression. This finding has been reported in the pulmonary vasculature of rescued ET_B receptor knockout rats (Ivy *et al.*, 2001). eNOS content was reduced and NO production diminished in this model, with a resultant increase in PAP. A diminished

pool of eNOS may impair the generation of NO via non-ET_B receptor-mediated pathways, producing generalised endothelial dysfunction. I observed impaired ACh-induced vasodilatation following acute pharmacological ET_B receptor antagonism. In the absence of a hypothetical ET_B receptor-dependent permissive effect upon muscarinic receptor activity, this finding might suggest that ET_B receptor-mediated NO release contributes importantly to basal vascular tone irrespective of eNOS protein content. The bioavailability of NO may be also be diminished by an increase in the production of reactive oxygen species (ROS) following ET_B receptor inhibition or down-regulation. Recently, an increase in vascular NADPH oxidase activity has been described in transgenic mice featuring EC-specific overexpression of preproET-1 (Dr E. Schriffrin, Montreal, personal communication). The increase in plasma ET-1 concentration in Flox/Flox Tie2 mice may have similarly upregulated NADPH oxidase activity with a consequent increase in ROS.

Were a decrease in NO bioavailability the cause of the impaired response to ACh, it might have been predicted that NE-induced aortic vasoconstriction would be potentiated in EC-specific ET_B receptor knockouts. I found no difference in the contractile response to NE between Flox/Flox Tie2 and wild type mice prior to inhibition of eNOS with L-NAME. However, the response to NE was decreased in W/W Tie2 mice and, although not statistically significant, there was also a trend towards greater ACh-induced vasodilatation in this genotype. The mechanisms underlying this observation are unclear, but perhaps suggest greater endogenous NO release in W/W Tie2 mice.

The pattern of Cre expression in Tie2-Cre transgenic mice may be used to predict the pattern of ET_B receptor down-regulation in Flox/Flox Tie2 mice. Double transgenic Tie2-Cre CAG-CAT-Z mice only express lacZ following Cre-mediated recombination. Staining patterns in these mice (Kisanuki *et al.*, 2001) suggest limitation of recombination events to ECs and to mesenchymal cells of the atrioventricular canal and proximal cardiac outflow tract (reviewed in section 2.1.3.1). To confirm the tissue-specific pattern of ET_B receptor down-regulation, I performed functional studies in

tracheal rings isolated from Flox/Flox Tie2 mice and littermate controls. Both ET_B and ET_A receptors mediate contractile responses to ET-1 in the mouse trachea (Hay *et al.*, 2001). My results, using the selective ET_B receptor agonist S6c, confirm that the ET_B receptor is an important mediator of tracheal constriction. This response may be completely blocked by the selective ET_B receptor antagonist A192621. S6c-induced tracheal constriction was maintained in Flox/Flox Tie2 mice and was inhibited by A192621, consistent with maintenance of normal expression of ET_B receptors in SMC. In contrast, piebald mice demonstrated no response to S6c, in keeping with previous studies (Hay *et al.*, 2001). ET-3 has been shown to elicit a bi-phasic contractile response in tracheal preparations. The initial phase is mediated via ET_B receptors and is followed by a second, ET_A receptor-mediated phase (Hay *et al.*, 2001). The absence of S6c-induced tracheal contraction in piebald mice further demonstrates that S6c is a selective agonist of the ET_B receptor in the trachea. Thus, I did not utilise selective ET_A receptor selective antagonists during our studies of tracheal responses.

I measured blood pressure under conscious unrestrained conditions via an in-dwelling carotid arterial cannula. This method permits the chronic direct measurement of systolic, diastolic and mean blood pressure and heart rate without the confounding cardio-depressant influence of most commonly used anaesthetic agents (Davisson *et al.*, 1998). I performed blood pressure measurement on days 2 and 3 following surgery. Problems with maintaining patency of the carotid cannulae for periods of greater than 5 days, despite daily flushing with heparin, precluded more prolonged recovery periods. Implantable telemetry devices for blood pressure measurement are now generally regarded as the 'gold standard' method for *in vivo* blood pressure monitoring and can provide recordings for up to 60 days (Butz and Davisson, 2001, Carlson and Wyss, 2000). These devices have demonstrated that restoration of normal circadian rhythm and normalisation of blood pressure and heart rate following surgery can require 5-7 days (Butz and Davisson, 2001). I observed no significant changes in blood pressure from days 1 to 5 in a limited sub-group of our mice, but I cannot discount that a further fall in blood pressure may occur at a later time point. The technique of carotid arterial

cannulation has several limitations. In common with all surgical procedures, there is an immediate associated mortality and morbidity, predominantly consisting of haemorrhage, cerebral infarction and post-operative infection. This is largely dependent upon the skill of the surgeon and in our hands was <10% of operated animals. However, late surgical complications were also apparent. These consisted of cerebral ischaemia/infarction during flushing of the cannula with heparinised saline and late blockage of the cannulae. Overall, around 40% of animals initially operated upon did not yield data. To overcome the limitations of this methodology, future studies might adopt the use of implantable telemetric devices for measurements of blood pressure using a modified technique in which the pressure-sensing catheter is located in the thoracic rather than the abdominal aorta (Butz and Davisson, 2001). Alternative methods for the *in vivo* measurement of systolic blood pressure include tail cuff plethysmography. However, this method requires extensive training, heating and restraint and, although well established in the rat, the small diameter of the mouse tail and the significant stress response associated with measurements, results in large variations in the observed pressure within groups. This method might, therefore, also be considered too insensitive to detect small but significant differences between experimental groups.

In summary, this chapter has described the effects upon blood pressure and *in vitro* vascular function of EC-specific ET_B receptor knockout mice. These mice demonstrate hypertension that is unaffected by dietary salt, suggesting that the EC ET_B receptor exerts a tonic hypotensive effect in the mouse and that salt-sensitivity is determined by IMCD ET_B receptors. Additionally, I noted impaired aortic vasodilatation to ACh and evidence to suggest a decrease in NO bioavailability following EC ET_B receptor downregulation. Finally, ET_B receptor-mediated tracheal constriction in these animals was preserved, consistent with EC-specific knockout of ET_B receptor expression.

8 Chapter 8

8.1 CONCLUSIONS

The endothelin system is a key regulator of cardiovascular homeostasis and plays an important role in the pathogenesis of hypertension (Cardillo *et al.*, 1999, Schiffrin, 1999) and cardiac failure (Krum *et al.*, 2001, Luscher *et al.*, 2002). However, despite initial promise as novel therapeutic agents, endothelin antagonists have not shown significant benefit in most long-term clinical trials in cardiac failure in humans. Although part of this failure may be ascribed to side effects related to the dose of the endothelin antagonist studied, considerable debate still remains over whether non-selective antagonism of endothelin receptors offers significant therapeutic advantages over selective ET_A receptor antagonism. To answer this question requires a more complete understanding of the complex physiological role of the ET_B receptor. The ET_B receptor serves multiple functions in the adult animal, including mediating vasodilatation (Takayanagi *et al.*, 1991), vasoconstriction (Sumner *et al.*, 1992), modulation of sodium reabsorbtion in the distal nephron (Gariepy *et al.*, 2000) and clearance of ET-1 from the circulation (Fukuroda *et al.*, 1994). Each of these functions may independently influence blood pressure and the response to salt loading. Current models of ET_B receptor deficiency and *in vivo* pharmacological studies are unable to differentiate the relative contribution of each of these functions to the complex homeostatic process of blood pressure control, since all ET_B receptors are blocked concurrently in these approaches. Hence, it has not been possible to assess the relative importance of ET_B receptors located on different cell types in the regulation of vessel tone, blood pressure and clearance of ET-1. To address these critical questions, I have developed a mouse model that permits the tissue-specific down-regulation of ET_B receptor expression (Bagnall *et al.*, 2003, Bagnall *et al.*, 2000). The 'floxed' ET_B receptor mouse features loxP sites located in intronic regions flanking exons 2 and 3 of the ET_B receptor gene, permitting cell specific removal of essential coding regions when crossed with mice in which expression of a Cre recombinase transgene is spatially restricted. The phenotypical effects of loss of ET_B

receptor function within an individual cell type, in the context of normal ET_B receptor function in all other cells, can, therefore, be examined. Detailed pharmacological studies of different tissue-specific ET_B receptor knockouts may also be used to permit precise cellular localisation of key regulatory functions and enable definition of the relative importance of ET_B receptor signalling in each cell type. My specific interest lay in understanding the role of the EC ET_B receptor in the control of blood pressure, vascular tone and the clearance of ET-1 from the circulation. In humans, activation of EC ET_B receptors results in the release of NO (Verhaar *et al.*, 1998), with the potentially beneficial cardiovascular effects of vasodilatation and inhibition of platelet aggregation. Preservation of ET_B receptor signalling through the use of selective ET_A receptor antagonists, may, therefore, have advantages over non-selective antagonists. To investigate the relative importance of EC ET_B receptor signalling, I have crossed the 'floxed' ET_B receptor mouse with the Tie2Cre transgenic mouse (Kisanuki *et al.*, 2001) to produce offspring in which ET_B receptor down-regulation is limited to EC and cells of the haematopoietic lineage. This thesis has described the generation of the 'floxed' ET_B receptor mouse and early experiments in the phenotyping of the EC-specific ET_B receptor knockout mouse. I have conducted experiments to confirm down-regulation of EC ET_B receptor expression and maintenance of ET_B receptor function in non-EC. I have examined the effects of EC-specific ET_B receptor knockout upon resting blood pressure under normal and salt-loaded conditions, vascular responses to ET_B receptor agonists, NE, ACh and NO donors, and upon the circulating concentration of ET-1 in the plasma. These findings are summarised below:

8.1.1 GENERATION OF FLOXED ET_B RECEPTOR MICE AND MICE FEATURING ENDOTHELIAL CELL-SPECIFIC ET_B RECEPTOR DOWN-REGULATION

LoxP sites flanking exons 2 and 3 of the ET_B receptor gene were introduced into the ET_B receptor gene locus through gene targeting events in ES cells. The targeting construct was prepared from fragments of the ET_B receptor genome isolated from a λ phage

129/SV mouse genomic library, combined with selection cassettes encoding for neomycin resistance, thymidine kinase and diphtheria toxin genes. Targeting events within the ET_B receptor locus were identified by selection with neomycin and screening by PCR and southern blotting used to detect homologous recombination events. The neomycin/thymidine kinase selection cassette was subsequently removed by initiation of a recombination reaction between loxP sites flanking the cassette. Clones underwent further selection with gancyclovir to remove clones retaining the thymidine kinase gene, followed by a second round of screening by PCR, and then were extensively sequenced prior to injection into blastocysts. Germline transmission of the targeted locus was achieved in a single clone (3B3 (2B5)) and the offspring of this mouse were intercrossed to produce mice homozygous for the floxed ET_B receptor allele. Floxed ET_B receptor mice were of normal appearance, birth weight and longevity, consistent with maintenance of functional ET_B receptor expression during embryogenesis (Gariepy *et al.*, 1996). The genetic background of floxed mice was ~50:50 129/SV:BKW strain.

To generate mice in which the expression of ET_B receptors was down-regulated in EC, 'floxed' ET_B receptor mice were crossed with Tie2Cre transgenic mice (Kisanuki *et al.*, 2001). When tail DNA was screened with PCR primers flanking the ET_B receptor gene, heterozygous Flox/W Tie2/- mice demonstrated bands of 186 bp in addition to the floxed and wild type bands, consistent with recombination events within the ET_B receptor gene locus in a proportion of cells. The recombined allele band was brighter when tail DNA derived from Flox/Flox Tie2 mice was amplified and direct sequencing of this band confirmed the predicted post-recombination sequence of the ET_B receptor gene. The results of previous reporter mouse studies (Constien *et al.*, 2001, Kisanuki *et al.*, 2001) using Tie2Cre transgenic mice suggest that these recombination events were present in the EC of the tail vasculature and I confirmed decreased ET_B receptor-mediated binding in EC (described in section 8.1.3). Mice featuring complete knockout of the ET_B receptor demonstrated only the recombined allele band.

8.1.2 RECOMBINATION-MEDIATED REMOVAL OF EXONS 2 AND 3 OF THE ET_B RECEPTOR GENE IS SUFFICIENT TO PREVENT EXPRESSION OF FUNCTIONAL ET_B RECEPTORS

Mice featuring gene knockouts that retain coding sequences within the targeted region have the potential for continued expression of truncated or mutated proteins. Such proteins may themselves be functional or assume transdominant interactions with other proteins, resulting in unexpected phenotypical outcomes (reviewed by (Muller, 1999). To investigate whether recombination between loxP sites flanking exons 2 and 3 of the ET_B receptor gene was sufficient to prevent expression of functional ET_B receptors, I utilised the then unexpected phenomenon of germ cell recombination. Consistent with the recent findings of other groups (Constien *et al.*, 2001, Koni *et al.*, 2001), I have noted germline recombination events in certain, but not all, female mice featuring the Tie2 Cre transgene and a floxed allele. Through intercross of offspring heterozygous for the recombined allele, I generated mice of piebald appearance that die shortly after weaning from aganglionic megacolon. PCR analysis of tail tip DNA from these animals demonstrated only the recombined allele. The phenotype of these mice was identical to that of the complete knockout (Gariepy *et al.*, 1996), demonstrating that exons 2 and 3 are necessary for the expression of functional ET_B receptors. Functional absence of ET_B receptors in piebald mice was confirmed in tracheal rings, which, in contrast to control and EC-specific ET_B receptor knockout mice, demonstrated loss of normal ET_B receptor-mediated contraction. A lack of ET_B receptor-mediated tracheal contraction in piebald mice has previously been demonstrated by other groups (Hay *et al.*, 2001). Recently, the requirement for exons 2 and 3 for the expression of functional ET_B receptors has been further demonstrated in a separate model. Mice featuring a spontaneous deletion of 318 nucleotides within this region develop aganglionic megacolon, abnormal pigmentation and deafness (Matsushima *et al.*, 2002). This phenotypical pattern is similar to that of the human Waardenburg syndrome type 4 in which mutations of the ET_B receptor gene have been described. Taken together, these data confirm that my strategy for the

recombination-mediated excision of exons 2 and 3 of the ET_B receptor gene was an appropriate technique to genetically inhibit functional ET_B receptor expression.

8.1.3 ET-1 BINDING BY PULMONARY EC IS SIGNIFICANTLY DECREASED IN FLOX/FLOX TIE2 MICE

To confirm that the recombined allele observed on genotyping was derived from ECs, ET_B receptor binding and functionality was examined in Flox/Flox Tie2 mice. Isolated populations of pulmonary EC from Flox/Flox Tie2 mice demonstrated significantly reduced ET_B receptor-mediated binding of ^{125}I ET-1. Binding in the presence of the selective ET_A receptor antagonist A147627 was decreased by ~82% in EC and total binding of ET-1 was decreased by ~18%, although this latter figure did not reach significance. These results suggest that down-regulation of ET_B receptors in EC was successfully achieved to an extent comparable to that of other Cre-LoxP knockout models (Orban *et al.*, 1992). However, the actual degree of ET_B receptor down regulation in EC may have been even greater. My results demonstrate that pulmonary EC-enriched populations contain at least some contaminating pulmonary SMC cells. ET_B receptor expression, and hence ^{125}I ET-1 binding, will be preserved such cells, thereby producing an over-estimation of the remaining ET_B receptor expression. The extent of contamination appears to be consistent in both wild type and Flox/Flox Tie2 populations. Other groups have examined expression of ET_B receptors in ET_B receptor-deficient models by direct visualisation following tissue staining with ET_B receptor antibodies (Gariepy *et al.*, 2000), or by RT-PCR of total mRNA from tissues using ET_B receptor-specific primers. Despite attempts with several commercially available ET_B receptor monoclonal antibodies, I have been unable to convincingly demonstrate absence of EC ET_B receptor staining. This is likely to be due to several factors. Firstly, although I have demonstrated that recombination-mediated removal of exons 2 and 3 of the ET_B receptor gene is sufficient to prevent expression of functional ET_B receptors, mutated non-functional ET_B receptors may still be expressed at the cell surface. Such non-functional proteins may still provide epitopes for ET_B receptor antibodies. Secondly,

most ET_B receptors are expressed upon the surface of the cell and hence spatial separation of ET_B receptors expressed upon the cell membranes of EC and adjacent VSMC is extremely difficult. To avoid this problem, our group has generated an ET_B receptor-LacZ 'knock-in' mouse (Adele Gordon, University of Edinburgh, personal communication) that includes a nuclear localisation signal. This mouse will enable precise definition of the cellular location of ET_B receptors found in close proximity to one another, such as in the vasculature and renal medulla (reviewed by (Kotelevtsev and Webb, 2001)). Further methods to co-localise EC staining and ET_B receptor staining might include the use of EC-specific antibodies, such as those to VE-cadherin (CD144), vascular endothelial growth factor and CD146. Alternatively, in-situ hybridisation or electron microscopic autoradiography might also be used to confirm EC-specific ET_B receptor down-regulation. With each of these methodologies, a mosaic pattern of EC ET_B receptor down-regulation may be seen (discussed in 8.2.2). The interpretation of such results must, therefore, also take into account the results of functional studies. The functional studies performed for this thesis are entirely consistent with significant EC-specific down regulation of ET_B receptor expression.

8.1.4 AORTIC VASODILATATION TO ET_B RECEPTOR AGONISTS IS IMPAIRED IN FLOX/FLOX TIE2 MICE

Bolus injection of ET-1 or S6c in the rat typically induces a transient fall in systemic blood pressure that is quickly followed by a sustained increase in blood pressure. The transient period of vasodilatation has been attributed, although not specifically shown, to be secondary to activation of EC ET_B receptors. Loss of this response has been used as a biological assay of inhibition of ET_B receptor function (Gariepy *et al.*, 2000, Wessale *et al.*, 2002). However, unlike most other species, previous studies in the mouse have demonstrated no transient fall in BP following bolus ET-1 injection (D'Orleans-Juste *et al.*, 2002). In order to examine whether ET_B receptor agonists induce vasodilatation in the mouse, I examined the *in vitro* response of aortic rings to S6c. S6c produced a modest vasodilatation of aortic rings from wild type mice that was ET_B receptor-dependent. This response was significantly impaired in Flox/Flox Tie2 mice (6.38% vs.

16.6%) suggesting that EC ET_B receptors mediate this response and that the Flox/Flox Tie2 mouse is a model of EC ET_B receptor deficiency. The mechanisms underlying the difference in response to exogenous endothelin receptor agonists between the rat and mouse are unclear. However, the increase in blood pressure in the mouse following loss of ET_B receptor activity suggests that the ET_B receptor exerts a tonic hypotensive effect. This effect may be obscured when pharmacological doses of agonists are infused.

8.1.5 FUNCTIONAL EXPRESSION OF SMOOTH MUSCLE CELL ET_B RECEPTORS IS MAINTAINED IN FLOX/FLOX TIE2 MICE

EC-specific ET_B receptor knockout mice are of normal coat colour and demonstrate normal growth, development and longevity. These findings are consistent with continued expression of ET_B receptors within epidermal melanocytes and ganglionic neurons. I investigated whether functional expression of ET_B receptors was maintained in other non-EC cell types, such as SMC. Maximal S6c-induced tracheal constriction of Flox/Flox Tie2 mice was not significantly different to that of wild type mice (18.7% vs. 20.1%). S6c-induced responses were completely inhibited by the selective ET_B receptor antagonist A192621, indicating that this response was ET_B receptor-mediated. Taken together, these findings suggest that the Flox/Flox Tie2 mouse maintains expression of functional ET_B receptors in non-EC. However, although the expression level of ET_B receptors in tracheal SMC is sufficient to produce normal responses to S6c, I have not directly assessed whether expression levels are similar to those of wild type mice. Unfortunately, there are no published data available regarding the tracheal responses of heterozygous ET_B receptor knockout mice to inform whether tracheal contraction is impaired. However, vascular responses to ET_B receptor-selective agonists are significantly reduced in heterozygous ET_B receptor knockouts (Berthiaume *et al.*, 1998), suggesting that continued expression from both ET_B receptor alleles is required to maintain normal physiological activity. As previously discussed, the high levels of non-specific binding seen with ET_B receptor antibodies have complicated direct measurement of ET_B receptor protein concentration by western blotting. Thus, currently, this method is unlikely to be of sufficient sensitivity to detect changes in ET_B receptor expression in

non-EC. An alternative approach might be to perform RT-PCR of vascular tissue or to measure ET_B receptor mRNA levels by RNase protection assay following removal of the endothelium. However, PCR screening of isolated non-EC populations to demonstrate the absence of the recombined allele is problematic because of the almost ubiquitous presence of either EC or cells of the haematopoietic lineage in tissue preparations.

8.1.6 ENDOTHELIAL CELL-SPECIFIC ET_B RECEPTOR KNOCKOUT MICE DEMONSTRATE IMPAIRED ACETYLCHOLINE-INDUCED AORTIC VASODILATATION AND DECREASED BIOAVAILABILITY OF NITRIC OXIDE

Enhanced endogenous ET_B-receptor mediated vascular relaxation has been proposed as a possible protective mechanism that prevents hypertension following a high salt diet (Giardina *et al.*, 2001). Previous investigators have demonstrated impaired endothelium-dependent NO-mediated vasodilatation in rats treated for 5 days with a selective ET_B receptor antagonist (Giardina *et al.*, 2001). The degree of endothelial dysfunction was significantly increased in rats additionally fed a high salt diet. Such animals also demonstrated a higher mean arterial pressure than animals treated with either an ET_B receptor antagonist or a high salt diet alone. I investigated whether endothelium-dependent vasodilatation was impaired in EC-specific ET_B receptor knockout mice fed a normal salt diet. Aortic rings from Flox/Flox Tie2 mice demonstrated a significant rightwards shift of the ACh concentration-response curve. The reduced ACh-induced relaxation may be due either to impaired release of vasorelaxant factors from the endothelium or to a decrease in the sensitivity of VSMC to these factors. I used deta/NO to demonstrate that exogenous NO-donor drugs elicit normal endothelium-independent vasodilatation in Flox/Flox Tie2 mice. Taken together, these data indicate that EC-specific ET_B receptor knockout results in impaired endothelium-dependent vasodilatation to ACh. Although this has been demonstrated in the rat following pharmacological ET_B receptor blockade (Giardina *et al.*, 2001), this is the first time that this phenomenon has been described in the mouse. This response may represent

generalised endothelial dysfunction as a result of EC ET_B receptor deficiency or a specific defect of ACh-induced vasodilatation.

Generalised endothelial dysfunction in EC-specific ET_B receptor knockout mice might result from impaired NO bioavailability secondary to loss of normal endogenous EC ET_B receptor signalling. Rescued ET_B receptor deficient rats demonstrate down-regulation of eNOS protein expression and diminished NO production in the lung, with a consequent increase in PAP (Ivy *et al.*, 2001). The ET_B receptor is thus thought to mediate ET-1-induced increases in eNOS expression. Similar down-regulation of eNOS activity may, therefore, occur in the aorta following EC ET_B receptor down-regulation. I examined the contribution of NO-mediated vasodilatation *in vitro* by measuring NE-induced aortic vasoconstriction before and following inhibition of eNOS with L-NAME. In Flox/Flox Tie2 mice, the leftwards shift of the NE concentration response curve following L-NAME was attenuated compared to wild type littermates. This suggests that endogenous bioavailability of NO is decreased following EC ET_B receptor down-regulation. Although this may result from a decrease in eNOS protein and consequent NO production, the decrease in ACh-induced vasodilatation of wild type vessels following acute ET_B receptor antagonism would suggest a mechanism independent of changes in eNOS protein content. Decreased bioavailability of NO might instead result from loss of endogenous ET_B receptor-mediated NO production, or an increase in reactive oxygen species. Mice featuring EC-specific overexpression of a human preproET-1 cDNA transgene have recently been shown to exhibit an increase in the production of reactive oxygen species (Dr E. Schriffrin, Montreal, personal communication). The increased plasma ET-1 concentration in Flox/Flox Tie2 mice may, therefore, have produced a similar effect.

An alternative hypothesis to explain the decrease in ACh-induced vasodilatation is that there is a specific, hitherto unidentified, permissive interaction between vascular ET_B receptors and muscarinic receptors. I have demonstrated impaired carbachol-mediated tracheal vasoconstriction in EC-specific ET_B receptor knockout mice. The mechanisms underlying this response are also unclear but indicate putative evidence of

such an interaction in other tissues. Specific interactions in the lung between cholinergic neurones and ET_B receptor-mediated responses have been noted previously. ET-1 enhances cholinergic nerve-mediated tracheal contraction in the rat through activation of pre-junctional ET_A and ET_B receptors, leading to an increase in ACh release from cholinergic nerve endings (Knott *et al.*, 1996). To further investigate the possibility that loss of EC ET_B receptor signalling modulates ACh-induced responses, I examined ACh-induced vasodilatation following acute ET_B receptor antagonism in wild type mice and in EC-specific knockouts. Acute pharmacological ET_B receptor blockade also produced a rightwards shift of the concentration response curve to ACh in wild type mice but not Flox/Flox Tie2 mice. This suggests that the VSMC ET_B receptor does not influence the vasodilator response to ACh and that, therefore, any permissive interaction is mediated by EC ET_B receptors.

8.1.7 ENDOTHELIAL CELL-SPECIFIC ET_B RECEPTOR KNOCKOUT MICE EXHIBIT HYPERTENSION THAT IS UNAFFECTED BY INCREASING DIETARY SALT

Previous rodent studies have demonstrated the importance of endogenous ET_B receptor signalling in the regulation of blood pressure under normal and high salt conditions (Berthiaume *et al.*, 2000, Gariepy *et al.*, 2000, Giardina *et al.*, 2001, Murakoshi *et al.*, 2002, Ohuchi *et al.*, 1999, Pollock, 2001, Wessale *et al.*, 2002). Collectively, this data suggests that endogenous ET_B receptor activation exerts a hypotensive effect in the rodent and this effect appears to assume greater importance under conditions of salt loading. The ET_B receptor is, therefore, likely to play an important role in the protection against salt-induced increases in blood pressure and ET_B receptor deficiency can be regarded as a single locus cause of severe salt sensitivity (Gariepy *et al.*, 2000). However, the relative contribution and importance of ET_B receptors expressed upon different cell types to both resting blood pressure and blood pressure in the face of high salt has not previously been evaluated. Indeed, this question cannot be easily addressed with any of the previously available *in vivo* models because they each feature concurrent

ET_B receptor blockade in all tissues. I have measured the resting blood pressure of mice featuring EC-specific down-regulation of ET_B receptor expression under normal and salt-loaded conditions. My data suggests that loss of EC ET_B receptor signalling results in hypertension in mice fed a normal salt diet and that the EC ET_B receptor exerts a tonic hypotensive effect. These findings are consistent with previous models of ET_B receptor deficiency (Berthiaume *et al.*, 2000, Gariepy *et al.*, 2000, Murakoshi *et al.*, 2002, Ohuchi *et al.*, 1999) and pharmacological blockade (Giardina *et al.*, 2001, Pollock, 2001, Wessale *et al.*, 2002), and the increase in blood pressure (MAP ~140 mmHg) suggests that EC ET_B receptor activation normally accounts for ~25 mmHg of the resting blood pressure. When earlier models of ET_B receptor deficiency have been exposed to high salt loads, there are further marked increases in blood pressure (MAP ~170 mmHg (Gariepy *et al.*, 2000, Giardina *et al.*, 2001, Pollock and Pollock, 2001)). The novel finding of this study is that preservation of non-EC ET_B receptor expression is protective against salt-induced increases in blood pressure. ET_B receptors located in the IMCD are likely to mediate the protection against salt through tonic inhibition of ENaC activity (Gariepy *et al.*, 2000), suggesting an autocrine ET-1/ET_B receptor signalling mechanism (Kotelevtsev and Webb, 2001) within the renal medulla. This hypothesis may be tested further by treatment of EC ET_B receptor-deficient mice on high salt diet with a selective ET_B receptor antagonist and examining the response of any exaggerated blood pressure increase to treatment with amiloride.

8.1.8 PATHOPHYSIOLOGY OF HYPERTENSION IN ENDOTHELIAL CELL ET_B RECEPTOR-DEFICIENT MICE

Although this study has demonstrated that the EC ET_B receptor contributes significantly to vascular tone and blood pressure, the predominant site at which this occurs has not been identified. Loss of endogenous ET_B receptor-mediated vasodilatation in resistance arterioles may have led to an increase in peripheral vascular resistance. Alternatively, loss of renovascular EC ET_B receptor signalling, particularly within the medulla may also have influenced blood pressure. Regulation of sodium and water excretion by the

kidney directly depends upon blood flow and vascular resistance within the glomeruli and vasa recta found in the cortex and medulla. Loss of ET_B receptors expressed upon EC of the vasa recta may have altered the pressure-natriuresis-diuresis relationship (Vassileva *et al.*, 2003). Thus, subtle changes in ET-1/ET_B natriuretic and diuretic pathways, whilst not producing overt salt sensitive hypertension, may have altered the 'set point' of blood pressure. Perhaps the most important question remaining is the extent to which ET_A receptor activation contributes to the hypertension observed in EC ET_B receptor-deficient mice. The increase in plasma ET-1 may have produced an increase in ET_A receptor signalling with consequent increase in peripheral vascular resistance, both in the peripheral and renal vasculature. In particular, alteration of the balance between ET_A and ET_B receptor signalling in the afferent and efferent glomerular arterioles may have a significant impact upon GFR (discussed in section 8.2.4). The importance of ET_A receptor signalling in previous genetic and pharmacological models of ET_B receptor deficiency remains controversial (Berthiaume *et al.*, 2000, Gariepy *et al.*, 2000, Matsumura *et al.*, 2000, Pollock and Pollock, 2001) (reviewed in section 8.2.3) and the effects upon blood pressure and renal haemodynamics of treatment of Flox/Flox Tie2 mice with selective ET_A receptor antagonists will be an interesting addition to the current debate.

8.1.9 PLASMA ET-1 CONCENTRATION IS INCREASED FOLLOWING DOWN-REGULATION OF ENDOTHELIAL CELL ET_B RECEPTORS

Clearance of ET-1 is mediated by ET_B receptors and occurs predominantly in the lungs and liver (Fukuroda *et al.*, 1994). Each of these organs contains a large population of EC and I wanted to investigate whether this cell type contributed to clearance of ET-1. Flox/Flox Tie2 mice demonstrate a 4-fold increase in plasma ET-1 concentration suggesting that the EC ET_B receptor contributes importantly to this process. However, I have not yet excluded the possibility that the increase in plasma ET-1 concentration is secondary to an increase in the production of ET-1. This could have occurred through loss of feedback mechanisms that might normally follow internalisation of clearance ET_B receptors. This question may be addressed by performing clearance studies using

^{125}I ET-1 in EC-specific knockout mice. Furthermore, I have not investigated the extent to which ET_B receptors on non-EC contribute to the process of clearance. This could be analysed in future cell type-specific ET_B receptor knockout models and in EC-specific knockouts additionally treated with ET_B receptor antagonists. However, the magnitude of increase in ET-1 concentration is comparable to that of rescued ET_B receptor rats (Gariepy *et al.*, 2000) and in models following chronic ET_B receptor antagonism, suggesting that EC may be the predominant cell type mediating clearance.

8.2 LIMITATIONS OF THE CURRENT STUDY

Many of our initial findings now need to be studied in greater detail to explore the underlying mechanisms of the observed phenotype. However, there are a number of limitations to the approach that I have taken and to murine models of cardiovascular disease in general.

8.2.1 GENETIC BACKGROUND

The genetic background of the model in question may have profound effects upon the observed phenotype. Current experience with ES cell isolation and manipulation dictates the use of 129/SV ES cells, since these are the simplest to maintain in an undifferentiated state in cell culture prior to gene targeting. Following production of chimaeric mice, germline transmission of the targeted allele is usually tested by crossing chimaeras with a further pure-bred strain, such as the BKW. Targeted offspring will, therefore, possess a mixed 129/SV and BKW background. In contrast, most transgenic mouse lines are produced on a C57/BL6J background. Intercross of targeted and transgenic lines thus leads to further mixing of genetic background with potentially profound influences upon cardiovascular phenotype (Ryan *et al.*, 2002). To minimise the effect of heterogeneity of genetic background upon the observed phenotype, I utilised single transgenic and wild type mice from the same litters as experimental controls. However, I cannot exclude the possibility that segregation of key genes influencing cardiovascular phenotype may have differed between double transgenic and control

littermates. Breeding of double transgenic mice onto a pure genetic background may be achieved by multiple backcrosses and detailed comparison of the influence of different genetic backgrounds may then be made. The genetic background may also influence the frequency of germline recombination events in female Flox/W Tie2/- mice and hence achievement of purebred background may provide a mechanism for simplification of breeding strategies.

8.2.2 CRE-LOXP APPROACHES TO CONDITIONAL GENE EXPRESSION

Analysis of cell type-specific receptor function is critically dependent upon both the efficiency of recombination events within a cell and the restriction of such events solely to the cell type of interest. Ideally, Cre-mediated recombination occurs in both alleles of the gene of interest, resulting in complete knockout of target gene expression in the desired cell-type. Conversely, expression in all other cells should be unchanged from the wild-type pattern. Leaky or deregulated transcription of the Cre recombinase transgene will result in unwanted recombination events in other cell types. At worst, this may result in lethality, but more commonly will complicate interpretation of the observed phenotypical outcomes. This problem was exemplified in this study by the unexpected finding of germline recombination events in some female mice featuring the Tie2Cre transgene and a floxed allele. Although this may be advantageous for studies in which 100% knockout of targ*et al*lele from EC is desirable and heterozygous knockout in other cells is inconsequential (Constien *et al.*, 2001), in our study it necessitated revision of the original breeding strategy. Because I wished to achieve normal expression of ET_B receptors in non-EC, I undertook breeding that only introduced the Tie2Cre transgene through the male germline and screened all control experimental animals by PCR for the presence of the recombined allele. To further ensure normal expression of ET_B receptors in non-EC, I designed a targeting vector that minimised the loss of intronic elements from the targeted allele. This design decreased the chances of inadvertently removing key gene transcription regulatory elements. I have demonstrated normal functional responses of SMC ET_B receptors within the trachea of EC-specific ET_B receptor knockout mice. However, I have not yet examined ET_B receptor binding in multiple

tissues to ensure that 'leaky' expression of Cre recombinase from adjacent EC has not initiated unwanted recombination events. As new ET_B receptor antibodies become available, it may be possible to more accurately quantify the expression of ET_B receptors in non-EC.

8.2.3 INCREASE IN PLASMA ET-1

EC-specific ET_B receptor knockout mice are hypertensive under conditions of normal and high salt, suggesting that EC ET_B receptors mediate a tonic vasodilator role. However, the contribution of EC ET_B receptors to clearance of ET-1 complicates interpretation of this finding. The increased plasma ET-1 concentration in Flox/Flox Tie2 mice may result in increased signalling through ET_A receptors, with consequent vasoconstriction and increased blood pressure. The importance of increased ET_A receptor signalling in ET_B receptor-deficient models remains contentious. In rescued ET_B receptor-deficient rats fed a high salt diet, acute treatment with a selective ET_A receptor antagonist did not normalise blood pressure, but the fall in blood pressure was greater than that observed in control rats (Gariepy *et al.*, 2000). In contrast, hypertension following selective ET_B receptor antagonism and high salt was completely reversed by 7 days treatment with an ET_A receptor antagonist (Pollock and Pollock, 2001). These different findings may reflect a difference between pharmacological and genetic models of ET_B receptor deficiency, but clearly require further clarification.

Sustained hypertension throughout development and the increase in plasma ET-1 concentration secondary to EC ET_B receptor deficiency may also have altered endothelial function and promoted vascular hypertrophy. Hypertensive models featuring an increase in vascular preproET-1 commonly demonstrate vascular hypertrophy to a greater extent than might be expected for the degree of hypertension (Schiffrin *et al.*, 1995). It is unknown whether increased plasma ET-1 resulting from abnormal clearance produces a similar synergistic effect upon vascular growth. I have not examined whether the aorta or resistance vessels of Flox/Flox Tie2 mice demonstrate significant vascular

hypertrophy or whether tissue preproET-1 levels are increased, but this may have contributed to the impairment of ACh-induced vasodilatation.

8.2.4 EFFECT OF ENDOTHELIAL CELL-SPECIFIC ET_B RECEPTOR DEFICIENCY UPON GLOMERULAR FILTRATION RATE

The kidney plays a central role in cardiovascular homeostasis, specifically in the long-term control of blood pressure. The regulation of sodium and water excretion by the kidney depends directly upon blood flow and vascular resistance within the glomeruli and vasa recta found in the cortex and medulla. In the medulla, ET-1 activates ET_B receptors, increasing medullary blood flow (Gurbanov *et al.*, 1996) and promoting natriuresis. This effect is mediated via the release of NO (Hoffman *et al.*, 2000) and ET_B receptor-dependent medullary vasodilatation appears to be particularly important under high salt conditions (Pollock *et al.*, 2000, Pollock and Pollock, 2001, Vassileva *et al.*, 2003). In the cortex, afferent arteriolar responses are mediated by both ET_A and ET_B receptors, whilst efferent arteriolar constriction is predominantly ET_B receptor-mediated (Endlich *et al.*, 1996). However, although exquisitely sensitive to exogenous ET-1, an endogenous ET_A-mediated vasomotor tone has been difficult to demonstrate in the rodent kidney. Selective ET_A receptor antagonists do not alter renal vascular resistance in normotensive anaesthetised rats (Matsuura *et al.*, 1997, Qiu *et al.*, 1995). In contrast, selective ET_B receptor antagonists decrease RBF and increase RVR by ~20% (Matsuura *et al.*, 1997) and GFR is markedly decreased in ET_B receptor deficient rats. Taken together, this data suggests an overall tonic vasodilator role for glomerular ET_B receptors (Hocher *et al.*, 2001) and that the regulation of renal vascular and glomerular tone may be more dependent upon endogenous activation of ET_B receptors than ET_A receptors. Thus, the balance between vasodilator EC and vasoconstrictor VSMC ET_B receptors within the afferent and efferent arterioles may have influenced the blood pressure of Flox/Flox Tie2 mice through changes in the pressure-natriuresis-diuresis relationship.

8.2.5 COMPENSATORY EFFECTS OF OTHER BLOOD PRESSURE REGULATORY PATHWAYS

The regulation of blood pressure is a complex process involving multiple neurohormonal pathways. Because recombination of the ET_B receptor gene in the target cell occurs during embryogenesis, I cannot exclude the possibility that other blood pressure regulatory mechanisms may have compensated for loss of EC ET_B receptor expression. This may have resulted in a less severe phenotype than perhaps was observed. Alternatively, the hypertension resulting from EC-specific down regulation of ET_B receptor expression during development may have produced pathophysiological changes in, for example, blood vessel structure. This in turn may have adversely altered endothelial function and the response to other vasoactive hormones, exaggerating the observed phenotype through non-ET_B receptor-dependent mechanisms. This criticism may be levelled at all genetic models of hypertension in which there is no temporal regulation of gene inactivation. However, 'floxed' ET_B receptor mice may also be used to examine the effects of loss of all ET_B receptors in the adult mouse without the confounding effects of ET_B receptor down-regulation during development. Adenovirus-mediated delivery of Cre recombinase to 'floxed' mice or inducible expression of Cre transgenes may each be used to down-regulate ET_B receptor expression in the adult animal. Such approaches will offer further insight into the pathophysiology of cardiovascular disease.

8.3 SUMMARY

This thesis has described the generation of the 'floxed' ET_B receptor mouse. Through crosses with tissue specific Cre recombinase expressing transgenic mouse lines, this model permits the selective down-regulation of ET_B receptor expression in the cell type of interest. I have demonstrated EC-specific down-regulation of ET_B receptor expression following intercross of 'floxed' ET_B receptor mice with Tie2-Cre transgenic mice. Binding studies in isolated pulmonary EC demonstrate a significant reduction of ET_B receptor-mediated binding whilst *in vitro* tracheal SMC contraction to ET_B receptor-

selective agonists is maintained. EC-specific ET_B receptor knockout mice are hypertensive on a normal salt diet but do not exhibit salt sensitivity. Plasma ET-1 concentration is increased and *in vitro* aortic vasodilatation to ACh is impaired, probably as a result of decreased bioavailability of NO. These findings suggest that the EC ET_B receptor mediates a tonic hypotensive effect in the mouse and contributes importantly to the process of clearance of ET-1.

The floxed ET_B receptor mouse was conceived with the intention of determining the relative importance of ET_B receptors expressed upon different cell types to the regulation of blood pressure. I have now demonstrated that endogenous EC ET_B receptor activation lowers blood pressure. The organ (kidney vs. peripheral resistance arterioles) in which EC ET_B receptors exert this effect has not yet been determined, but may be investigated using this model and other tissue-specific ET_B receptor knockouts produced from the floxed ET_B receptor mouse. The ET_B receptor is likely to protect against salt-induced changes in blood pressure through 3 major mechanisms: regulation of distal tubular sodium re-absorption by IMCD cells, up-regulation of endothelium-dependent vasorelaxant pathways in resistance arterioles or medullary vasa recta, and by regulation of glomerular and medullary blood flow. The detailed phenotyping of EC-, VSMC- and IMCD-specific ET_B receptor knockouts will allow definition of the importance of each cell type, and their likely interactions, in each of these pathways, permitting further novel insights into the role of the ET_B receptor in cardiovascular physiology and pathophysiology.

9 Bibliography

1. Abassi ZA, Tate JE, Golomb E, Keiser HR. Role of neutral endopeptidase in the metabolism of endothelin. *Hypertension.* 1992;20:89-95.
2. Adachi M, Furuichi Y, Miyamoto C. Identification of a ligand-binding site of the human endothelin-A receptor and specific regions required for ligand selectivity. *Eur J Biochem.* 1994;220:37-43.
3. Adachi M, Hashido K, Trzeciak A, Watanabe T, Furuichi Y, Miyamoto C. Functional domains of human endothelin receptor. *J Cardiovasc Pharmacol.* 1993;22:S121-4.
4. Arai H, Hori S, Aramori I, Ohkubo H, Nakanishi S. Cloning and expression of a cDNA encoding an endothelin receptor. *Nature.* 1990;370:216-8.
5. Arai H, Nakao K, Takaya K, Hosoda K, Ogawa Y, *et al.* The human endothelin-B receptor gene. Structural organization and chromosomal assignment. *J Biol Chem.* 1993;268:3463-70.
6. Araki K, Araki M, Miyazaki J, Vassalli P. Site-specific recombination of a transgene in fertilized eggs by transient expression of Cre recombinase. *Proc Natl Acad Sci U S A.* 1995;92:160-4.
7. Attie T, Till M, Pelet A, Amiel J, Edery P, *et al.* Mutation of the endothelin-receptor B gene in Waardenburg-Hirschsprung disease. *Hum Mol Genet.* 1995;4:2407-9.
8. Auricchio A, Casari G, Staiano A, Ballabio A. Endothelin-B receptor mutations in patients with isolated Hirschsprung disease from a non-inbred population. *Embo J.* 1996;15:1292-300.
9. Bagnall A, Gulliver-Sloan F, Kelland N, Yanagisawa M, Webb DJ, Kotelevtsev Y. Increased plasma endothelin-1 and impaired vasorelaxation in mice featuring endothelial cell-specific knockout of the endothelin B receptor. *American Journal of Hypertension.* 2003;16:22A.
10. Bagnall A, Webb D, Kotelevtsev Y. A transgenic strategy for analysis of the function of the endothelin-B- receptor. *J Cardiovasc Pharmacol.* 2000;36:S90-2.
11. Barnes K, Brown C, Turner AJ. Endothelin-converting enzyme: ultrastructural localization and its recycling from the cell surface. *Hypertension.* 1998;31:3-9.
12. Barnett RL, Ruffini L, Hart D, Mancuso P, Nord EP. Mechanism of endothelin activation of phospholipase A2 in rat renal medullary interstitial cells. *Am J Physiol.* 1994;266:F46-56.
13. Barton M, d'Uscio LV. Hypertension, diabetes mellitus, hypercholesterolemia, and endothelin B receptor-mediated renal nitric oxide release. *Circulation.* 2000;101:E228-9.
14. Barton M, d'Uscio LV, Shaw S, Meyer P, Moreau P, Luscher TF. ET(A) receptor blockade prevents increased tissue endothelin-1, vascular hypertrophy, and endothelial dysfunction in salt-sensitive hypertension. *Hypertension.* 1998;31:499-504.
15. Barton M, Vos I, Shaw S, Boer P, D'Uscio LV, *et al.* Dysfunctional renal nitric oxide synthase as a determinant of salt- sensitive hypertension: mechanisms of renal artery endothelial dysfunction and role of endothelin for vascular hypertrophyandGlomerulosclerosis. *J Am Soc Nephrol.* 2000;11:835-45.

16. Baynash AG, Hosoda K, Giaid A, Richardson JA, Emoto N, *et al.* Interaction of endothelin-3 with endothelin-B receptor is essential for development of epidermal melanocyte and enteric neurons. *Cell.* 1994;79:1277-1285.
17. Benatti L, Fabbrini MS, Patrono C. Regulation of endothelin-1 biosynthesis. *Ann N Y Acad Sci.* 1994;714:109-21.
18. Benton WD, Davis RW. Screening lambdagt recombinant clones by hybridization to single plaques in situ. *Science.* 1977;196:180-2.
19. Berrazueta JR, Bhagat K, Vallance P, MacAllister RJ. Dose- and time-dependency of the dilator effects of the endothelin antagonist, BQ-123, in the human forearm. *Br J Clin Pharmacol.* 1997;44:569-71.
20. Berthiaume N, Yanagisawa M, D'Orleans-Juste P. Contribution of endogenous endothelin-1 and endothelin-A-receptors to the hypertensive state of endothelin-B heterozygous (+/-) knockout mice. *J Cardiovasc Pharmacol.* 2000;36:S72-4.
21. Berthiaume N, Yanagisawa M, Labonte J, D'Orleans-Juste P. Heterozygous knock-out of ET(B) receptors induces BQ-123-sensitive hypertension in the mouse. *Hypertension.* 2000;36:1002-7.
22. Berthiaume N, Yanagisawa M, Yanagisawa H, deWit D, D'Orleans-Juste P. Pharmacology of endothelins in vascular circuits of normal or heterozygous endothelin-A or endothelin-B knockout transgenic mice. *J Cardiovasc Pharmacol.* 1998;31:S561-4.
23. Bitar KN, Stein S, Omann GM. Specific G proteins mediate endothelin induced contraction. *Life Sci.* 1992;50:2119-24.
24. Boarder MR. A role for phospholipase D in control of mitogenesis. *Trends Pharmacol Sci.* 1994;15:57-62.
25. Borck K, Beggs JD, Brammar WJ, Hopkins AS, Murray NE. The construction in vitro of transducing derivatives of phage lambda. *Mol Gen Genet.* 1976;146:199-207.
26. Bradford MM. A rapid and sensitive method for the quantitation of microgram quantities of protein utilizing the principle of protein-dye binding. *Anal Biochem.* 1976;72:248-54.
27. Bradley A. Production of chimaeric mice. In: *Teratocarcinoma and Embryonic Stem Cells: A Practical Approach.* Oxford: IRL Press; 1987:113-52.
28. Bronson SK, Smithies O, Mascarello JT. High incidence of XXY and XYY males among the offspring of female chimeras from embryonic stem cells. *Proc Natl Acad Sci U S A.* 1995;92:3120-3.
29. Brunner F, Doherty AM. Role of ET(B) receptors in local clearance of endothelin-1 in rat heart: studies with the antagonists PD 155080 and BQ-788. *FEBS Lett.* 1996;396:238-42.
30. Bullock WO, Fernandez JM, Short JM. XL1-Blue: A high efficiency plasmid transforming recA *Escherichia coli* strain with beta-galactosidase selection. *BioTechniques.* 1987;5:376.
31. Butz GM, Davisson RL. Long-term telemetric measurement of cardiovascular parameters in awake mice: a physiological genomics tool. *Physiol Genomics.* 2001;5:89-97.
32. Capecchi MR. Altering the genome by homologous recombination. *Science.* 1989;244:1288-92.

33. Cardillo C, Kilcoyne CM, Waclawiw M, Cannon RO, 3rd, Panza JA. Role of endothelin in the increased vascular tone of patients with essential hypertension. *Hypertension.* 1999;33:753-8.
34. Carlson SH, Wyss JM. Long-term telemetric recording of arterial pressure and heart rate in mice fed basal and high NaCl diets. *Hypertension.* 2000;35:E1-5.
35. Carr MJ, Goldie RG, Henry PJ. Influence of respiratory tract viral infection on endothelin-1-induced potentiation of cholinergic nerve-mediated contraction in mouse trachea. *Life Sci.* 1997;61:1529-38.
36. Cheng S, Fockler C, Barnes WM, Higuchi R. Effective amplification of long targets from cloned inserts and human genomic DNA. *Proc Natl Acad Sci U S A.* 1994;91:5695-9.
37. Chomczynski P, Qasba PK. Alkaline transfer of DNA to plastic membrane. *Biochem Biophys Res Commun.* 1984;122:340-4.
38. Chun M, Lin HY, Henis YI, Lodish HF. Endothelin-induced endocytosis of cell surface ETA receptors. Endothelin remains intact and bound to the ETA receptor. *J Lab Clin Med.* 1995;126:559-70.
39. Chung CT, Niemela SL, Miller RH. One-step preparation of competent Escherichia coli: transformation and storage of bacterial cells in the same solution. *Proc Natl Acad Sci U S A.* 1989;86:2172-5.
40. Clavell AL, Stingo AJ, Margulies KB, Brandt RR, Burnett JC, Jr. Role of endothelin receptor subtypes in the in vivo regulation of renal function. *Am J Physiol.* 1995;268:F455-60.
41. Clouthier DE, Hosoda K, Richardson JA, Williams SC, Yanagisawa H, *et al.* Cranial and cardiac neural crest defects in endothelin-A receptor- deficient mice. *Development.* 1998;125:813-24.
42. Constien R, Forde A, Liliensiek B, Grone HJ, Nawroth P, *et al.* Characterization of a novel EGFP reporter mouse to monitor Cre recombination as demonstrated by a Tie2 Cre mouse line. *Genesis.* 2001;30:36-44.
43. Cramer H, Muller-Esterl W, Schroeder C. Subtype-specific endothelin-A and endothelin-B receptor desensitization correlates with differential receptor phosphorylation. *Biochemistry.* 1999;38:1300-9.
44. Cyr CR, Devi LA, Rudy B, Kris RM. Heterologous desensitization of the human endothelin A and neurokinin A receptors in Xenopus laevis oocytes. *J Biol Chem.* 1997;272:17734-43.
45. D'Orleans-Juste P, Labonte J, Bkaily G, Choufani S, Plante M, Honore JC. Function of the endothelin(B) receptor in cardiovascular physiology and pathophysiology. *Pharmacol Ther.* 2002;95:221-38.
46. d'Uscio LV, Moreau P, Shaw S, Takase H, Barton M, Luscher TF. Effects of chronic ETA-receptor blockade in angiotensin II-induced hypertension. *Hypertension.* 1997;29:763-9.
47. Danthuluri NR, Brock TA. Endothelin receptor-coupling mechanisms in vascular smooth muscle: a role for protein kinase C. *J Pharmacol Exp Ther.* 1990;254:393-9.

48. Davenport AP, Kuc RE. Cellular expression of isoforms of endothelin-converting enzyme-1 (ECE- 1c, ECE-1b and ECE-1a) and endothelin-converting enzyme-2. *J Cardiovasc Pharmacol.* 2000;36:S55-7.
49. Davenport AP, Kuc RE. Radioligand binding assays and quantitative autoradiography of endothelin receptors. *Methods Mol Biol.* 2002;206:45-70.
50. Davisson RL, Yang G, Beltz TG, Cassell MD, Johnson AK, Sigmund CD. The brain renin-angiotensin system contributes to the hypertension in mice containing both the human renin and human angiotensinogen transgenes. *Circ Res.* 1998;83:1047-58.
51. De Vriese AS, Van de Voorde J, Lameire NH. Effects of connexin-mimetic peptides on nitric oxide synthase- and cyclooxygenase-independent renal vasodilation. *Kidney Int.* 2002;61:177-85.
52. Dean R, Zhuo J, Alcorn D, Casley D, Mendelsohn FA. Cellular localization of endothelin receptor subtypes in the rat kidney following in vitro labelling. *Clin Exp Pharmacol Physiol.* 1996;23:524-31.
53. Decker ER, Brock TA. Endothelin receptor-signalling mechanisms in vascular smooth muscle. In: Highsmith RF, ed. *Endothelin Molecular Biology, Physiology and Pathology.* Totowa, New Jersey: Humana Press; 1998:93-120.
54. Deng C, Capecchi MR. Reexamination of gene targeting frequency as a function of the extent of homology between the targeting vector and the target locus. *Mol Cell Biol.* 1992;12:3365-71.
55. Dong QG, Bernasconi S, Lostaglio S, De Calmanovici RW, Martin-Padura I, *et al.* A general strategy for isolation of endothelial cells from murine tissues. Characterization of two endothelial cell lines from the murine lung and subcutaneous sponge implants. *Arterioscler Thromb Vasc Biol.* 1997;17:1599-604.
56. Dorfman DM, Wilson DB, Bruns GA, Orkin SH. Human transcription factor GATA-2. Evidence for regulation of preproendothelin-1 gene expression in endothelial cells. *J Biol Chem.* 1992;267:1279-85.
57. Doucet J, Gonzalez W, Michel JB. Endothelin antagonists in salt-dependent hypertension associated with renal insufficiency. *J Cardiovasc Pharmacol.* 1996;27:643-51.
58. Douglas SA. Clinical development of endothelin receptor antagonists. *Trends Pharmacol Sci.* 1997;18:408-12.
59. Douglas SA, Ohlstein EH. Signal transduction mechanisms mediating the vascular actions of endothelin. *J Vasc Res.* 1997;34:152-64.
60. Elledge SJ, Mulligan JT, Ramer SW, Spottswood M, Davis RW. Lambda YES: a multifunctional cDNA expression vector for the isolation of genes by complementation of yeast and Escherichia coli mutations. *Proc Natl Acad Sci U S A.* 1991;88:1731-5.
61. Elshourbagy NA, Korman DR, Wu HL, Sylvester DR, Lee JA, *et al.* Molecular characterization and regulation of the human endothelin receptors. *J Biol Chem.* 1993;268:3873-9.
62. Endlich K, Hoffend J, Steinhausen M. Localization of endothelin ETA and ETB receptor-mediated constriction in the renal microcirculation of rats. *J Physiol (Lond).* 1996;497:211-8.

63. Fan J, Unoki H, Iwasa S, Watanabe T. Role of endothelin-1 in atherosclerosis. *J Hypertens.* 2000;18:1429-36.
64. Feinberg AP, Vogelstein B. A technique for radiolabeling DNA restriction endonuclease fragments to high specific activity. *Anal Biochem.* 1983;132:6-13.
65. Freedman NJ, Ament AS, Oppermann M, Stoffel RH, Exum ST, Lefkowitz RJ. Phosphorylation and desensitization of human endothelin A and B receptors. Evidence for G protein-coupled receptor kinase specificity. *Biochemistry.* 1997;36:13325-32.
66. Fujita K, Matsumura Y, Miyazaki Y, Hashimoto N, Takaoka M, Morimoto S. ETA receptor-mediated role of endothelin in the kidney of DOCA-salt hypertensive rats. *Life Sci.* 1996;58:L1-7.
67. Fujita K, Matsumura Y, Miyazaki Y, Takaoka M, Morimoto S. Role of endothelin-1 in hypertension induced by long-term inhibition of nitric oxide synthase. *Eur J Pharmacol.* 1995;280:311-6.
68. Fukuroda T, Fujikawa T, Ozaki S, Ishikawa K, Yano M, Nishikibe M. Clearance of circulating endothelin-1 by ETB receptors in rats. *Biochem Biophys Res Commun.* 1994;199:1461-5.
69. Gariepy CE, Cass DT, Yanagisawa M. Null mutation of endothelin receptor type B gene in spotting lethal rats causes aganglionic megacolon and white coat color. *Proc Natl Acad Sci U S A.* 1996;93:867 72.
70. Gariepy CE, Ohuchi T, Williams SC, Richardson JA, Yanagisawa M. Salt-sensitive hypertension in endothelin-B receptor-deficient rats. *J Clin Invest.* 2000;105:925-33.
71. Gariepy CE, Williams SC, Richardson JA, Hammer RE, Yanagisawa M. Transgenic expression of the endothelin-B receptor prevents congenital intestinal aganglionosis in a rat model of Hirschsprung disease. *J Clin Invest.* 1998;102:1092-101.
72. Giardina JB, Green GM, Rinewalt AN, Granger JP, Khalil RA. Role of endothelin B receptors in enhancing endothelium-dependent nitric oxide-mediated vascular relaxation during high salt diet. *Hypertension.* 2001;37:516-23.
73. Giller T, Breu V, Valdenaire O, Clozel M. Absence of ET(B)-mediated contraction in Piebald-lethal mice. *Life Sci.* 1997;61:255-63.
74. Gray G. Generation of Endothelin. In: Webb DJ, Gray G, eds. *Molecular Biology and Pharmacology of the Endothelins.* Georgetown, Texas: R.G. Landes Company; 1995:1-173.
75. Gray GA, Mickley EJ, Webb DJ, McEwan PE. Localization and function of ET-1 and ET receptors in small arteries post-myocardial infarction: upregulation of smooth muscle ET(B) receptors that modulate contraction. *Br J Pharmacol.* 2000;130:1735-44.
76. Gu H, Marth JD, Orban PC, Mossmann H, Rajewsky K. Deletion of a DNA polymerase beta gene segment in T cells using cell type-specific gene targeting. *Science.* 1994;265:103-6.
77. Gurbanov K, Rubinstein I, Hoffman A, Abassi Z, Better OS, Winaver J. Differential regulation of renal regional blood flow by endothelin-1. *Am J Physiol.* 1996;271:F1166-72.
78. Harris PJ, Zhuo J, Mendelsohn FA, Skinner SL. Haemodynamic and renal tubular effects of low doses of endothelin in anaesthetized rats. *J Physiol (Lond).* 1991;433:25-39.

79. Hasegawa H, Hiki K, Sawamura T, Aoyama T, Okamoto Y, *et al.* Purification of a novel endothelin-converting enzyme specific for big endothelin-3. *Circulation.* 1999;99:292-8.
80. Hashimoto N, Kuro T, Fujita K, Azuma S, Matsumura Y. Endothelin ET(B) receptor-mediated action on systemic and renal hemodynamics and urine formation in deoxycorticosterone acetate-salt- induced hypertensive rats. *Biol Pharm Bull.* 1998;21:800-4.
81. Hay DW, Douglas SA, Ao Z, Moesker RM, Self GJ, *et al.* Differential modulation of endothelin ligand-induced contraction in isolated tracheae from endothelin B (ET(B)) receptor knockout mice. *Br J Pharmacol.* 2001;132:1905-15.
82. Haynes WG, Webb DJ. Contribution of endogenous generation of endothelin-1 to basal vascular tone. *Lancet.* 1994;344:852-4.
83. Haynes WG, Webb DJ. Endothelin as a regulator of cardiovascular function in health and disease. *J Hypertens.* 1998;16:1081-98.
84. Henry PJ. Endothelin-1 (ET-1)-induced contraction in rat isolated trachea: involvement of ETA and ETB receptors and multiple signal transduction systems. *Br J Pharmacol.* 1993;110:435-41.
85. Hirata Y, Takagi Y, Fukuda Y, Marumo F. Endothelin is a potent mitogen for rat vascular smooth muscle cells. *Atherosclerosis.* 1989;78:225-8.
86. Hirata Y, Yoshimi H, Takaichi S, Yanagisawa M, Masaki T. Binding and receptor down-regulation of a novel vasoconstrictor endothelin in cultured rat vascular smooth muscle cells. *FEBS Lett.* 1988;239:13-7.
87. Hocher B, Dembowski C, Slowinski T, Friese ST, Schwarz A, *et al.* Impaired sodium excretion, decreased glomerular filtration rate and elevated blood pressure in endothelin receptor type B deficient rats. *J Mol Med.* 2001;78:633-41.
88. Hocher B, Liefeldt L, Thone-Reineke C, Orzechowski HD, Distler A, *et al.* Characterization of the renal phenotype of transgenic rats expressing the human endothelin-2 gene. *Hypertension.* 1996;28:196-201.
89. Hocher B, Rohmeiss P, Thone-Reineke C, Schwarz A, Burst V, *et al.* Apoptosis in kidneys of endothelin-1 transgenic mice. *J Cardiovasc Pharmacol.* 1998;31:S554-6.
90. Hocher B, Rohmeiss P, Zart R, Diekmann F, Vogt V, *et al.* Significance of endothelin receptor subtypes in the kidneys of spontaneously hypertensive rats: renal and hemodynamic effects of endothelin receptor antagonists. *J Cardiovasc Pharmacol.* 1995;26:S470-2.
91. Hocher B, Thone-Reineke C, Rohmeiss P, Schmager F, Slowinski T, *et al.* Endothelin-1 transgenic mice develop glomerulosclerosis, interstitial fibrosis, and renal cysts but not hypertension. *J Clin Invest.* 1997;99:1380-9.
92. Hoffman A, Abassi ZA, Brodsky S, Ramadan R, Winaver J. Mechanisms of big endothelin-1-induced diuresis and natriuresis : role of ET(B) receptors. *Hypertension.* 2000;35:732-9.
93. Hori S, Komatsu Y, Shigemoto R, Mizuno N, Nakanishi S. Distinct tissue distribution and cellular localization of two messenger ribonucleic acids encoding different subtypes of rat endothelin receptors. *Endocrinology.* 1992;130:1885-95.

94. Horstmann A, Menzel L, Gabler R, Jentsch A, Urban W, Lehmann J. Release of nitric oxide from novel diazeniumdiolates monitored by laser magnetic resonance spectroscopy. *Nitric Oxide.* 2002;6:135-41.
95. Horstmeyer A, Cramer H, Sauer T, Muller-Esterl W, Schroeder C. Palmitoylation of endothelin receptor A. Differential modulation of signal transduction activity by post-translational modification. *J Biol Chem.* 1996;271:20811-9.
96. Hosoda K, Hammer RE, Richardson JA, Baynash AG, Cheung JC, *et al.* Targeted and natural (piebald-lethal) mutations of endothelin-B receptor gene produce megacolon associated with spotted coat color in mice. *Cell.* 1994;79:1267-76.
97. Hosoda K, Hammer RE, Richardson JA, Baynash AG, Cheung JC, *et al.* Targetted and natural (piebald-lethal) mutations of endothelin-B receptor gene produce megacolon associated with spotted coat colour in mice. *Cell.* 1994;79:1267-1276.
98. Hosoda K, Nakao K, Hiroshi A, Suga S, Ogawa Y, *et al.* Cloning and expression of human endothelin-1 receptor cDNA. *FEBS Lett.* 1991;287:23-6.
99. Hosoda K, Nakao K, Tamura N, Arai H, Ogawa Y, *et al.* Organization, structure, chromosomal assignment, and expression of the gene encoding the human endothelin-A receptor. *J Biol Chem.* 1992;267:18797-804.
100. Inoue A, Yanagisawa M, Kimura S, Kasuya Y, Miyauchi T, *et al.* The human endothelin family: three structurally and pharmacologically distinct isopeptides predicted by three separate genes. *Proc Natl Acad Sci U S A.* 1989;86:2863-7.
101. Inoue A, Yanagisawa M, Takuwa Y, Mitsui Y, Kobayashi M, Masaki T. The human preproendothelin-1 gene. Complete nucleotide sequence and regulation of expression. *J Biol Chem.* 1989;264:14954-9.
102. Intengan HD, He G, Schiffrin EL. Effect of vasopressin antagonism on structure and mechanics of small arteries and vascular expression of endothelin-1 in deoxycorticosterone acetate salt hypertensive rats. *J Hypertens.* 1998;16:1907-12.
103. Intengan HD, Park JB, Schiffrin EL. Blood pressure and small arteries in DOCA-salt-treated genetically AVP- deficient rats: role of endothelin. *Hypertension.* 1998;32:770-7.
104. Ishibashi KI, Imamura T, Sharma PM, Huang J, Ugi S, Olefsky JM. Chronic endothelin-1 treatment leads to heterologous desensitization of insulin signaling in 3T3-L1 adipocytes. *J Clin Invest.* 2001;107:1193-202.
105. Ishikawa K, Ihara M, Noguchi K, Mase T, Mino N, *et al.* Biochemical and pharmacological profile of a potent and selective endothelin B-receptor antagonist, BQ-788. *Proc Natl Acad Sci U S A.* 1994;91:4892-6.
106. Ivy D, McMurtry IF, Yanagisawa M, Gariepy CE, Le Cras TD, *et al.* Endothelin B receptor deficiency potentiates ET-1 and hypoxic pulmonary vasoconstriction. *Am J Physiol Lung Cell Mol Physiol.* 2001;280:L1040-8.
107. James AF, Xie L-H, Fujitani Y, Hayashi S, Horie M. Inhibition of the cardiac protein kinase A-dependent chloride conductance by endothelin-1. *Nature.* 1994;370:297-300.
108. Jougasaki M, Schirger JA, Simari RD, Burnett JC, Jr. Autocrine role for the endothelin-B receptor in the secretion of adrenomedullin. *J Hypertens Suppl.* 1999;17:S37-43.

109. Karne S, Jayawickreme CK, Lerner MR. Cloning and characterization of an endothelin-3 specific receptor (ETC receptor) from Xenopus laevis dermal melanophores. *Shock.* 1994;1:184-7.
110. King AJ, Brenner BM, Anderson S. Endothelin: a potent renal and systemic vasoconstrictor peptide. *Am J Physiol.* 1989;256:F1051-8.
111. Kisanuki YY, Hammer RE, Miyazaki J, Williams SC, Richardson JA, Yanagisawa M. Tie2-Cre transgenic mice: a new model for endothelial cell-lineage analysis in vivo. *Dev Biol.* 2001;230:230-42.
112. Kitamura K, Tanaka T, Kato J, Ogawa T, Eto T, Tanaka K. Immunoreactive endothelin in rat kidney inner medulla: marked decrease in spontaneously hypertensive rats. *Eur J Pharmacol.* 1993;250:447-53.
113. Klenow H, Henningsen I. Selective elimination of the exonuclease activity of the deoxyribonucleic acid polymerase from Escherichia coli B by limited proteolysis. *Proc Natl Acad Sci U S A.* 1970;65:168-75.
114. Knott PG, Fernandes LB, Henry PJ, Goldie RG. Influence of endothelin-1 on cholinergic nerve-mediated contractions and acetylcholine release in rat isolated tracheal smooth muscle. *J Pharmacol Exp Ther.* 1996;279:1142-7.
115. Kobayshi T, Miyauchi T, Sakai S, Maeda S, Yamaguchi I, *et al.* Down-regulation of ET(B) receptor, but not ET(A) receptor, in congestive lung secondary to heart failure. Are marked increases in circulating endothelin-1 partly attributable to decreases in lung ET(B) receptor-mediated clearance of endothelin-1? *Life Sci.* 1998;62:185-93.
116. Kohan DE. Endothelins: renal tubule synthesis and actions. *Clin Exp Pharmacol Physiol.* 1996;23:337-44.
117. Kohan DE. Endothelins in the normal and diseased kidney. *Am J Kidney Dis.* 1997;29:2-26.
118. Kohan DE, Fiedorek FT, Jr. Endothelin synthesis by rat inner medullary collecting duct cells. *J Am Soc Nephrol.* 1991;2:150-5.
119. Kohan DE, Hughes AK. Autocrine role of endothelin in rat IMCD: inhibition of AVP-induced cAMP accumulation. *Am J Physiol.* 1993;265:F670-6.
120. Kohan DE, Hughes AK, Perkins SL. Characterization of endothelin receptors in the inner medullary collecting duct of the rat. *J Biol Chem.* 1992;267:12336-40.
121. Kohan DE, Padilla E. Endothelin-1 is an autocrine factor in rat inner medullary collecting ducts. *Am J Physiol.* 1992;263:F607-12.
122. Koni PA, Joshi SK, Temann UA, Olson D, Burkly L, Flavell RA. Conditional vascular cell adhesion molecule 1 deletion in mice: impaired lymphocyte migration to bone marrow. *J Exp Med.* 2001;193:741-54.
123. Kotelevtsev Y, Webb DJ. Endothelin as a natriuretic hormone: the case for a paracrine action mediated by nitric oxide. *Cardiovasc Res.* 2001;51:481-8.
124. Kotelevtsev Y, Webb DJ. Endothelin as a natriuretic hormone: the case for a paracrine action mediated by nitric oxide. *Cardiovasc Res.* 2001;51:481-8.
125. Krum H, Denver R, Tzanidis A, Martin P. Diagnostic and therapeutic potential of the endothelin system in patients with chronic heart failure. *Heart Fail Rev.* 2001;6:341-52.

126. Krum H, Viskoper RJ, Lacourciere Y, Budde M, Charlon V. The effect of an endothelin-receptor antagonist, bosentan, on blood pressure in patients with essential hypertension. Bosentan Hypertension Investigators. *N Engl J Med.* 1998;338:784-90.
127. Kumar C, Mwangi V, Nuthulaganti P, Wu HL, Pullen M, *et al.* Cloning and characterization of a novel endothelin receptor from Xenopus heart. *J Med Chem.* 1994;37:1553-7.
128. Kurihara Y, Kurihara H, Suzuki H, Kodama T, Maemura K, *et al.* Elevated blood pressure and craniofacial abnormalities in mice deficient in endothelin-1. *Nature.* 1994;368:703-10.
129. Kuwaki T, Cao WH, Kurihara Y, Kurihara H, Ling GY, *et al.* Impaired ventilatory responses to hypoxia and hypercapnia in mutant mice deficient in endothelin-1. *Am J Physiol.* 1996;270:R1279-86.
130. Ladoux A, Frelin C. Endothelins inhibit adenylate cyclase in brain capillary endothelial cells. *Biochem Biophys Res Commun.* 1991;180:169-73.
131. Laird PW, Zijderveld A, Linders K, Rudnicki MA, Jaenisch R, Berns A. Simplified mammalian DNA isolation procedure. *Nucleic Acids Res.* 1991;19:4293.
132. Lariviere R, Thibault G, Schiffrin EL. Increased endothelin-1 content in blood vessels of deoxycorticosterone acetate-salt hypertensive but not in spontaneously hypertensive rats. *Hypertension.* 1993;21:294-300.
133. Le Monnier de Gouville AC, Lippton H, Cohen G, Cavero I, Hyman A. Vasodilator activity of endothelin-1 and endothelin-3: rapid development of cross-tachyphylaxis and dependence on the rate of endothelin administration. *J Pharmacol Exp Ther.* 1990;254:1024-8.
134. Lewandoski M. Mouse genomic technologiesconditional control of gene expression in the mouse. *Nat Rev Genet.* 2001;2:743-55.
135. Li JS, Knafo L, Turgeon A, Garcia R, Schiffrin EL. Effect of endothelin antagonism on blood pressure and vascular structure in renovascular hypertensive rats. *Am J Physiol.* 1996;271:H88-93.
136. Li JS, Schiffrin EL. Effect of chronic treatment of adult spontaneously hypertensive rats with an endothelin receptor antagonist. *Hypertension.* 1995;25:495-500.
137. Liefeldt L, Schonfelder G, Bocker W, Hocher B, Talsness CE, *et al.* Transgenic rats expressing the human ET-2 gene: a model for the study of endothelin actions in vivo. *J Mol Med.* 1999;77:565-74.
138. Lincoln TM. Cyclic GMP and mechanisms of vasodilation. *Pharmacol Ther.* 1989;41:479-502.
139. Ling GY, Cao WH, Onodera M, Ju KH, Kurihara H, *et al.* Renal sympathetic nerve activity in mice: comparison between mice and rats and between normal and endothelin-1 deficient mice. *Brain Res.* 1998;808:238-49.
140. Little PJ, Neylon CB, Tkachuk VA, Bobik A. Endothelin-1 and endothelin-3 stimulate calcium mobilization by different mechanisms in vascular smooth muscle. *Biochem Biophys Res Commun.* 1992;183:694-700.
141. Liu Y, Geisbuhler B, Jones AW. Activation of multiple mechanisms including phospholipase D by endothelin-1 in rat aorta. *Am J Physiol.* 1992;262:C941-9.

142. Loffler BM, Kalina B, Kunze H. Partial characterisation and subcellular distribution patterns of endothelin-1, -2 and -3 binding sites in human liver. *Biochem Biophys Res Commun.* 1991;181:840-5.
143. Lorens JB. Rapid and reliable cloning of PCR products. *PCR Methods Appl.* 1991;1:140-1.
144. Luscher TF, Enseleit F, Pacher R, Mitrovic V, Schulze MR, *et al.* Hemodynamic and neurohumoral effects of selective endothelin A (ET(A)) receptor blockade in chronic heart failure: the Heart Failure ET(A) Receptor Blockade Trial (HEAT). *Circulation.* 2002;106:2666-72.
145. Maemura K, Kurihara H, Kurihara Y, Kuwaki T, Kumada M, Yazaki Y. Gene expression of endothelin isoforms and receptors in endothelin-1 knockout mice. *J Cardiovasc Pharmacol.* 1995;26:S17-21.
146. Mantamadiotis T, Taraviras S, Tronche F, Schutz G. PCR-based strategy for genotyping mice and ES cells harboring loxP sites. *Biotechniques.* 1998;25:968-70, 972.
147. Marsault R, Feolde E, Frelin C. Receptor externalization determines sustained contractile responses to endothelin-1 in the rat aorta. *Am J Physiol.* 1993;264:C687-93.
148. Marsault R, Vigne P, Frelin C. The irreversibility of endothelin action is a property of a late intracellular signalling event. *Am J Physiol.* 1991;261:C987-93.
149. Marsden PA, Danthuluri NR, Brenner BM, Ballermann BJ, Brock TA. Endothelin action on vascular smooth muscle involves inositol trisphosphate and calcium mobilization. *Biochem Biophys Res Commun.* 1989;158:86-93.
150. Masaki T. The endothelin family: an overview. *J Cardiovasc Pharmacol.* 2000;36:S105-6.
151. Matsumura Y, Fujita K, Miyazaki Y, Takaoka M, Morimoto S. Involvement of endothelin-1 in deoxycorticosterone acetate-salt-induced hypertension and cardiovascular hypertrophy. *J Cardiovasc Pharmacol.* 1995;26:S456-8.
152. Matsumura Y, Hashimoto N, Taira S, Kuro T, Kitano R, *et al.* Different contributions of endothelin-A and endothelin-B receptors in the pathogenesis of deoxycorticosterone acetate-salt-induced hypertension in rats. *Hypertension.* 1999;33:759-65.
153. Matsumura Y, Kuro T, Kobayashi Y, Konishi F, Takaoka M, *et al.* Exaggerated vascular and renal pathology in endothelin-B receptor- deficient rats With deoxycorticosterone acetate-salt hypertension. *Circulation.* 2000;102:2765-2773.
154. Matsumura Y, Kuro T, Kobayashi Y, Konishi F, Takaoka M, *et al.* Exaggerated vascular and renal pathology in endothelin-B receptor-deficient rats with deoxycorticosterone acetate-salt hypertension. *Circulation.* 2000;102:2765-73.
155. Matsushima Y, Shinkai Y, Kobayashi Y, Sakamoto M, Kunieda T, Tachibana M. A mouse model of Waardenburg syndrome type 4 with a new spontaneous mutation of the endothelin-B receptor gene. *Mamm Genome.* 2002;13:30-5.
156. Matsuura T, Miura K, Ebara T, Yukimura T, Yamanaka S, *et al.* Renal vascular effects of the selective endothelin receptor antagonists in anaesthetized rats. *Br J Pharmacol.* 1997;122:81-6.
157. Matsuura T, Yukimura T, Kim S, Miura K, Iwao H. Selective blockade of endothelin receptor subtypes on systemic and renal vascular responses to endothelin-1

and IRL1620, a selective endothelin ETB-receptor agonist, in anesthetized rats. *Jpn J Pharmacol.* 1996;71:213-22.
158. Meyer-Lehnert H, Wanning C, Predel HG, Backer A, Stelkens H, Kramer HJ. Effects of endothelin on sodium transport mechanisms: potential role in cellular Ca2+ mobilization. *Biochem Biophys Res Commun.* 1989;163:458-65.
159. Miki S, Takeda K, Kiyama M, Hatta T, Morimoto S, *et al.* Augmented response of endothelin-A and endothelin-B receptor stimulation in coronary arteries of hypertensive hearts. *Am J Physiol.* 1998;274:R1613-8.
160. Miyoshi Y, Nakaya Y, Wakatsuki T, Nakaya S, Fujino K, *et al.* Endothelin blocks ATP-sensitive K+ channels and depolarizes smooth muscle cells of porcine coronary artery. *Circ Res.* 1992;70:612-6.
161. Molenaar P, O' Reilly G, Sharkey A, Kuc RE, Harding DP, *et al.* Characterisation and localisation of endothelin receptor subtypes in the human atrioventricular conducting system and myocardium. *Circulation.* 1993;72:526-538.
162. Moreau P, D'Uscio LV, Shaw S, Takase H, Barton M, Luscher TF. Angiotensin II increases tissue endothelin and induces vascular hypertrophy: reversal by ET(A)-receptor antagonist. *Circulation.* 1997;96:1593-1597.
163. Moreland S, McMullen DM, Delaney CL, Lee VG, Hunt JT. Venous smooth muscle contains vasoconstrictor ETB-like receptors. *Biochem Biophys Res Commun.* 1992;184:100-6.
164. Morita H, Kurihara H, Kurihara Y, Shindo T, Kuwaki T, *et al.* Systemic and renal response to salt loading in endothelin-1 knockout mice. *J Cardiovasc Pharmacol.* 1998;31:S557-60.
165. Mosqueda-Garcia R, Inagami T, Appalsamy M, Sugiura M, Robertson RM. Endothelin as a neuropeptide. Cardiovascular effects in the brainstem of normotensive rats. *Circ Res.* 1993;72:20-35.
166. Muller U. Ten years of gene targeting: targeted mouse mutants, from vector design to phenotype analysis. *Mech Dev.* 1999;82:3-21.
167. Mulvany MJ, Halpern W. Mechanical properties of vascular smooth muscle cells in situ. *Nature.* 1976;260:617-9.
168. Mulvany MJ, Hansen OK, Aalkjaer C. Direct evidence that the greater contractility of resistance vessels in spontaneously hypertensive rats is associated with a narrowed lumen, a thickened media, and an increased number of smooth muscle cell layers. *Circ Res.* 1978;43:854-64.
169. Murakoshi N, Miyauchi T, Kakinuma Y, Ohuchi T, Goto K, *et al.* Vascular endothelin-B receptor system in vivo plays a favorable inhibitory role in vascular remodeling after injury revealed by endothelin-B receptor-knockout mice. *Circulation.* 2002;106:1991-8.
170. Nakamura A, Kuwaki T, Kuriyama T, Yanagisawa M, Fukuda Y. Normal ventilation and ventilatory responses to chemical stimuli in juvenile mutant mice deficient in endothelin-3. *Faseb J.* 2001;15:618-26.
171. Nakamura K, Sasaki S, Moriguchi J, Morimoto S, Miki S, *et al.* Central effects of endothelin and its antagonists on sympathetic and cardiovascular regulation in SHR-SP. *J Cardiovasc Pharmacol.* 1999;33:876-82.

172. Nakano A, Kishi F, Minami K, Wakabayashi H, Nakaya Y, Kido H. Selective conversion of big endothelins to tracheal smooth muscle- constricting 31-amino acid-length endothelins by chymase from human mast cells. *J Immunol.* 1997;159:1987-92.
173. Namiki A, Hirata Y, Ishikawa M, Moroi M, Aikawa J, Machii K. Endothelin-1- and endothelin-3-induced vasorelaxation via common generation of endothelium-derived nitric oxide. *Life Sci.* 1992;50:677-82.
174. Nehls M, Messerle M, Sirulnik A, Smith AJ, Boehm T. Two large insert vectors, lambda PS and lambda KO, facilitate rapid mapping and targeted disruption of mammalian genes. *Biotechniques.* 1994;17:770-5.
175. Nelson RD, Stricklett P, Gustafson C, Stevens A, Ausiello D, *et al.* Expression of an AQP2 Cre recombinase transgene in kidney and male reproductive system of transgenic mice. *Am J Physiol.* 1998;275:C216-26.
176. Niranjan V, Telemaque S, deWit D, Gerard RD, Yanagisawa M. Systemic hypertension induced by hepatic overexpression of human preproendothelin-1 in rats. *J Clin Invest.* 1996;98:2364-72.
177. Nishimura J, Moreland S, Ahn HY, Kawase T, Moreland RS, van Breemen C. Endothelin increases myofilament Ca2+ sensitivity in alpha-toxin- permeabilized rabbit mesenteric artery. *Circ Res.* 1992;71:951-9.
178. Ohnaka K, Takayanagi R, Yamauchi T, Okazaki H, Ohashi M, *et al.* Identification and characterization of endothelin converting activity in cultured bovine endothelial cells. *Biochem Biophys Res Commun.* 1990;168:1128-36.
179. Ohuchi T, Kuwaki T, Ling GY, Dewit D, Ju KH, *et al.* Elevation of blood pressure by genetic and pharmacological disruption of the ETB receptor in mice. *Am J Physiol.* 1999;276:R1071-7.
180. Oksche A, Boese G, Horstmeyer A, Papsdorf G, Furkert J, *et al.* Evidence for downregulation of the endothelin-B-receptor by the use of fluorescent endothelin-1 and a fusion protein consisting of the endothelin-B-receptor and the green fluorescent protein. *J Cardiovasc Pharmacol.* 2000;36:S44-7.
181. Orban PC, Chui D, Marth JD. Tissue- and site-specific DNA recombination in transgenic mice. *Proc Natl Acad Sci U S A.* 1992;89:6861-5.
182. Ozaki S, Ihara M, Saeki T, Fukami T, Ishikawa K, Yano M. Endothelin ETB receptors couple to two distinct signaling pathways in porcine kidney epithelial LLC-PK1 cells. *J Pharmacol Exp Ther.* 1994;270:1035-40.
183. Pollock DM. Contrasting pharmacological ETB receptor blockade with genetic ETB deficiency in renal responses to big ET-1. *Physiol Genomics.* 2001;6:39-43.
184. Pollock DM, Allcock GH, Krishnan A, Dayton BD, Pollock JS. Upregulation of endothelin B receptors in kidneys of DOCA-salt hypertensive rats. *Am J Physiol Renal Physiol.* 2000;278:F279-86.
185. Pollock DM, Pollock JS. Evidence for endothelin involvement in the response to high salt. *Am J Physiol Renal Physiol.* 2001;281:F144-50.
186. Puffenberger EG, Hosada K, Washington SS, Nakao K, deWit D, *et al.* A missense mutation of the endothelin receptor B gene in multigenic Hirschsprung's disease. *Cell.* 1994;79:1257-1266.

187. Qiu C, Ding SS, Hess P, Clozel JP, Clozel M. Endothelin mediates the altered renal hemodynamics associated with experimental congestive heart failure. *J Cardiovasc Pharmacol.* 2001;38:317-24.
188. Qiu C, Samsell L, Baylis C. Actions of endogenous endothelin on glomerular hemodynamics in the rat. *Am J Physiol.* 1995;269:R469-73.
189. Reed KC, Mann DA. Rapid transfer of DNA from agarose gels to nylon membranes. *Nucleic Acids Res.* 1985;13:8999-9009.
190. Rolinski B, Sadri I, Bogner J, Goebel FD. Determination of endothelin-1 immunoreactivity in plasma, cerebrospinal fluid and urine. *Res Exp Med (Berl).* 1994;194:9-24.
191. Roos M, Soskic V, Poznanovic S, Godovac-Zimmermann J. Post-translational modifications of endothelin receptor B from bovine lungs analyzed by mass spectrometry. *J Biol Chem.* 1998;273:924-31.
192. Roubert P, Gillard V, Plas P, Chabrier PE, Braquet P. Binding characteristics of endothelin isoforms (ET-1, ET-2, and ET-3) in vascular smooth muscle cells. *J Cardiovasc Pharmacol.* 1991;17:S104-8.
193. Rubanyi GM, Polokoff MA. Endothelins: molecular biology, biochemistry, pharmacology, physiology, and pathophysiology. *Pharmacol Rev.* 1994;46:325-415.
194. Russell FD, Davenport AP. Evidence for intracellular endothelin-converting enzyme-2 expression in cultured human vascular endothelial cells. *Circ Res.* 1999;84:891-6.
195. Russell FD, Skepper JN, Davenport AP. Evidence using immunoelectron microscopy for regulated and constitutive pathways in the transport and release of endothelin. *J Cardiovasc Pharmacol.* 1998;31:S19-21.
196. Russell FD, Skepper JN, Davenport AP. Human endothelial cell storage granules: a novel intracellular site for isoforms of the endothelin-converting enzyme. *Circ Res.* 1998;83:314-21.
197. Ryan MJ, Didion SP, Davis DR, Faraci FM, Sigmund CD. Endothelial dysfunction and blood pressure variability in selected inbred mouse strains. *Arterioscler Thromb Vasc Biol.* 2002;22:42-8.
198. Sakamoto A, Yanagisawa M, Sakurai T, Takuwa Y, Yanagisawa H, Masaki T. Cloning and functional expression of human cDNA for the ETB endothelin receptor. *Biochem Biophys Res Commun.* 1991;178:656-63.
199. Sakamoto A, Yanagisawa M, Sawamura T, Enoki T, Ohtani T, *et al.* Distinct subdomains of human endothelin receptors determine their selectivity to endothelinA-selective antagonist and endothelinB- selective agonists. *J Biol Chem.* 1993;268:8547-53.
200. Sakurai T, Yanagisawa M, Takuwa Y, Miyazaki H, Kimura S, *et al.* Cloning of a cDNA encoding a non-isopeptide-selective subtype of the endothelin receptor. *Nature.* 1990;348:730-2.
201. Sambrook J, Fritsch EF, Maniatis T. *Molecular cloning. A laboratory manual.* New York: Cold Spring Harbour Laboratory Press; 1989.
202. Sauer B, Henderson N. Cre-stimulated recombination at loxP-containing DNA sequences placed into the mammalian genome. *Nucleic Acids Res.* 1989;17:147-61.

203. Schiffrin EL. State-of-the-Art lecture. Role of endothelin-1 in hypertension. *Hypertension.* 1999;34:876-81.
204. Schiffrin EL, Lariviere R, Li JS, Sventek P, Touyz RM. Deoxycorticosterone acetate plus salt induces overexpression of vascular endothelin-1 and severe vascular hypertrophy in spontaneously hypertensive rats. *Hypertension.* 1995;25:769-73.
205. Schiffrin EL, Lariviere R, Li JS, Sventek P, Touyz RM. Endothelin-1 gene expression and vascular hypertrophy in DOCA-salt hypertension compared to spontaneously hypertensive rats. *Clin Exp Pharmacol Physiol Suppl.* 1995;1:S188-90.
206. Schlaeger TM, Bartunkova S, Lawitts JA, Teichmann G, Risau W, *et al.* Uniform vascular-endothelial-cell-specific gene expression in both embryonic and adult transgenic mice. *Proc Natl Acad Sci U S A.* 1997;94:3058-63.
207. Sharifi AM, He G, Touyz RM, Schiffrin EL. Vascular endothelin-1 expression and effect of an endothelin ETA antagonist on structure and function of small arteries from stroke- prone spontaneously hypertensive rats. *J Cardiovasc Pharmacol.* 1998;31:S309-12.
208. Shin MK, Levorse JM, Ingram RS, Tilghman SM. The temporal requirement for endothelin receptor-B signalling during neural crest development. *Nature.* 1999;402:496-501.
209. Shindo T, Kurihara H, Maemura K, Kurihara Y, Ueda O, *et al.* Renal damage and salt-dependent hypertension in aged transgenic mice overexpressing endothelin-1. *J Mol Med.* 2002;80:105-16.
210. Shukla SD, Halenda SP. Phospholipase D in cell signalling and its relationship to phospholipase C. *Life Sci.* 1991;48:851-66.
211. Shyamala V, Moulthrop TH, Stratton-Thomas J, Tekamp-Olson P. Two distinct human endothelin B receptors generated by alternative splicing from a single gene. *J Biol Chem.* 1993;268:19126-33.
212. Smith AG, Heath JK, Donaldson DD, Wong GG, Moreau J, *et al.* Inhibition of pluripotential embryonic stem cell differentiation by purified polypeptides. *Nature.* 1988;336:688-90.
213. Sokolovsky M, Ambar I, Galron R. A novel subtype of endothelin receptors. *J Biol Chem.* 1992;267:20551-4.
214. Southern EM. Detection of specific sequences among DNA fragments separated by gel electrophoresis. *J Mol Biol.* 1975;98:503-17.
215. Spokes RA, Ghatei MA, Bloom SR. Studies with endothelin-3 and endothelin-1 on rat blood pressure and isolated tissues: evidence for multiple endothelin receptor subtypes. *J Cardiovasc Pharmacol.* 1989;13:S191-2.
216. Spratt JC, Goddard J, Patel N, Strachan FE, Rankin AJ, Webb DJ. Systemic ETA receptor antagonism with BQ-123 blocks ET-1 induced forearm vasoconstriction and decreases peripheral vascular resistance in healthy men. *Hypertension.* 1999;33:581-5.
217. Stasch JP, Kazda S. Endothelin-1-induced vascular contractions: interactions with drugs affecting the calcium channel. *J Cardiovasc Pharmacol.* 1989;13:S63-6; discussion S74.

218. Strachan FE, Spratt JC, Wilkinson IB, Johnston NR, Gray GA, Webb DJ. Systemic blockade of the endothelin-B receptor increases peripheral vascular resistance in healthy men. *Hypertension.* 1999;33:581-5.
219. Sudjarwo SA, Hori M, Tanaka T, Matsuda Y, Okada T, Karaki H. Subtypes of endothelin ETA and ETB receptors mediating venous smooth muscle contraction. *Eur J Pharmacol.* 1994;262:255-9.
220. Sumner MJ, Cannon TR, Mundin JW, White DG, Watts IS. Endothelin ETA and ETB receptors mediate vascular smooth muscle contraction. *Br J Pharmacol.* 1992;107:858-60.
221. Suri C, Jones PF, Patan S, Bartunkova S, Maisonpierre PC, *et al.* Requisite role of angiopoietin-1, a ligand for the TIE2 receptor, during embryonic angiogenesis. *Cell.* 1996;87:1171-80.
222. Sventek P, Turgeon A, Schiffrin EL. Vascular endothelin-1 gene expression and effect on blood pressure of chronic ETA endothelin receptor antagonism after nitric oxide synthase inhibition with L-NAME in normal rats. *Circulation.* 1997;95:240-4.
223. Taddei S, Virdis A, Ghiadoni L, Sudano I, Notari M, Salvetti A. Vasoconstriction to endogenous endothelin-1 is increased in the peripheral circulation of patients with essential hypertension. *Circulation.* 1999;100:1680-3.
224. Takagi Y, Ninomiya H, Sakamoto A, Miwa S, Masaki T. Structural basis of G protein specificity of human endothelin receptors. A study with endothelinA/B chimeras. *J Biol Chem.* 1995;270:13961-7.
225. Takasuka T, Sakurai T, Goto K, Furuichi Y, Watanabe T. Human endothelin receptor ETB. Amino acid sequence requirements for super stable complex formation with its ligand. *J Biol Chem.* 1994;269:7509-13.
226. Takayanagi R, Kitazumi K, Takasaki C, Ohnaka K, Aimoto S, *et al.* Presence of non-selective type of endothelin receptor on vascular endothelium and its linkage to vasodilation. *Biochem Biophys Res Commun.* 1991;177:34-9.
227. Takayanagi R, Ohnaka K, Liu W, Ito T, Nawata H. Molecular biology of endothelin-converting enzyme. In: Highsmith RF, ed. *Endothelin Molecular Biology, Physiology and Pathology.* Totowa, New Jersey: Humana Press; 1998:75-92.
228. te Riele H, Maandag ER, Berns A. Highly efficient gene targeting in embryonic stem cells through homologous recombination with isogenic DNA constructs. *Proc Natl Acad Sci U S A.* 1992;89:5128-32.
229. Theis M, de Wit C, Schlaeger TM, Eckardt D, Kruger O, *et al.* Endothelium-specific replacement of the connexin43 coding region by a lacZ reporter gene. *Genesis.* 2001;29:1-13.
230. Tsukahara H, Ende H, Magazine HI, Bahou WF, Goligorsky MS. Molecular and functional characterization of the non-isopeptide-selective ETB receptor in endothelial cells. Receptor coupling to nitric oxide synthase. *J Biol Chem.* 1994;269:21778-85.
231. Valdenaire O, Barret A, Schweizer A, Rohrbacher E, Mongiat F, *et al.* Two di-leucine-based motifs account for the different subcellular localizations of the human endothelin-converting enzyme (ECE-1) isoforms. *J Cell Sci.* 1999;112 Pt 18:3115-25.

232. Valdenaire O, Barret A, Schweizer A, Rohrbacher E, Mongiat F, *et al.* Two di-leucine-based motifs account for the different subcellular localizations of the human endothelin-converting enzyme (ECE-1) isoforms. *Br J Pharmacol.* 2001;132:213-20.
233. Valdenaire O, Rohrbacher E, Mattei MG. Organization of the gene encoding the human endothelin-converting enzyme (ECE-1). *J Biol Chem.* 1995;270:29794-8.
234. Vassileva I, Mountain C, Pollock DM. Functional role of ETB receptors in the renal medulla. *Hypertension.* 2003;41:1359-63.
235. Verhaar MC, Strachan FE, Newby DE, Cruden NL, Koomans HA, *et al.* Endothelin-A receptor antagonist-mediated vasodilatation is attenuated by inhibition of nitric oxide synthesis and by endothelin-B receptor blockade. *Circulation.* 1998;97:752-6.
236. Wagner AH, Krzesz R, Gao D, Schroeder C, Cattaruzza M, Hecker M. Decoy oligodeoxynucleotide characterization of transcription factors controlling endothelin-B receptor expression in vascular smooth muscle cells. *Mol Pharmacol.* 2000;58:1333-40.
237. Wang X, Douglas SA, Louden C, Vickery-Clark LM, Feuerstein GZ, Ohlstein EH. Expression of endothelin-1, endothelin-3, endothelin-converting enzyme- 1, and endothelin-A and endothelin-B receptor mRNA after angioplasty- induced neointimal formation in the rat. *Circ Res.* 1996;78:322-8.
238. Wessale JL, Adler AL, Novosad EI, Calzadilla SV, Dayton BD, *et al.* Pharmacology of endothelin receptor antagonists ABT-627, ABT-546, A-182086 and A-192621: ex vivo and in vivo studies. *Clin Sci (Lond).* 2002;103 Suppl 48:112S-117S.
239. Wilkes LC, Boarder MR. Characterization of endothelin receptors on a human neuroblastoma cell line: evidence for the ETA subtype. *Br J Pharmacol.* 1991;104:750-4.
240. Willette RN, Sauermelch CF, Storer BL, Guiney S, Luengo JI, *et al.* Plasma- and cerebrospinal fluid-immunoreactive endothelin-1: effects of nonpeptide endothelin receptor antagonists with diverse affinity profiles for endothelin-A and endothelin-B receptors. *J Cardiovasc Pharmacol.* 1998;31:S149-57.
241. Williams DL, Jr., Jones KL, Pettibone DJ, Lis EV, Clineschmidt BV. Sarafotoxin S6c: an agonist which distinguishes between endothelin receptor subtypes. *Biochem Biophys Res Commun.* 1991;175:556-61.
242. Williams RL, Hilton DJ, Pease S, Willson TA, Stewart CL, *et al.* Myeloid leukaemia inhibitory factor maintains the developmental potential of embryonic stem cells. *Nature.* 1988;336:684-7.
243. Wong NL, Wong BP, Tsui JK. Vasopressin regulates endothelin-B receptor in rat inner medullary collecting duct. *Am J Physiol Renal Physiol.* 2000;278:F369-74.
244. Xu D, Emoto N, Giaid A, Slaughter C, Kaw S, *et al.* ECE-1: a membrane bound metalloprotease that catalyses the proteolytic activation of big endothelin-1. *Cell.* 1994;78:473-485.
245. Yagi T, Ikawa Y, Yoshida K, Shigetani Y, Takeda N, *et al.* Homologous recombination at c-fyn locus of mouse embryonic stem cells with use of diphtheria toxin A-fragment gene in negative selection. *Proc Natl Acad Sci U S A.* 1990;87:9918-22.

246. Yanagisawa H, Hammer RE, Richardson JA, Emoto N, Williams SC, *et al.* Disruption of ECE-1 and ECE-2 reveals a role for endothelin-converting enzyme-2 in murine cardiac development. *J Clin Invest.* 2000;105:1373-82.
247. Yanagisawa H, Yanagisawa M, Kapur RP, Richardson JA, Williams SC, *et al.* Dual genetic pathways of endothelin-mediated intercellular signaling revealed by targeted disruption of endothelin converting enzyme-1 gene. *Development.* 1998;125:825-36.
248. Yanagisawa M, Kurihara H, Kimura S, Tomobe Y, Kobayashi M, *et al.* A novel potent vasoconstrictor peptide produced by vascular endothelial cells. *Nature.* 1988;332:411-415.
249. Yu M, Gopalakrishnan V, McNeill JR. Hemodynamic effects of a selective endothelin--a receptor antagonist in deoxycorticosterone acetate-salt hypertensive rats. *J Cardiovasc Pharmacol.* 1998;31:S262-4.
250. Yukimura T, Notoya M, Mizojiri K, Mizuhira V, Matsuura T, *et al.* High resolution localization of endothelin receptors in rat renal medulla. *Kidney Int.* 1996;50:135-47.
251. Zhang M, Luo B, Chen SJ, Abrams GA, Fallon MB. Endothelin-1 stimulation of endothelial nitric oxide synthase in the pathogenesis of hepatopulmonary syndrome. *Am J Physiol.* 1999;277:G944-52.

10 Appendix

10.1 AUTORADIOGRAPHIC STUDIES

10.1.1 METHODS

W/W -/-, Flox/Flox -/- and Flox/Flox Tie2 mice (n = 3) were sacrificed, frozen and longitudinally sectioned. Autoradiographic binding studies using the selective ET_B receptor ligand, BQ3020 (Amersham Biosciences, UK) were performed as described (Davenport and Kuc, 2002). Briefly, 30 μm sections were incubated with 0.1 pmol of [^{125}I]-BQ3020. Non-specific binding was determined in the presence of excess unlabelled BQ3020. Autoradiograms were exposed for 6 days at room temperature prior to development.

10.1.2 RESULTS

Qualitative ET_B receptor expression was visualised using the radiolabelled ET_B receptor ligand [^{125}I]-BQ3020 (Figure 10.1). W/W -/- and Flox/Flox -/- mice demonstrated intense ET_B receptor-mediated binding within the kidney, liver and lung. Binding of [^{125}I]-BQ3020 in Flox/Flox -/- mice in the absence of the Cre recombinase transgene was indistinguishable from that of W/W -/- mice. In EC-specific KOs, binding was substantially reduced within the lung parenchyma, but could be clearly seen within the SMC layer surrounding bronchioles. Binding was also detected in gut epithelial cells and the heart. Binding was substantially reduced within the renal medulla of Flox/Flox Tie2 mice, presumably as a result of decreased ET_B receptor expression on vasa recta EC. The liver of Flox/Flox Tie2 mice showed only a moderate reduction in ET_B receptor-mediated binding, consistent with continued expression on hepatocytes.

(i) (ii) (iii)

Figure 10.1

Autoradiographic analysis of W/W -/- (i) Flox/Flox -/- (ii) and Flox/Flox Tie2 (iii) mice following labelling with [^{125}I]-BQ3020. K = kidney, Li = liver, H = heart, G = gut, L = lung.